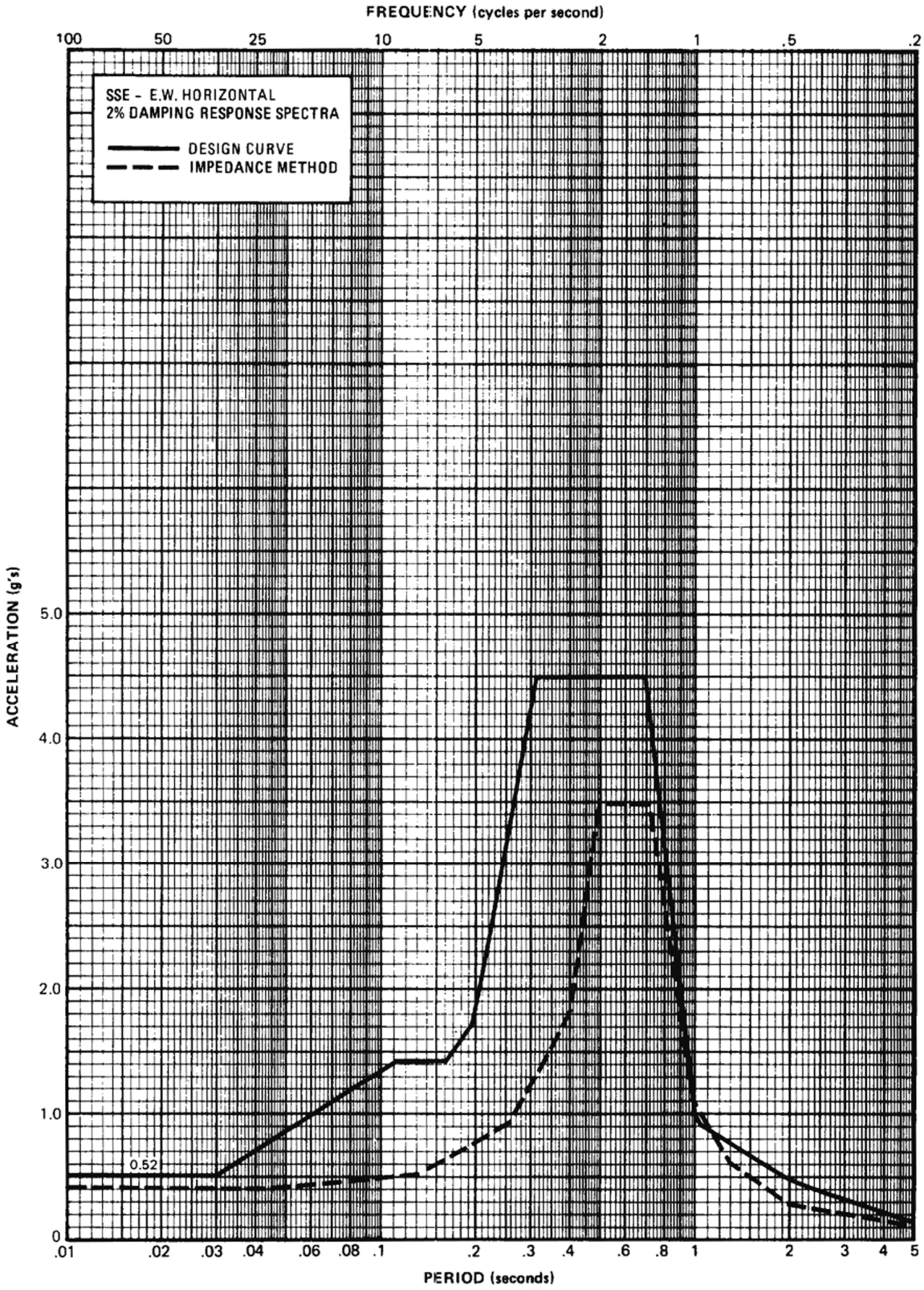

REV 14 10/07

SOUTHERN COMPANY
Energy to Serve Your World®

VOGTLE
ELECTRIC GENERATING PLANT
UNIT 1 AND UNIT 2

CONTAINMENT BUILDING
EL. 323 FT.POLAR CRANE

FIGURE 3D–137

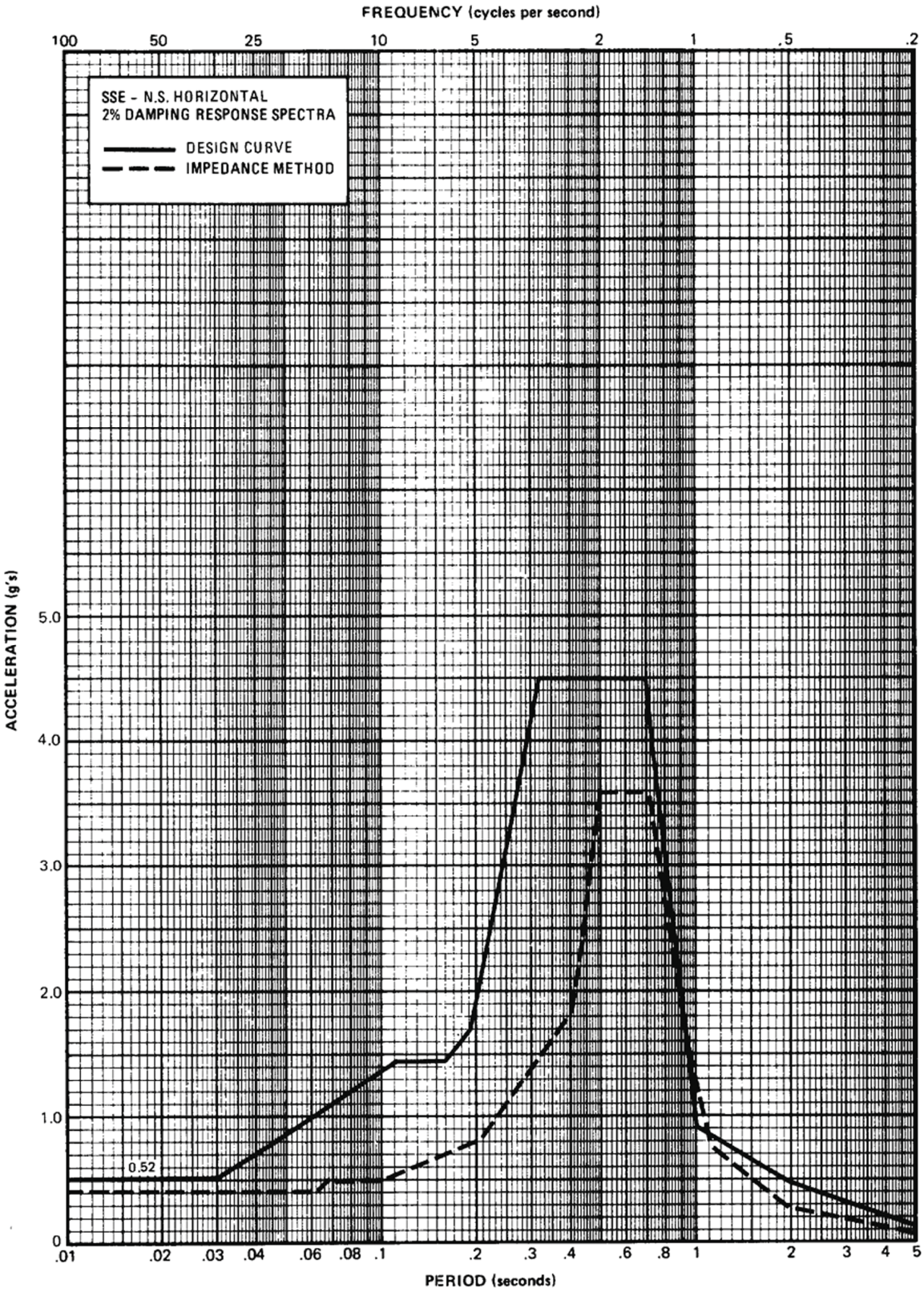

REV 14 10/07

SOUTHERN COMPANY
Energy to Serve Your World®

VOGTLE
ELECTRIC GENERATING PLANT
UNIT 1 AND UNIT 2

CONTAINMENT BUILDING
EL. 323 FT. POLAR CRANE

FIGURE 3D–138

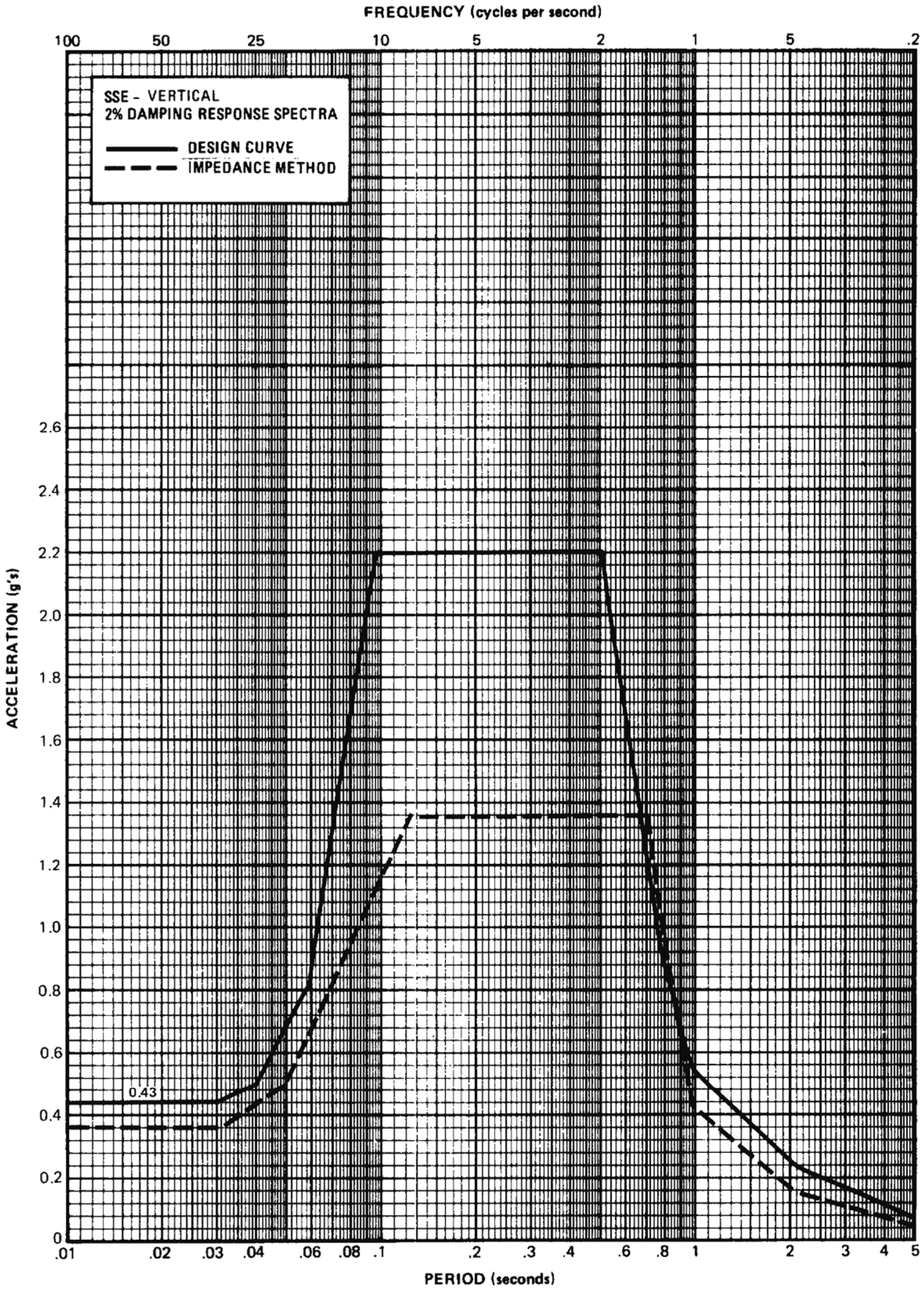

REV 14 10/07

SOUTHERN COMPANY
Energy to Serve Your World®

VOGTLE
ELECTRIC GENERATING PLANT
UNIT 1 AND UNIT 2

CONTAINMENT BUILDING
EL. 323 FT. POLAR CRANE

FIGURE 3D–139

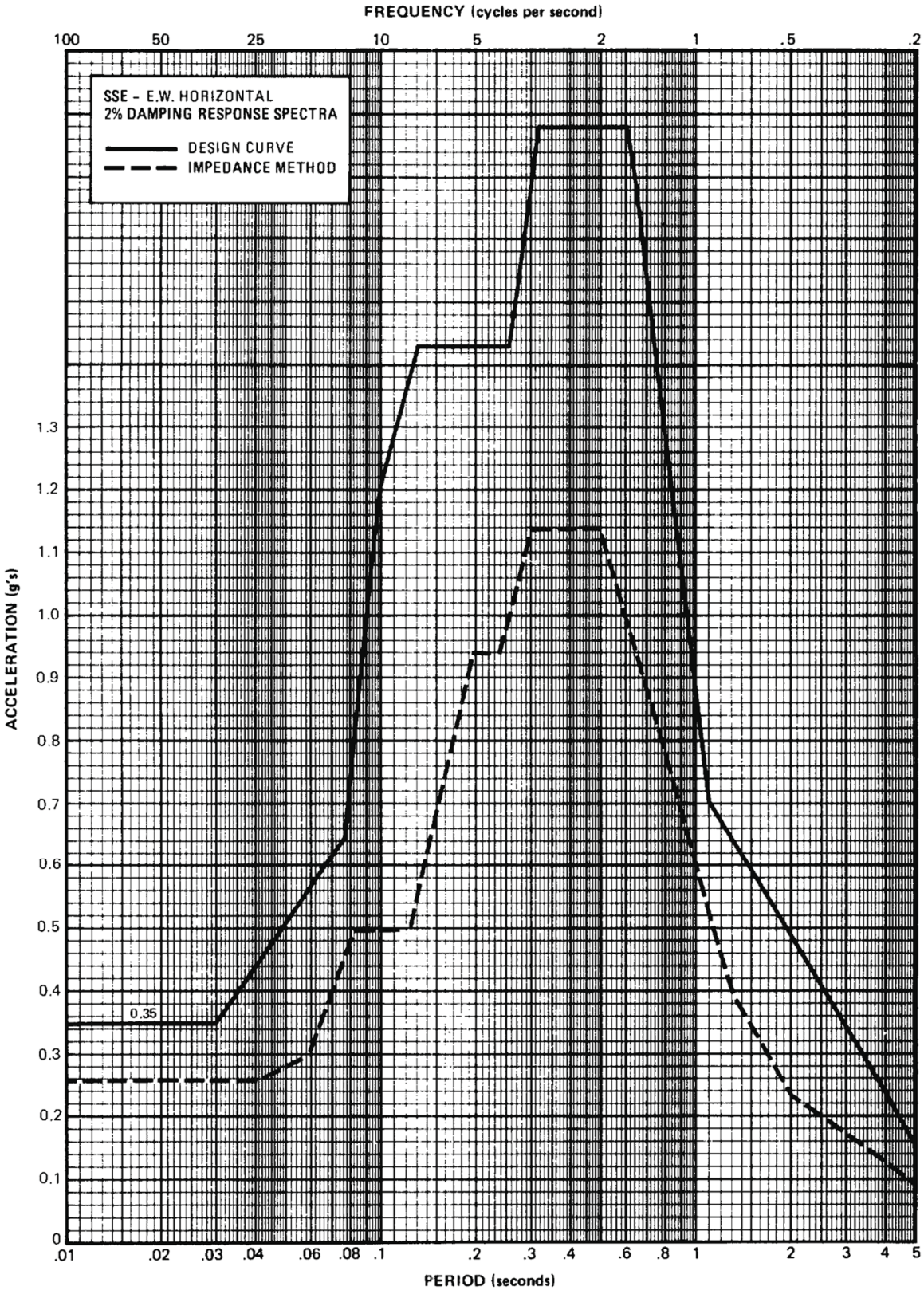

REV 14 10/07

SOUTHERN COMPANY
Energy to Serve Your World®

VOGTLE
ELECTRIC GENERATING PLANT
UNIT 1 AND UNIT 2

CONTROL BUILDING
EL. 180 FT. BASEMAT

FIGURE 3D–140

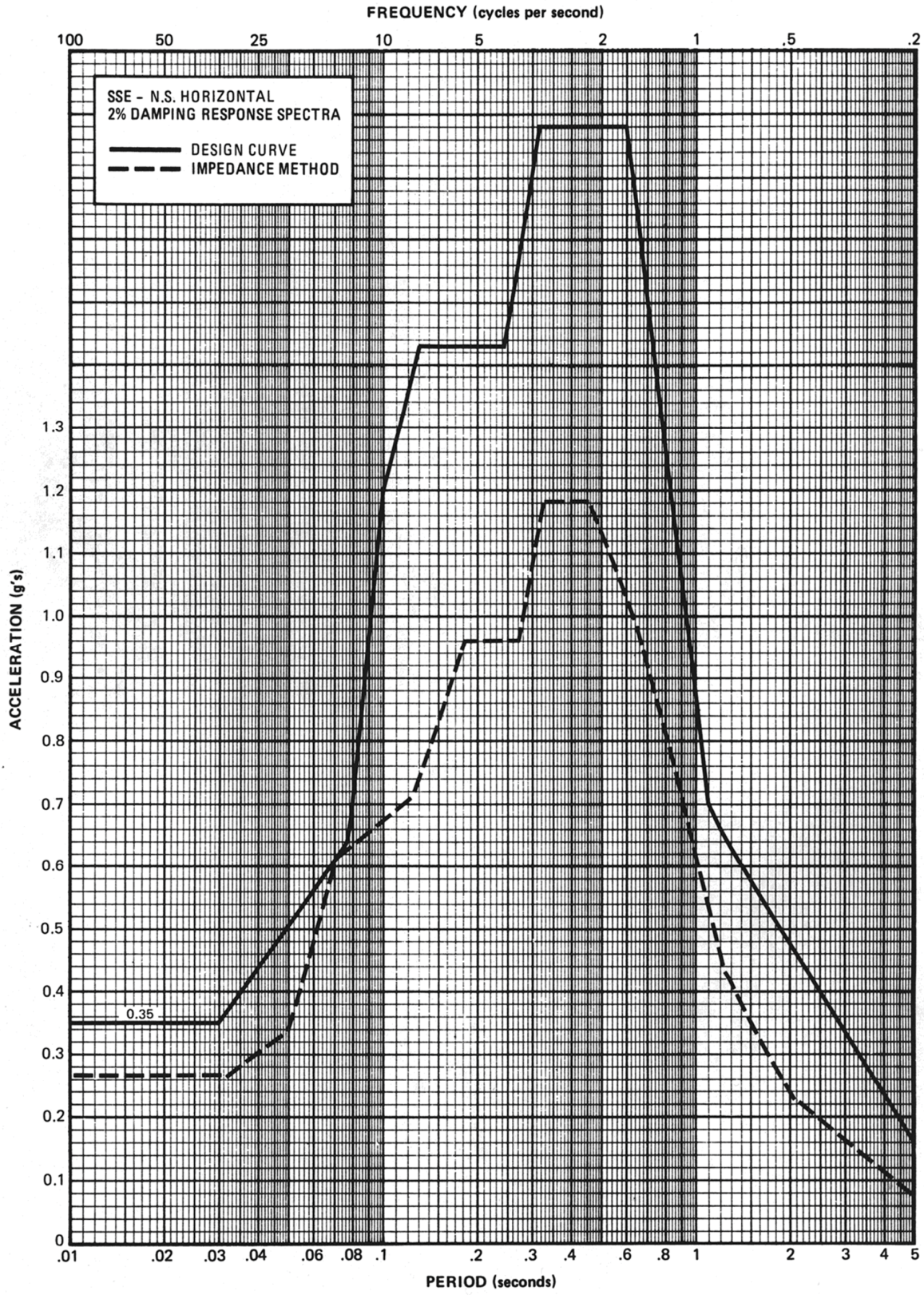

REV 14 10/07

SOUTHERN COMPANY
Energy to Serve Your World®

VOGTLE
ELECTRIC GENERATING PLANT
UNIT 1 AND UNIT 2

CONTROL BUILDING
EL. 180 FT. BASEMAT

FIGURE 3D–141

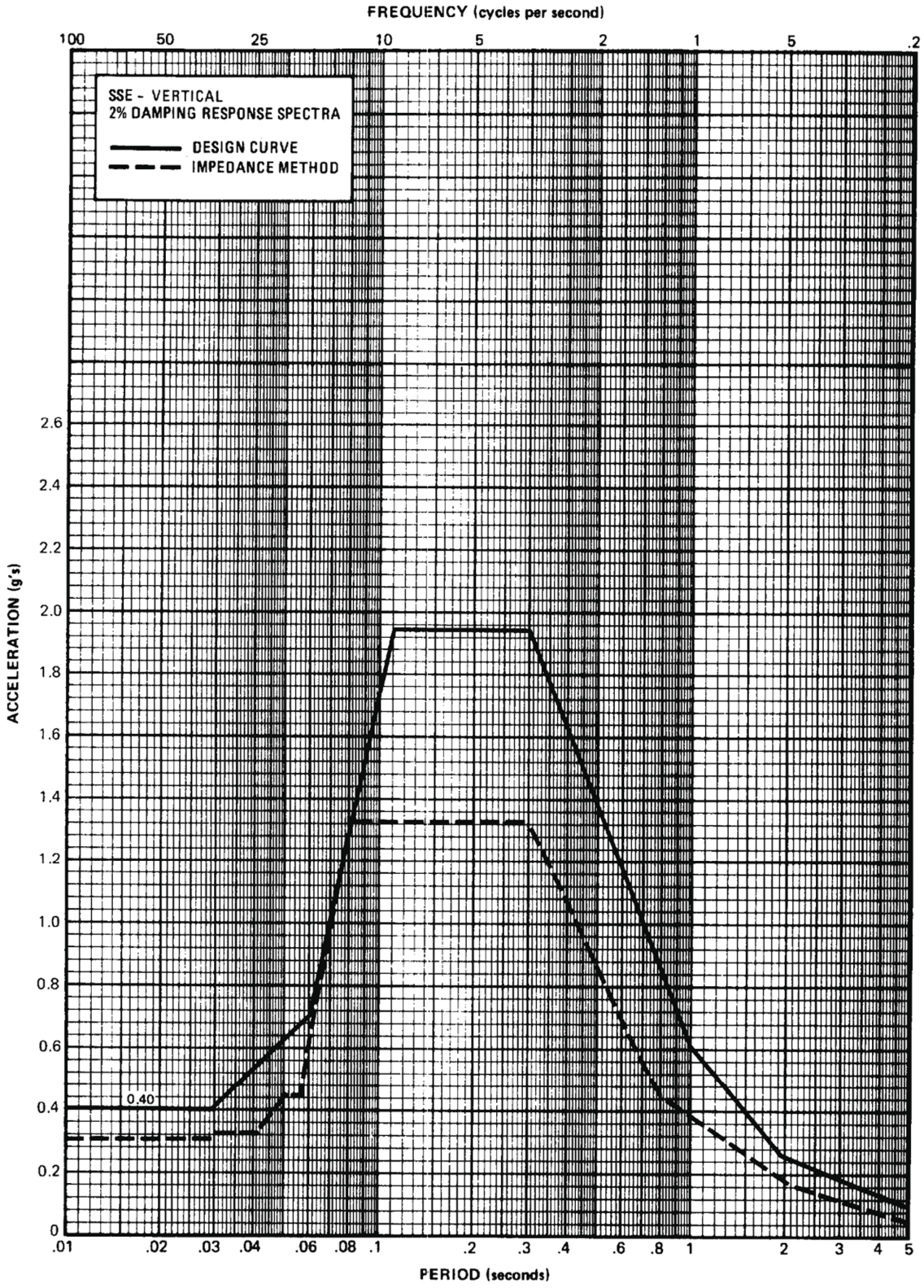

REV 14 10/07

SOUTHERN COMPANY
Energy to Serve Your World®

VOGTLE
ELECTRIC GENERATING PLANT
UNIT 1 AND UNIT 2

CONTROL BUILDING
EL. 180 FT. BASEMAT

FIGURE 3D–142

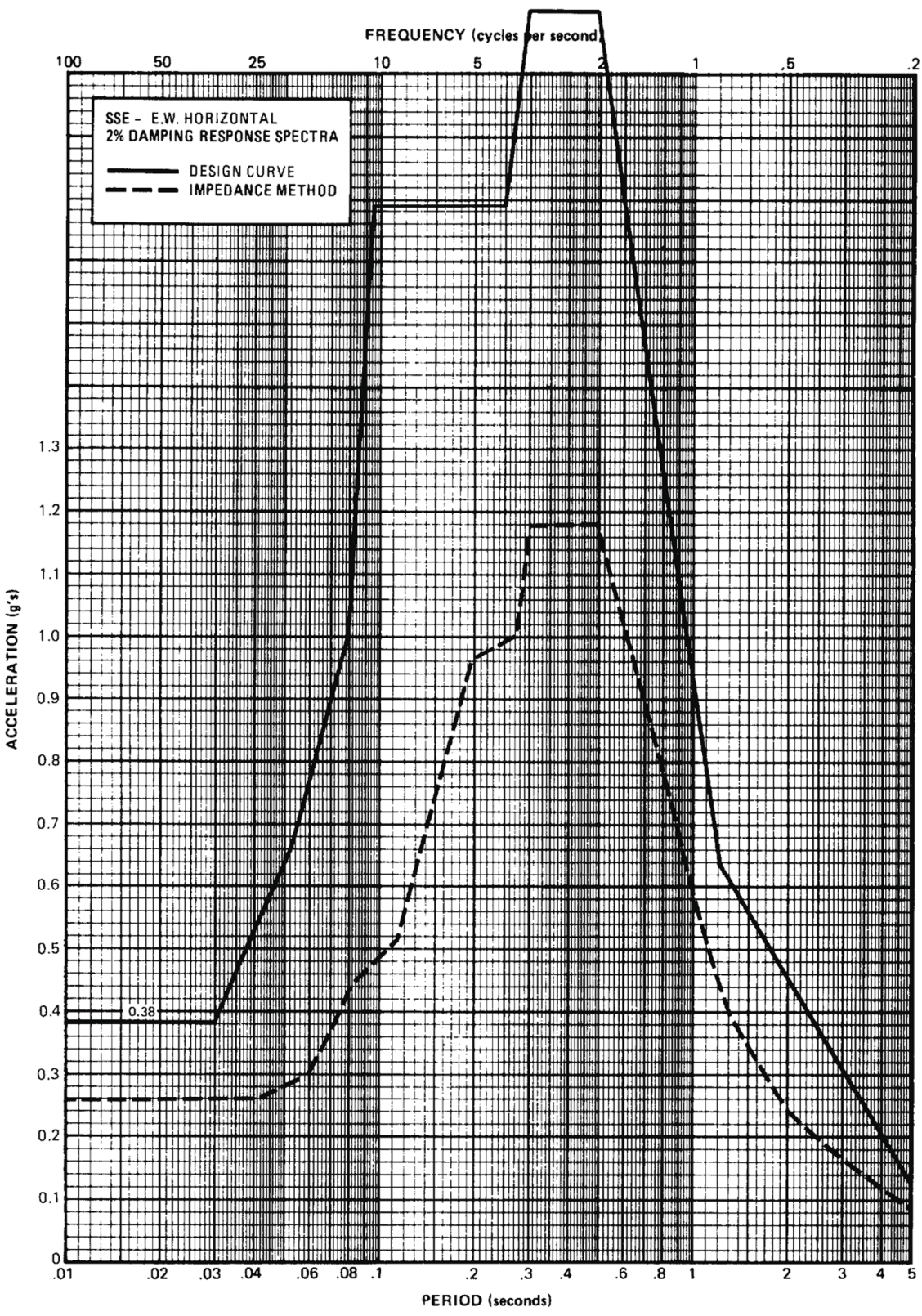

REV 14 10/07

SOUTHERN COMPANY
Energy to Serve Your World®

VOGTLE
ELECTRIC GENERATING PLANT
UNIT 1 AND UNIT 2

CONTROL BUILDING
EL. 220 FT.

FIGURE 3D–143

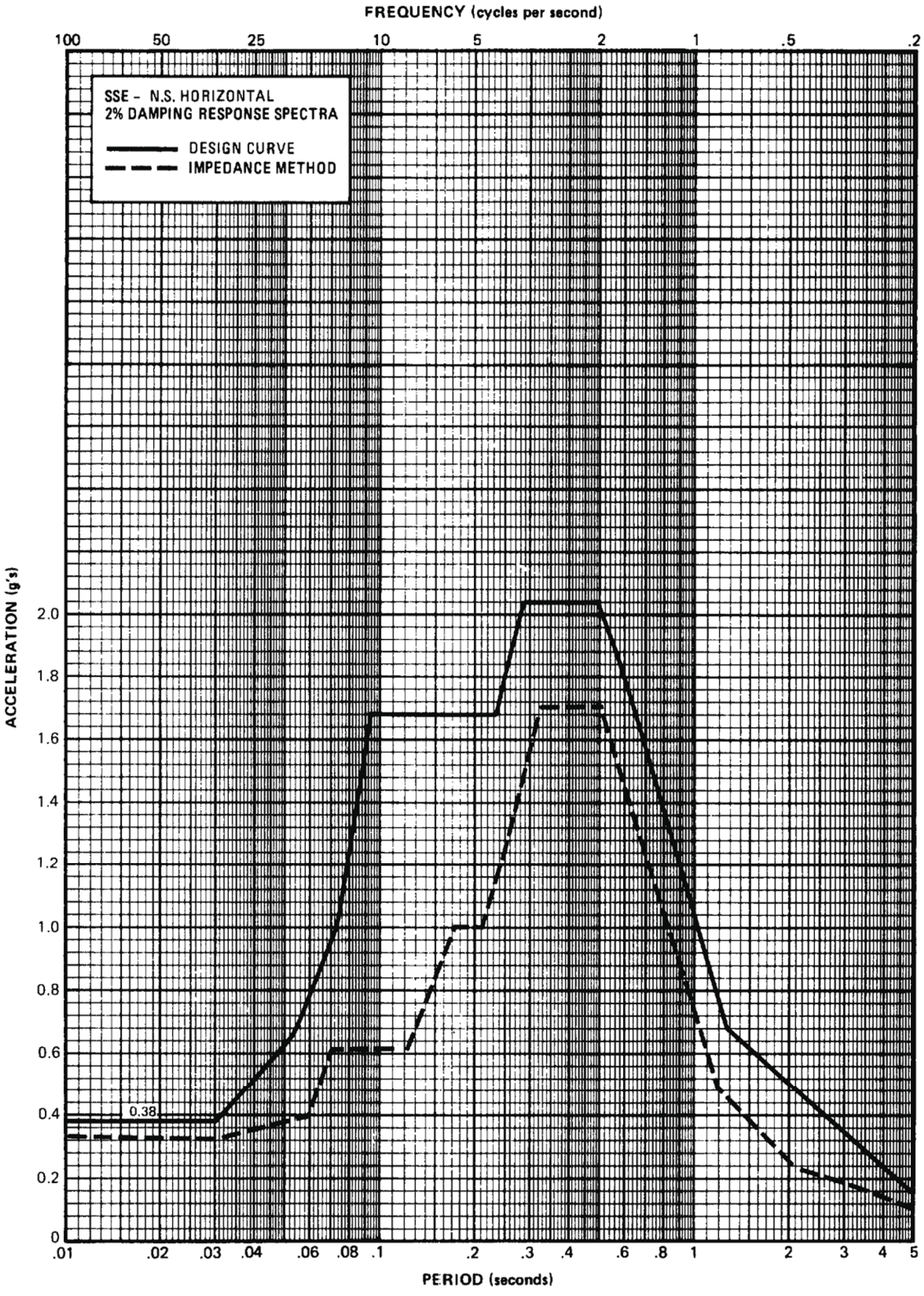

REV 14 10/07

SOUTHERN COMPANY
Energy to Serve Your World®

VOGTLE
ELECTRIC GENERATING PLANT
UNIT 1 AND UNIT 2

CONTROL BUILDING
EL. 220 FT.

FIGURE 3D–144

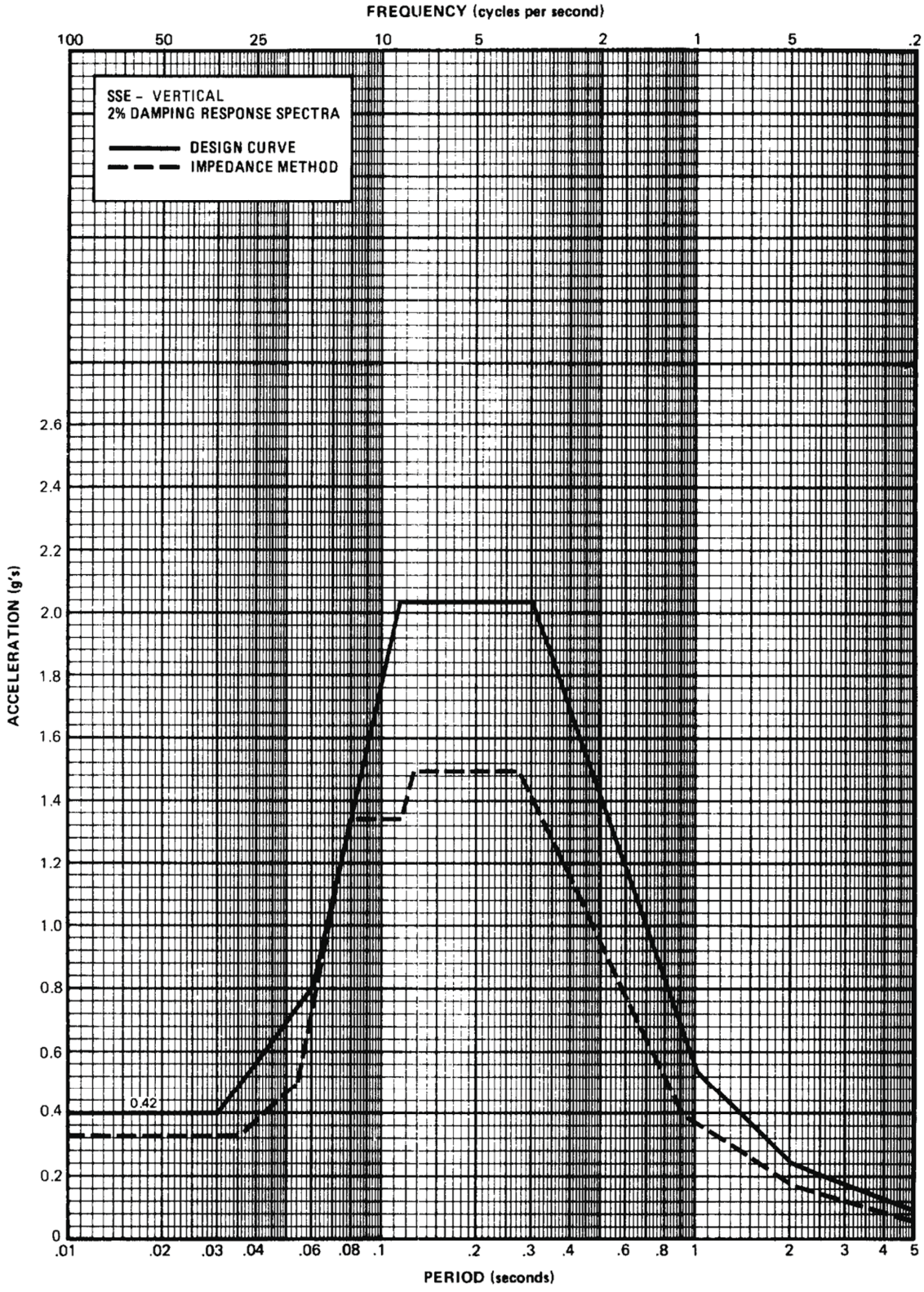

REV 14 10/07

SOUTHERN COMPANY
Energy to Serve Your World®

VOGTLE
ELECTRIC GENERATING PLANT
UNIT 1 AND UNIT 2

CONTROL BUILDING
EL. 220 FT.

FIGURE 3D–145

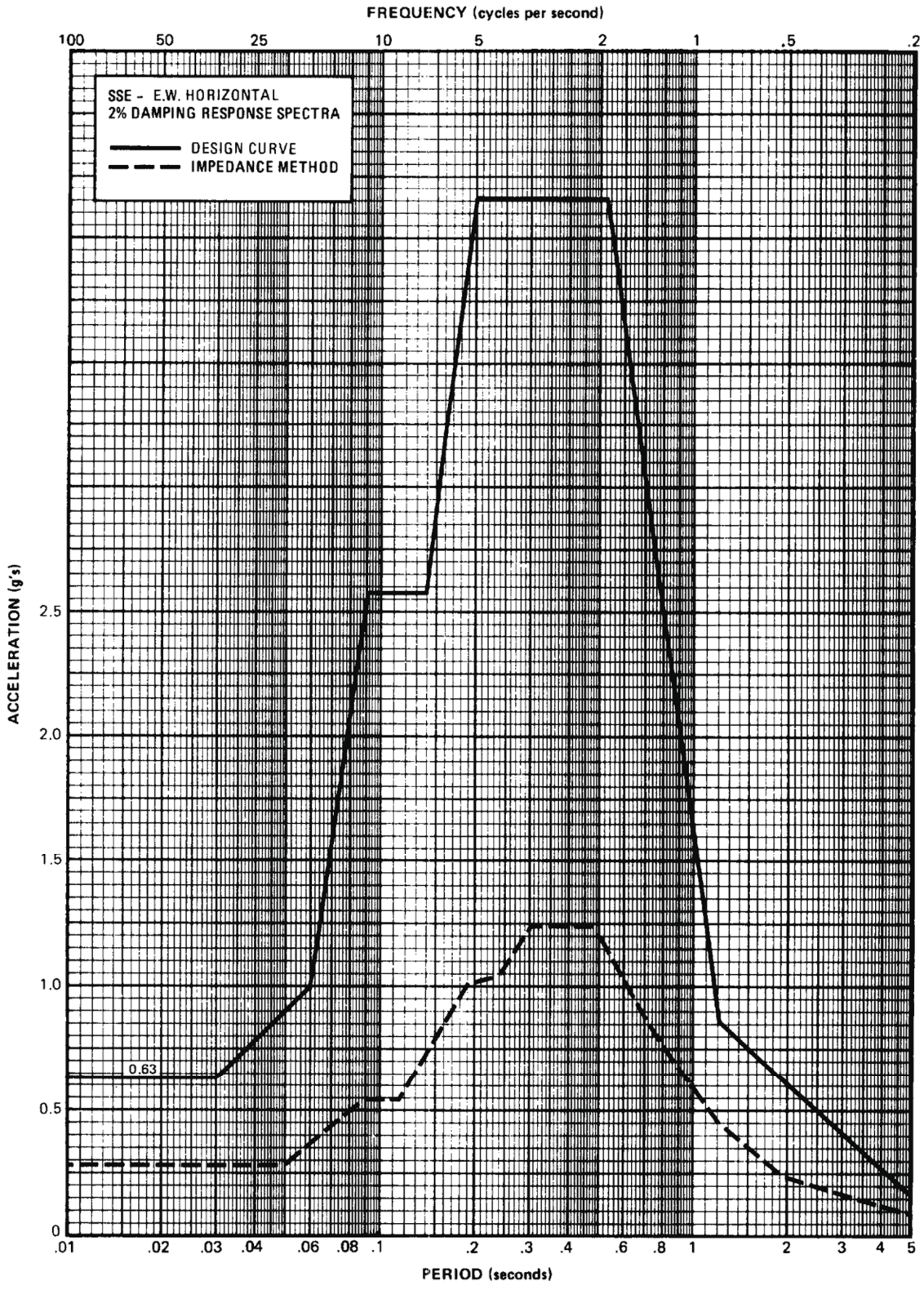

REV 14 10/07

SOUTHERN COMPANY
Energy to Serve Your World®

VOGTLE
ELECTRIC GENERATING PLANT
UNIT 1 AND UNIT 2

CONTROL BUILDING
EL. 260 FT.

FIGURE 3D–146

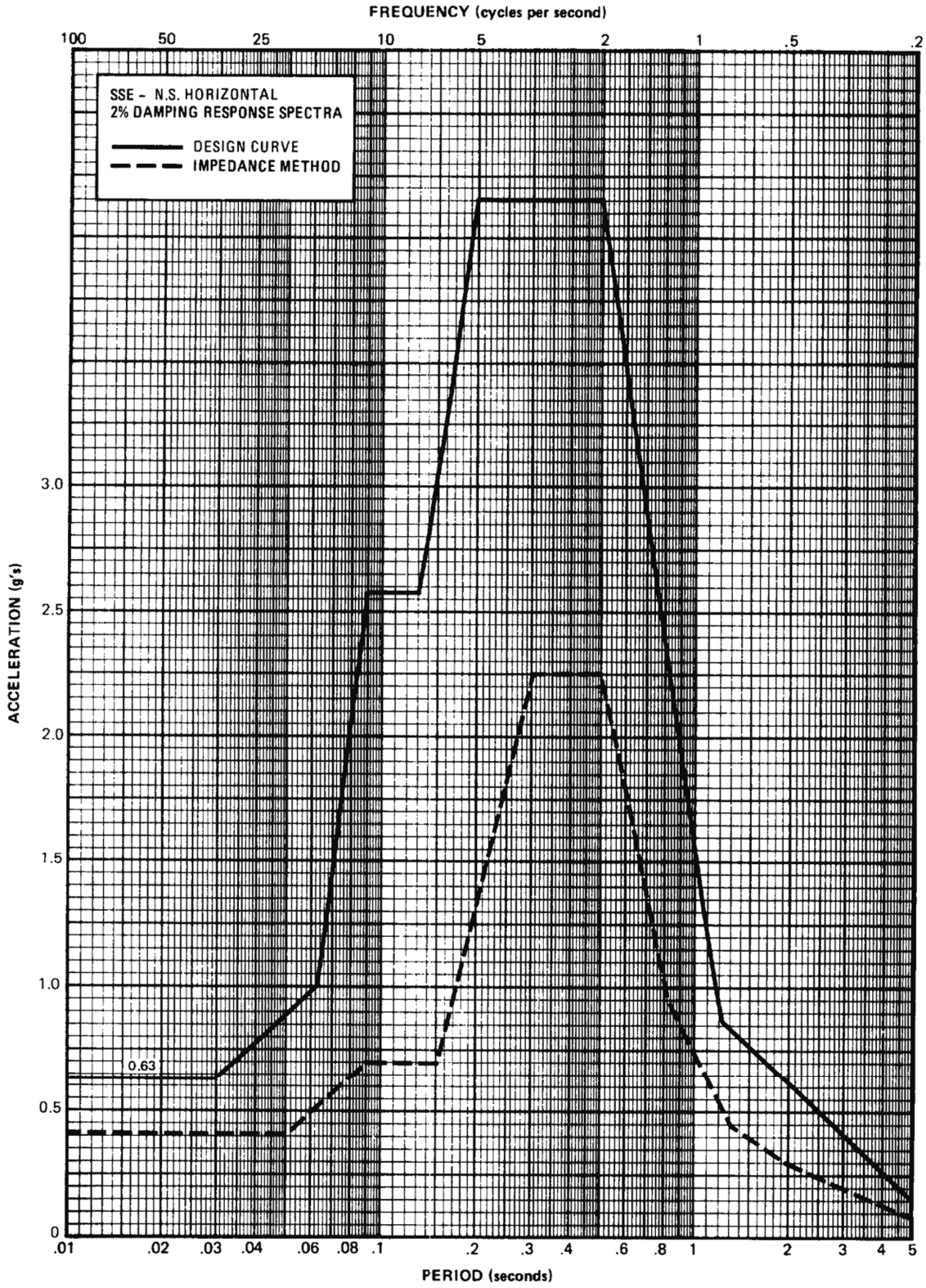

REV 14 10/07

SOUTHERN COMPANY *Energy to Serve Your World®* **VOGTLE** **ELECTRIC GENERATING PLANT** **UNIT 1 AND UNIT 2**	CONTROL BUILDING EL. 260 FT. FIGURE 3D–147

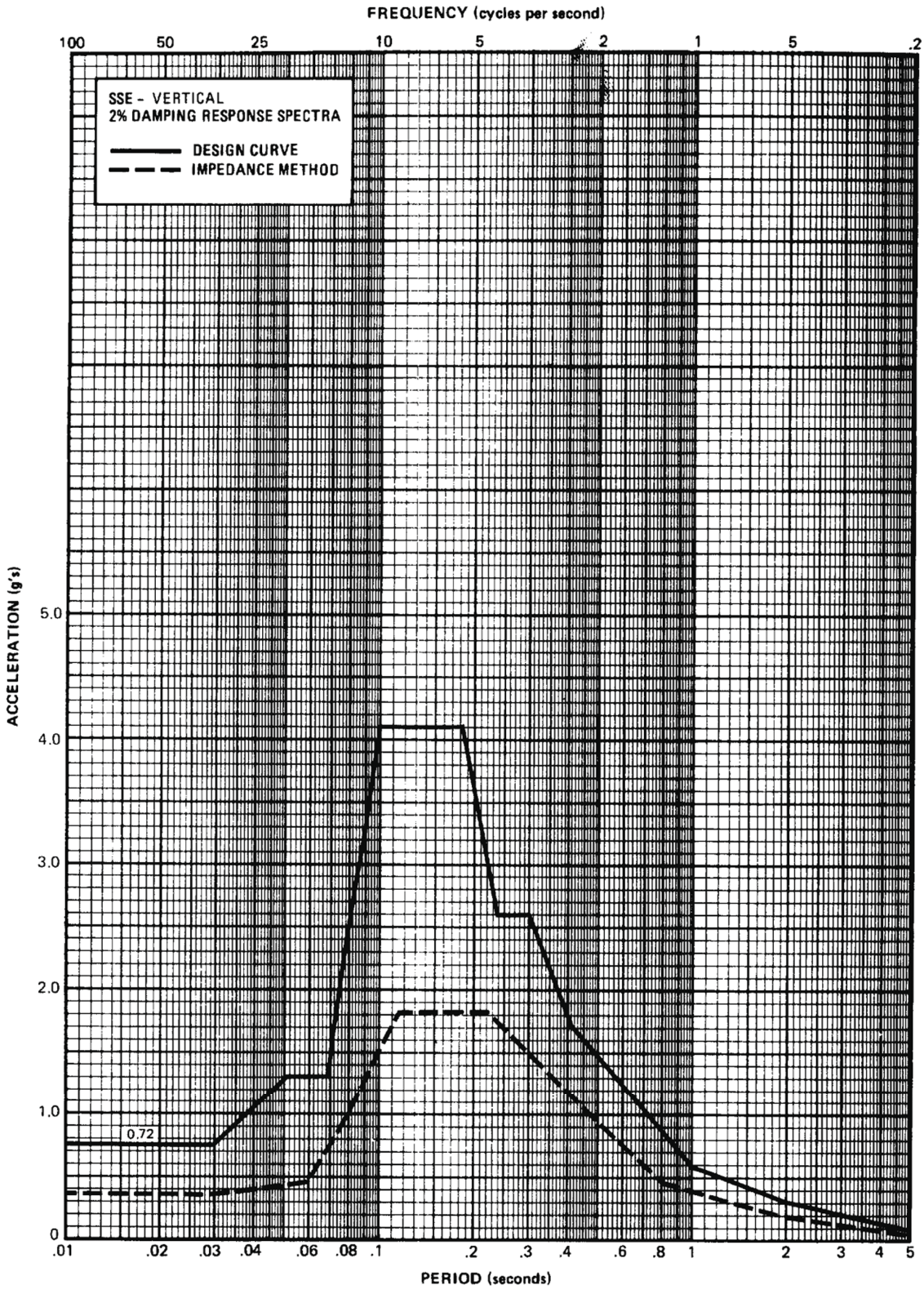

REV 14 10/07

SOUTHERN COMPANY *Energy to Serve Your World®* **VOGTLE** **ELECTRIC GENERATING PLANT** **UNIT 1 AND UNIT 2**	CONTROL BUILDING EL. 260 FT.
	FIGURE 3D–148

APPENDIX 3E

IMPEDANCE FUNCTIONS FOR AN ARBITRARILY SHAPED FOUNDATION ON A LAYERED MEDIUM

This appendix describes the procedure used to compute the impedance functions for an arbitrarily shaped foundation resting on a layered soil medium, for use in the soil-structure interaction analysis as specified in subsection 3.7.B.2.

The analytical techniques to obtain the impedance functions for flat rigid foundations of arbitrary shape placed on the surface of an elastic half space have been developed by Wong and Luco.[1] The equation of motion for the forced steady-state vibrations of an elastic half space excited by harmonic loads distributed over a region S of the plane surface (figure 3E-1) is:

$$(c^2 - \beta^2)\,\nabla(\nabla \cdot u) + \beta^2\nabla^2 u + \omega^2 u = 0 \qquad \chi_3 \geq 0 \tag{1}$$

in which u is the displacement vector $(u_1,u_2,u_3)e^{i\omega t}$ in the cartesian system of coordinates (χ_1,χ_2,χ_3) such that $\chi_3 = 0$ corresponds to the surface of the half space with $\chi_3 > 0$ representing the points within the half space. The symbols c and ß are the compressional and shear wave velocities, respectively.

Assuming that the surface tractions on the loaded region S are known, or equivalently, assuming that the stress components σ_{j_3} (j = 1,2,3) on S are known, then a solution of equation (1) satisfying the mixed boundary-value problem on $\chi_3 = 0$, in which displacements are prescribed along the contact between the foundation and the soil while tractions are prescribed on the soil surface not covered by the foundation, is given by:

$$u_i(\chi_1,\chi_2,0) = - - \sum_{j=1}^{3} \int_S G_{ij}\,(\chi_i - \chi_1^0,\ \chi_2 - \chi_2^0)\,\sigma_{j3}\,(\chi_1^0,\ \chi_2^0,\ 0)\,d\chi_1^0\,d\chi_2^0 \tag{2}$$

for $\chi_3 = 0$. In equation 2, $G_{ij}(\chi_1^0 - \chi_1^0, \chi_2 - \chi_2^0, 0)$ denotes the ith displacement component at $(\chi_1,\chi_2,0)$ generated by a unit harmonic load acting at $(\chi_1^0,\chi_2^0,0)$.

To solve this integral equation 2 for an arbitrarily shaped foundation, the following numerical procedure is used:

A. The region S is divided into n rectangular subregions Sk (k = 1,2,...,n) as indicated in figure 3E-1.

B. The stress components σ_{j3} are assumed to have constant values $\sigma_{j3}^{(k)}$ within each subregion S_k.

C. The boundary conditions are satisfied approximately by matching the average displacements within each subregion to the average value of the required compatible displacements.

Using the above approximations, integral equation 2 can be expressed in matrix equations as:

$$\begin{Bmatrix} \bar{u}_1 \\ \bar{u}_2 \\ . \\ . \\ . \\ \bar{u}_n \end{Bmatrix} = \begin{bmatrix} [\phi]11\ [\phi]12.\ .\ .\ .\ .[\phi]1n \\ \\ [\phi]21\ [\phi]22.\ .\ .\ .\ .[\phi]2n \\ .\quad .\quad . \\ .\quad .\quad . \\ .\quad .\quad . \\ [\phi]n1\ [\phi]n2.\ .\ .\ .\ .[\phi]nn \\ \\ \end{bmatrix} \begin{Bmatrix} \sigma_{j3}^{(1)} A_1 \\ \sigma_{j3}^{(2)} A_2 \\ . \\ . \\ . \\ \sigma_{j3}^{(n)} n \end{Bmatrix} \quad (3)$$

in which:

$\underset{\sim}{\bar{u}}_1 = \left\{ \bar{u}_{1i}, \bar{u}_{2i}, \bar{u}_{3i} \right\}^T$ are average displacements in subregion S_i.

A_i = area if subregion S_i.

$[\phi]_{ij}$ = a 3x3 compliance submatrix relating the average displacements at subregion S_i to the tractions at subregion S_j.

To calculate the compliance submatrices, four linear integrals on the Green's functions are performed for point loads at the surface of a layered stratum. The formula for $[\phi]_{ij}$ is:

$$[\phi]_{ij} = -\int_{Si} ds \int_{Sj} ds_o \left[G(\omega, \underset{\sim}{r} - \underset{\sim o}{r}, \underset{\sim}{P}) \right] \quad (4)$$

in which [G] is the 3x3 Green's function matrix relating the displacement at the observation point $r = (\chi_1, \chi_2, 0)^T$ to a set of point loads at the source point $\underset{\sim o}{r} \cong \left(\chi_1^0, \chi_2^0, 0\right)^T$ • $\underset{\sim}{P}$ is the property vector associated with the underlying half space. By use of the average displacement matching approximation, the following symmetry exists even if $A_i \neq A_j$:

$$[\phi]_{ij}^T = [\phi]_{ji} \quad (5)$$

The property vector $\underset{\sim}{P}$ for a horizontally layered stratum can be characterized as:

$$\underset{\sim}{P} = (m, \mu_i, \beta_i, \rho_i, h_i, \nu_i, \varepsilon_i) \quad (6)$$

where:

- m = the number of layers.
- μ_i = the shear modulus of the ith layer.
- β_i = the shear wave velocity of the ith layer.
- ρ_i = the mass density of the ith layer.
- H_i = the thickness of the ith layer.

ν_i = the Poisson's ratio of the ith layer.

ξ_i = the critical damping coefficient of the ith layer.

The matrix [G] contains six independent elements. In order to reduce the number of independent variables and to render [G] dimensionless, a new matrix [G′] may be defined in the polar coordinate system {r, ψ, z}, as shown in figure 3E-2:

$$\left[G(\omega, \underset{\sim}{r} - \underset{\sim}{r_o}, \underset{\sim}{P})\right] = \frac{1}{\bar{\mu} r} \left[G'(b_0, \psi, \underset{\sim}{P'})\right] \quad (7)$$

where:

$$r = \left| \underset{\sim}{r} - \underset{\sim}{r_o} \right| = \sqrt{(\chi_1 - \chi_1^o)^2 + (\chi_2 - \chi_2^o)^2}$$

$$\psi = \arg\left(\underset{\sim}{r} - \underset{\sim}{r_o}\right) = \tan^{-1}\left(\frac{\chi_2 \chi_2^o}{\chi_1 - \chi_1^o}\right)$$

$$b_o = \frac{\omega r}{\bar{\beta}}$$

$\underset{\sim}{P'} = \{m, \mu_i', \beta_i', \rho_i', h_i', \nu_i, \varepsilon\}$, the normalized property vector in which:

$$\mu_i' = \frac{\mu_i}{\bar{\mu}}$$

$$\beta_i' = \frac{\beta_i}{\bar{\beta}}$$

$$\rho_i' = \frac{\rho_i}{\bar{\rho}}$$

$$h_i' = \frac{\omega h_i}{\bar{\beta}}$$

The reference values of $\bar{\mu}$, $\bar{\beta}$ and $\bar{\rho}$, used to normalize $\underset{\sim}{P'}$ and [G´], are usually taken to be those of the top layer.

The dimensionless matrix [G´] is a function of four variables, f_{rr}, $f_{\psi r}$, f_{rz}, and f_{zz}, which are the Green's functions in the polar coordinate system.

The Green's functions for three-dimensional wave propagation in layered viscoelastic media have been formulated and solved by Luco and Apsel.[(2)(3)] In frequency domain, solution of the Green's functions in polar coordinates, which involve the Hankel transform-type integral representations of the displacement and stress components, can be expressed in the form:

$$I_n(b_o) = \int_0^\infty F(k, \omega, \underset{\sim}{P'}) J_n(k b_o) \, dk \quad (8)$$

for the concentrated point load applied at surface and displacement at the free surface observed at b_o distance from the load point. The kernel F depends upon wave number k, frequency ω, and layer properties $\underset{\sim}{P'}$; whereas, the Bessel functions J_n depend only upon kb_o.

The F integrands are evaluated in terms of factorizations of the upgoing and downgoing wave amplitudes in each layer. The semi-infinite integral in equation 8 can be reduced to the following finite integral:

$$I_n(b_o) = I_n(0) + \int_0^{k_\ell} [F(k,\omega,\underset{\sim}{P}') - F(k,0,P')]\, J_n(kb_o)\, dk \qquad (9)$$

in which the upper limit of integration, k_ℓ, is defined by the convergence of the dynamic integrands to the static integrands, and $I_n(0)$ represents the static (= 0) integrals. Since the radial dependence b_o appears only in the Bessel functions J_n, it is expedient to calculate the integrals; begin at $b_o = 0$ and end at $b_o = \frac{\omega r_{max}}{\beta}$ (r_{max} is the maximum length of the foundation) in equally spaced intervals. This precalculated Green's function table can be repeatedly used in solving the compliance submatrices $[\phi]_{ij}$ in integral equation 4 using the Gaussian quadrature.

For a rigid foundation, the average displacements $\bar{u}_i$, evaluated at the center of subregion S_i are given by:

$$\begin{aligned}
\bar{u}_{1i}(\chi_1^i,\chi_2^i,0) &= \Delta_1 - \theta_3\chi_2^i \\
\bar{u}_{2i}(\chi_1^i,\chi_2^i,0) &= \Delta_2 + \theta_3\chi_2^i \qquad (10) \\
\bar{u}_{3i}(\chi_1^i,\chi_2^i,0) &= \Delta_3 + \theta_1\chi_2^i - \theta_2\chi_2^i
\end{aligned}$$

where Δ_i (i = 1, 2, 3) corresponds to the amplitudes of the translational displacements at (0,0,0), while θ_i (i = 1,2,3), which is assumed to be small, corresponds to the amplitudes of the rotational displacements about the χ_i (i = 1, 2, 3) axes. From equation 3, the three corresponding traction components $\sigma_{j^3}^{(k)} A_k$ can be expressed in terms of $\bar{\underset{\sim}{u}}_i$, by inverting the matrix $[\phi]$. By substituting for $\bar{\underset{\sim}{u}}_i$ from equation 10, the surface tractions on the contact area may be expressed in terms of the translation Δ_1 and rotation θ_i of the rigid foundation. Finally, the total harmonic load with components (P_1,P_2,P_3) and the total harmonic moment with components (M_1,M_2,M_3) acting on the contact area can be expressed in terms of traction components by means of the following relationships:

$$\begin{aligned}
P_1 &= \sum_{j=1}^{n} \sigma_{i3}^{(j)} Aj \qquad (i = 1,2,3) \\
M_1 &= \sum_{j=1}^{n} \chi_2^j \sigma_{33}^{(j)} \qquad (11) \\
M_2 &= \sum_{j=1}^{n} \chi_1^j \sigma_{33}^{(j)} \\
M_3 &= \sum_{j=1}^{n} \left[\chi_1^j \sigma_{23}^{(j)} Aj - \chi_2^j \sigma_{13}^{(j)} Aj \right]
\end{aligned}$$

Substitution for contact tractions in terms of Δ_i and θ_i into equation 11 leads to the desired force-displacement relationship for the rigid foundation:

$$\begin{Bmatrix} P \\ M \end{Bmatrix} = [K] \begin{Bmatrix} \Delta \\ \theta \end{Bmatrix} \qquad (12)$$

where [K] is the complex frequency dependent impedance functions for flat rigid foundations placed on the surface of an elastic half space.

3E.1 REFERENCES

1. Wong, H. L., and Luco, J. E., "Dynamic Response of Rigid Foundations of Arbitrary Shape," Earthquake Engineering and Structural Dynamics, Vol 4, pp 579-587, 1976.

2. Luco, J. E., and Apsel, R. J., "On the Green's Functions for the Layered Half Space," Part 1, Bulletin of the Seismological Society of America, Vol 73, pp 901-929, 1983.

3. Apsel, R. J., and Luco, J. E., "On the Green's Functions for the Layered Half Space," Part 2, Bulletin of the Seismological Society of America, Vol 73, pp 931-951, 1983.

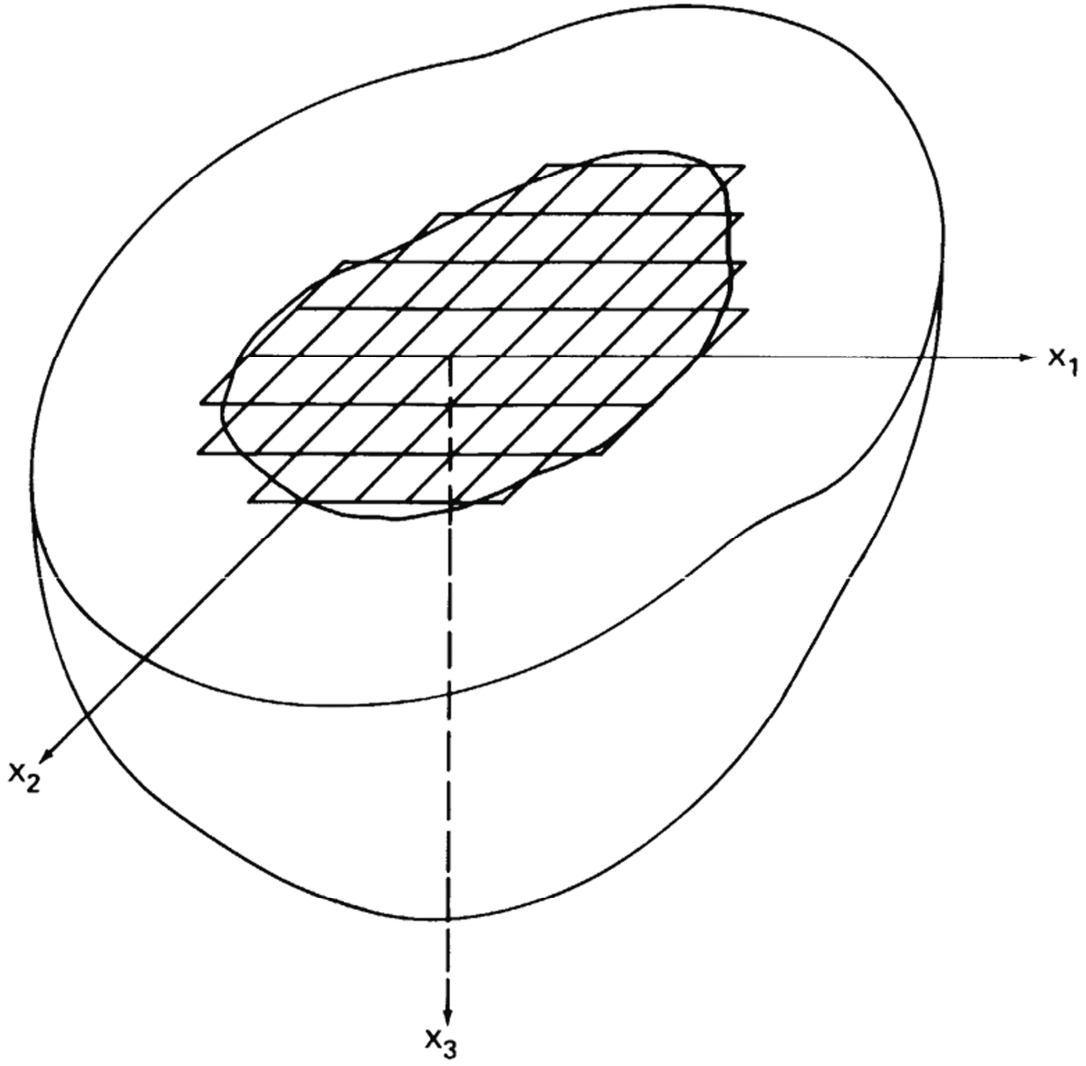

REV 14 10/07

SOUTHERN COMPANY
Energy to Serve Your World®

VOGTLE
ELECTRIC GENERATING PLANT
UNIT 1 AND UNIT 2

MODEL AND COORDINATE SYSTEM

FIGURE 3E–1

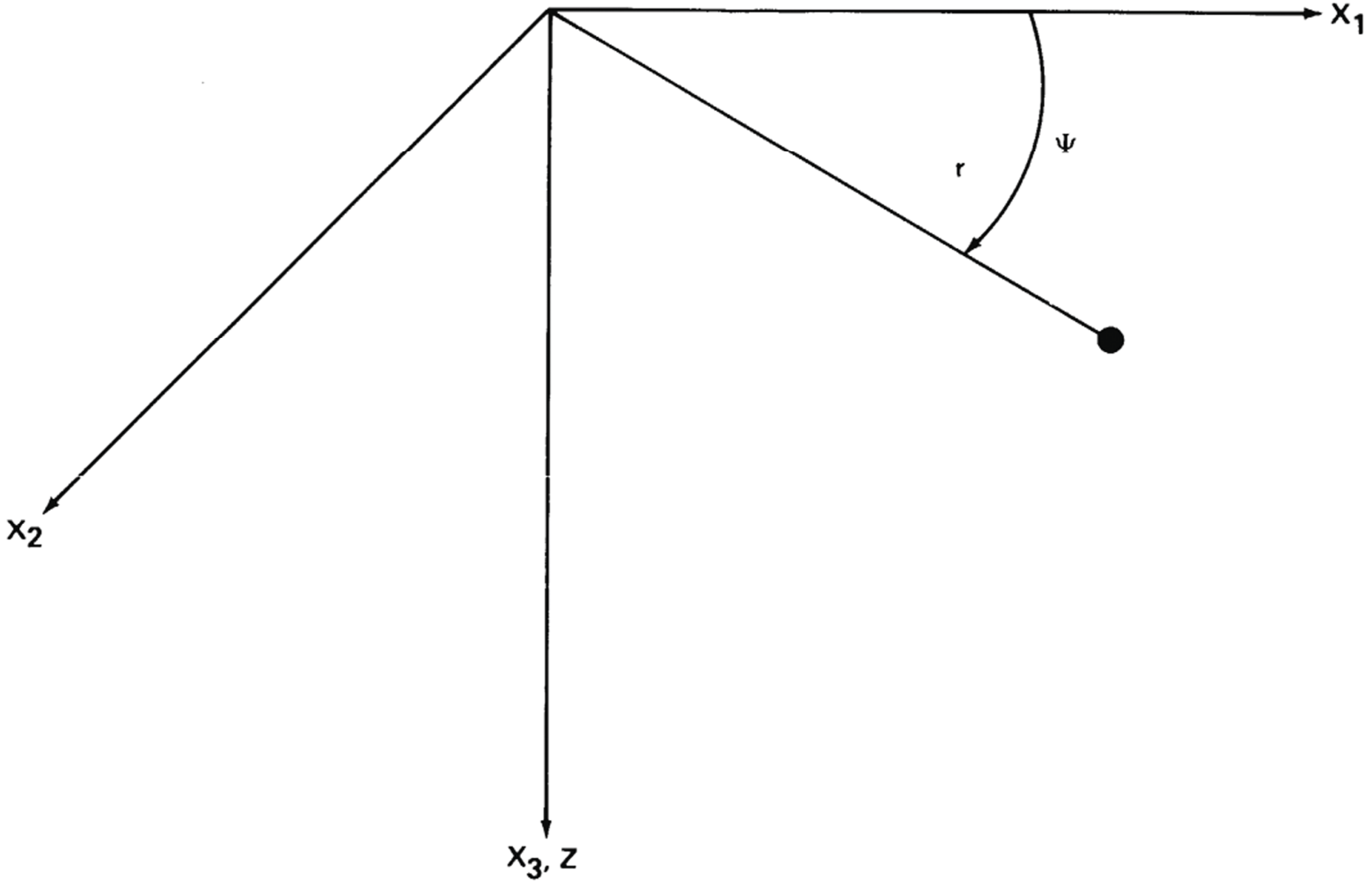

REV 14 10/07

SOUTHERN COMPANY
Energy to Serve Your World®

VOGTLE
ELECTRIC GENERATING PLANT
UNIT 1 AND UNIT 2

POLAR COORDINATE SYSTEM

FIGURE 3E–2

APPENDIX 3F

HAZARDS ANALYSIS

3F.1 INTRODUCTION

The VEGP power block has been designed to provide protection for safety-related equipment from hazards and events which could reasonably be expected to occur. This protection is provided to ensure that recovery from the event is possible, to ensure the integrity of the reactor coolant pressure boundary, to minimize the release of radioactivity, and to enable the plant to be placed in a safe condition.

This appendix provides the results of integrated hazards analyses for selected areas of the plant to demonstrate the type of analyses conducted for each safety-related area of the plant to ensure that the VEGP units can withstand the postulated events. A sample of the results of the analysis of level C and safety-related pump rooms on levels B and D of the auxiliary building as shown in table 3F-1 provides this example. Analyses are also provided for the pressure/temperature effects of a pipe rupture in the Unit 1 control building main steam line and main feedwater line isolation valve compartment, the flooding effects of pipe ruptures in the Unit 1 auxiliary and control building main steam line and main feedwater line isolation valve compartments, the effects of pipe ruptures in the Unit 1 auxiliary feedwater pump rooms, and the effects of a circulating water pipe rupture.

The items considered in the evaluation of each plant area include tornadoes, floods, missiles, pipe breaks, fires, and seismic events. (Refer to sections 3.3 through 3.7 and subsection 9.5.1.) Even though each area of the plant and each system are designed individually to properly consider the above events, an integrated analysis of rooms, systems, and events is performed to ensure that the above objectives are realized for each postulated event.

The hazards analyses are conducted on a room-by-room basis. All components within the room are reviewed for the effects of earthquake-induced failures, effects of high- and moderate-energy piping breaks (flooding, sprays, and jet impingement), and the effects of missiles.

The effects of the high-energy pipe breaks on equipment are reported in paragraph 3.6.2.5. Fire protection and the effects of fires in the various fire areas are discussed in subsection 9.5.1.

3F.2 ANALYSIS ASSUMPTIONS

In the analysis of an event or hazard, it is assumed that the plant is being operated in accordance with the requirements of the Technical Specifications. Should the event result in a turbine or reactor trip, the plant will be placed in a hot shutdown condition. If required by a limiting condition of operation or if recovery from the event will cause the plant to be shut down for an extended period of time, the plant will be taken to a cold shutdown condition. (Safe shutdown is discussed in section 7.4.)

During the hot shutdown condition, an adequate heat sink is provided to remove reactor core residual heat. Boration capability is provided to compensate for xenon decay and to maintain the required core shutdown margin. Boration is a long-term need because it is not required until approximately 25 h after shutdown.

Redundancy or diversity of systems and components is provided to enable continued operation at hot shutdown or to cool the reactor to a cold shutdown condition. If time is available, it is assumed that temporary repairs can be made to circumvent damages resulting from the hazard. Loss of offsite power (LOSP) is not assumed, unless a trip of the turbine-generator system or

the reactor protection system is a direct consequence of the hazard. All available systems, including nonsafety-related systems and those systems requiring operator action, may be employed to mitigate the consequences of the hazards.

In determining the availability of the systems required to mitigate the consequences of a hazard and those required to place the reactor in a safe condition, the direct consequences of the hazard are considered. The feasibility of carrying out operator actions is based on ample time and adequate access to the controls, motor control center, switchgear, etc., associated with the component required to accomplish the proposed action.

When the postulated hazard occurs in one of two or more redundant trains of a dual-purpose moderate-energy system, single failures of components in other trains (and associated supporting trains) are not assumed.

3F.2.1 EARTHQUAKE ANALYSIS ASSUMPTIONS

When evaluating the effects of any earthquake, no other major hazard or event is assumed, and no Seismic Category 1 equipment is assumed to fail as a result of the earthquake. Non-Seismic Category 1 equipment would not be available following the seismic event. Certain non-Seismic Category 1 components are designed and constructed to ensure that their failure could not reduce the functioning of a safe shutdown component to an unacceptable safety level. This criterion meets the intent of Regulatory Guide 1.29, Position C.2. Evaluation of component failure includes drop impact forces and secondary effects, such as spray and flooding from piping failures.

LOSP is assumed following a safe shutdown earthquake (SSE). An earthquake, as a single event, will affect the entire plant; hence, all the rooms dedicated to items associated with either safety-related train are considered in total.

3F.2.2 PIPE BREAK ANALYSIS ASSUMPTIONS

All high- and moderate-energy lines whose failure could reduce the functioning of a safe shutdown component to an unacceptable safety level are evaluated for pipe breaks or cracks. Thrust forces, jet impingement forces, and environmental effects are considered. Section 3.6 provides a description of the location and types of breaks and the forcing functions that are considered for analyzing pipe breaks.

Evaluation of environmental effects of moderate-energy pipe cracks has been made based on the characteristics of the flow from the postulated cracks. The locations of the cracks are discussed in paragraph 3.6.2.1. The evaluations include the effects of spraying or wetting on the safe shutdown equipment to assure that electrical safe shutdown equipment is not affected. The evaluation also includes the effect of flooding from the worst-case pipe crack in each room or general area. Flooding volumes are based on assuming automatic isolation or operator termination of flow to the pipe failure within a reasonable period after indication of the hazard. An interval of 30 min for operator's action after indication of flood is assumed.

3F.2.3 MISSILES ANALYSIS ASSUMPTIONS

There are two general sources of postulated internally generated missiles outside the containment, rotating component failure and pressurized component failure.

Section 3.5 provides a description of the design bases for the selection of missiles. Tables 3.5.1-1, 3.5.1-2, and 3.5.1-3 provide a listing of major missiles generated within the plant.

Analysis of impact from missiles is done for all rotating equipment and high-energy pressurized components.

3F.2.4 FLOODING ANALYSIS ASSUMPTIONS

In the event of a pipe failure, significant flooding might result and jeopardize the function of safety-related equipment required to mitigate the consequences of the pipe break or to maintain the plant in a safe shutdown condition.

Flooding rates are based on the worst-case pipe failure in each safety-related room or area. Through-wall cracks are postulated on moderate energy lines, seismic or non-seismic piping, to substantiate the effects due to spray and flooding on components which are required to mitigate the consequences of the event and/or safely shut down the plant; i.e., essential equipment. On high energy lines, terminal and intermediate breaks are postulated based on the lines' stress analyses. Full ruptures are assumed on all postulated breaks and are analyzed in part to determine flooding effects on essential equipment for the area in which the break is postulated.

The failure mode of non-Seismic Category 1 piping will be a critical crack rather than double-ended rupture, non-Seismic Category 1 piping in areas of safety-related structures where Seismic Category 2 over 1 interactions or flooding from a double-ended rupture could result in unacceptable interactions has been supported to withstand safe shutdown earthquake loads. The pipe support loads are determined by analyzing the piping system. For SSE loading, with the exception of the piping listed below, pipe stresses are also calculated to demonstrate they are maintained within faulted allowables:

- Duriron lines.
- Copper lines.
- ASTM A-120 galvanized lines.
- Air service lines.
- Process tubing $\leq$ 3/8 in.
- Instrument tubing.
- Moderate energy, non-Seismic Category 1 piping 2 in. and smaller in Unit 2 only.

For each area the worst flooding source is identified and analyzed for spray and/or flooding effects. The flooding rate is calculated based on the flooding sources reservoir capacity, piping dimensions, and fluid parameters. The level of the flood water is based on automatic isolation or operator action after a reasonable delay time following indication of flow from the breaks or crack. The delay time of 30 min for operator's action after indication of flood is assumed. If detection is not available, the full volume of the reservoir is assumed to flood the affected area. The maximum flood level is determined by distributing the flood volume over a surface area determined by room size and the size and geometry of large components within the room. Flow paths out of the room; i.e., open doors, grating, stairs, or large openings, are also considered.

The contents of the flooded area are then reviewed to ensure that no essential equipment is adversely affected. Additionally, flooding communication to adjacent rooms is evaluated to ensure that the event does not result in failure of essential components in adjacent rooms.

The analysis for flooding caused by failure of non-Seismic Category 1 tanks inside Category 1 buildings assumes each tank to completely rupture and empty into adjacent areas. The effects of open doors, stairs, and large openings are considered in the analysis. The tank's contents are then divided by the established boundaries' surface area to determine a flood level. The

contents of the flooded area are then reviewed to ensure that no essential equipment is adversely affected. The analysis considers the effects of the worst single active failure taken concurrent with the break. The effects of flooding from non-Seismic Category 1 tanks in the outside areas are discussed in paragraph 3.4.1.1.2.

Potential flooding due to probable maximum flood and probable maximum precipitation is discussed in section 3.4.

The equipment and floor drainage system is discussed in subsection 9.3.3. All water, released because of pipe breaks in the auxiliary building, drains to the common sump. Refer to paragraph 9.3.3.2.2.3 for a discussion of this design.

3F.3 PROTECTION MECHANISMS

The plant layout arrangement is based on maximizing the physical separation of redundant or diverse safety-related components and systems from each other and from nonsafety- related items. Therefore, if an accident occurs within the plant, there is minimal effect on other systems or components which are required for safe shutdown of the plant or to mitigate the consequence of the hazard.

Since it is not always feasible to provide separation in every hazard situation, other protection features are employed. These protection features include the following:

- Structural enclosures.
- Structural barriers.
- Restraints.
- Seismically designed components.
- Hardening.
- Orientation.

3F.4 HAZARDS EVALUATIONS

As stated previously, table 3F-1 provides a hazards evaluation of level C and safety-related pump rooms on levels B and D of the auxiliary building. Each room on those elevations is shown in drawings AX1D08A03-3, AX1D08A03-4, AX1D08A31, AX1D08A02-3, AX1D08A02-2 and AX1D08A04-4 and has been reviewed to ensure that the integrated design of the plant acceptably addresses all postulated hazards. Since the evaluations for equipment and components in all safety-related areas are documented in the project files and are available for audit, they are not provided in the FSAR.

Specific evaluations of certain areas of the plant have been of licensing concern in the past. These evaluations are provided in the following subsections.

3F.4.1 AUXILIARY FEEDWATER (AFW) PUMP ROOMS

The effects of a pipe break in the AFW pump rooms have been evaluated and the results of the Unit 1 analysis are presented in this appendix. The Unit 2 analysis is similar. The effects include room pressurization, temperature, flooding, and operability of the AFW system.

There are three separate AFW pump rooms, each housing one pump. Drawing 1X6DD300 provides plan and elevation views and nodal boundary of this area. Each of two motor-driven pumps is sized to deliver the feedwater flow required for decay heat removal. The single

turbine-driven pump supplies twice the capacity of a motor-driven pump and is sufficient to remove decay heat and, additionally, to cool down the reactor at a rate of up to 100°F/h not to exceed 100°F in any 1 hour period. The turbine-driven pump provides system diversity to both motor-driven pumps.

The results of the pressure/temperature analysis for the Unit 1 turbine-driven AFW pump room, as shown in table 3F-2, indicate that the maximum differential pressure on the walls will be less than 1.0 psi. The walls are capable of withstanding this pressure.

Analysis of AFW piping failures shows that loss of a redundant train does not prevent decay heat removal. The capability to provide adequate feedwater flow to remove decay heat is ensured by operation of either one of two motor-driven pumps or by operation of the turbine-driven pump.

Pressure-temperature response analysis for design basis main steam and main feedwater pipe breaks in the main steam tunnel has been performed. Design basis pipe breaks and locations are selected to identify maximum tunnel pressures to be accommodated by the AFW structure adjacent to the main steam tunnel.

The maximum flooding occurs within the AFW pumphouse when considering a single failure of a check valve that results in backflow from the turbine-driven AFW pump. In this scenario, flooding will propagate to the adjacent motor-driven pump room. However, no failure of the turbine-driven pump is postulated, and the system is capable of providing the required flow. For all other cases, flooding is contained such that it will not propagate to the other pumps.

Analysis of the other hazards shows that adequate redundancy and separation are provided to ensure the operability of at least one train of the AFW system.

3F.4.2 MAIN STEAM ISOLATION VALVE (MSIV) AND MAIN FEEDWATER ISOLATION VALVE (MFIV) COMPARTMENT

The MSIV/MFIV compartment is located in the wing areas of the auxiliary building and the control building. Drawings 1X6DD301, 1X6DD302, AX6DD300, AX6DD301, and AX6DD302 provide plan and elevation views of this area. The main steam and main feedwater piping in this area consists of straight piping runs extending from the containment penetrations to torsional restraints mounted in the auxiliary building and control building walls through which these lines enter the main steam tunnel. The MSIVs, main steam safety valves, atmospheric relief valves, and MFIVs are in this compartment. Also in the compartment are branch piping lines of the AFW system, chemical addition system, steam supply to the turbine-driven AFW pump, bypass loops of the MSIVs, pressure instrumentation, and drains.

3F.4.2.1 Break Size and Location

Main steam and feedwater piping in this compartment is designed to the criteria stated in paragraph 3.6.2.1 for those portions of the piping passing through the primary containment and extending to the first pipe whip restraint past the first outside isolation valve. In accordance with these criteria, no specific pipe breaks are postulated in the main run of these lines in the MSIV/MFIV compartment. However, to provide an additional level of assurance of operability of safety-related equipment in this compartment, the building structure and safety-related equipment are designed for the environmental conditions (pressure, temperature, and flooding) that would result from a break, equal in area to one cross-sectional pipe area, of either a main steam line or main feedwater line without steam generator tube bundle being uncovered. Main steam line breaks up to 1.0 ft^2 with steam generator tube bundle being uncovered have been considered for equipment qualification as discussed in paragraph 3.11.B.1.1.

Pressurization of the MSIV/MFIV compartment due to such a rupture is limited by providing adequate venting of the compartment and designing the compartment to withstand the maximum resultant pressure. Venting is accomplished by including adequate passageways between compartments or by other acceptable venting schemes. Engineered safety features required to bring the reactor to safe shutdown, which are located within these compartments, are designed to withstand the associated temperature, pressure, and humidity conditions.

The following cases are analyzed to determine the worst environmental conditions for the MSIV/MFIV compartment:

A. Case 1: Saturated steam blowdown from a main steam line break (MSLB) equivalent to the flow area of a single area rupture inside the restraint wall and a double area rupture outside the restraint wall. This case results in the maximum compartment pressure.
B. Case 2: Blowdown from a main feedwater line break equivalent to the flow area of a single area rupture. This case results in the maximum compartment flood level.
C. Case 3: Blowdown from MSLBs up to 1.0 ft^2 equivalent flow area with steam generator tube bundle being uncovered producing superheated blowdown. This case results in the maximum compartment temperatures and is discussed in paragraph 3.11.B.1.1.

3F.4.2.2 Method of Analysis

The case 1 analysis was performed using the Bechtel COPDA computer code, which is described in reference 1. The case 2 analysis was performed using the fluid flow equations identified in reference 2 for cold water flow. The case 3 analysis was performed using the GOTHIC computer code which is described in reference 4.

The MSIV area MSLB environmental conditions and the resulting impact on equipment qualification were evaluated using both the COPDA and GOTHIC computer codes. COPDA modeled the control and auxiliary sides of the MSIV/MFIV vault areas. Because reference 3 indicates the transient temperature for the auxiliary building MSIV/MFIV vault area is extremely similar to the transient for the same break in the control building, the detailed GOTHIC model was performed only on the control building MSIV/MFIV vault area. This area has compartments with smaller volumes and less flow area out of the break compartment than the auxiliary building MSIV/MFIV vault area (reference 3).

3F.4.2.3 Mass and Energy Release for Main Steam Line Break

For cases 1 and 2, blowdown mass and energy releases were calculated for a single area rupture inside the restraint wall and a double area rupture outside the restraint wall for both the auxiliary and control building MSIV/MFIV areas. The blowdown data for the double area rupture outside the restraint wall of the auxiliary building MSIV/MFIV area (Node 10) are presented in table 3F-3A.

For case 3, a spectrum of blowdown mass and energy releases was calculated for a spectrum of break sizes and power levels. The blowdown data for a 1.0 ft^2 single area rupture at 102% power (102% of 3579 MWt) inside the restraint wall in the control building MSIV/MFIV area are presented in table 3F-3B.

3F.4.2.4 Compartment Volumes and Vent Areas

For the Unit 1 analyses of the pressure temperature-transient following a MSLB (cases 1 and 3), the flow model of control volumes and intercompartment flow paths are illustrated in figures 3F-1 and 3F-2 and listed in tables 3F-3A and 3F-3B. The calculated Unit 1 flooding results from the case 2 analysis are shown in table 3F-3A. The calculated Unit 1 compartment pressure (case 1) and temperature (case 3) responses are listed in table 3F-3A and table 3F-3B. The Unit 2 analysis is similar.

3F.4.2.5 Initial Conditions

Tables 3F-3A and 3F-3B provide the Unit 1 initial conditions for case 1, case 2, and case 3 analyses.

3F.4.2.6 Design Provisions

The Plot of the time-history of the Unit 1 maximum break node compartment composite temperature for case 3 is given in figure 3F-3. The calculated Unit 1 flooding results from the case 2 analysis are shown in table 3F-3A.

Table 3F-3A provides the peak transient values of the Unit 1 compartment pressure analyses. Table 3F-3B provides the peak transient values of the Unit 1 compartment temperature analyses. The MSIV/MFIV compartment is designed to withstand these conditions. Essential safety-related equipment is qualified to these environmental conditions as discussed in section 3.11.

3F.4.3 EVALUATION OF REACTOR COOLANT SYSTEM (RCS) LOOP BRANCH LINE BREAKS

The evaluation of effects on safety-related equipment resulting from branch line breaks in the RCS is presented in table 3F-4. The evaluation shows that breaks in the RCS will not compromise the capability to safely shut down the plant.

3F.4.4 TURBINE BUILDING FLOODING EVALUATION

The flooding effects of a pipe break in the turbine building have been evaluated. Although the turbine building does not contain any essential safety-related equipment (however, see paragraph 7.2.1.1.2.F for trip instrumentation in the turbine building), it is connected to other safety-related structures by piping and electrical tunnels. However, it has been shown that the propagation of flood waters into the safety-related structures is precluded by design.

The design basis pipe failure in the turbine building is postulated to be a full circumferential break in the 96-in. circulating water piping to the condensers. A complete rupture of the condenser riser expansion joints has not been postulated as such joints have not been implemented in the VEGP design. The circulating water system design pressure is 80 psig, with a normal anticipated operating pressure of 45 psig. The maximum transient analysis pressure (unscheduled shutdown) is 54 psig. The flowrate through the break is conservatively estimated to be 612,000 gal/min, which is the combined runout flow of two circulating water pumps. This flowrate will cause the water level in the turbine building to rise at a rate of 0.72 ft/min.

If it is assumed that the turbine building flood detectors and the circulating water basin level detectors fail, the flooding could continue until the basin is empty. As the water level rises in one unit, the concrete block wall between units will fail due to high static water pressure, allowing the water to spread into both halves of the building. Calculations have shown that the

block wall will not withstand more than 8 ft of water and will fail before the water level reaches the operating deck at el 220 ft 0 in. If the entire circulating water system volume of 1.2×10^6 ft^3 is pumped into the turbine building, the resulting flood level in both units would be 211 ft.

Should flood water enter the main steam tunnels at the east or west end of the turbine building, it is precluded from entering the control and auxiliary buildings by sealed penetrations in the walls of the safety-related structures. The piping and electrical tunnels along the south wall at the centerline of the turbine building extend above grade level. Penetrations into the tunnels below grade are sealed.

A failure of the condensate feedwater system piping would result in significantly less flooding than a circulating water system failure. Even if the entire condensate/feedwater inventory flooded into the turbine building, the final flood level would be less than 1 ft above the level A floor.

3F.5 REFERENCES

1. Braddy, R.W. and Thiesing, J.W., Subcompartment Pressure and Temperature Transient Analysis, BN-TOP-4, Revision 0, Bechtel Corporation, San Francisco, California, July 1976.
2. Design for Pipe Break Effects, BN-TOP-2, Revision 2, Bechtel Corporation, San Francisco, California, June 1974.
3. Spryshak, J. J. and Iyengar, J., "Vogtle Electric Generating Plant Units 1 and 2. Main Steam Isolation Valve Area Equipment Thermal Response to Superheated Steam Releases," WCAP-13169, December 1991.
4. NAI 8907-02, Revision 8, “GOTHIC Containment Analysis Package User Manual.”

TABLE 3F-1 (SHEET 1 OF 84)

SAMPLE OF HAZARDS ANALYSIS RESULTS FOR AUXILIARY BUILDING (LEVELS B, C, AND D)

Room Number R-B15 Title Safety Injection Pump Room Train A

Flooding Analysis

_X_ Flooding from sources within the room, coincident with the most limiting single active failure (assumed in accordance with paragraphs 3.6.1.1.F and 3.6.1.1.G) will not preclude mitigation of the event or safe shutdown of the plant.

_X_ Flooding from sources external to the room is not credible even with a single active failure.

___ Other, see remarks.

Seismic Design Analysis

___ Only safety-related equipment (SRE) is in the room; therefore, there are no seismically induced failures (Category 2/1 interactions).

_X_ The nonsafety-related equipment (NSRE) in the room is seismically restrained (upgraded to Category 1 requirements); therefore, no seismically induced failures of these restraints are postulated.

___ The NSRE, which is postulated to fail as a result of an SSE, does not impact SRE.

___ Other, see remarks.

Missile Analysis

_X_ No credible missile sources exist in the room.

___ Missiles from rotating components generated within the room contain insufficient energy to escape their equipment housing(s).

___ Other, see remarks.

Pipe Break Analysis

___ There are no high-energy lines in the room.

___ The high-energy line breaks have been evaluated and do not adversely affect SRE.

_X_ Other, see remarks.

Remarks

1. The high-energy line breaks have been evaluated and will not preclude mitigation of the event or safe shutdown of the plant.

TABLE 3F-1 (SHEET 2 OF 84)

Listing of safety-related items in room R-B15

Item Number	Description	Equipment Designation	Essential Equipment	Seismic Category 1
1.	Safety injection pump suction header isolation valve	HV-8807 A		Y
2.	Safety injection pump train A miniflow valve	HV-8814		Y
3.	SIP A to RCS Cold Leg Isolation valve	HV-8821 A		Y
4.	Safety injection pump P6003 inlet valve	HV-8923 A		Y
5.	Safety injection pump room leak detection switch	LSH-9812		Y
6.	Safety injection pump room leak detection switch	LSH-9816		Y
7.	Charging pump header valve	HV-8924	Y	Y
8.	Cable tray	Train A	Y	Y
9.	Safety injection pump	1-1204-P6-003		Y
10	Air-handling units	1-1555-A7-015-000		Y
11.	Piping	1-1204-003-1 1/2 in.	Y	Y
		1-1204-008-6 in.	Y	Y
		1-1202-117-3 in.	Y	Y
		1-1208-411-6 in.	Y	Y
		1-1204-011-6 in.	Y	Y
		1-1202-118-2 in.	Y	Y
		1-1202-116-2 in.	Y	Y
		1-1204-028-4 in.		
		1-1204-014-4 in.		
		1-1202-115-3 in.		
		1-1202-113-2 in.		
		1-1202-115-1 in.	Y	Y
		1-1202-117-1 in.	Y	Y
		1-1202-281-3/4 in.	Y	Y
		1-1202-297-1 in.	Y	Y
		1-1202-298-3/4 in.	Y	Y
		1-1202-372-2 in.	Y	Y
		1-1202-373-2 in.	Y	Y
		1-1202-475-2 in.	Y	Y
		1-1202-476-2 in.	Y	Y
		1-1204-008-3/4 in.	Y	Y
		1-1204-015-4 in.	Y	Y
		1-1204-028-3/4 in.	Y	Y
		1-1204-052-2 in.	Y	Y
		1-1204-128-3/4 in.	Y	Y
		1-1204-129-3/4 in.	Y	Y
		1-1204-130-3/4 in.	Y	Y
		1-1204-131-3/4 in.	Y	Y
		1-1204-280-1/2 in.	Y	Y
		1-1555-066-1 1/2 in.	Y	Y
		1-1609-031-3/4 in.	Y	Y

TABLE 3F-1 (SHEET 3 OF 84)

Listing of safety-related items in room R-B15

Item Number	Description	Equipment Designation	Essential Equipment	Seismic Category 1
12.	Safety injection pump discharge, flow transmitter	FT-0918		Y
13.	Safety injection pump outlet, relief valve	PSV-8853A		Y
14.	Safety injection pump inlet, relief valve	PSV-8858		Y
15.	Safety injection pump room cooler, high temperature switch	TISH-12210		Y
16.	Train A raceway	Conduit and cabletrays	Y	Y

TABLE 3F-1 (SHEET 4 OF 84)

Room Number R-B18 Title Valve Gallery

Flooding Analysis

___ Flooding from sources within the room coincident with the most limiting single active failure (assumed in accordance with paragraphs 3.6.1.1.F and 3.6.1.1.G), will not preclude mitigation of the event or safe shutdown of the plant.
___ Flooding from sources external to the room is not credible even with a single active failure.
_X_ Other, see remarks.

Seismic Design Analysis

___ Only SRE is in the room; therefore, there are no seismically induced failures (Category 2/1 interactions).
_X_ The NSRE in the room is seismically restrained (upgraded to Category 1 requirements); therefore, no seismically induced failures of these restraints are postulated.
___ The NSRE, which is postulated to fail as a result of an SSE, does not impact SRE.
___ Other, see remarks.

Missile Analysis

_X_ No credible missile sources exist in the room.
___ Missiles from rotating components generated within the room contain insufficient energy to escape their equipment housing(s).
___ Other, see remarks.

Pipe Break Analysis

___ There are no high-energy lines in the room.
_X_ The high-energy line breaks have been evaluated and do not adversely affect SRE.
___ Other, see remarks.

Remarks

1. Flooding from sources located in this room will not impair the safe shutdown capability of the SRE.

TABLE 3F-1 (SHEET 5 OF 84)

Listing of safety-related items in room R-B18

Item Number	Description	Equipment Designation	Essential Equipment	Seismic Category 1
1.	Piping	1-1202-162-3 in.	Y	Y
		1-1204-010-6 in.	Y	Y
		1-1204-004-3/4 in.	Y	Y
		1-1204-008-8 in.	Y	Y

TABLE 3F-1 (SHEET 6 OF 84)

Room Number R-B19 Title Safety Injection Pump Room Train B

Flooding Analysis

_X_ Flooding from sources within the room, coincident with the most limiting single active failure (assumed in accordance with paragraphs 3.6.1.1.F and 3.6.1.1.G), will not preclude mitigation of the event or safe shutdown of the plant.

_X_ Flooding from sources external to the room is not credible even with a single active failure.

___ Other, see remarks.

Seismic Design Analysis

___ Only SRE is in the room; therefore, there are no seismically induced failures (Category 2/1 interactions).

_X_ The NSRE in the room is seismically restrained (upgraded to Category 1 requirements); therefore, no seismically induced failures of these restraints are postulated.

___ The NSRE, which is postulated to fail as a result of an SSE, does not impact SRE.

___ Other, see remarks.

Missile Analysis

_X_ No credible missile sources exist in the room.

___ Missiles from rotating components generated within the room contain insufficient energy to escape their equipment housing(s).

___ Other, see remarks.

Pipe Break Analysis

___ There are no high-energy lines in the room.

___ The high-energy line breaks have been evaluated and do not adversely affect SRE.

___ Other, see remarks.

Remarks

1. The high-energy line breaks have been evaluated and will not preclude mitigation of the event or safe shutdown of the plant.

TABLE 3F-1 (SHEET 7 OF 84)

Listing of safety-related items in room R-B19

Item Number	Description	Equipment Designation	Essential Equipment	Seismic Category 1
1.	Safety injection pump suction header valve	HV-8807B		Y
2.	Safety injection pump miniflow isolation train B valve	HV-8813		Y
3.	SIP B to RCS Cold Leg Isolation valve	HV-8821B		Y
4.	Safety injection pump inlet and miniflow isolation valve	HV-8920		Y
5.	Safety injection pump P6004 inlet valve	HV-8923B		Y
6.	Safety injection pump room leak detection switch	LSH-9813		Y
7.	Safety injection pump room leak detection switch	LSH-9817		Y
8.	Cooler motor control switch	TISH 12216		Y
9.	Train B raceway	Conduits and cabletrays	Y	Y
10.	Safety injection pump	1-1204-P6-004		Y
11.	Air-handling unit	1-1555-A7-016-000		Y
12.	Piping	1-1204-004-3 in.	Y	Y
		1-1202-381-2 in.	Y	Y
		1-1202-160-3 in.	Y	Y
		1-1202-162-3 in.	Y	Y
		1-1202-163-2 in.	Y	Y
		1-1204-004-1 1/2 in.	Y	Y
		1-1204-010-6 in.	Y	Y
		1-1204-012-8 in.	Y	Y
		1-1204-015-4 in.	Y	Y
		1-1202-161-2 in.	Y	Y
		1-1592-059-1 1/2 in.	Y	Y
		1-1592-050-1 1/2 in.	Y	Y
		1-1202-160-1 in.	Y	Y
		1-1202-289-3/4 in.	Y	Y
		1-1202-313-1 in.	Y	Y
		1-1202-380-2 in.	Y	Y
		1-1202-481-2 in.	Y	Y
		1-1204-002-3 in.	Y	Y
		1-1204-004-3/4 in.	Y	Y
		1-1204-004-1 1/2 in.	Y	Y
		1-1204-011-6 in.	Y	Y
		1-1204-015-3/4 in.	Y	Y
		1-1204-037-4 in.	Y	Y
		1-1204-280-1/2 in.	Y	Y
		1-1204-281-1/2 in.	Y	Y
		1-1204-314-3/4 in.	Y	Y
		1-1555-074-1 1/2 in.	Y	Y
		1-1609-030-3/4 in.	Y	Y

TABLE 3F-1 (SHEET 8 OF 84)

Listing of safety-related items in room R-B19

Item Number	Description	Equipment Designation	Essential Equipment	Seismic Category 1
13.	Safety injection pump discharge, flow transmitter	FT-0922		Y
14.	Safety injection pump inlet, relief valve	PSV-8853B		Y
15.	Safety injection pump room cooler, high temperature switch.	TISH-12211		Y

TABLE 3F-1 (SHEET 9 OF 84)

(Recycle Evaporator Abandoned in Place)

TABLE 3F-1 (SHEET 10 OF 84)

Listing of safety-related items in room R-C64, C65

Item Number	Description	Equipment Designation	Essential Equipment	Seismic Category 1
1.	Piping	1-1228-174-in.	Y	Y

TABLE 3F-1 (SHEET 11 OF 84)

(Waste Evaporator Abandoned in Place)

TABLE 3F-1 (SHEET 12 OF 84)

Listing of safety-related items in room R-C66, C67

Item Number	Description	Equipment Designation	Essential Equipment	Seismic Category 1
1.	Piping	1-1228-168-2 in.	Y	Y

TABLE 3F-1 (SHEET 13 OF 84)

Room Number R-C77 Title Boron Recycle Holdup Tank Room

Flooding Analysis

___ Flooding from sources within the room, coincident with the most limiting single active failure (assumed in accordance with paragraphs 3.6.1.1.F and 3.6.1.1.G), will not preclude mitigation of the event or safe shutdown of the plant.
___ Flooding from sources external to the room is not credible even with a single active failure.
_X_ Other, see remarks.

Seismic Design Analysis

___ Only SRE is in the room; therefore, there are no seismically induced failures (Category 2/1 interactions).
_X_ The NSRE in the room is seismically restrained (upgraded to Category 1 requirements); therefore, no seismically induced failures of these restraints are postulated.
___ The NSRE, which is postulated to fail as a result of an SSE, does not impact SRE.
___ Other, see remarks.

Missile Analysis

_X_ No credible missile sources exist in the room.
___ Missiles from rotating components generated within the room contain insufficient energy to escape their equipment housing(s).
___ Other, see remarks.

Pipe Break Analysis

_X_ There are no high-energy lines in the room.
___ The high-energy line breaks have been evaluated and do not adversely affect SRE.
___ Other, see remarks.

Remarks

1. Flooding from sources located in this room will not impair the safe shutdown capability of the SRE.

TABLE 3F-1 (SHEET 14 OF 84)

Listing of safety-related items in room R-C77

Item Number	Description	Equipment Designation	Essential Equipment	Seismic Category 1
1.	Boron recycle holdup tank	A-1210-T4-001		Y
2.	Piping	1-1208-151-3/4 in.	Y	Y
		1-1208-437-3/4 in.	Y	Y
		1-1208-493-3/4 in.	Y	Y
		A-1561-102-10 in.	Y	Y
		1-1561-165-10 in.	Y	Y
			Y	Y

TABLE 3F-1 (SHEET 15 OF 84)

Room Number R-C83 Title Corridor

Flooding Analysis

___ Flooding from sources within the room, coincident with the most limiting single active failure (assumed in accordance with paragraphs 3.6.1.1.F and 3.6.1.1.G), will preclude mitigation of the event or safe shutdown of the plant.
___ Flooding from sources external to the room is not credible even with a single active failure.
_X_ Other, see remark 1.

Seismic Design Analysis

___ Only SRE is in the room; therefore, there are no seismically induced failures (Category 2/1 interactions).
_X_ The NSRE in the room is seismically restrained (upgraded to Category 1 requirements); therefore, no seismically induced failures of these restraints are postulated.
___ The NSRE, which is postulated to fail as a result of an SSE, does not impact SRE.
___ Other, see remarks.

Missile Analysis

_X_ No credible missile sources exist in the room.
___ Missiles from rotating components generated within the room contain insufficient energy to escape their equipment housing(s).
___ Other, see remarks.

Pipe Break Analysis

_X_ There are no high-energy lines in the room.
___ The high-energy line breaks have been evaluated and do not adversely affect SRE.
___ Other, see remarks.

Remarks

1. The SRE located in this room is not required for safe shutdown.

TABLE 3F-1 (SHEET 16 OF 84)

Listing of safety-related
items in room R-C83

Item Number	Description	Equipment Designation	Essential Equipment	Seismic Category 1
1.	Recycle holdup tank/heating, ventilation, and air-conditioning (HVAC) vent valve	HV-12596	N	Y
2.	Recycle holdup tank/HVAC vent valve	HV-12597	N	Y
3.	Train A raceway	Conduits and cabletrays	N	Y
4.	Train B raceway	Conduits and cabletrays	N	Y
5.	Piping	1-1208-017-2 in.	Y	Y
		2-1208-017-2 in.	Y	Y
		1-1208-020-2 in.	Y	Y
		1-1208-090-3 in.	Y	Y
		1-1208-093-3 in.	Y	Y
		1-1208-095-3 in.	Y	Y
		1-1208-340-3/8 in.	Y	Y
		1-1208-410-3 in.	Y	Y
		1-1208-437-3/8 in.	Y	Y
		1-1208-493-3/4 in.	Y	Y
		1-1213-026-3 in.	Y	Y
		1-1224-005-1 1/2 in.	Y	Y
		1-1224-006-4 in.	Y	Y
		1-1224-008-3 in.	Y	Y
		1-1224-011-2 in.	Y	Y
		1-1224-013-2 in.	Y	Y
		1-1224-014-2 in.	Y	Y
		1-1224-015-2 in.	Y	Y
		1-1224-016-2 in.	Y	Y
		1-1224-026-3 in.	Y	Y
		1-1224-027-3 in.	Y	Y
		1-1224-028-3 in.	Y	Y
		1-1224-066-3 in.	Y	Y
		1-1407-021-2 in.	Y	Y

TABLE 3F-1 (SHEET 17 OF 84)

Room Number R-C88 Title Electrical Chase Train A

Flooding Analysis

___ Flooding from sources within the room, coincident with the most limiting single active failure (assumed in accordance with paragraphs 3.6.1.1.F and 3.6.1.1.G), will not preclude mitigation of the event or safe shutdown of the plant.
___ Flooding from sources external to the room is not credible even with a single active failure.
_X_ Other, see remarks.

Seismic Design Analysis

___ Only SRE is in the room; therefore, there are no seismically induced failures (Category 2/1 interactions).
_X_ The NSRE in the room is seismically restrained (upgraded to Category 1 requirements); therefore, no seismically induced failures of these restraints are postulated.
___ The NSRE, which is postulated to fail as a result of an SSE, does not impact SRE.
___ Other, see remarks.

Missile Analysis

_X_ No credible missile sources exist in the room.
___ Missiles from rotating components generated within the room contain insufficient energy to escape their equipment housing(s).
___ Other, see remarks.

Pipe Break Analysis

_X_ There are no high-energy lines in the room.
___ The high-energy line breaks have been evaluated and do not adversely affect SRE.
___ Other, see remarks.

Remarks

1. The safe shutdown capability of the SRE located in this room is not impaired by this flood level.

TABLE 3F-1 (SHEET 18 OF 84)

Listing of safety-related
items in room R-C88

Item Number	Description	Equipment Designation	Essential Equipment	Seismic Category 1
1.	Train C Raceway	Conduits and cabletrays	Y	Y
2.	Piping	1-1202-104-8 in.	Y	Y
		1-1202-134-8 in.	Y	Y

TABLE 3F-1 (SHEET 19 OF 84)

Room Number R-C89 Title Storage Room

Flooding Analysis

___ Flooding from sources within the room, coincident with the most limiting single active failure (assumed in accordance with paragraphs 3.6.1.1.F and 3.6.1.1.G), will not preclude mitigation of the event or safe shutdown of the plant.
___ Flooding from sources external to the room is not credible even with a single active failure.
_X_ Other, see remarks.

Seismic Design Analysis

___ Only SRE is in the room; therefore, there are no seismically induced failures (Category 2/1 interactions).
_X_ The NSRE in the room is seismically restrained (upgraded to Category 1 requirements); therefore, no seismically induced failures of these restraints are postulated.
___ The NSRE, which is postulated to fail as a result of an SSE, does not impact SRE.
___ Other, see remarks.

Missile Analysis

_X_ No credible missile sources exist in the room.
___ Missiles from rotating components generated within the room contain insufficient energy to escape their equipment housing(s).
___ Other, see remarks.

Pipe Break Analysis

_X_ There are no high-energy lines in the room.
___ The high-energy line breaks have been evaluated and do not adversely affect SRE.
___ Other, see remarks.

Remarks

1. Flooding from sources located in this room will not impair the safe shutdown capability of the SRE.

TABLE 3F-1 (SHEET 20 OF 84)

Listing of safety-related items in room R-C89

Item Number	Description	Equipment Designation	Essential Equipment	Seismic Category 1
1.	Train D raceway	Conduits and cabletrays	Y	Y

TABLE 3F-1 (SHEET 21 OF 84)

Room Number R-C90 Title Residual Heat Removal (RHR) Exchanger Room Train A

Remarks

Flooding Analysis

_X_ Flooding from sources within the room, coincident with the most limiting single active failure (assumed in accordance with paragraphs 3.6.1.1.F and 3.1.1.6.G), will not preclude mitigation of the event or safe shutdown of the plant.

___ Flooding from sources external to the room is not credible even with a single active failure.

___ Other, see remarks.

Seismic Design Analysis

___ Only SRE is in the room; therefore, there are no seismically induced failures (Category 2/1 interactions).

_X_ The NSRE in the room is seismically restrained (upgraded to Category 1 requirements); therefore, no seismically induced failures of these restraints are postulated.

___ The NSRE, which is postulated to fail as a result of an SSE, does not impact SRE.

___ Other, see remarks.

Missile Analysis

_X_ No credible missile sources exist in the room.

___ Missiles from rotating components generated within the room contain insufficient energy to escape their equipment housing(s).

___ Other, see remarks.

Pipe Break Analysis

_X_ There are no high-energy lines in the room.

___ The high-energy line breaks have been evaluated and do not adversely affect SRE.

___ Other, see remarks.

TABLE 3F-1 (SHEET 22 OF 84)

Listing of safety-related items in room R-C90

Item Number	Description	Equipment Designation	Essential Equipment	Seismic Category 1
1.	Train A and B raceway	Conduits and cabletrays	Y	Y
2.	RHR heat exchanger room leak detection switch	LSH 9874	Y	Y
3.	RHR miniflow valve	FV 0610	Y	Y
4.	RHR heat exchanger to pump valve	HV 8804A	Y	Y
5.	RHR exchanger	1-1205-E6-001	Y	Y
6.	Piping	1-1205-007-8 in.	Y	Y
		1-1205-007-2 in.	Y	Y
		1-1205-013-3/4 in.	Y	Y
		1-1205-013-3 in.	Y	Y
		1-1208-411-8 in.	Y	Y
		1-1205-46-3/4 in.	Y	Y
		1-1205-005-8 in.	Y	Y
		1-1203-021-18 in.	Y	Y
		1-1203-021-14 in.	Y	Y
		1-1205-033-3/8 in.	Y	Y
		1-1203-122-1 in.	Y	Y
		1-1203-088-1 in.	Y	Y
		1-1203-086-1 in.	Y	Y
		1-1205-005-8 in.	Y	Y
		1-1205-008-8 in.	Y	Y
		1-1205-012-2 in.	Y	Y
		1-1205-014-3/4 in.	Y	Y
		1-1205-014-3 in.	Y	Y
		1-1205-022-3/4 in.	Y	Y
		1-1205-029-3/4 in.	Y	Y
		1-1205-030-2 in.	Y	Y
		1-1205-070-1/2 in.	Y	Y
7.	HVAC ducts	Train A	Y	Y
8.	Residual heat exchanger outlet valve	HV-0606	Y	Y
9.	Residual heat removal LP return bypass valve	FV-0618	Y	Y

TABLE 3F-1 (SHEET 23 OF 84)

Room Number R-C91 Title RHR Heat Exchanger Room Train B

Remarks

Flooding Analysis

_X_ Flooding from sources within the room, coincident with the most limiting single active failure (assumed in accordance with paragraphs 3.6.1.1.F and 3.6.1.1.G), will not preclude mitigation of the event or safe shutdown of the plant.

___ Flooding from sources external to the room is not credible even with a single active failure.

___ Other, see remarks.

Seismic Design Analysis

___ Only SRE is in the room; therefore, there are no seismically induced failures (Category 2/1 interactions).

_X_ The NSRE in the room is seismically restrained (upgraded to Category 1 requirements); therefore, no seismically induced failures of these restraints are postulated.

___ The NSRE, which is postulated to fail as a result of an SSE, does not impact SRE.

___ Other, see remarks.

Missile Analysis

_X_ No credible missile sources exist in the room.

___ Missiles from rotating components generated within the room contain insufficient energy to escape their equipment housing(s).

___ Other, see remarks.

Pipe Break Analysis

_X_ There are no high-energy lines in the room.

___ The high-energy line breaks have been evaluated and do not adversely affect SRE.

___ Other, see remarks.

TABLE 3F-1 (SHEET 24 OF 84)

Listing of safety-related items in room R-C91

Item Number	Description	Equipment Designation	Essential Equipment	Seismic Category 1
1.	Train A and B raceways	Conduits and cabletrays	Y	Y
2.	RHR pump to miniflow valve	FV 0611	Y	Y
3.	RHR heat exchanger room leak detection switch	LSH 9855	Y	Y
4.	RHR exchanger	1-1205-E6-002	Y	Y
5.	Conduit	-	Y	Y
6.	Piping	1-1205-014-3/4 in.	Y	Y
		1-1205-014-3 in.	Y	Y
		1-1203-042-18 in.	Y	Y
		1-1203-042-14 in.	Y	Y
		1-1205-006-8 in.	Y	Y
		1-1204-012-8 in.	Y	Y
		1-1203-114-1 in.	Y	Y
		1-1203-116-1 in.	Y	Y
		1-1205-034-3/8 in.	Y	Y
		1-1205-045-3/4 in.	Y	Y
		1-1205-008-2 in.	Y	Y
		1-1205-008-8 in.	Y	Y
		1-1203-071-3/4 in.	Y	Y
		1-1203-075-3/4 in.	Y	Y
		1-1203-084-3/4 in.	Y	Y
		1-1203-111-3/4 in.	Y	Y
		1-1205-005-8 in.	Y	Y
		1-1205-007-8 in.	Y	Y
		1-1205-012-2 in.	Y	Y
		1-1205-018-1 in.	Y	Y
		1-1205-021-1 in.	Y	Y
		1-1205-029-3/4 in.	Y	Y
		1-1205-031-1 in.	Y	Y
		1-1205-032-1 in.	Y	Y
		1-1205-035-1 in.	Y	Y
		1-1205-036-1 in.	Y	Y
		1-1205-037-1 in.	Y	Y
		1-1205-038-1 in.	Y	Y
		1-1205-043-1 in.	Y	Y
		1-1205-044-1 in.	Y	Y
		1-1205-051-1 in.	Y	Y
		1-1205-052-1 in.	Y	Y
		1-1205-053-1 in.	Y	Y
		1-1205-054-1 in.	Y	Y
		1-1205-056-1 in.	Y	Y
		1-1205-057-1 in.	Y	Y
		1-1205-058-1 in.	Y	Y
		1-1205-059-1 in.	Y	Y

TABLE 3F-1 (SHEET 25 OF 84)

Listing of safety-related items in room R-C91

Item Number	Description	Equipment Designation	Essential Equipment	Seismic Category 1
		1-1205-072-1/2 in.	Y	Y
		1-1205-073-1/2 in.	Y	Y
		1-1205-074-1/2 in.	Y	Y
		1-1205-075-1/2 in.	Y	Y
7.	HVAC ducts	Train B	Y	Y
8.	Residual heat exchanger outlet valve	HV-0607	Y	Y
9.	Residual heat removal LP return bypass valve	FV-0619	Y	Y
10.	Residual heat removal exchanger train B to H injection pump valve	HV-8804B	Y	Y

TABLE 3F-1 (SHEET 26 OF 84)

Room Number R-C95 Title Pipe Chase Train B

Flooding Analysis

___ Flooding from sources within the room, coincident with the most limiting single active failure (assumed in accordance with paragraphs 3.6.1.1.F and 3.6.1.1.G), will not preclude mitigation of the event or safe shutdown of the plant.
___ Flooding from sources external to the room is not credible even with a single active failure.
_X_ Other, see remark 1.

Seismic Design Analysis

___ Only SRE is in the room; therefore, there are no seismically induced failures (Category 2/1 interactions).
_X_ The NSRE in the room is seismically restrained (upgraded to Category 1 requirements); therefore, no seismically induced failures of these restraints are postulated.
___ The NSRE, which is postulated to fail as a result of an SSE, does not impact SRE.
___ Other, see remarks.

Missile Analysis

_X_ No credible missile sources exist in the room.
___ Missiles from rotating components generated within the room contain insufficient energy to escape their equipment housing(s).
___ Other, see remarks.

Pipe Break Analysis

___ There are no high-energy lines in the room.
_X_ The high-energy line breaks have been evaluated and do not adversely affect SRE.
___ Other, see remarks.

Remarks

1. Flooding from sources located in this room will not impair the safe shutdown capability of the SRE.

TABLE 3F-1 (SHEET 27 OF 84)

Listing of safety-related items in room R-C95

Item Number	Description	Equipment Designation	Essential Equipment	Seismic Category 1
1.	Train C raceway	Conduits and cableways	Y	Y
2.	Piping	1-1208-411-8 in.	Y	Y
		1-1204-012-8 in.	Y	Y
		1-1205-008-8 in.	Y	Y
		1-1206-006-8 in.	Y	Y
		1-1204-002-3 in.	Y	Y
		1-1204-037-4 in.	Y	Y
		1-1204-221-2 in.	Y	Y
		1-1208-003-3 in.	Y	Y
		1-1208-022-2 in.	Y	Y
		1-1208-095-3 in.	Y	Y
		1-1208-097-3 in.	Y	Y
		1-1208-103-3 in.	Y	Y
		1-1208-123-4 in.	Y	Y
		1-1208-131-2 in.	Y	Y
		1-1208-146-3 in.	Y	Y
		1-1208-410-3 in.	Y	Y
		1-1208-485-1 in.	Y	Y
		1-1208-493-3/4 in.	Y	Y
		1-1213-014-2 in.	Y	Y
		1-1213-017-2 in.	Y	Y
		1-1213-043-3 in.	Y	Y
		1-1407-007-4 in.	Y	Y
		1-1407-034-4 in.	Y	Y
		1-1561-103-10 in.	Y	Y
3.	HVAC ducts	Train A		Y
4.	HVAC ducts	Train B		Y
5.	Temperature elements	TE-19723E		Y
		TE-19722E		

TABLE 3F-1 (SHEET 28 OF 84)

Room Number R-C99 Title Nonradioactive Pipe Chase

Flooding Analysis

___ Flooding from sources within the room, coincident with the most limiting single active failure (assumed in accordance with paragraphs 3.6.1.1.F and 3.6.1.1.G), will not preclude mitigation of the event or safe shutdown of the plant.

_X_ Flooding from sources external to the room is not credible even with a single active failure.

___ Other, see remarks.

Seismic Design Analysis

___ Only SRE is in the room; therefore, there are no seismically induced failures (Category 2/1 interactions).

_X_ The NSRE in the room is seismically restrained (upgraded to Category 1 requirements); therefore, no seismically induced failures of these restraints are postulated.

___ The NSRE, which is postulated to fail as a result of an SSE, does not impact SRE.

___ Other, see remarks.

Missile Analysis

_X_ No credible missile sources exist in the room.

___ Missiles from rotating components generated within the room contain insufficient energy to escape their equipment housing(s).

___ Other, see remarks.

Pipe Break Analysis

_X_ There are no high-energy lines in the room.

___ The high-energy line breaks have been evaluated and do not adversely affect SRE.

___ Other, see remarks.

Remarks

1. The flooding from sources located in this room will not impair the safe shutdown capability of the SRE.

TABLE 3F-1 (SHEET 29 OF 84)

Listing of safety-related items in room R-C99

Item Number	Description	Equipment Designation	Essential Equipment	Seismic Category 1
1.	Train B raceway	Conduits and cabletrays	Y	Y
2.	Essential chilled water	1-1592-020-2 1/2 in. piping	Y	Y
		1-1592-020-3 in.	Y	Y
		1-1592-031-2 1/2 in.	Y	Y
		1-1592-031-3 in.	Y	Y
		1-1592-052-1 1/2 in.	Y	Y
		1-1592-057-1 1/2 in.	Y	Y
		1-1592-044-2 1/2 in.	Y	Y
		1-1592-054-2 1/2 in.	Y	Y
		1-1592-026-2 in.	Y	Y
		1-1592-038-2 in.	Y	Y
		A-1228-166-2 in.	Y	Y
		1-1228-166-2 in.	Y	Y
		1-1228-170-1 in.	Y	Y
		1-1228-174-2 in.	Y	Y
		1-1228-174-3 in.	Y	Y
		A-1561-103-10 in.	Y	Y
		1-1592-044-2 in.	Y	Y
		1-1592-054-2 in.	Y	Y

TABLE 3F-1 (SHEET 30 OF 84)

Room Number R-C99 Title Nonradioactive

Flooding Analysis

___ Flooding from sources within the room, coincident with the most limiting single active failure (assumed in accordance with paragraphs 3.6.1.1.F and 3.6.1.1.G), will not preclude mitigation of the event or safe shutdown of the plant.
___ Flooding from sources external to the room is not credible even with a single active failure.
_X_ Other, see remarks.

Seismic Design Analysis

___ Only SRE is in the room; therefore, there are no seismically induced failures (Category 2/1 interactions).
_X_ The NSRE in the room is seismically restrained (upgraded to Category 1 requirements); therefore, no seismically induced failures of these restraints are postulated.
___ The NSRE, which is postulated to fail as a result of an SSE, does not impact SRE.
___ Other, see remarks.

Missile Analysis

_X_ No credible missile sources exist in the room.
___ Missiles from rotating components generated within the room contain insufficient energy to escape their equipment housing(s).
___ Other, see remarks.

Pipe Break Analysis

_X_ There are no high-energy lines in the room.
___ The high-energy line breaks have been evaluated and do not adversely affect SRE.
___ Other, see remarks.

Remarks

1. Safety-related function is not impaired by flooding or water spray.

TABLE 3F-1 (SHEET 31 OF 84)

Listing of safety-related items in room R-C103

Item Number	Description	Equipment Designation	Essential Equipment	Seismic Category 1
1.	Piping	1-1205-003-14 in.	Y	Y
		1-1205-010-12 in.	Y	Y
		1-1205-007-8 in.	Y	Y
		1-1205-005-8 in.	Y	Y
2.	Train A raceway	Conduits and cabletrays	Y	Y
3.	HVAC ducts	Train A		Y

TABLE 3F-1 (SHEET 32 OF 84)

Room Number R-C104 Title Electrical Chase

Flooding Analysis

___ Flooding from sources within the room, coincident with the most limiting single active failure (assumed in accordance with paragraphs 3.6.1.1.F and 3.6.1.1.G), will not preclude mitigation of the event or safe shutdown of the plant.
___ Flooding from sources external to the room is not credible even with a single active failure.
_X_ Other, see remarks.

Seismic Design Analysis

_X_ Only SRE is in the room; therefore, there are no seismically induced failures (Category 2/1 interactions).
___ The NSRE in the room is seismically restrained (upgraded to Category 1 requirements); therefore, no seismically induced failures of these restraints are postulated.
___ The NSRE, which is postulated to fail as a result of an SSE, does not impact SRE.
___ Other, see remarks.

Missile Analysis

_X_ No credible missile sources exist in the room.
___ Missiles from rotating components generated within the room contain insufficient energy to escape their equipment housing(s).
___ Other, see remarks.

Pipe Break Analysis

_X_ There are no high-energy lines in the room.
___ The high-energy line breaks have been evaluated and do not adversely affect SRE.
___ Other, see remarks.

Remarks

1. The flooding from sources located in this room will not impair the safe shutdown capability of the SRE.

TABLE 3F-1 (SHEET 33 OF 84)

Listing of safety-related items in room R-C104

Item Number	Description	Equipment Designation	Essential Equipment	Seismic Category 1
1.	Train A and C raceway	Conduits and cabletrays	Y	Y

TABLE 3F-1 (SHEET 34 OF 84)

Room Number R-C105 Title Pipe Penetration Room Train A

Flooding Analysis

___ Flooding from sources within the room, coincident with the most limiting single active failure (assumed in accordance with paragraphs 3.6.1.1.F and 3.6.1.1.G), will not preclude mitigation of the event or safe shutdown of the plant.
___ Flooding from sources external to the room is not credible even with a single active failure.
_X_ Other, see remarks.

Seismic Design Analysis

___ Only SRE is in the room; therefore, there are no seismically induced failures (Category 2/1 interactions).
_X_ The NSRE in the room is seismically restrained (upgraded to Category 1 requirements); therefore, no seismically induced failures of these restraints are postulated.
___ The NSRE, which is postulated to fail as a result of an SSE, does not impact SRE.
___ Other, see remarks.

Missile Analysis

_X_ No credible missile sources exist in the room.
___ Missiles from rotating components generated within the room contain insufficient energy to escape their equipment housing(s).
___ Other, see remarks.

Pipe Break Analysis

_X_ There are no high-energy lines in the room.
___ The high-energy line breaks have been evaluated and do not adversely affect SRE.
___ Other, see remarks.

Remarks

1. Safety-related function is not impaired by flooding or water spray.

TABLE 3F-1 (SHEET 35 OF 84)

Listing of safety-related items in room R-C105

Item Number	Description	Equipment Designation	Essential Equipment	Seismic Category 1
1.	HVAC ducts	Train A		Y
2.	Containment sump isolation valve	HV-8811A		Y
3.	Containment spray pump No. 1 suction	HV-9002A		Y
4.	Containment spray pump No. 2 suction	HV-9003A		Y
5.	Train D raceway	Conduits and cabletrays	Y	Y

TABLE 3F-1 (SHEET 36 OF 84)

Room Number R-C107 Title Vestibule

Flooding Analysis

___ Flooding from sources within the room, coincident with the most limiting single active failure (assumed in accordance with paragraphs 3.6.1.1.F and 3.6.1.1.G), will not preclude mitigation of the event or safe shutdown of the plant.
___ Flooding from sources external to the room is not credible even with a single active failure.
_X_ Other, see remarks.

Seismic Design Analysis

___ Only SRE is in the room; therefore, there are no seismically induced failures (Category 2/1 interactions).
_X_ The NSRE in the room is seismically restrained (upgraded to Category 1 requirements); therefore, no seismically induced failures of these restraints are postulated.
___ The NSRE, which is postulated to fail as a result of an SSE, does not impact SRE.
___ Other, see remarks.

Missile Analysis

_X_ No credible missile sources exist in the room.
___ Missiles from rotating components generated within the room contain insufficient energy to escape their equipment housing(s).
___ Other, see remarks.

Pipe Break Analysis

_X_ There are no high-energy lines in the room.
___ The high-energy line breaks have been evaluated and do not adversely affect SRE.
___ Other, see remarks.

Remarks

1. Safety-related function is not impaired by flooding or water spray.

TABLE 3F-1 (SHEET 37 OF 84)

Listing of safety-related items in room R-C107

Item Number	Description	Equipment Designation	Essential Equipment	Seismic Category 1
1.	HVAC ducts	Train A		Y
2.	Temperature elements	TE-15212C		Y
		TE-15216C		Y
3.	Train D raceway	Conduits and cabletrays	Y	Y

TABLE 3F-1 (SHEET 38 OF 84)

Room Number R-C108 Title Steam Generator Blowdown Heat Exchanger Room

Flooding Analysis

___ Flooding from sources within the room, coincident with the most limiting single active failure (assumed in accordance with paragraphs 3.6.1.1.F and 3.6.1.1.G), will not preclude mitigation of the event or safe shutdown of the plant.
___ Flooding from sources external to the room is not credible even with a single active failure.
_X_ Other, see remark 1.

Seismic Design Analysis

___ Only SRE is in the room; therefore, there are no seismically induced failures (Category 2/1 interactions).
___ The NSRE in the room is seismically restrained (upgraded to Category 1 requirements); therefore, no seismically induced failures of these restraints are postulated.
___ The NSRE, which is postulated to fail as a result of an SSE, does not impact SRE.
_X_ Other, see remark 2.

Missile Analysis

___ No credible missile sources exist in the room.
_X_ Missiles from rotating components generated within the room contain insufficient energy to escape their equipment housing(s).
__ Other, see remarks.

Pipe Break Analysis

___ There are no high-energy lines in the room.
_X_ The high-energy line breaks have been evaluated and do not adversely affect SRE.
___ Other, see remarks.

Remarks

1. Safety-related function is not impaired by flooding or water spray.
2. There is no essential equipment for safe shutdown located in this room; therefore, the postulated hazards have no effect on the safe shutdown capability.

TABLE 3F-1 (SHEET 39 OF 84)

Listing of safety-related items in room R-C108

Item Number	Description	Equipment Designation	Essential Equipment	Seismic Category 1
1.	Train C raceway	Conduits and cabletrays	Y	Y
2.	Piping	1-1206-001-12 in.		Y
		1-1305-067-2 1/2 in.	Y	Y
		1-1305-068-2 1/2 in.	Y	Y
		1-1305-080-3 in.	Y	Y
		1-1305-080-4 in.	Y	Y
		1-1305-080-6 in.	Y	Y
		1-1305-098-3 in.	Y	Y
		1-1305-098-4 in.	Y	Y
		1-1305-099-3 in.	Y	Y
		1-1305-107-1 1/2 in.	Y	Y
		1-1305-107-3 in.	Y	Y
		1-1305-108-2 1/2 in.	Y	Y
		1-1305-109-2 1/2 in.	Y	Y
		1-1407-001-3 in.	Y	Y
		1-1407-002-3 in.	Y	Y
		1-1407-003-1 in.	Y	Y
		1-1407-003-3 in.	Y	Y
		1-1407-004-3 in.	Y	Y
		1-1407-005-1 in.	Y	Y
		1-1407-006-3 in.	Y	Y
		1-1407-015-3 in.	Y	Y
		1-1407-029-1 in.	Y	Y
		1-1407-035-4 in.	Y	Y
		1-1407-038-4 in.	Y	Y
		1-1407-039-4 in.	Y	Y
		1-1407-062-3 in.	Y	Y
		1-1407-066-3 in.	Y	Y
		1-1407-066-4 in.	Y	Y
		1-1407-067-3 in.	Y	Y
		1-1407-098-1 1/2 in.	Y	Y
		1-1407-124-3/4 in.	Y	Y
		1-1407-125-3/4 in.	Y	Y
		1-1407-126-3/4 in.	Y	Y
		1-1407-127-3/4 in.	Y	Y
		1-1407-128-3/4 in.	Y	Y
		1-1407-129-3/4 in.	Y	Y
		1-1407-130-3/4 in.	Y	Y
		1-1407-131-3/4 in.	Y	Y
		1-1407-132-3/4 in.	Y	Y
		1-1592-026-1 in.	Y	Y
		1-1592-038-1 in.	Y	Y
3.	Temperature elements	TE-15212D		Y
		TE-15216D		Y

TABLE 3F-1 (SHEET 40 OF 84)

Room Number R-C109 Title Motor Control Center (MCC) Room

Flooding Analysis

___ Flooding from sources within the room, coincident with the most limiting single active failure (assumed in accordance with paragraphs 3.6.1.1.F and 3.6.1.1.G), will not preclude mitigation of the event or safe shutdown of the plant.
___ Flooding from sources external to the room is not credible even with a single active failure.
_X_ Other, see remarks.

Seismic Design Analysis

_X_ Only SRE is in the room; therefore, there are no seismically induced failures (Category 2/1 interactions).
___ The NSRE in the room is seismically restrained (upgraded to Category 1 requirements); therefore, no seismically induced failures of these restraints are postulated.
___ The NSRE, which is postulated to fail as a result of an SSE, does not impact SRE.
___ Other, see remarks.

Missile Analysis

_X_ No credible missile sources exist in the room.
___ Missiles from rotating components generated within the room contain insufficient energy to escape their equipment housing(s).
___ Other, see remarks.

Pipe Break Analysis

_X_ There are no high-energy lines in the room.
___ The high-energy line breaks have been evaluated and do not adversely affect SRE.
___ Other, see remarks.

Remarks

1. Safety related function is not impaired by flooding or water spray.

TABLE 3F-1 (SHEET 41 OF 84)

Listing of safety-related
items in room R-C109

Item Number	Description	Equipment Designation	Essential Equipment	Seismic Category 1
1.	Train A raceway	Conduits and cabletrays	Y	Y

TABLE 3F-1 (SHEET 42 OF 84)

Room Number R-C111

Title Chemical and Volume Control System (CVCS)
Normal Charging Pump Room

Remarks

Flooding Analysis

_X_ Flooding from sources within the room, coincident with the most limiting single active failure (assumed in accordance with paragraphs 3.6.1.1.F and 3.6.1.1.G) will not preclude mitigation of the event or safe shutdown of the plant.

___ Flooding from sources external to the room is not credible even with a single active failure.

___ Other, see remarks.

Seismic Design Analysis

___ Only SRE is in the room; therefore, there are no seismically induced failures (Category 2/1 interactions).

_X_ The NSRE in the room is seismically restrained (upgraded to Category 1 requirements); therefore, no seismically induced failures of these restraints are postulated.

____The NSRE, which is postulated to fail as a result of an SSE, does not impact SRE.

____Other, see remarks.

Missile Analysis

____No credible missile sources exist in the room.

_X_ Missiles from rotating components generated within the room contain insufficient energy to escape their equipment housing(s).

____Other, see remarks.

Pipe Break Analysis

___ There are no high-energy lines in the room.

_X_ The high-energy line breaks have been evaluated and do not adversely affect SRE.

___ Other, see remarks.

TABLE 3F-1 (SHEET 43 OF 84)

Listing of safety-related items in room R-C111

Item Number	Description	Equipment Designation	Essential Equipment	Seismic Category 1
1.	CVCS normal charging pump	1-1208-P4-001	N	Y
2.	Piping	1-1204-037-4 in.	Y	Y
		1-1204-168-3/4 in.	Y	Y
		1-1208-002-3 in.	Y	Y
		1-1208-003-2 in.	Y	Y
		1-1208-016-3 in.	Y	Y
		1-1208-123-4 in.	Y	Y
		1-1208-140-3/4 in.	Y	Y
		1-1208-142-3/4 in.	Y	Y
		1-1208-187-3/4 in.	Y	Y
		1-1208-189-3/4 in.	Y	Y
		1-1208-190-3/4 in.	Y	Y
		1-1208-280-1/2 in.	Y	Y
		1-1208-411-6 in.	Y	Y
		1-1208-440-2 in.	Y	Y
		1-1208-482-3/4 in.	Y	Y
		1-1208-483-3/4 in.	Y	Y

TABLE 3F-1 (SHEET 44 OF 84)

Room Number R-C113 Title Boric Acid Batching Tank Room

Flooding Analysis

___ Flooding from sources within the room, coincident with the most limiting single active failure (assumed in accordance with paragraphs 3.6.1.1.F and 3.6.1.1.G), will not preclude mitigation of the event or safe shutdown of the plant.
___ Flooding from sources external to the room is not credible even with a single active failure.
_X_ Other, see remarks.

Seismic Design Analysis

___ Only SRE is in the room; therefore, there are no seismically induced failures (Category 2/1 interactions).
_X_ The NSRE in the room is seismically restrained (upgraded to Category 1 requirements); therefore, no seismically induced failures of these restraints are postulated.
___ The NSRE, which is postulated to fail as a result of an SSE, does not impact SRE.
___ Other, see remarks.

Missile Analysis

_X_ No credible missile sources exist in the room.
___ Missiles from rotating components generated within the room contain insufficient energy to escape their equipment housing(s).
___ Other, see remarks.

Pipe Break Analysis

_X_ There are no high-energy lines in the room.
___ The high-energy line breaks have been evaluated and do not adversely affect SRE.
___ Other, see remarks.

Remarks

1. Flooding from sources located in this room room will not impair the safe shutdown capability of the SRE.

TABLE 3F-1 (SHEET 45 OF 84)

Listing of safety-related
items in room R-C113

Item Number	Description	Equipment Designation	Essential Equipment	Seismic Category 1
1.	Train A raceway	Conduits and cabletrays	Y	Y
2.	Piping	1-1202-122-1 1/2 in.	Y	Y
		1-1202-122-3 in.	Y	Y
		1-1202-125-2 in.	Y	Y
		A-1208-232-3 in.	Y	Y
		1-1202-125-1 1/2 in	Y	Y
		1-1202-124-3 in.	Y	Y
		1/2-1208-241-3 in.	Y	Y
		A-1208-034-3 in.	Y	Y
		A-1208-230-1 in.	Y	Y
		A-1208-230-3/4 in.	Y	Y
		1-1202-123-2 in.	Y	Y
		1-1202-124-1 1/2 in.	Y	Y
		1-1202-300-3/4 in.	Y	Y
		1-1202-473-2 in.	Y	Y
		1-1202-474-2 in.	Y	Y
		1-1204-177-8 in.	Y	Y
		1-1208-137-8 in.	Y	Y
		1-1208-241-3 in.	Y	Y
		A-1208-492-3 in.	Y	Y
		A-1228-166-2 in.	Y	Y
		A-1228-166-1/2 in.	Y	Y
		A-1228-228-3 in.	Y	Y
		A-1609-034-3/4 in.	Y	Y

TABLE 3F-1 (SHEET 46 OF 84)

Room Number R-C114 Title Valve Gallery

Remarks

Flooding Analysis

_X_ Flooding from sources within the room, coincident with the most limiting single active failure (assumed in accordance with paragraphs 3.6.1.1.F and 3.6.1.1.G), will not preclude mitigation of the event or safe shutdown of the plant.

___ Flooding from sources external to the room is not credible even with a single active failure.

___ Other, see remarks.

Seismic Design Analysis

___ Only SRE is in the room; therefore, there are no seismically induced failures (Category 2/1 interactions).

_X_ The NSRE in the room is seismically restrained (upgraded to Category 1 requirements); therefore, no seismically induced failures of these restraints are postulated.

___ The NSRE, which is postulated to fail as a result of an SSE, does not impact SRE.

___ Other, see remarks.

Missile Analysis

_X_ No credible missile sources exist in the room.

___ Missiles from rotating components generated within the room contain insufficient energy to escape their equipment housing(s).

___ Other, see remarks.

Pipe Break Analysis

___ There are no high-energy lines in the room.

_X_ The high-energy line breaks have been evaluated and do not adversely affect SRE.

___ Other, see remarks.

TABLE 3F-1 (SHEET 47 OF 84)

Listing of safety-related items in room R-C114

Item Number	Description	Equipment Designation	Essential Equipment	Seismic Category 1
1.	Train A raceway	Conduits and cabletrays	Y	Y
2.	Refuel water tank to charging pump valve	LV 0112D	Y	Y
3.	Piping	1-1202-122-1 1/2 in.	Y	Y
		1-1202-123-2 in.	Y	Y
		1-1202-124-1 1/2 in.	Y	Y
		1-1202-125-2 in.	Y	Y
		1-1592-027-1 1/2 in.	Y	Y
		1-1592-037-1 1/2 in.	Y	Y
		1-1208-141-6 in.	Y	Y
		1-1208-144-4 in.	Y	Y
		1-1203-101-2 in.	Y	Y
		1-1203-144-4 in.	Y	Y
		1-1208-157-8 in.	Y	Y
		1-1208-095-3 in.	Y	Y
		1-1208-101-2 in.	Y	Y
		1-1208-137-8 in.	Y	Y
		1-1208-139-8 in.	Y	Y
		1-1208-147-3 in.	Y	Y
		1-1208-411-8 in.	Y	Y
		1-1208-485-1 in.	Y	Y
		1-1208-497-2 in.	Y	Y
		1-1208-498-2 in.	Y	Y
		1-1208-501-2 in.	Y	Y
4.	Charging pump miniflow isolation valve	HV-8111A	Y	Y
5.	Charging pump A suction valve	HV-8471A	Y	Y
6.	Charging pump A discharge valve	HV-8485A	Y	Y
7.	Charging pump miniflow isolation to RWST valve	HV-8508A, 8509B	Y	Y
8.	Normal charging pump miniflow isolation valve	1-1208-U4-150	Y	Y

TABLE 3F-1 (SHEET 48 OF 84)

Room Number R-C115 Title Centrifugal Charging Pump Room Train A

Remarks

Flooding Analysis

_X_ Flooding from sources within the room, coincident with the most limiting single active failure (assumed in accordance with paragraphs 3.6.1.1.F and 3.6.1.1.G), will not preclude mitigation of the event or safe shutdown of the plant.

___ Flooding from sources external to the room is not credible even with a single active failure.

___ Other, see remarks.

Seismic Design Analysis

___ Only SRE is in the room; therefore, there are no seismically induced failures (Category 2/1 interactions).

_X_ The NSRE in the room is seismically restrained (upgraded to Category 1 requirements); therefore, no seismically induced failures of these restraints are postulated.

___ The NSRE, which is postulated to fail as a result of an SSE, does not impact SRE.

___ Other, see remarks.

Missile Analysis

___ No credible missile sources exist in the room.

_X_ Missiles from rotating components generated within the room contain insufficient energy to escape their equipment housing(s).

___ Other, see remarks.

Pipe Break Analysis

___ There are no high-energy lines in the room.

_X_ The high-energy line breaks have been evaluated and do not adversely affect SRE.

___ Other, see remarks.

TABLE 3F-1 (SHEET 49 OF 84)

Listing of safety-related items in room R-C115

Item Number	Description	Equipment Designation	Essential Equipment	Seismic Category 1
1.	Train A raceway	Conduits and cabletrays	Y	Y
2.	CVCS centrifugal charging pump	1-1208-P6-002	Y	Y
3.	Charging pump room leak detection switch	LSH 9826		Y
4.	Charging pump room leak detection switch	LSH 9830		Y
5.	Air-handling unit	1-1555A7-013	Y	Y
6.	Piping	1-1202-122-1 1/2 in.	Y	Y
		1-1202-123-2 in.	Y	Y
		1-1202-124-1 1/2 in.	Y	Y
		1-1202-125-2 in.	Y	Y
		1-1202-370-2 in.	Y	Y
		1-1202-371-2 in.	Y	Y
		1-1208-141-6 in.	Y	Y
		1-1208-144-4 in.	Y	Y
		1-1592-027-1 1/2 in.	Y	Y
		1-1592-037-1 1/2 in.	Y	Y
		1-1204-012-8 in.	Y	Y
		1-1208-132-2 in.	Y	Y
		1-1208-191-1 in.	Y	Y
		1-1208-197-3/4 in.	Y	Y
		1-1208-198-1 in.	Y	Y
		1-1555-101-1 1/2 in.	Y	Y
		1-1555-134-1 1/2 in.	Y	Y
7.	HVAC ducts	Train A		Y
8.	HVAC ducts	Train B		Y
9.	Charging pump room cooler temperature element	TE-12209		Y

TABLE 3F-1 (SHEET 50 OF 84)

Room Number R-C116 Title Vestibule

Flooding Analysis

___ Flooding from sources within the room, coincident with the most limiting single active failure (assumed in accordance with paragraphs 3.6.1.1.F and 3.6.1.1.G), will not preclude mitigation of the event or safe shutdown of the plant.

___ Flooding from sources external to the room is not credible even with a single active failure.

_X_ Other, see remarks.

Seismic Design Analysis

___ Only SRE is in the room; therefore, there are no seismically induced failures (Category 2/1 interactions).

_X_ The NSRE in the room is seismically restrained (upgraded to Category 1 requirements); therefore, no seismically induced failures of these restraints are postulated.

___ The NSRE, which is postulated to fail as a result of an SSE, does not impact SRE.

___ Other, see remarks.

Missile Analysis

_X_ No credible missile sources exist in the room.

___ Missiles from rotating components generated within the room contain insufficient energy to escape their equipment housing(s).

___ Other, see remarks.

Pipe Break Analysis

___ There are no high-energy lines in the room.

_X_ The high-energy line breaks have been evaluated and do not adversely affect SRE.

___ Other, see remarks.

Remarks

1. Safety-related equipment is not impaired by flooding or water spray.

TABLE 3F-1 (SHEET 51 OF 84)

Listing of safety-related items in room R-C116

Item Number	Description	Equipment Designation	Essential Equipment	Seismic Category 1
1.	Piping	1-1202-003-4 in.	Y	Y
2.	Train A and C raceway	1-1202-004-4 in.	Y	Y
		1-1202-004-3 in.	Y	Y
		1-1202-003-3 in.	Y	Y
		1-1202-122-3 in.	Y	Y
		1-1202-124-3 in.	Y	Y
		1-1305-080-6 in.	Y	Y
		Conduits and cabletrays	Y	Y

TABLE 3F-1 (SHEET 52 OF 84)

Room Number R-C118 Title Centrifugal Charging Pump Train B

Remarks

Flooding Analysis

_X_ Flooding from sources within the room, coincident with the most limiting single active failure (assumed in accordance with paragraphs 3.6.1.1.F and 3.6.1.1.G), will not preclude mitigation of the event or safe shutdown of the plant.

_X_ Flooding from sources external to the room is not credible even with a single active failure.

___ Other, see remarks.

Seismic Design Analysis

___ Only SRE is in the room; therefore, there are no seismically induced failures (Category 2/1 interactions).

_X_ The NSRE in the room is seismically restrained (upgraded to Category 1 requirements); therefore, no seismically induced failures of these restraints are postulated.

___ The NSRE, which is postulated to fail as a result of an SSE, does not impact SRE.

___ Other, see remarks.

Missile Analysis

___ No credible missile sources exist in the room.

_X_ Missiles from rotating components generated within the room contain insufficient energy to escape their equipment housing(s).

___ Other, see remarks.

Pipe Break Analysis

___ There are no high-energy lines in the room.

_X_ The high-energy line breaks have been evaluated and do not adversely affect SRE.

___ Other, see remarks.

TABLE 3F-1 (SHEET 53 OF 84)

Listing of safety-related items in room R-C118

Item Number	Description	Equipment Designation	Essential Equipment	Seismic Category 1
1.	Train B raceway	Conduits and cabletrays	Y	Y
2.	CVCS centrifugal charging pump	1-1208-P6-003	Y	Y
3.	Charging pump room leak detection switch	LSH 9827		Y
4.	Charging pump room leak detection switch	LSH 9831		Y
5.	Air-handling unit	1-1555-A7-014	Y	Y
6.	Piping	1-1202-167-1 1/2 in.	Y	Y
		1-1202-167-1 1/2 in.	Y	Y
		1-1202-168-2 in.	Y	Y
		1-1202-169-1 1/2 in.	Y	Y
		1-1202-170-2 in.	Y	Y
		1-1202-379-2 in.	Y	Y
		1-1202-378-2 in.	Y	Y
		1-1208-139-6 in.	Y	Y
		1-1208-145-4 in.	Y	Y
		1-1592-052-1 1/2 in.	Y	Y
		1-1592-067-1 1/2 in.	Y	Y
		1-1208-135-1 in.	Y	Y
		1-1208-200-3/4 in.	Y	Y
		1-1208-200-1 in.	Y	Y
		1-1208-201-3/4 in.	Y	Y
		1-1208-203-1 in.	Y	Y
		1-1208-204-3/4 in.	Y	Y
		1-1555-091-1 1/2 in.	Y	Y
		1-1555-135-1 1/2 in.	Y	Y
		1-1592-057-1 1/2 in.	Y	Y
7.	HVAC ducts	Train A		Y
8.	Charging pump room cooler, high temperature switch and indicator	T1SH-12215		Y

TABLE 3F-1 (SHEET 54 OF 84)

Room Number R-C119 Title Valve Gallery

Remarks

Flooding Analysis

_X_ Flooding from sources within the room, coincident with the most limiting single active failure (assumed in accordance with paragraphs 3.6.1.1.F and 3.6.1.1.G), will not preclude mitigation of the event or safe shutdown of the plant.

___ Flooding from sources external to the room is not credible even with a single active failure.

___ Other, see remarks.

Seismic Design Analysis

___ Only SRE is in the room; therefore, there are no seismically induced failures (Category 2/1 interactions).

_X_ The NSRE in the room is seismically restrained (upgraded to Category 1 requirements); therefore, no seismically induced failures of these restraints are postulated.

___ The NSRE, which is postulated to fail as a result of an SSE, does not impact SRE.

___ Other, see remarks.

Missile Analysis

_X_ No credible missile sources exist in the room.

___ Missiles from rotating components generated within the room contain insufficient energy to escape their equipment housing(s).

Pipe Break Analysis

___ There are no high-energy lines in the room.

_X_ The high-energy line breaks have been evaluated and do not adversely affect SRE.

___ Other, see remarks.

TABLE 3F-1 (SHEET 55 OF 84)

Listing of safety-related items in room R-C119

Item Number	Description	Equipment Designation	Essential Equipment	Seismic Category 1
1.	Train B raceway	Conduits and cabletrays	Y	Y
2.	Charging pump train B, throttling valve	HV 1090B	Y	Y
		HY-1090B		
		ZT-1090B		
3.	Piping	1-1592-038-2 in.	Y	Y
		1-1592-026-2 in.	Y	Y
		1-1202-167-1 1/2 in.	Y	Y
		1-1202-168-2 in.	Y	Y
		1-1202-169-1 1/2 in.	Y	Y
		1-1202-170-2 in.	Y	Y
		1-1208-146-3 in.	Y	Y
		1-1208-099-3 in.	Y	Y
		1-1208-139-6 in.	Y	Y
		1-1208-145-4 in.	Y	Y
		1-1204-057-4 in.	Y	Y
		1-1208-099-2 in.	Y	Y
		1-1208-135-1 in.	Y	Y
		1-1208-137-8 in.	Y	Y
		1-1208-145-1 in.	Y	Y
		1-1208-303-2 in.	Y	Y
		1-1208-499-2 in.	Y	Y
		1-1592-052-1 1/2 in.	Y	Y
		1-1592-057-1 1/2 in.	Y	Y
4.	Charging pump miniflow isolation valve	HV-8111B		Y
5.	Charging pump discharge, train B valve	HV-8438, HV-8485V	Y	Y
6.	Charging pump suction, train B valve	HV-8471B	Y	Y
7.	Charging pump miniflow isolation to RWST valves	HV-8508B, HV-8509B		

TABLE 3F-1 (SHEET 56 OF 84)

Room Number R-C120 Title Vestibule

Flooding Analysis

___ Flooding from sources within the room, coincident with the most limiting single active failure (assumed in accordance with paragraphs 3.6.1.1.F and 3.6.1.1.F), will not preclude mitigation of the event or safe shutdown of the plant.
__ Flooding from sources external to the room is not credible even with a single active failure.
_X_ Other, see remarks.

Seismic Design Analysis

___ Only SRE is in the room; therefore, there are no seismically induced failures (Category 2/1 interactions).
_X_ The NSRE in the room is seismically restrained (upgraded to Category 1 requirements); therefore, no seismically induced failures of these restraints are postulated.
___ The NSRE, which is postulated to fail as a result of an SSE, does not impact SRE.
___ Other, see remarks.

Missile Analysis

_X_ No credible missile sources exist in the room.
___ Missiles from rotating components generated within the room contain insufficient energy to escape their equipment housing(s).
___ Other, see remarks.

Pipe Break Analysis

_X_ There are no high-energy lines in the room.
___ The high-energy line breaks have been evaluated and do not adversely affect SRE.
___ Other, see remarks.

Remarks

1. The flooding from sources located in this room will not impair the safe shutdown capability of the SRE.

TABLE 3F-1 (SHEET 57 OF 84)

Listing of safety-related items in room R-C120

Item Number	Description	Equipment Designation	Essential Equipment	Seismic Category 1
1.	Train B raceway	Conduit and cabletrays	Y	Y
2.	Piping	1-1592-038-2 in.	Y	Y
		1-1592-026-2 in.	Y	Y
		1-1592-052-1 1/2 in.	Y	Y
		1-1592-057-1 1/2 in.	Y	Y
		1-1202-167-1 1/2 in.	Y	Y
		1-1202-168-2 in.	Y	Y
		1-1202-169-1 1/2 in.	Y	Y
		1-1202-170-2 in.	Y	Y
		1-1202-151-4 in.	Y	Y
		1-1202-169-3 in.	Y	Y
		1-1202-151-3 in.	Y	Y
		1-1202-006-3 in.	Y	Y
		1-1202-006-4 in.	Y	Y
		1-1202-151-4 in.	Y	Y
		1-1202-167-3 in.	Y	Y
		1-1202-290-3/4 in.	Y	Y
		1-1202-316-3/4 in.	Y	Y
		1-1202-479-2 in.	Y	Y
		1-1202-480-2 in.	Y	Y
		1-1228-166-2 in.	Y	Y
		1-1609-030-3/4 in.	Y	Y
		1-1609-031-3/4 in.	Y	Y
		1-1609-032-3/4 in.	Y	Y
		1-1609-033-3/4 in.	Y	Y
		1-1609-034-3/4 in.	Y	Y
3.	Refueling water tank to charging pump valve	LV-0112E		

TABLE 3F-1 (SHEET 58 OF 84)

Room Number R-C131 Title Vestibule

Flooding Analysis

__ Flooding from sources within the room coincident with the most limiting single active failure (assumed in accordance with paragraphs 3.6.1.1.F and 3.6.1.1.G), will not preclude mitigation of the event or safe shutdown of the plant.
__ Flooding from sources external to the room is not credible even with a single active failure.
_X_ Other, see remark 1.

Seismic Design Analysis

__ Only SRE is in the room; therefore, there are no seismically induced failures (Category 2/1 interactions).
_X_ The NSRE in the room is seismically restrained (upgraded to Category 1 requirements); therefore, no seismically induced failures of these restraints are postulated.
__ The NSRE, which is postulated to fail as a result of an SSE, does not impact SRE.
__ Other, see remarks.

Missile Analysis

_X_ No credible missile sources exist in the room.
__ Missiles from rotating components generated within the room contain insufficient energy to escape their equipment housing(s).
__ Other, see remarks.

Pipe Break Analysis

__ There are no high-energy lines in the room.
_X_ The high-energy line breaks have been evaluated and do not adversely affect SRE.
__ Other, see remarks.

Remarks

1. Flooding from sources located in this room will not impair the safe shutdown, capability of the SRE.

TABLE 3F-1 (SHEET 59 OF 84)

Listing of safety-related items in room R-C131

Item Number	Description	Equipment Designation	Essential Equipment	Seismic Category 1
1.	Piping	1-1205-003-12 in.	Y	Y
		1-1407-001-3 in.	Y	Y
		1-1407-002-3 in.	Y	Y
		1-1407-003-3 in.	Y	Y
		1-1407-004-3 in.	Y	Y

TABLE 3F-1 (SHEET 60 OF 84)

Room Number R-C133 Title Pipe Penetration Room Train A

Flooding Analysis

___ Flooding from sources within the room, coincident with the most limiting single active failure (assumed in accordance with paragraphs 3.6.1.1.F and 3.6.1.1.G), will not preclude mitigation of the event or safe shutdown of the plant.
___ Flooding from sources external to the room is not credible even with a single active failure.
_X_ Other, see remarks.

Seismic Design Analysis

___ Only SRE is in the room; therefore, there are no seismically induced failures (Category 2/1 interactions).
_X_ The NSRE in the room is seismically restrained (upgraded to Category 1 requirements); therefore, no seismically induced failures of these restraints are postulated.
___ The NSRE, which is postulated to fail as a result of an SSE, does not impact SRE.
___ Other, see remarks.

Missile Analysis

_X_ No credible missile sources exist in the room.
___ Missiles from rotating components generated within the room contain insufficient energy to escape their equipment housing(s).
___ Other, see remarks.

Pipe Break Analysis

_X_ There are no high-energy lines in the room.
___ The high-energy line breaks have been evaluated and do not adversely affect SRE.
___ Other, see remarks.

Remarks

1. Flooding from sources located in this room will not impair the safe shutdown capability of the SRE.

TABLE 3F-1 (SHEET 61 OF 84)

Listing of safety-related items in room R-C133

Item Number	Description	Equipment Designation	Essential Equipment	Seismic Category 1
1.	Train A raceway	Conduits and cabletrays	Y	Y
2.	Piping	1-1205-003-14 in.	Y	Y
		1-1205-003-12 in.	Y	Y
		1-1205-010-12 in.	Y	Y
		1-1205-007-8 in.	Y	Y
		1-1206-005-8 in.	Y	Y
		1-1205-028-1 in.	Y	Y
		1-1205-066-1 1/2 in.	Y	Y
3.	HVAC ducts	Train A		Y

TABLE 3F-1 (SHEET 62 OF 84)

Room Number R-C134 Title Pipe Penetration Room Train A

Flooding Analysis
___ Flooding from sources within the room, coincident with the most limiting single active failure (assumed in accordance with paragraphs 3.6.1.1.F and 3.6.1.1.G), will not preclude mitigation of the event or safe shutdown of the plant.
___ Flooding from sources external to the room is not credible even with a single active failure.
_X_ Other, see remarks.

Seismic Design Analysis
___ Only SRE is in the room; therefore, there are no seismically induced failures (Category 2/1 interactions).
_X_ The NSRE in the room is seismically restrained (upgraded to Category 1 requirements); therefore, no seismically induced failures of these restraints are postulated.
___ The NSRE, which is postulated to fail as a result of an SSE, does not impact SRE.
___ Other, see remarks.

Missile Analysis
_X_ No credible missile sources exist in the room.
___ Missiles from rotating components generated within the room contain insufficient energy to escape their equipment housing(s).
___ Other, see remarks.

Pipe Break Analysis
_X_ There are no high-energy lines in the room.
___ The high-energy line breaks have been evaluated and do not adversely affect SRE.
___ Other, see remarks.

Remarks

1. Flooding from sources located in this room will not impair the safe shutdown capability of the SRE.

TABLE 3F-1 (SHEET 63 OF 84)

Listing of safety-related items in room R-C134

Item Number	Description	Equipment Designation	Essential Equipment	Seismic Category 1
1.	Containment sump isolation valve	HV-8811A		Y
2.	RHR encapsulation vessel	V-1-1205 V4 001	Y	Y
3.	Containment spray pump emergency sump isolation valve	HV-9002A		Y
4.	Containment spray pump suction valve	HV-9003A		Y
5.	Piping	1-1205-028-14 in.	Y	Y
		1-1205-061-20 in.	Y	Y
		1-1205-041-14 in.	Y	Y
		1-1206-001-12 in.	Y	Y
		1-1206-061-18 in.	Y	Y
		1-1205-003-12 in.	Y	Y
		1-1205-062-3/4 in.	Y	Y
		1-1205-063-3/4 in.	Y	Y
		1-1206-001-1 in.	Y	Y
		1-1206-076-3/4 in.	Y	Y
		1-1206-077-3/4 in.	Y	Y

TABLE 3F-1 (SHEET 64 OF 84)

Room Number UC-C14 Title Pipe Chase

Flooding Analysis

___ Flooding from sources within the room, coincident with the most limiting single active failure (assumed in accordance with paragraphs 3.6.1.1.F and 3.6.1.1.G), will not preclude mitigation of the event or safe shutdown of the plant.
___ Flooding from sources external to the room is not credible even with a single active failure.
_X_ Other, see remark 1.

Seismic Design Analysis

___ Only SRE is in the room; therefore, there are no seismically induced failures (Category 2/1 interactions).
_X_ The NSRE in the room is seismically restrained (upgraded to Category 1 requirements); therefore, no seismically induced failures of these restraints are postulated.
___ The NSRE, which is postulated to fail as a result of an SSE, does not impact SRE.
___ Other, see remarks.

Missile Analysis

___ No credible missile sources exist in the room.
_X_ Missiles from rotating components generated within the room contain insufficient energy to escape their equipment housing(s).
___ Other, see remarks.

Pipe Break Analysis

___ There are no high-energy lines in the room.
_X_ The high-energy line breaks have been evaluated and do not adversely affect SRE.
___ Other, see remarks.

Remarks

1. The flooding from sources located in this room will not impair the safe shutdown capability of the SRE.

TABLE 3F-1 (SHEET 65 OF 84)

Listing of safety-related items in room UC-C14

Item Number	Description	Equipment Designation	Essential Equipment	Seismic Category 1
1.	Piping	1-1204-002-3 in.	Y	Y
		1-1208-146-3 in.	Y	Y
		1-1208-103-3 in.	Y	Y
		1-1208-097-3 in.	Y	Y
		1-1208-095-3 in.	Y	Y
		1-1208-411-8 in.	Y	Y
		1-1208-123-4 in.	Y	Y
		1-1208-410-3 in.	Y	Y
		1-1208-107-1 in.	Y	Y
		1-1208-022-2 in.	Y	Y
		1-1208-003-3 in.	Y	Y
		1-1204-037-4 in.	Y	Y
		1-1204-012-8 in.	Y	Y
		1-1208-485-1 in.	Y	Y

TABLE 3F-1 (SHEET 66 OF 84)

Room Number R-D48 Title RHR Pump Room Train A

Flooding Analysis

___ Flooding from sources within the room, coincident with the most limiting single active failure (assumed in accordance with paragraphs 3.6.1.1.F and 3.6.1.1.G), will not preclude mitigation of the event or safe shutdown of the plant.

_X_ Flooding from sources external to the room is not credible even with a single active failure.

___ Other, see remark 1.

Seismic Design Analysis

___ Only SRE is in the room; therefore, there are no seismically induced failures (Category 2/1 interactions).

_X_ The NSRE in the room is seismically restrained (upgraded to Category 1 requirements); therefore, no seismically induced failures of these restraints are postulated.

___ The NSRE, which is postulated to fail as a result of an SSE, does not impact SRE.

___ Other, see remarks.

Missile Analysis

_X_ No credible missile sources exist in the room.

___ Missiles from rotating components generated within the room contain insufficient energy to escape their equipment housing(s).

__ Other, see remark 2.

Pipe Break Analysis

_X_ There are no high-energy lines in the room.

___ The high-energy line breaks have been evaluated and do not adversely affect SRE.

___ Other, see remarks.

Remarks

1. The SRE will not be adversely affected by the maximum design flood.

TABLE 3F-1 (SHEET 67 OF 84)

Listing of safety-related items in room R-D48

Item Number	Description	Equipment Designation	Essential Equipment	Seismic Category 1
1.	Leak detection switch	LSH 9856		Y
2.	Leak detection switch	LSH 9860		Y
3.	RHR pump 1 inlet valve	HV 8812A	Y	Y
4.	RHR 1 cold leg isolation valve	HV 8716A	Y	Y
5.	Residual heat removal pump cooler temperature element	TE-12206	Y	Y
6.	Train A raceway	Conduits and cabletrays	Y	Y
7.	RHR pump	1-1205-P6-001	Y	Y
8.	Piping	1-1205-019-2 in.	Y	Y
		1-1205-023-2 in.	Y	Y
		1-1205-039-12 in.	Y	Y
		1-1205-013-3 in.	Y	Y
		1-1202-110-2 in.	Y	Y
		1-1202-111-2 in.	Y	Y
		1-1203-088-1 in.	Y	Y
		1-1203-086-1 in.	Y	Y
		1-1205-007-8 in.	Y	Y
		1-1205-003-14 in.	Y	Y
		1-1205-009-8 in.	Y	Y
		1-1205-005-8 in.	Y	Y
		1-1205-005-2 in.	Y	Y
		1-1204-001-12 in.	Y	Y
		1-1205-016-2 in.	Y	Y
		1-1205-039-2 in.	Y	Y
		1-1205-070-1/2 in.	Y	Y
		1-1205-071-1/2 in.	Y	Y
		1-1205-192-8 in.	Y	Y
		1-1202-478-2 in.	Y	Y

TABLE 3F-1 (SHEET 68 OF 84)

Room Number R-D76 Title Containment Spray Pump Room Train A

Flooding Analysis

___ Flooding from sources within the room, coincident with the most limiting single active failure (assumed in accordance with paragraphs 3.6.1.1.F and 3.6.1.1.G), will not preclude mitigation of the event or safe shutdown of the plant.
_X_ Flooding from sources external to the room is not credible even with a single active failure.
_X_ Other, see remarks.

Seismic Design Analysis

___ Only SRE is in the room; therefore, there are no seismically induced failures (Category 2/1 interactions).
_X_ The NSRE in the room is seismically restrained (upgraded to Category 1 requirements); therefore, no seismically induced failures of these restraints are postulated.
___ The NSRE, which is postulated to fail as a result of an SSE, does not impact SRE.
___ Other, see remarks.

Missile Analysis

_X_ No credible missile sources exist in the room.
___ Missiles from rotating components generated within the room contain insufficient energy to escape their equipment housing(s).
___ Other, see remarks.

Pipe Break Analysis

_X_ There are no high-energy lines in the room.
___ The high-energy line breaks have been evaluated and do not adversely affect SRE.
___ Other, see remarks.

Remarks

1. The flooding from sources located in this room will not impair the safe shutdown capability of the SRE

TABLE 3F-1 (SHEET 69 OF 84)

Listing of safety-related items in room R-D76

Item Number	Description	Equipment Designation	Essential Equipment	Seismic Category 1
1.	Leak detection switch	LSH 9872		Y
2.	Refueling water storage tank to containment spray pump 1, valve	HV 9017A		Y
3.	Leak detection switch	LSH 9868A		Y
4.	Train A raceway	Conduits and cabletrays	Y	Y
5.	Containment spray pump	1-1206-P6-001	Y	Y
6.	Piping	1-1206-001-12 in.	Y	Y
		1-1206-005-8 in.	Y	Y
		1-1202-110-2 in.	Y	Y
		1-1202-111-2 in.	Y	Y
		1-1206-036-3 in.	Y	Y
		1-1206-003-10 in.	Y	Y
		1-1202-003-2 in.	Y	Y
		1-1202-003-3 in.	Y	Y
		1-1204-007-10 in.	Y	Y
		1-1202-004-2 in.	Y	Y
		1-1202-004-3 in.	Y	Y
		1-1202-105-2 in.	Y	Y
		1-1202-294-3/4 in.	Y	Y
		1-1202-477-2 in.	Y	Y
		1-1206-005-3 in.	Y	Y
		1-1206-022-3/4 in.	Y	Y
		1-1206-023-3/4 in.	Y	Y
		1-1206-031-3/4 in.	Y	Y
		1-1206-047-3 in.	Y	Y
		1-1206-051-3/4 in.	Y	Y
		1-1206-070-1 in.	Y	Y
		1-1206-152-2 in.	Y	Y
		1-1206-223-2 in.	Y	Y
7.	Containment sump pump relief valve	PSV-9007A		Y
8.	Containment spray pump room cooler temperature switch	TISH-12207	Y	Y
9.	Containment spray train A	1-1206-6001		

TABLE 3F-1 (SHEET 70 OF 84)

Room Number R-D77 Title Containment Spray Pump Room Train B

Flooding Analysis

___ Flooding from sources within the room, coincident with the most limiting single active failure (assumed in accordance with paragraphs 3.6.1.1.F and 3.6.1.1.G) will not preclude mitigation of the event or safe shutdown of the plant.
_X_ Flooding from sources external to the room is not credible even with a single active failure.
___ Other, see remarks.

Seismic Design Analysis

___ Only SRE is in the room; therefore, there are no seismically induced failures (Category 2/1 interactions).
_X_ The NSRE in the room is seismically restrained (upgraded to Category 1 requirements); therefore, no seismically induced failures of these restraints are postulated.
___ The NSRE, which is postulated to fail as a result of an SSE, does not impact SRE.
___ Other, see remarks.

Missile Analysis

___ No credible missile sources exist in the room.
_X_ Missiles from rotating components generated within the room contain insufficient energy to escape their equipment housing(s).
___ Other, see remarks.

Pipe Break Analysis

_X_ There are no high-energy lines in the room.
___ The high-energy line breaks have been evaluated and do not adversely affect SRE.
___ Other, see remarks.

Remarks

1. The only equipment in this room is associated with containment spray system, which is not essential in this case.

TABLE 3F-1 (SHEET 71 OF 84)

Listing of safety-related
items in room R-D77

Item Number	Description	Equipment Designation	Essential Equipment	Seismic Category 1
1.	Leak detection switch	LSH 9869		Y
2.	Radwaste to containment spray pump 2, valve	HV 9017B		Y
3.	Train B raceway	Conduits and cabletrays	Y	Y
4.	Containment spray pump	1-1206-P6-002		Y
5.	Air-handling unit	1-1555-A7-010		Y
6.	Piping	1-1202-151-2 in.	Y	Y
		1-1202-006-2 in.	Y	Y
		1-1204-038-10 in.	Y	Y
		1-1206-004-12 in.	Y	Y
		1-1206-002-12 in.	Y	Y
		1-1206-006-8 in.	Y	Y
		1-1592-044-1 1/2 in.	Y	Y
		1-1592-054-1 1/2 in.	Y	Y
		1-1202-006-3 in.	Y	Y
		1-1202-310-3/4 in.	Y	Y
		1-1202-483-2 in.	Y	Y
		1-1204-221-2 in.	Y	Y
		1-1206-004-10 in.	Y	Y
		1-1206-006-2 in.	Y	Y
		1-1206-019-3 in.	Y	Y
		1-1206-027-3/4 in.	Y	Y
		1-1206-048-3 in.	Y	Y
		1-1206-052-3/4 in.	Y	Y
		1-1206-071-1 in.	Y	Y
		1-1555-070-1/2 in.	Y	Y
		1-1609-035-3/4 in.	Y	Y
		1-1609-036-3/4 in.	Y	Y
7.	Containment spray pumproom cooler temperature switch	TISH-12207	Y	Y
8.	Containment spray pumproom, train B level switch	LSH-9873	Y	Y
9.	Containment spray pumproom cooler temperature switch	TISH-12213	Y	Y

TABLE 3F-1 (SHEET 72 OF 84)

Room Number R-D100 Title Pipe Chase Train A

Flooding Analysis

___ Flooding from sources within the room, coincident with the most limiting single active failure (assumed in accordance with paragraphs 3.6.1.1.F and 3.6.1.1.G), will not preclude mitigation of the event or safe shutdown of the plant.
___ Flooding from sources external to the room is not credible even with a single active failure.
_X_ Other, see remarks.

Seismic Design Analysis

___ Only SRE is in the room; therefore, there are no seismically induced failures (Category 2/1 interactions).
_X_ The NSRE in the room is seismically restrained (upgraded to Category 1 requirements); therefore, no seismically induced failures of these restraints are postulated.
___ The NSRE, which is postulated to fail as a result of an SSE, does not impact SRE.
___ Other, see remarks.

Missile Analysis

X No credible missile sources exist in the room.
___ Missiles from rotating component generated within the room contain insufficient energy to escape their equipment housing(s).
___ Other, see remarks.

Pipe Break Analysis

_X_ There are no high-energy lines in the room.
___ The high-energy line breaks have been evaluated and do not adversely affect SRE.
___ Other, see remarks.

Remarks

1. The flooding from sources located in this room will not impair the safe shutdown capability of the SRE.

TABLE 3F-1 (SHEET 73 OF 84)

Listing of safety-related
items in room R-D100

Item Number	Description	Equipment Designation	Essential Equipment	Seismic Category 1
1.	Pipe chase leak detection switch	LSH 9842		Y
2.	Pipe chase leak detection switch	LSH 9846		Y
3.	Train A raceway	Conduits and cabletrays	Y	Y
4.	Piping	1-1205-007-8 in.	Y	Y
		1-1592-031-2 1/2 in.	Y	Y
		1-1592-020-2 1/2 in.	Y	Y
		1-1205-003-14 in.	Y	Y
		1-1204-001-12 in.		Y
		1-1202-111-2 in.	Y	Y
		1-1202-110-2 in.	Y	Y
		1-1205-010-12 in.	Y	Y
		1-1205-009-8 in.	Y	Y
		1-1204-006-24 in.	Y	Y
		1-1204-192-8 in.	Y	Y

TABLE 3F-1 (SHEET 74 OF 84)

Room Number R-D101 Title Pipe Chase Train B

Flooding Analysis

___ Flooding from sources within the room, coincident with the most limiting single active failure (assumed in accordance with paragraphs 3.6.1.1.F and 3.6.1.1.G), will not preclude mitigation of the event or safe shutdown of the plant.
___ Flooding from sources external to the room is not credible even with a single active failure.
_X_ Other, see remarks.

Seismic Design Analysis

___ Only SRE is in the room; therefore, there are no seismically induced failures (Category 2/1 interactions).
_X_ The NSRE in the room is seismically restrained (upgraded to Category 1 requirements); therefore, no seismically induced failures of these restraints are postulated.
___ The NSRE, which is postulated to fail as a result of an SSE, does not impact SRE.
___ Other, see remarks.

Missile Analysis

_X_ No credible missile sources exist in the room.
___ Missiles from rotating components generated within the room contain insufficient energy to escape their equipment housing(s).
___ Other, see remarks.

Pipe Break Analysis

_X_ There are no high-energy lines in the room.
___ The high-energy line breaks have been evaluated and do not adversely affect SRE.
___ Other, see remarks.

Remarks

1. The flooding from sources located in this room will not impair the safe shutdown capability of the SRE.

TABLE 3F-1 (SHEET 75 OF 84)

Listing of safety-related items in room R-D101

Item Number	Description	Equipment Designation	Essential Equipment	Seismic Category 1
1.	Train B raceway	Conduits and cabletrays	Y	Y
2.	Piping	1-1205-004-14 in.	Y	Y
		1-1205-008-8 in.	Y	Y
		1-1206-006-8 in.		Y
		1-1206-002-12 in.		Y
		1-1202-155-2 in.	Y	Y
		1-1202-156-2 in.	Y	Y
		1-1205-009-8 in.	Y	Y
		1-1204-006-12 in.	Y	Y
		1-1204-038-14 in.	Y	Y
		1-1204-006-24 in.	Y	Y
		1-1208-131-2 in.	Y	Y
		1-1208-241-3 in.	Y	Y
		1-1208-242-2 in.	Y	Y
		1-1204-221-2 in.	Y	Y
		1-1205-105-2 in.	Y	Y
		1-1208-017-2 in.	Y	Y
		1-1208-241-3 in.	Y	Y
		1-1208-450-2 in.	Y	Y

TABLE 3F-1 (SHEET 76 OF 84)

Room Number R-D121 Title Passage

Flooding Analysis

___ Flooding from sources within the room, coincident with the most limiting single active failure (assumed in accordance with paragraphs 3.6.1.1.F and 3.6.1.1.G), will not preclude mitigation of the event or safe shutdown of the plant.
___ Flooding from sources external to the room is not credible even with a single active failure.
_X_ Other, see remarks.

Seismic Design Analysis

___ Only SRE is in the room; therefore, there are no seismically induced failures (Category 2/1 interactions).
_X_ The NSRE in the room is seismically restrained (upgraded to Category 1 requirements); therefore, no seismically induced failures of these restraints are postulated.
___ The NSRE, which is postulated to fail as a result of an SSE, does not impact SRE.
___ Other, see remarks.

Missile Analysis

_X_ No credible missile sources exist in the room.
___ Missiles from rotating components generated within the room contain insufficient energy to escape their equipment housing(s).
___ Other, see remarks.

Pipe Break Analysis

_X_ There are no high-energy lines in the room.
___ The high-energy line breaks have been evaluated and do not adversely affect SRE.
___ Other, see remarks.

Remarks

1. Flooding from sources located in this room will not impair the safe shutdown capability of the SRE.

TABLE 3F-1 (SHEET 77 OF 84)

Listing of safety-related items in room R-D121

Item Number	Description	Equipment Designation	Essential Equipment	Seismic Category 1
1.	RHR miniflow switch	FIS-0610	Y	Y
2.	Train A raceway	Conduits and cabletrays	Y	Y
3.	Residual heat removal LP Yet bypass, train A flow transmitter	FT-0618	Y	Y

TABLE 3F-1 (SHEET 78 OF 84)

Room Number R-D122 Title Passage

Flooding Analysis

___ Flooding from sources within the room, coincident with the most limiting single active failure (assumed in accordance with paragraphs 3.6.1.1.F and 3.6.1.1.G), will not preclude mitigation of the event or safe shutdown of the plant.
_X_ Flooding from sources external to the room is not credible even with a single active failure.
___ Other, see remarks.

Seismic Design Analysis

___ Only SRE is in the room; therefore, there are no seismically induced failures (Category 2/1 interactions).
_X_ The NSRE in the room is seismically restrained (upgraded to Category 1 requirements); therefore, no seismically induced failures of these restraints are postulated.
___ The NSRE, which is postulated to fail as a result of an SSE, does not impact SRE.
___ Other, see remarks.

Missile Analysis

_X_ No credible missile sources exist in the room.
___ Missiles from rotating components generated within the room contain insufficient energy to escape their equipment housing(s).
___ Other, see remarks.

Pipe Break Analysis

_X_ There are no high-energy lines in the room.
___ The high-energy line breaks have been evaluated and do not adversely affect SRE.
___ Other, see remarks.

Remarks

1. The flooding from sources located in this room will not impair the safe shutdown capability of the SRE.

TABLE 3F-1 (SHEET 79 OF 84)

Listing of safety-related items in room R-D122

Item Number	Description	Equipment Designation	Essential Equipment	Seismic Category 1
1.	Train A raceway	Conduits and cabletrays	Y	Y
2.	Piping	1-1205-026-3/4 in.	Y	Y
		1-1555-061-1 1/2 in.	Y	Y
		1-1592-020-2 1/2 in.	Y	Y
		1-1592-028-1 1/2 in.	Y	Y
		1-1592-031-2 1/2 in.	Y	Y
		1-1592-036-1 1/2 in.	Y	Y
		1-1592-053-1 1/2 in.	Y	Y
		1-1592-056 1 1/2 in.	Y	Y

TABLE 3F-1 (SHEET 80 OF 84)

Room Number R-D128 Title Cooler Room Train A

Flooding Analysis

_X_ Flooding from sources within the room, coincident with the most limiting single active failure (assumed in accordance with paragraphs 3.6.1.1.F and 3.6.1.1.G) will not preclude mitigation of the event or safe shutdown of the plant.

___ Flooding from sources external to the room is not credible even with a single active failure.

___ Other, see remarks.

Seismic Design Analysis

___ Only SRE is in the room; therefore, there are no seismically induced failures (Category 2/1 interactions).

_X_ The NSRE in the room is seismically restrained (upgraded to Category 1 requirements); therefore, no seismically induced failures of these restraints are postulated.

___ The NSRE, which is postulated to fail as a result of an SSE, does not impact SRE.

___ Other, see remarks.

Missile Analysis

___ No credible missile sources exist in the room.

___ Missiles from rotating components generated within the room contain insufficient energy to escape their equipment housing(s).

_X_ Other, see remarks.

Pipe Break Analysis

_X_ There are no high-energy lines in the room.

___ The high-energy line breaks have been evaluated and do not adversely affect SRE.

___ Other, see remarks.

Remarks

1. Missiles from sources within the room, coincident with the most limiting single active failure (assumed in accordance with paragraphs 3.6.1.1.F and 3.6.1.1.G) will not preclude mitigation of the event or safe shutdown of the plant.

TABLE 3F-1 (SHEET 81 OF 84)

Listing of safety-related items in room R-D128

Item Number	Description	Equipment Designation	Essential Equipment	Seismic Category 1
1.	Train A raceway	Conduits and cableways	Y	Y
2.	Piping	1-1592-036-1 1/2 in.	Y	Y
		1-1592-028-1 1/2 in.	Y	Y
		1-1592-020-2 1/2 in.	Y	Y
		1-1592-031-2 1/2 in.	Y	Y
3.	Air-handling unit	1-1555-A7-007	Y	Y

TABLE 3F-1 (SHEET 82 OF 84)

Room Number R-D130 Title Cooler Room Train B

Flooding Analysis

_X_ Flooding from sources within the room, coincident with the most limiting single active failure (assumed in accordance with paragraphs 3.6.1.1.F and 3.6.1.1.G), will not preclude mitigation of the event or safe shutdown of the plant.
___ Flooding from sources external to the room is not credible even with a single active failure.
___ Other, see remarks.

Seismic Design Analysis

___ Only SRE is in the room; therefore, there are no seismically induced failures (Category 2/1 interactions).
_X_ The NSRE in the room is seismically restrained (upgraded to Category 1 requirements); therefore, no seismically induced failures of these restraints are postulated.
___ The NSRE, which is postulated to fail as a result of an SSE, does not impact SRE.
___ Other, see remarks.

Missile Analysis

___ No credible missile sources exist in the room.
___ Missiles from rotating components generated within the room contain insufficient energy to escape their equipment housing(s).
_X_ Other, see remarks.

Pipe Break Analysis

_X_ There are no high-energy lines in the room.
___ The high-energy line breaks have been evaluated and do not adversely affect SRE.
___ Other, see remarks.

Remarks

1. Missiles from sources within the room, coincident with the most limiting single active failure (assumed in accordance with paragraphs 3.6.1.1.F and 3.6.1.1.G), will not preclude mitigation of the event or safe shutdown of the plant.

TABLE 3F-1 (SHEET 83 OF 84)

Listing of safety-related items in room R-D130

Item Number	Description	Equipment Designation	Essential Equipment	Seismic Category 1
1.	Train B raceway	Conduits and cabletrays	Y	Y
2.	Air-handling unit	1-1555-A7-008	Y	Y

TABLE 3F-1 (SHEET 84 0F 84)

Rooms: R-C60; R-C106; R-C110; R-C125; R-C130

Effects analysis:

Pressure/temperature - There are no high-energy line breaks located in the above rooms. As the above rooms do not have high-energy line breaks and are not break nodes, they are included as a flowpath in the nodal model used in the pressure/temperature analysis of the steam generator blowdown system.

The above rooms are affected by pressure/temperature analysis.

Equipment is designed to withstand the effects of pressure, temperature, and humidity. For the pressure/temperature/humidity data, see table 3.11.B.1-1.

Structures are designed to withstand the short-term pressure/ temperature effects of high-energy line breaks.

TABLE 3F-2

UNIT 1 AFW PUMP HOUSE DESIGN PARAMETERS

Node No.[a] (Btu/lb)	Initial Conditions			Design Conditions			Flood Level (in.)	Nodal Volume (ft^3)	Nodes[a]	Press. Flow Area (ft^2)	Calc. after Break (psia)	Peak Temp. (°F)	Blowdown		
	Pressure (psia)	Temp. (°F)	Rel. Hum. (%)	Pressure (psia)	Temp.[b] (°F)	Rel. Hum. (%)							Time (s)	Mass Flowrate (lb/s)	Enthalpy
													Steam Line		
1.	14.7	120	50	17.7	320	0-100	(c)	12.6×10^3	1-2	24.0	15.4	184	0	0	0
2.	14.7	120	50	17.7	320	0-100	(d)	10.9×10^3	1-3	20.0	15.5	249	0.004	237.4	1188.6
													0.01	210.5	1156.7
3. (atm)	14.7	120	50	-	-	-	-	-	-	-	-	-	0.1	143.8	1187.3
												0.2	126.7	1191.1	
												0.5	110.8	1191.7	
												0.9	104.5	1191.3	
												2.0	100.9	1190.4	
												20	100.7	1190.1	
													Auxiliary Feedwater		
													0	0	
													60	282	
													1800	142	

a. Refer to drawing 1X6DD300 for nodal boundary.

b. The design of the structure assumes a 2-h duration for peak temperature.

c. Node 1 Flood level (in.):
Room 104 - 86
Room 105 - 97.2

d. Node 2 Flood level (in.):
Room 106 - 11

TABLE 3F-3A (SHEET 1 OF 4)

UNIT 1 MSIV/MFIV ROOM FLOODING (CASE 2) AND PRESSURE (CASE 1) ANALYSIS

Node[(a)] No.	Initial Conditions Pressure (psia)	Temp. (°F)	Rel. Hum. (%)	Design Conditions Pressure (psia)	Temp (°F)	Rel. Hum. (%)	Flood Level (in.)	Node Volume (ft^3)	Calc Peak Pressure (psia)
I. Auxiliary Building MSIV/MFIV Area									
1	14.7	120	50	29.7	320	0-100	NA	5520.0	18.4
2	14.7	120	50	29.7	320	0-100	NA	17423.0	18.0
3	14.7	120	50	29.7	320	0-100	7	3505.5	19.1
4	14.7	120	50	29.7	320	0-100	67	6033.88	19.4
5	14.7	120	50	29.7	320	0-100	NA	4138.8	20.3
6	14.7	120	50	29.7	320	0-100	67	4237.0	19.4
7	14.7	120	50	29.7	320	0-100	7	1989.8	18.8
8	14.7	120	50	29.7	320	0-100	NA	12684.8	18.0
9	14.7	120	50	29.7	320	0-100	67	22883.9	20.8
10	14.7	120	50	29.7	320	0-100	NA	9577.0	24.4
11	14.7	120	50	29.7	320	0-100	138	5415.0	23.5
12	14.7	120	50	29.7	320	0-100	NA	4651.2	18.8
13	atm								

TABLE 3F-3A (SHEET 2 OF 4)

Node[a] No.	Initial Conditions Pressure (psia)	Temp. (°F)	Rel. Hum. (%)	Design Conditions Pressure (psia)	Temp (°F)	Rel. Hum. (%)	Flood Level (in.)	Node Volume (ft^3)	Calc Peak Pressure (psia)
II. Auxiliary Building MSIV/MFIV Area Outside Restraint Wall									
1	14.7	120	50	29.7	320	0-100	NA	5520.0	17.5
2	14.7	120	50	29.7	320	0-100	NA	17423.0	17.3
3	14.7	120	50	29.7	320	0-100	7	3505.5	17.4
4	14.7	120	50	29.7	320	0-100	67	6033.88	17.5
5	14.7	120	50	29.7	320	0-100	NA	4138.8	17.2
6	14.7	120	50	29.7	320	0-100	67	4273.0	17.9
7	14.7	120	50	29.7	320	0-100	7	1989.8	17.9
8	14.7	120	50	29.7	320	0-100	NA	12684.8	17.4
9	14.7	120	50	29.7	320	0-100	67	22883.9	17.4
10	14.7	120	50	29.7	320	0-100	NA	9577.0	24.4
11	14.7	120	50	29.7	320	0-100	138	5415.0	23.5
12	14.7	120	50	29.7	320	0-100	NA	4651.2	18.8
13	atm								

TABLE 3F-3A (SHEET 3 OF 4)

Node[a] No.	Initial Conditions Pressure (psia)	Temp. (°F)	Rel. Hum. (%)	Design Conditions Pressure (psia)	Temp (°F)	Rel. Hum. (%)	Flood Level (in.)	Node Volume (ft^3)	Calc Peak Pressure (psia)
III. Control Building MSIV/MFIV Area									
1	14.7	120	50	29.7	320	0-100	NA	3079.9	21.4
2	14.7	120	50	29.7	320	0-100	NA	17617.0	20.2
3	14.7	120	50	29.7	320	0-100	22	11295.2	20.4
4	14.7	120	50	29.7	320	0-100	NA	3769.6	19.8
5	14.7	120	50	29.7	320	0-100	NA	21514.5	19.5
6	14.7	120	50	29.7	320	0-100	22	13740.5	20.3
7	14.7	120	50	29.7	320	0-100	NA	8853.6	16.8
8	atm								
IV. Control Building MSIV/MFIV Area Outside Restraint Wall									
1	14.7	120	50	29.7	320	0-100	16	28805.2	23.5

a. Refer to figure 3F-1 (sheets 1 through 4) for nodal boundary.

TABLE 3F-3A (SHEET 4 OF 4)

Blowdown Data (Case 1)
(Break at Node 10)

Time (s)	Mass Flowrate (lbm/s)	Enthalpy (BTU/lbm)
0.0	0	1188
0.004	18,959	1138
0.008	19,905	1139
0.01	19,399	1137
0.03	17,567	1136
0.06	16,747	1139
0.10	16,030	1140
0.15	15,450	1140
0.20	15,312	1142
1.0	12,994	1153
1.2	12,378	1141
1.4	9304	1119
1.6	14,163	814
1.65	15,040	791
1.80	17,716	725
1.90	18,414	712
2.00	18,831	706
2.15	19,854	700
2.30	19,597	695
3.0	17,259	688
3.4	21,428	668
4.0	20,755	661
4.8	20,415	653

TABLE 3F-3B (SHEET 1 OF 2)

UNIT 1 CONTROL BUILDING MSIV/MFIV VAULT AREA MSLB TEMPERATURE (CASE 3) ANALYSIS

		Initial Conditions			Design Conditions					
Node No.[a]	Description	Pressure (psia)	Temp. (°F)	Rel. Hum. (%)	Pressure (psia)	Temp. (°F)	Rel. Hum. (%)	Volume (ft^3)	Node Elev. (ft)	Calc. Peak[c] Temp. (°F)
1	West Steam Line Room (Lower)	14.7	120	50	29.7	320	0-100	18,361.4	224.0	483.2[c]
2	West Aux. Feedline Room	14.7	120	50	29.7	320	0-100	11,300.0	200.5	399.0
3	East SL Room (Lower)	14.7	120	50	29.7	320	0-100	11,370.0	224.0	413.1
4	East AFL Room	14.7	120	50	29.7	320	0-100	13,740.0	200.5	360.9
5	Entrance Room (Lower)	14.7	120	50	29.7	320	0-100	4,234.0	221.0	390.2
6	Entrance Room (Upper)	14.7	120	50	29.7	320	0-100	4,234.0	239.0	398.7
7	East Penthouse	14.7	120	50	29.7	320	0-100	3,208.0	257.0	428.3
8	West Penthouse	14.7	120	50	29.7	320	0-100	2,338.6	257.0	477.4
9	East SL Room (Upper)	14.7	120	50	29.7	320	0-100	11,370.0	240.5	429.1
10	West Steam Line Room (Upper)	14.7	120	50	29.7	320	0-100	9,180.0	240.5	478.3

TABLE 3F-3B (SHEET 2 OF 2)

Flow Path Data				Blowdown Data (1.0 ft^2 MSLB[b] at 102% Power)		
Flow Path No.	Upstream Node	Downstream Node	Flow Area ft^2	Time (s)	Mass Flow-rate (lbm/s)	Enthalpy (Btu/lbm)
1	4	3	145.0	0.0	0.0	0.0
2	2	1	139.0	1.5	1980.0	1192.0
3	1	3	218.6	6.5	1904.0	1194.0
4	2	4	245.0	14.0	2282.0	1188.0
5	3	5	95.0	15.0	2283.0	1189.0
6	9	6	144.0	15.5	2173.0	1191.0
7	9	7	139.5	23.5	1490.0	1201.0
8	1	8	120.0	33.0	1187.0	1204.0
9	1	9	205.5	55.5	924.2	1204.0
10	3	9	876.6	64.5	762.0	1236.0
11	1	atm	4.5	81.5	203.9	1288.0
12	2	atm	6.85	90.5	100.3	1298.0
13	3	atm	4.5	123.5	78.0	1304.0
14	4	atm	6.85	162.5	78.0	1305.0
15	5	atm	141.0	1800.0	78.0	1287.0
16	6	atm	141.0	1812.0	12.5	1295.0
17	7	atm	164.35			
18	8	atm	135.85			
19	5	6	268.0			
20	1	break	1.0			
21	1	10	725.0			

a. Refer to figure 3F-2 for nodal diagrams.

b. Main steam line break.

c. The calculated peak temperatures correspond to a 1.0 ft^2 MSLB at 102% power (102% of 3579 MWt). This break resulted in the overall highest peak temperature which occurred in break node 1. The peak temperatures and pressures for other nodes actually may be higher for other breaks.

TABLE 3F-4 (SHEET 1 OF 3)

EVALUATION OF RCS LOOP BRANCH LINE BREAKS

RCS Loop Nozzle No.	Branch Line Description	Branch Line Identification	Pipe Break Evaluation
Loop 1 cold leg			
Nozzle - 5	Boron injection tank (safety injection system (SIS))	1204-243-1£ in.	Pipe whip: Pipe whips but does not result in the failure of any essential components. Jet impingement: Breaks do not result in the failure of any essential components.
Nozzle - 14	Accumulator injection	1204-124-10 in.	Pipe whip: Two restraints were installed to prevent pipe whip.(b) Jet impingement: One barrier was installed to prevent the failure of any essential components.(b)
	Upstream of valve 083	1204-120-10 in. 1204-042-6 in. 1204-036-2 in.	Pipe whip: Two restraints were installed to prevent pipe whip. Jet impingement: Breaks do not result in the failure of any essential components.
Nozzle - 11	CVCS normal charging line	1208-009-3 in. to valve 035 (second check valve)	Pipe whip: Three restraints were installed to prevent pipe whip. Jet impingement: Breaks do not result in the failure of any essential components.
	CVCS normal charging upstream of valve 035(second valve)	1208-008-3 in.	Pipe whip: One restraint was installed to prevent pipe whip. Jet impingement: Breaks do not result in the failure of any essential components.
Nozzle - 12	Pressurizer spray header	1201-029-4 in.	Pipe whip: One restraint was installed to prevent pipe whip. Jet impingement: Breaks do not result in the failure of any essential components.
Loop 1 crossover leg			
Nozzle - 18	Reactor coolant loop drain	1201-031-2 in.	Pipe whip: Pipe whips but does not result in the failure of any essential components. Jet impingement: Breaks do not result in the failure of any essential components.
Loop 1 hot leg			
Nozzle - 15	RHR system recirculation/SIS	1201-036-12 in. (b)	Pipe whip: Pipe whips but does not result in the failure of any essential components. Jet impingement: Breaks do not result in the failure of any essential components.

TABLE 3F-4 (SHEET 2 OF 3)

RCS Loop Nozzle No.	Branch Line Description	Branch Line Identification	Pipe Break Evaluation
Loop 2 cold leg			
Nozzle - 5	Boron injection tank (SIS)	1204-244-1 1/2 in.	Pipe whip: Pipe whips but does not result in the failure of any essential components. Jet impingement: Breaks do not result in the failure of any essential components.
Nozzle - 14	Accumulator injection	1204-125-10 in.[b]	Pipe whip: Two restraints were installed to prevent pipe whip.[b] Jet impingement: Breaks do not result in the failure of any essential components.[b]
	Upstream of valve 084	1204-121-10 in. 1204-043-6 in. 1204-035-2 in.	Pipe whip: Pipe whips but does not result in the failure of any essential components. Jet impingement: Breaks do not result in the failure of any essential components.
Loop 2 crossover leg			
Nozzle - 18	Reactor coolant loop drain	1201-042-2 in.	Pipe whip: Pipe whips but does not result in the failure of any essential components. Jet impingement: Breaks do not result in the failure of any essential components.
Loop 2 hot leg			
Nozzle - 13	RHR SIS injection	1204-024-6 in.	Pipe whip: One restraint was installed to prevent pipe whip. Jet impingement: Breaks do not result in the failure of any essential components.
Loop 3 cold leg			
Nozzle - 5	Boron injection tank (SIS)	1204-245-1 1/2 in.	Pipe whip: Pipe whips but does result in the failure of any essential components. Jet impingement: Breaks do not result in the failure of any essential components.
Nozzle - 14	Accumulator injection	1204-126-10 in.[b]	Pipe whip: Two restraints were installed to prevent pipe whip.[b] Jet impingement: Breaks do not result in the failure of any essential components.[b]
	Upstream of valve 085	1204-122-10 in. 1204-044-6 in. 1204-034-2 in.	Pipe whip: Two restraints were installed to prevent pipe whip. Jet impingement: Breaks do not result in the failure of any essential components.
Nozzle - 4	Letdown (CVCS)	1201-048-3 in.	Pipe whip: Pipe whips but does not result in the failure of any essential components. Jet impingement: Breaks do not result in the failure of any essential components.
Loop 3 crossover leg			
Nozzle - 18	Reactor coolant loop drain	1201-046-2 in.[c]	Pipe whip: Pipe whips but does not result in the failure of any essential components. Jet impingement: Breaks do not result in the failure of any essential components.

TABLE 3F-4 (SHEET 3 OF 3)

RCS Loop Nozzle No.	Branch Line Description	Branch Line Identification	Pipe Break Evaluation
Loop 3 hot leg			
Nozzle - 13	RHR SIS injection	1204-025-6 in.	Pipe whip: One restraint was installed to prevent pipe whip. Jet impingement: Breaks do not result in the failure of any essential components.
Loop 4 cold leg			
Nozzle - 5	Boron injection tank (SIS)	1204-246-1 1/2 in.	Pipe whip: Pipe whips but does not result in the failure of any essential components. Jet impingement: Breaks do not result in the failure of any essential components.
Nozzle - 14	Accumulator injection	1204-127-10 in.(b)	Pipe whip: Two restraints were installed to prevent pipe whip.(b) Jet impingement: One barrier was installed to prevent the failure of any essential components.(b)
	Upstream of valve 086	1204-123-10 in.(b) 1204-045-6 in. 1204-033-2 in.	Pipe whip: Pipe whips but does not result in the failure of any essential components. Jet impingement: Breaks do not result in the failure of any essential components.
Nozzle - 12	Pressurizer spray header	1201-030-4 in. 1201-030-6 in. 1208-012-2 in.	Pipe whip: One restraint was installed to prevent pipe whip. Jet impingement: Breaks do not result in the failure of any essential components.
Nozzle - 11	CVCS alternate charging line	1208-007-3 in. to valve 037 (second check valve)	Pipe whip: Three restraints were installed to prevent pipe whip. Jet impingement: Breaks do not result in the failure of any essential components.
	Upstream of valve 037 (second valve)	1208-488-3 in.	Pipe whip: One restraint was installed to prevent pipe whip. Jet impingement: Breaks do not result in the failure of any essential components.
Loop 4 crossover leg			
Nozzle - 18	Reactor coolant loop drain	1201-051-2 in. with excess letdown	Pipe whip: Pipe whips but does not result in the failure of any essential components. Jet impingement: Breaks do not result in the failure of any essential components.
Loop 4 hot leg			
Nozzle - 15	RHR system recirculation/SIS injection	1201-049-12 in.(b) 1204-021-6 in.	Pipe whip: One restraint was installed. Pipe whips but does not result in failure of any essential components. Jet impingement: One barrier was installed to prevent the failure of any essential components.(b)

a. See drawing AX6DD309.
b. Applies to Unit 1 only.
c. Applies to Unit 2 only.

TABLE 3F-5

JET IMPINGEMENT BARRIERS

System Line Number	Break Location	Target Number	Barrier Number	Building
Accumulator injection loop-4 1204-127-10 in.	P-14DB-0411-L-1 P-14DB-0411-L-2	1201-029-4 in.	BC-3	Containment (Unit 1 only)
Main safety loops 1 and 4 from auxiliary building to main steam tunnel 1301-008-38 in.	P-17CA-1059-C	1305-056-26 in.	BT-2	Tunnel IT1
Main feedwater loops 1-4 (tunnel to turbine building) 1305-055-36 in.	P-12EA-1135-C	1301-007-36 in.	BT-1	Tunnel IT1

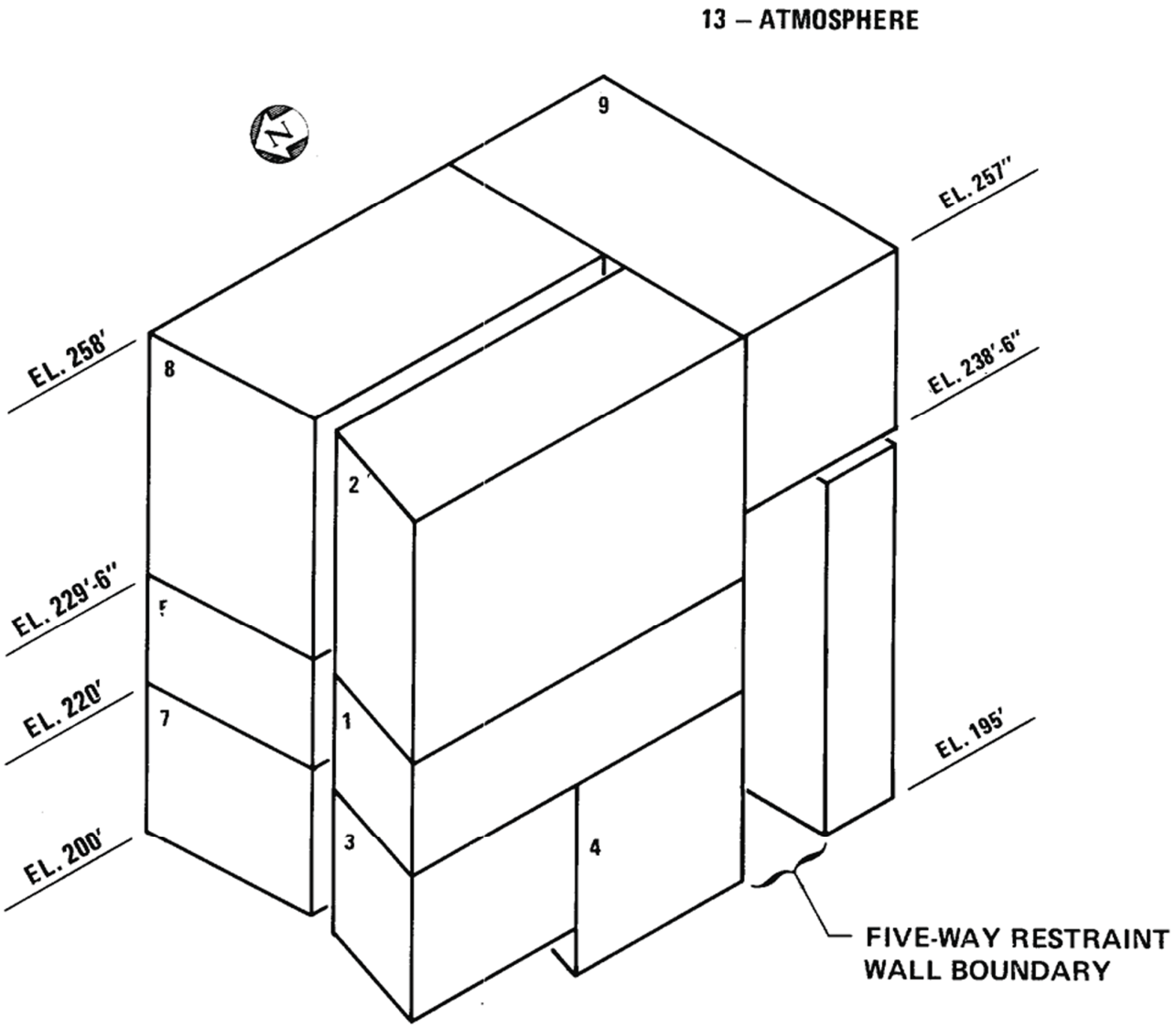

REV 14 10/07

SOUTHERN COMPANY *Energy to Serve Your World®* VOGTLE ELECTRIC GENERATING PLANT UNIT 1 AND UNIT 2	NODAL BOUNDARY FOR AUXILIARY BUILDING – MSIV/MFIV ROOMS
	FIGURE 3F–1 (SHEET 1 OF 4)

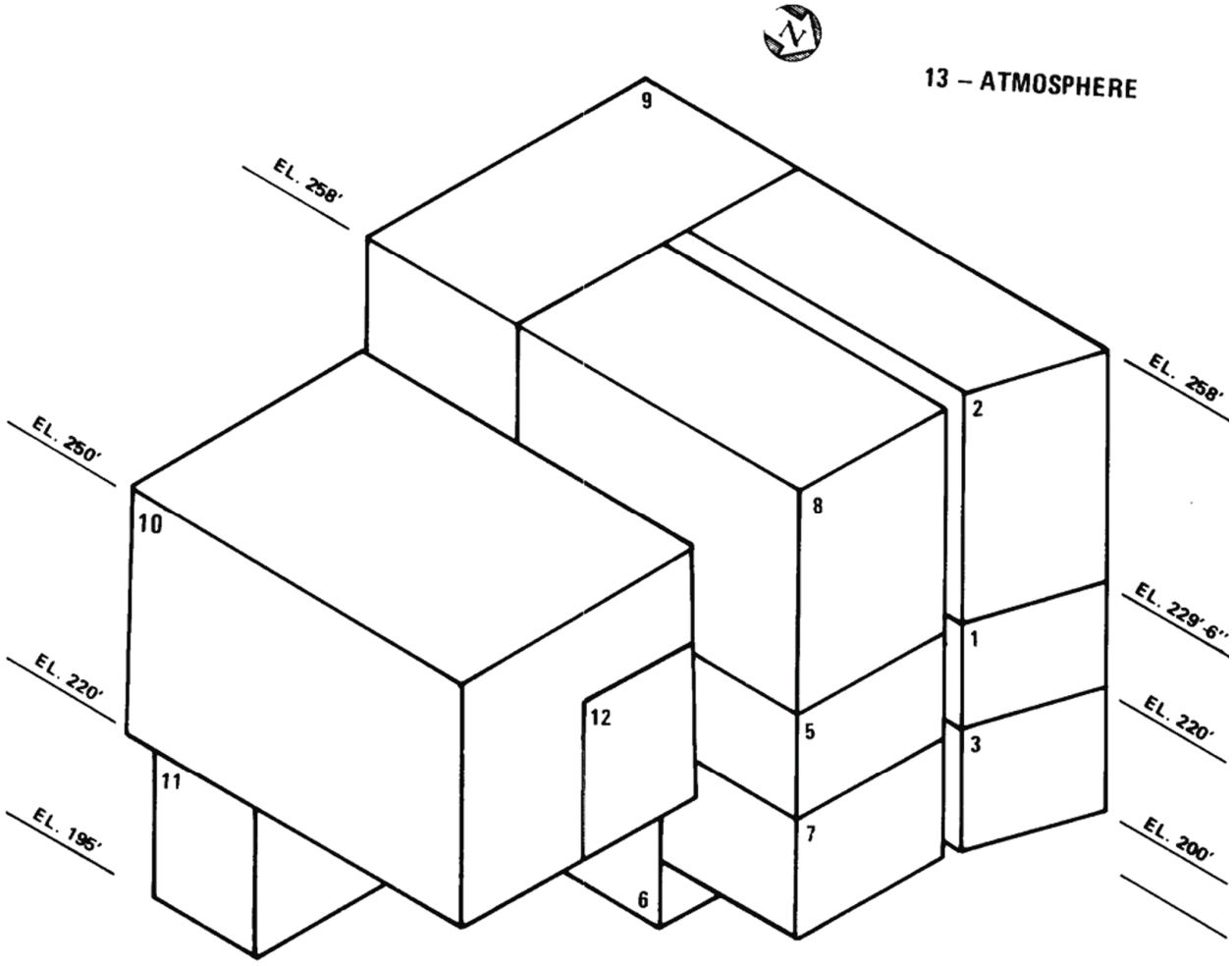

REV 14 10/07

SOUTHERN COMPANY *Energy to Serve Your World®* VOGTLE ELECTRIC GENERATING PLANT UNIT 1 AND UNIT 2	NODAL BOUNDARY FOR AUXILIARY BUILDING – MSIV/MFIV ROOMS
	FIGURE 3F–1 (SHEET 2 OF 4)

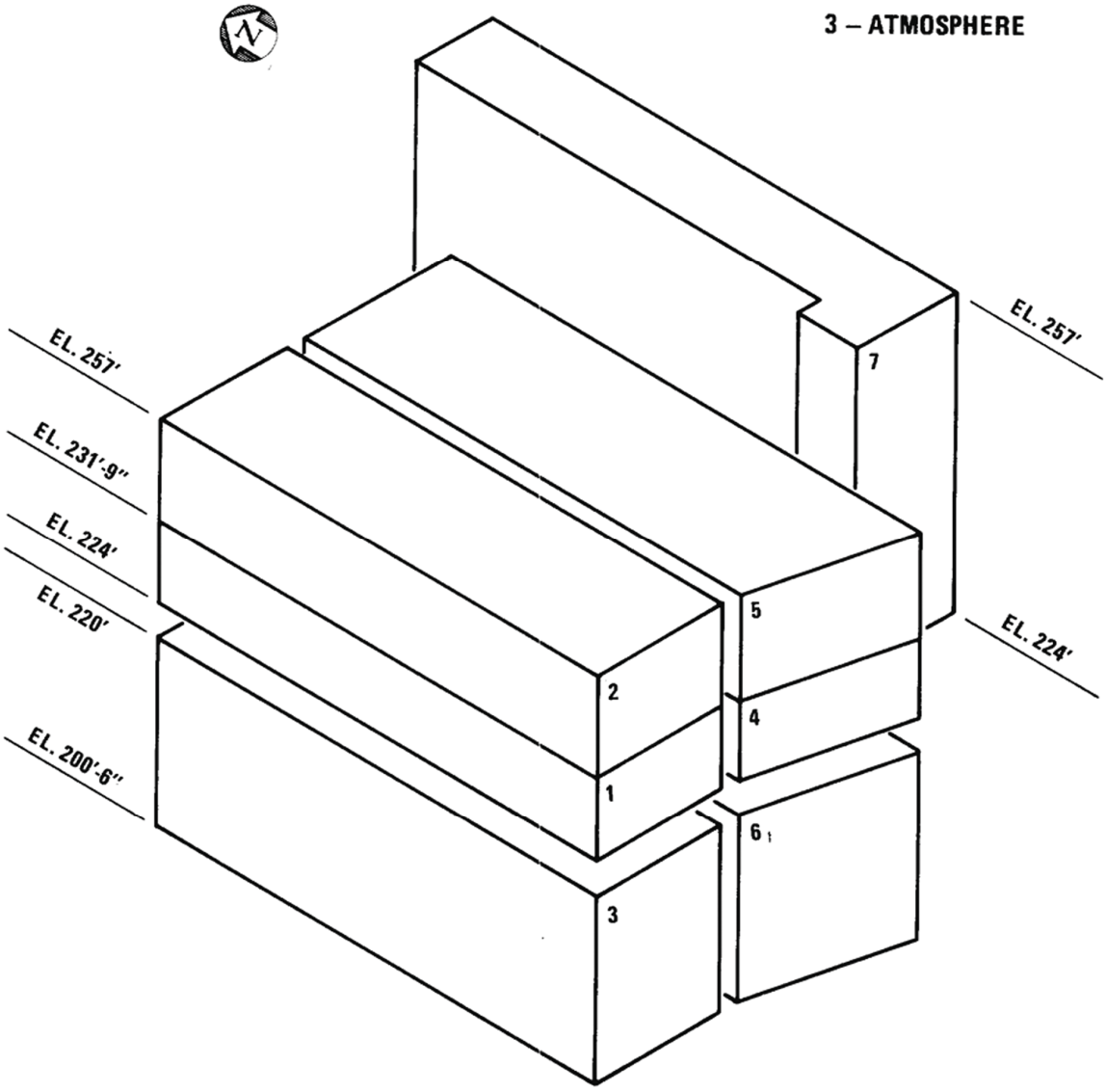

REV 14 10/07

SOUTHERN COMPANY *Energy to Serve Your World®* **VOGTLE** **ELECTRIC GENERATING PLANT** **UNIT 1 AND UNIT 2**	NODAL BOUNDARY FOR CONTROL BUILDING – MSIV/MFIV ROOMS (INSIDE RESTRAINT WALL)
	FIGURE 3F–1 (SHEET 3 OF 4)

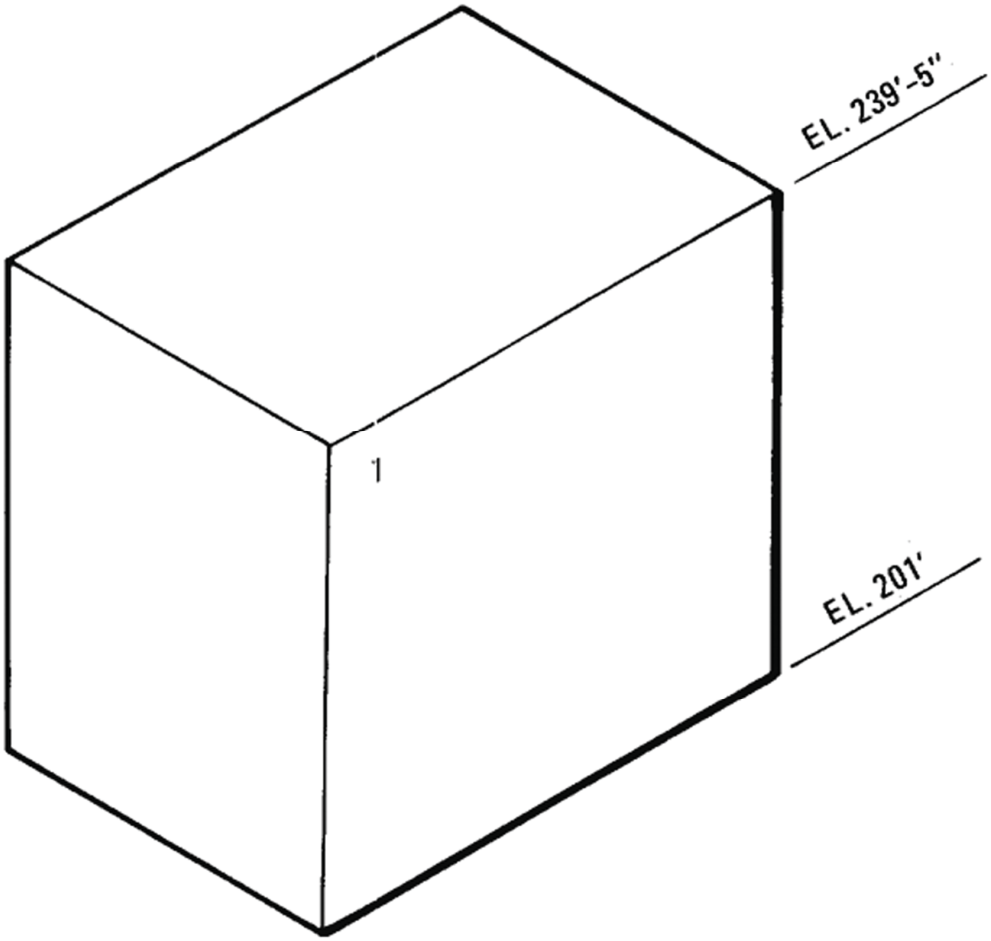

REV 14 10/07

SOUTHERN COMPANY
Energy to Serve Your World®

VOGTLE
ELECTRIC GENERATING PLANT
UNIT 1 AND UNIT 2

NODAL BOUNDARY FOR CONTROL BUILDING – MSIV/MFIV ROOMS (OUTSIDE RESTRAINT WALL)

FIGURE 3F–1 (SHEET 4 OF 4)

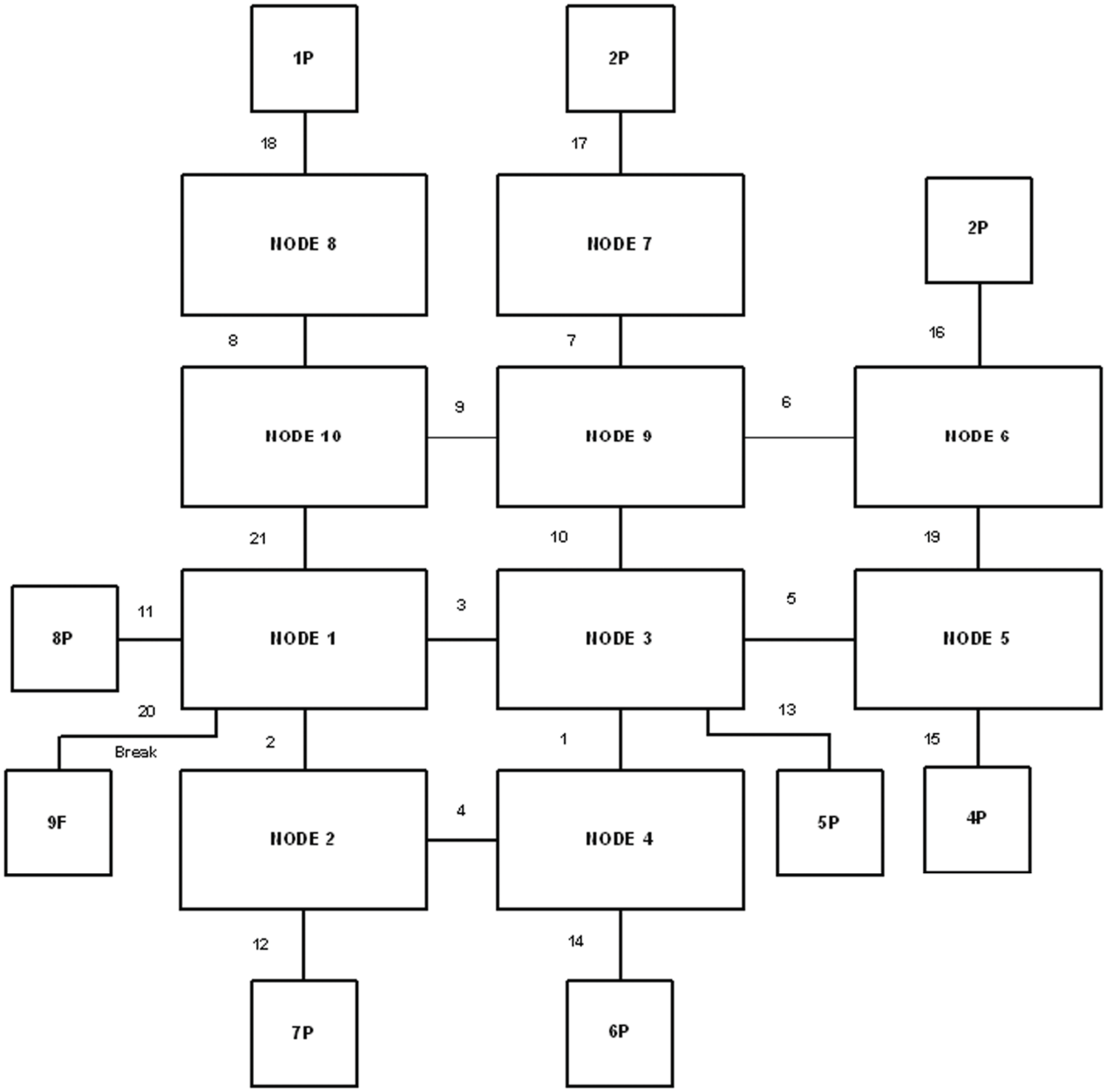

REV 14 10/07

SOUTHERN COMPANY *Energy to Serve Your World®* **VOGTLE ELECTRIC GENERATING PLANT UNIT 1 AND UNIT 2**	NODAL DIAGRAM FOR MSIV/MFIV GOTHIC ANALYSIS FIGURE 3F–2

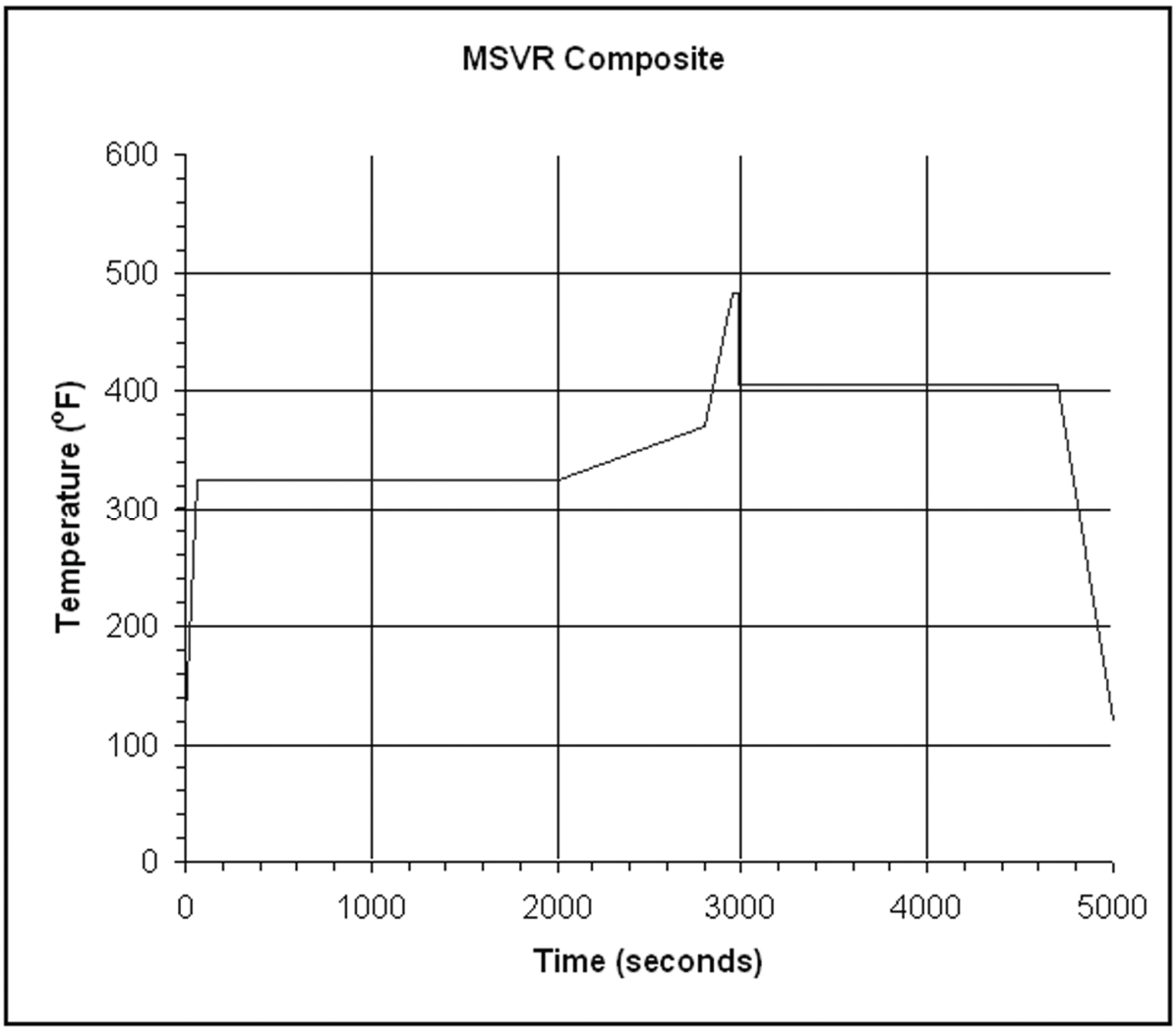

REV 14 10/07

SOUTHERN COMPANY
Energy to Serve Your World®

VOGTLE
ELECTRIC GENERATING PLANT
UNIT 1 AND UNIT 2

TIME–HISTORY PLOT MAXIMUM
COMPARTMENT COMPOSITE TEMPERATURE
FOR MSIV AREA BREAK NODE

FIGURE 3F–3

4.0 REACTOR

4.1 SUMMARY DESCRIPTION

This chapter describes:

A. The mechanical components of the reactor and reactor core, including the fuel rods and fuel assemblies.

B. The nuclear design.

C. The thermal-hydraulic design.

The initial reactor core is composed of an array of fuel assemblies that are identical in mechanical design but different in fuel enrichment. Within each fuel assembly all rods are of the same enrichment. Three different enrichments are employed in the first core: 2.10 (region 1), 2.60 (region 2), and 3.10 (region 3) weight percents. It was required that the initial core loading maximum enrichment not exceed 3.2 weight percent U-235. For subsequent reloads, the target maximum enrichment is up to 5.0 weight percent. Reload fuel shall be similar in physical design to the initial core loading and shall have a maximum enrichment not to exceed 5.0 weight percent U-235.

Reload cores are comprised of 17 x 17 VANTAGE+ with Debris Mitigation Features (VANTAGE+) and/or VANTAGE 5 fuel assemblies. The original referenced design described herein consisted of LOPAR fuel assemblies arranged in a checkered, low-leakage core loading pattern.

The significant mechanical design features of the VANTAGE 5 design, as described in reference 1, relative to the LOPAR fuel design include the following: integral fuel burnable absorbers (IFBA), intermediate flow mixer (IFM) grids, reconstitutable top nozzle (RTN), extended burnup capability, and axial blankets. In addition, a debris filter bottom nozzle (DFBN) replacing the standard nozzle has been implemented. The RTN, DFBN, and extended burnup capability have been introduced in both VEGP Units 1 and 2. Fuel reloads contain an advanced zirconium alloy clad fuel known as ZIRLO®, which is the key feature of the VANTAGE+ fuel design, reference 2, or Optimized ZIRLO™ cladding, reference 3, as well as improved design features including:

- Protective bottom grid,
- Long fuel rod end plugs,
- Annular blanket pellets,
- ZIRLO guide thimbles,
- Instrumentation tube,
- Mid grid, and
- IFM grid.

Beginning with the Region 27 (Cycle 25) reload for Unit 1 and the Region 25 (Cycle 23) reload for Unit 2, the Vogtle units implement the Westinghouse 17x17 OFA PRIME™ fuel assembly

design which is an improved version of the 17x17 VANTAGE+ fuel design. The PRIME™ fuel assembly design incorporates advanced features to improve fuel reliability, dimensional stability and corrosion resistance of the 17x17 VANTAGE+ with Debris Mitigation Features fuel design. The PRIME™ fuel features include Low Tin ZIRLO grid strap material to improve corrosion resistances, the PRIME™ Bottom Nozzle incorporates a low pressure drop design along with lower side skirts to help improve debris resistance and the external dashpot tube which stiffens the dashpot region of the fuel assembly to minimize the potential for incomplete rod insertion. The PRIME™ advanced fuel design has been extensively evaluated, tested and analyzed and it was demonstrated that it meets all of the applicable mechanical design and safety criteria.

A fuel assembly is composed of 264 fuel rods in a 17 x 17 square array. The center position in the fuel assembly is reserved for incore instrumentation. The remaining 24 positions in the fuel assembly have guide thimbles which are joined to the top and bottom nozzles of the fuel assembly and serve to support the fuel grids. A fuel assembly may have limited substitution of zirconium alloy or stainless steel filler rods in place of fuel rods, in accordance with NRC approved applications of fuel rod configurations. The fuel grids consist of an egg crate arrangement of interlocked straps that maintain lateral spacing between the rods. The grid straps have spring fingers and dimples which grip and support the fuel rods. The middle grids also have coolant-mixing vanes. The flow mixer grid straps contain only support dimples and coolant mixing vanes.

The fuel rods consist of enriched uranium, in the form of cylindrical pellets of uranium dioxide, contained in Zircaloy-4 tubing. Commencing with Unit 2 Cycle 6, the fresh fuel region uses an advanced zirconium alloy tubing known as ZIRLO to provide improved fuel performance, reference 2. Additionally, Optimized ZIRLO cladding material has been approved for use in Vogtle 1 and 2 by the NRC, reference 4. The tubing is plugged and seal welded at the ends to encapsulate the fuel. An axial blanket of natural, mid-enriched, or fully enriched solid or annular UO_2 fuel pellets may be placed at the ends of the enriched fuel pellet stack. The natural or mid-enriched axial blanket pellets are used to reduce the neutron leakage and to improve fuel utilization. The annular blanket pellets are used to increase the void volume for gas accommodation within the fuel rod. A second fuel rod type is utilized to varying degrees within some fuel assemblies. These rods use zirc diboride (ZrB_2) coated fuel pellets in the central portion of the fuel stack. All fuel rods are pressurized internally with helium during fabrication to reduce clad creep-down during operation and thereby to increase fatigue life.

Depending on the position of the assembly in the core, the guide thimbles are used for rod cluster control assemblies (RCCAs), neutron source assemblies, burnable absorber (BA) assemblies, or stainless steel rod insert assemblies (SSRIA). If none of these is required, the guide thimbles may be fitted with plugging devices to limit bypass flow. Standard borosilicate glass rods were used in first cycles. Wet annular burnable absorbers (WABA) and/or IFBA coated fuel pellets are used in subsequent reloads.

The bottom nozzle is a boxlike structure which serves as the lower structural element of the fuel assembly and directs the coolant flow distribution to the assembly. The top nozzle assembly serves as the upper structural element of the fuel assembly and provides a partial protective housing for the RCCA or other components.

The RCCAs consist of 24 absorber rods fastened at the top end to a common hub or spider assembly. Each absorber rod consists of either hafnium or an alloy of silver-indium-cadmium clad in stainless steel. The control rod assemblies shall contain a nominal 142 in. of absorber material. The nominal absorber composition shall be 95.5 percent natural hafnium and 4.5 percent natural zirconium and/or 80 percent silver, 15 percent indium, and 5 percent cadmium. All control rods shall be clad with stainless steel. The RCCAs are used to control relatively rapid changes in reactivity and to control the axial power distribution.

The reactor core is cooled and moderated by light water at a pressure of 2250 psia. Soluble boron in the moderator/coolant serves as a neutron absorber. The concentration of boron is varied to control reactivity changes that occur relatively slowly, including the effects of fuel burnup and transient xenon. Burnable absorber rods are also employed in the first core to limit the amount of soluble boron required and, thereby, to maintain the desired negative reactivity coefficients. Additional boron in the form of WABAs and/or IFBAs may be employed to limit the moderator temperature coefficient and the local power peaking.

The nuclear design analyses establish the core locations for control rods and BAs and define design parameters, such as fuel enrichments and boron concentration in the coolant. The nuclear design analyses establish that the reactor core and the reactor control system satisfy all design criteria, even if the RCCA of highest reactivity worth is in the fully withdrawn position. The core has inherent stability against diametral and azimuthal power oscillations. Axial power oscillations which may be induced by load changes and resultant transient xenon may be suppressed by the use of the RCCAs.

The thermal-hydraulic design analyses establish that adequate heat transfer is provided between the fuel clad and the reactor coolant. The thermal design takes into account local variations in dimensions, power generation, flow distribution, and mixing. The mixing vanes incorporated in the fuel assembly spacer grid design and the VANTAGE 5 fuel assembly IFMs induce additional flow mixing between the various flow channels within a fuel assembly as well as between adjacent assemblies.

The performance of the core is monitored by fixed neutron detectors outside the core, movable neutron detectors within the core, and thermocouples at the outlet of selected fuel assemblies. The excore nuclear instrumentation provides input to automatic control functions.

Table 4.1-1 presents a comparison of the principal nuclear, thermal-hydraulic, and mechanical design parameters of the VEGP units with parameters of the SNUPPS units (Docket No. STN 50-482, STN 50-483, STN 50-485, and STN 50-486).

The analytical techniques employed in the core design are tabulated in table 4.1-2. The mechanical loading conditions considered for the core internals and components are tabulated in table 4.1-3. Specific or limiting loads considered for design purposes of the various components are listed as follows: fuel assemblies in paragraph 4.2.1.5; control rods, BA rods, neutron source rods, thimble plug assemblies, and the SSRIA in paragraph 4.2.1.6. The dynamic analyses, input forcing functions, and response loadings for the control rod drive system and reactor vessel internals are presented in subsections 3.9.4 and 3.9.5.

4.1.1 REFERENCES

1. Davidson, S. L. and Kramer, W. R., eds, "Reference Core Report VANTAGE 5 Fuel Assembly," WCAP-10444-P-A (Proprietary) and WCAP-10445-NP-A (Nonproprietary), September 1985.

2. Davidson, S. L. and Nuhfer, D. L., "VANTAGE+ Fuel Assembly Reference Core Report," WCAP-12610-A (Proprietary) and WCAP-14342-A (Nonproprietary), April 1995.

3. Shah, H., “Optimized ZIRLO™,” WCAP-12610-P-A & CENPD-404-P-A Addendum 1-A, July 2006.

4. U.S. NRC, R. E. Martin letter to SNC, C. R. Pierce, “Joseph M. Farley Nuclear Plant, Units 1 and 2, and Vogtle Electric Generating Plant, Units 1 and 2, Issuance of

Amendments Regarding Use of Optimized ZIRLO (CAC Nos. MF7480, MF7481, MF7482, and MF7483),” August 04, 2016 (Agencywide Documents Access and Management System (ADAMS) Accession No. ML16179A386).

TABLE 4.1-1 (SHEET 1 OF 4)

REACTOR DESIGN COMPARISON TABLE

	Thermal and Hydraulic Design Parameters		VEGP (ORIGINAL DESIGN)	VEGP (UPRATE DESIGN)[h]	SNUPPS
1.	Reactor core heat output (MWt)		3411	3626	3411
2.	Reactor core heat output (10^6 Btu/h)		11,639	12,372	11,639
3.	Heat generated in fuel (%)		97.4	97.4	97.4
4.	System pressure, nominal (psia)		2250	2250	2250
5	System pressure, minimum steady state (psia)		2220	2200	2220
6.	Minimum DNBR for design transients				
	Typical flow channel	(LOPAR) (VANTAGE + / VANTAGE 5)	1.30	(g) 1.24	1.30
	Thimble (cold wall) flow channel	(LOPAR) (VANTAGE + / VANTAGE 5)		(g) 1.23	
7.	DNB correlation	(LOPAR) VANTAGE + / (VANTAGE 5)	R (W-3 with modified spacer factor)	(g) WRB-2 [d]	R (W-3 with modified spacer factor)
Coolant flow[e]					
8.	Total vessel flowrate (10^6 lbm/h) (Based on thermal design flow) (Based on minimum measured flow)		142.1	139.5 143.0 [f]	142.1
9.	Effective flowrate for heat transfer (106 lbm/h)		133.9	130.6	133.9
10.	Effective flow area for heat transfer(ft^2)	(LOPAR) (VANTAGE + / VANTAGE 5)	51.1	(g) 54.1	51.1
11.	Average velocity along fuel rods (ft/s)	(LOPAR) (VANTAGE + / VANTAGE 5)	16.6	(g) 15.3	16.6
					2.62
12.	Average mass velocity (10^6 lbm/h-ft^2)	(LOPAR) (VANTAGE + / VANTAGE 5)	2.62	(g) 2.41	
Coolant temperature					
13.	Nominal inlet (°F)		558.8	556.3	558.8
14.	Average rise in vessel (°F)		59.4	64.2	59.4
15.	Average rise in core (°F)		62.6	68.0	62.6
16.	Average in core (°F)		591.8	592.3	591.8

TABLE 4.1-1 (SHEET 2 OF 4)

	Thermal and Hydraulic Design Parameters		VEGP (ORIGINAL DESIGN)	VEGP (UPRATE DESIGN)[h]	SNUPPS
Heat transfer					
17.	Average in vessel (°F)		588.5	588.4	588.5
18.	Active heat transfer surface area, (ft^2)	(LOPAR) (VANTAGE + / VANTAGE 5)	59,700	(g) 57,505	59,700
19.	Average heat flux (Btu/h-ft^2)	(LOPAR) (VANTAGE + / VANTAGE 5)	189,800	(g) 209,612	189,800
20.	Maximum heat flux for normal operation (Btu/h-ft^2)	(LOPAR) (VANTAGE + / VANTAGE 5)	436,500[a]	(g) 524,030 (a)	440,300[a]
21	Average linear power (kW/ft)		5.44	5.788 (i)	5.44
22.	Peak Linear power for normal operation (kW/ft) [a]		12.5	14.47 (i)	12.6
23.	Peak linear power resulting from overpower transients/operator errors, assuming a maximum overpower of 120% (KW/ft)		18.0	22.4(b)	18.0
24.	Heat flux hot channel factor (F_Q)		2.30[c]	2.50[c]	2.32[c]
25.	Peak fuel central temperature for prevention of centerline melt (°F)		4700	4700	4700
26.	Design		RCC canless 17 x 17	RCC canless 17 x 17	RCC canless 17 x 17
27.	Number of fuel assemblies		193	193	193
28.	UO_2 rods per assembly		264	264	264
29.	Rod pitch (in.)		0.496	0.496	0.496
30.	Overall dimensions (in.)		8.426 x 8.426	8.426 x 8.426	8.426 x 8.426
31.	Fuel weight, as UO_2 (lb)	(LOPAR) (VANTAGE + / VANTAGE 5)	222,739	(g) 204,231[j]	222,739
32.	Zircaloy/ZIRLO/Optimized ZIRLO weight (lb) (active core)	(LOPAR) (VANTAGE + / VANTAGE 5)	45,296	(g) 45,914	45,296
33.	Number of grids per assembly	(LOPAR) (VANTAGE + / VANTAGE 5)	8-Rtype	(g) 2 – R type 6 – Z type 3 - IFM 1-P-Grid	8 – R type
34.	Loading technique (first cycle)		3 region nonuniform	N/A	3 region nonuniform
Fuel rods					
35.	Number		50,952	50,952	50,952

TABLE 4.1-1 (SHEET 3 OF 4)

	Thermal and Hydraulic Design Parameters		VEGP (ORIGINAL DESIGN)	VEGP (UPRATE DESIGN)[h]	SNUPPS
36.	Outside diameter (in.)	(LOPAR) (VANTAGE + / VANTAGE 5)	0.374	(g) 0.360	0.374
37.	Diametral gap (in.)	(LOPAR) (VANTAGE + / VANTAGE 5)	0.0065	(g) 0.0062 (non-IFBA)	0.0065
38.	Clad thickness (in.)		0.0225	0.0225	0.0225
39.	Clad material	(LOPAR) (VANTAGE + / VANTAGE 5)	Zircaloy-4	(g) Zircaloy-4/ZIRLO/ Optimized ZIRLO	Zircaloy-4
Fuel pellets					
40.	Material		UO_2 sintered	UO_2 sintered	UO_2 sintered
41.	Density (% of theoretical)		95	95	95
42.	Diameter (in.)	(LOPAR) (VANTAGE + / VANTAGE 5)	0.3225	(g) 0.3088 (non-IFBA)	0.3225
43.	Length (in.)	(LOPAR) (VANTAGE + / VANTAGE 5) (Blanket Pellet)	0.530	(g) 0.370 0.462/0.500	0.530
Rod cluster control assemblies					
44.	Neutron absorber		Ag-In-Cd or hafnium	Ag-In-Cd or hafnium	Ag-In-Cd or hafnium
45.	Cladding material		Type 304 SS, cold-worked[a]	Type 304 SS, cold-worked[a]	Type 304 SS, cold-worked[a]
46.	Clad thickness Ad-In-Cd or hafnium		0.0185	0.0185	0.0185
47.	Number of clusters		53	53	53
48.	Number of absorber rods per cluster		24	24	24
Core structure					
49.	Core barrel, ID/OD (in.)		148.0/152.5	148.0/152.5	148.0/152.5
50.	Thermal shield		Neutron panel design	Neutron panel design	Neutron panel design
51.	Baffle thickness (in.)		0.88	0.88	0.88
Structure characteristics					
52.	Core diameter, equivalent (in.)		132.7	132.7	132.7
53.	Core height, active fuel (in.)		143.7	143.7	143.7

a. 316L SS cladding material applicable to Framatome RCCA only.

TABLE 4.1-1 (SHEET 4 OF 4)

			VEGP (ORIGINAL DESIGN)	VEGP (UPRATE DESIGN)[h]	SNUPPS	
Reflector thickness and composition						
54.	Top, water plus steel (in.)		10	10	10	
55.	Bottom, water plus steel (in.)		10	10	10	
56.	Side, water plus steel (in.)		15	15	15	
57.	H_2O/U molecular ratio core, lattice, cold	(LOPAR)	2.41	(g)	2.41	
		(VANTAGE + / VANTAGE 5)		2.73		
	First Cycle Fuel Enrichments (Weight Percent					
58.	Region 1		Units 1 and 2	N/A	Core A	Core B
59.	Region 2		2.10	N/A	2.10	1.40
60.	Region 3		2.60	N/A	2.60	2.60
			3.10		3.10	2.90

a. This limit is associated with the values F_Q = 2.32 for SNUPPS, F_Q = 2.30 for VEGP (Original Design) and F_Q = 2.50 for VEGP (Uprate Design).

b. See paragraph 4.3.2.2.6.

c. This is the maximum value of F_Q for normal operation.

d. See paragraph 4.4.2.2.1 for the use of the W-3 correlation.

e. Flowrates are based on 10% steam generator tube plugging for VEGP (Uprate Design) and 0% plugging for VEGP (Original Design) and SNUPPS.

f. Inlet temperature = 557.0°F.

g. LOPAR fuel is not analyzed for the VEGP MUR power uprate to 3626 MWt.

h. The VEGP MUR power uprate increases the licensed reactor core power level from 3565 MWt to 3625.6 MWt.

i. Based on densified active fuel length.

j. The decrease in fuel weight due to annular axial blanket pellets is not considered.

TABLE 4.1-2 (SHEET 1 OF 2)

ANALYTICAL TECHNIQUES IN CORE DESIGN

Analysis	Technique	Computer Code	Section Referenced
Mechanical design of core internals loads, deflections, and stress analysis	Static and dynamic modeling	Blowdown code, FORCE, finite element, structural analysis code, and others	3.7.2.1 3.9.2 3.9.3
Fuel rod design			
Full performance characteristics (temperature, internal pressure, clad stress, etc.)	Semiempirical thermal model of fuel rod with consideration of fuel density changes, heat transfer, fission gas release, etc.	Westinghouse fuel rod design model	4.2.1.1 4.2.3.2 4.2.3.3 4.3.3.1 4.4.2.11
Nuclear design			
Cross-sections and group constants	Microscopic data; macroscopic constants for homogenized core regions	Modified ENDF/B library LEOPARD/CINDER type or PHOENIX-P or NEXUS/PARAGON	4.3.3.2
	Group constants for control rods with self-shielding	HAMMER-AIM or PHOENIX-P or NEXUS/PARAGON	4.3.3.2
X-Y and X-Y-Z power distributions, fuel depletion, critical boron concentrations, X-Y and X-Y-Z xenon distributions, reactivity coefficients	2-group diffusion theory	TURTLE (2-D) or ANC (2-D or 3-D)	4.3.3.3
Axial power distributions, control rod worths, and axial xenon distribution	1-D, 2-group diffusion theory	PANDA	4.3.3.3
Fuel rod power	Integral transport theory	LASER	4.3.3.1
Effective resonance temperature	Monte Carlo weighting function	REPAD	4.3.3.1
Criticality of reactor and fuel assemblies	2-D, 2-group diffusion theory	APX system of codes, KENO-IV	4.3.2.6
Vessel irradiation	Multigroup spatial dependent transport theory	DOT	4.3.2.8

TABLE 4.1-2 (SHEET 2 OF 2)

Analysis	Technique	Computer Code	Section Referenced
Thermal-hydraulic design Steady state	Subchannel analysis of local fluid conditions in rod bundles, including inertial and crossflow resistance terms; solution is based on a one-pass model which simulates the core and hot channels.	VIPRE-01	4.4.4.5.2
Transient departure from nucleate boiling	Subchannel analysis of local fluid conditions in rod bundles during transients by including accumulation terms in conservation equations; solution is based on a one-pass model which simulates the core and hot channels.	VIPRE-01	4.4.4.5.4

TABLE 4.1-3

DESIGN LOADING CONDITIONS FOR REACTOR CORE COMPONENTS

1. Fuel assembly weight and core component weights (BAs, sources, plugging devices)
2. Fuel assembly spring forces and core component spring forces
3. Internals weight
4. Control rod trip (equivalent static load)
5. Differential pressure
6. Spring preloads
7. Coolant flow forces (static)
8. Temperature gradients
9. Differences in thermal expansion
   a. Due to temperature differences
   b. Due to expansion of different materials
10. Interference between components
11. Vibration (mechanically or hydraulically induced)
12. One or more loops out of service
13. All operational transients listed in table 3.9.N.1-1
14. Pump overspeed
15. Seismic loads (operating basis earthquake and safe shutdown earthquake)
16. Blowdown forces (due to cold and hot leg break)

4.2 FUEL SYSTEM DESIGN

The plant conditions for design are divided into four categories in accordance with their anticipated frequency of occurrence and risk to the public:

- Condition 1 - Normal operation.
- Condition 2 - Incidents of moderate frequency.
- Condition 3 - Infrequent incidents.
- Condition 4 - Limiting faults.

Chapter 15 describes bases and plant operation and events involving each condition.

The reactor is designed so that its components meet the following performance and safety criteria:

A. The mechanical design of the reactor core components and their physical arrangement, together with corrective actions of the reactor control, protection, and emergency cooling systems (when applicable) ensure that:

1. Fuel damage is not expected during Condition 1 and Condition 2 events.[a] It is not possible, however, to preclude a very small amount of fuel damage. This is within the capability of the plant cleanup system and is consistent with plant design bases.

2. The reactor can be brought to a safe state following a Condition 3 event with only a small fraction of fuel rods damaged, although sufficient fuel damage might occur to preclude immediate resumption of operation.[b]

3. The reactor can be brought to a safe state and the core can be kept subcritical with acceptable heat transfer geometry following transients arising from Condition 4 events.

B. The fuel assemblies are designed to withstand loads induced during shipping, handling, and core loading without exceeding the criteria of paragraph 4.2.1.5.

C. The fuel assemblies are designed to accept control rod insertions in order to provide the required reactivity control for power operations and reactivity shutdown conditions.

D. All fuel assemblies have provisions for the insertion of incore instrumentation necessary for plant operation.

E. The reactor vessel and internals, in conjunction with the fuel assemblies and incore control components, direct reactor coolant through the core. This achieves acceptable flow distribution and restricts bypass flow so that the heat transfer performance requirements can be met for all modes of operation.

The following subsection provides the fuel system design bases and design limits. This information, augmented by the clarifying information submitted to the Nuclear Regulatory

[a] Fuel damage as used here is defined as penetration of the fission product barrier; i.e., the fuel rod clad.
[b] In any case, the fraction of fuel rods damaged must be limited so as to meet the dose guidelines of 10 CFR 100.

Commission (NRC) during their review of Westinghouse topical report WCAP-9500, Reference Core Report - 17 x 17 Optimized Fuel Assembly (ref. 1 and 2) is consistent with the acceptance criteria of the Standard Review Plan (SRP) 4.2.

4.2.1 DESIGN BASES

The fuel rod and fuel assembly design bases are established to satisfy the general performance and safety criteria presented in section 4.2.

The fuel rods are designed for extended burnup as described in the Extended Burnup Evaluation Report (Ref. 24).

The detailed fuel rod design establishes such parameters as pellet size and density, clad/pellet diametral gap, gas plenum size, and helium prepressurization level. The design also considers effects such as fuel density changes, fission gas release, clad creep, and other physical properties which vary with burnup. The integrity of the fuel rods is ensured by designing to prevent excessive fuel temperatures (paragraph 4.2.1.2A); excessive internal rod gas pressures (paragraphs 4.2.1.3A and 4.2.1.3B) due to fission gas releases; and excessive cladding stresses, strains, and strain fatigue (paragraph 4.2.1.1C). This is achieved by designing the fuel rods so that the conservative design bases in the following subsections are satisfied during Condition 1 and Condition 2 events over the fuel lifetime. For each design basis, the performance of the limiting fuel rod must not exceed the limits specified by the design basis.

Integrity of the fuel assembly structure is ensured by setting limits on stresses and deformations due to various loads and by preventing the assembly structure from interfering with the functioning of other components. Three types of loads are considered:

A. Nonoperational loads such as those due to shipping and handling.

B. Normal and abnormal loads which are defined for Conditions 1 and 2.

C. Abnormal loads which are defined for Conditions 3 and 4.

The design bases for the incore control components are described in paragraph 4.2.1.6.

4.2.1.1 Cladding

A. Zircaloy-4/ZIRLO/Optimized ZIRLO cladding material combines neutron economy (low absorption cross-section); high corrosion resistance to coolant, fuel, and fission products; and high strength and ductility at operating temperatures. Reference 3 documents the operating experience with Zircaloy-4/ ZIRLO and reference 28 documents the operating experience with Optimized ZIRLO as a clad material. Information on the materials chemical and mechanical properties of the cladding is given in reference 4 for Zircaloy-4, reference 25 for ZIRLO, and reference 28 for Optimized ZIRLO.

B. Stress-Strain Limits

1. Clad Stress

The clad stresses under Condition 1 and 2 events are less than the Zircaloy/ZIRLO/Optimized ZIRLO clad material yield stress, with due consideration of temperature and irradiation effects. While the clad has some capability for accommodating plastic strain, the yield stress has been accepted as a conservative design basis.

2. Clad Tensile Strain

The total tensile creep strain is less than 1 percent from the unirradiated condition. The cluster tensile strain during a transient is less than 1 percent from the pretransient value. This limit is consistent with proven practice. (Ref. 3)

C. Vibration and Fatigue

1. Strain Fatigue

The cumulative strain fatigue cycles are less than the design strain fatigue life. This basis is consistent with proven practice. (Ref. 3)

2. Vibration

Potential fretting wear due to vibration is prevented, ensuring that the stress-strain limits are not exceeded during design life. Fretting of the clad surface can occur due to flow-induced vibration between the fuel rods and fuel assembly grid springs. Vibration and fretting forces vary during the fuel life due to clad diameter creep-down combined with grid spring relaxation.

D. Chemical properties of the cladding are discussed in reference 4 for Zircaloy-4, reference 25 for ZIRLO, and reference 28 for Optimized ZIRLO.

4.2.1.2 Fuel Material

A. Thermal-Physical Properties

The center temperature of the hottest pellet is below the melting temperature of the UO_2 (melting point of 5080°F (ref. 4) unirradiated and decreasing by 58°F per 10,000 MWd/tonne of uranium). While a limited amount of center melting can be tolerated, the design conservatively precludes center melting. A calculated fuel centerline temperature of 4700°F has been selected as an overpower limit to ensure no fuel melting. This provides sufficient margin for uncertainties as described in paragraph 4.4.2.9.

The normal design density of the fuel is 95 percent of theoretical. Additional information on fuel properties is given in reference 4.

B. Fuel Densification and Fission Product Swelling

The design bases and models used for fuel densification and swelling are provided in references 5, 6, and 23.

C. Chemical Properties

Reference 4 for Zircaloy-4, reference 25 for ZIRLO, and reference 28 for Optimized ZIRLO provide the basis for justifying that no adverse chemical interactions occur between the fuel and its adjacent material.

4.2.1.3 Fuel Rod Performance

A. Fuel Rod Models

The basic fuel rod models and the ability to predict operating characteristics are given in references 23, 25, and 27, and subsection 4.2.3. Beginning with Unit 2 Cycle 9 and Unit 1 Cycle 11, the NRC-approved fuel performance model, PAD 4.0 (ref. 27) is acceptable for use in fuel rod design.

B. Mechanical Design Limits

Cladding collapse shall be precluded during the fuel rod design lifetime. The models described in references 7 and 26 are used for this evaluation.

The rod internal gas pressure remains below the value which causes the fuel/clad diametral gap to increase due to outward cladding creep during steady-state operation. Rod pressure is also limited such that extensive departure from nucleate boiling (DNB) propagation does not occur during normal operation and any accident event. Reference 8 shows that the DNB propagation criteria are satisfied.

4.2.1.4 Spacer Grids

A. Mechanical Limits and Materials Properties

The grid component strength criteria are based on experimental tests. The limit is established at 0.9 Pc, where Pc is the experimental collapse load. This limit is sufficient to ensure that, under worst-case combined seismic and blowdown loads from a Condition 4 loss-of-coolant accident (LOCA), the core will maintain a geometry amenable to cooling. As an integral part of the fuel assembly structure, the grids satisfy the applicable fuel assembly design bases and limits defined in paragraph 4.2.1.5.

The grid material and chemical properties are given in references 4, 5 and 25.

B. Vibration and Fatigue

The grids provide sufficient fuel rod support to limit fuel rod vibration and maintain clad fretting wear within acceptable limits (defined in paragraph 4.2.1.1).

4.2.1.5 Fuel Assembly Structural Design

As previously discussed in subsection 4.2.1, the structural integrity of the fuel assemblies is ensured by setting design limits on stresses and deformations due to various nonoperational, operational, and accident loads. These limit bases are applied to the design and evaluation of the top and bottom nozzles, guide thimbles, grids, and thimble joints.

The design bases for evaluating the structural integrity of the fuel assemblies are:

A. Nonoperational

This is a loading of 4 g axial and 6 g lateral with dimensional stability.

B. Normal Operating and Upset Conditions

The fuel assembly component structural design criteria are established for the two primary material categories, austenitic steels and Zircaloy/ZIRLO. The stress categories and strength theory presented in the American Society of Mechanical Engineers (ASME) Boiler and Pressure Vessel (B&PV) Code, Section III, are used as a general guide. The maximum shear theory (Tresca criterion) for combined stresses is used to determine the stress intensities for the austenitic steel components. The stress intensity is defined as the numerically largest difference between the various principal stresses in a three-dimensional field. The allowable stress intensity value for austenitic steels, such as nickel-chromium-iron alloys, is given by the lowest of the following:

1. One-third of the specified minimum tensile strength or two-thirds of the specified minimum yield strength at room temperature.

2. One-third of the tensile strength or 90 percent of the yield strength at room temperature but not to exceed two-thirds of the specified minimum yield strength at room temperature.

   The stress limits for the austenitic steel components are given below. All stress nomenclature is per the ASME Code, Section III.

Stress Intensity Limits

Categories	Limit
General primary membrane stress intensity	S_m
Local primary membrane stress intensity	1.5 S_m
Primary membrane plus bending stress intensity	1.5 S_m
Total primary plus secondary stress intensity	3.0 S_m

The Zircaloy/ZIRLO structural components, which consist of guide thimbles and fuel tubes, are in turn subdivided into two categories because of material differences and functional requirements. The fuel tube design criteria are covered separately in paragraph 4.2.1.1. The maximum shear theory is used to evaluate the guide thimble design. For conservative purposes, the Zircaloy/ZIRLO unirradiated properties are used to define the stress limits.

3. Abnormal loads during Conditions 3 or 4, worst cases represented by seismic and blowdown loads, are as follows:

   a. Deflections or failures of components cannot interfere with the reactor shutdown or emergency cooling of the fuel rods.

   b. The fuel assembly structural component stresses under faulted conditions are evaluated using primarily the methods outlined in Appendix F of the ASME Code, Section III. Since the current

analytical methods utilize elastic analysis, the stress allowables are defined as the small value of 2.4 S_m or 0.70 S_u for primary membrane and 3.6 S_m or 1.05 S_u for primary membrane plus primary bending. For the austenitic steel fuel assembly components, the stress intensity is defined in accordance with the rules described in the previous section for normal operating conditions. For the Zircaloy components, the stress intensity limits are set at two-thirds of the material yield strength, S_y, at reactor operating temperature. This results in Zircaloy stress limits being the smaller of 1.6 S_y or 0.70 S_u for primary membrane and 2.4 S_y or 1.05 S_u for primary membrane plus bending. For conservative purposes, the Zircaloy/ZIRLO unirradiated properties are used to define the stress limits.

The material and chemical properties of the fuel assembly components are given in reference 4 for Zircaloy-4 and reference 25 for ZIRLO. See paragraph 4.2.3.4 for a discussion of the spacer grid crush testing.

c. Thermal-hydraulic design is discussed in section 4.4.

4.2.1.6 Incore Control Components

The control components are subdivided into permanent and temporary devices.

The permanent components are the rod cluster control assemblies (RCCAs), secondary neutron source assemblies, and thimble plug assemblies. The temporary components are the burnable absorber (BA) assemblies, stainless steel rod insert assemblies (SSRIA), and the primary neutron source assemblies, which are normally used only in the initial core.

Materials are selected for:

A. Compatibility in a pressurized water reactor (PWR) environment.

B. Adequate mechanical properties at room and operating temperatures.

C. Resistance to adverse property changes in a radioactive environment.

D. Compatibility with interfacing components.

Material properties are given in reference 4.

The design bases for each of the mentioned components are given in the following paragraphs.

A. Control Rods

For Conditions 1 and 2, the stress categories and strength theory presented in the ASME B&PV Code, Section III, Subsection NG-3000, are used as a general guide in the design of the control rod cladding.

Design conditions considered under the ASME Code, Section III, are as follows:

1. External pressure equal to the reactor coolant system (RCS) operating pressure with appropriate allowance for overpressure transients.

2. Wear allowance equivalent to 1000 reactor trips.

3. Bending of the rod due to a misalignment in the guide tube.

4. Forces imposed on the rods during rod drop.

5. Loads imposed by the accelerations of the control rod drive mechanism.

6. Radiation exposure during maximum core life. The absorber material temperature does not exceed its melting temperature (1472°F for silver-indium-cadmium (Ag-In-Cd) (ref. 4) or 3913°F for hafnium (ref. 9)).

7. Temperature effects at operating conditions.

B. BA Rods

For Conditions 1 and 2, the stress categories and strength theory presented in the ASME B&PV Code, Section III, Subsection NG-3000, are used as a general guide in the design of the BA cladding. For abnormal loads during Conditions 3 and 4, code stresses are not considered limiting. Failure of the BA rods during these conditions must not interfere with reactor shutdown or cooling of the fuel rods. Thus the structural elements are designed to prevent excessive slumping.

The standard burnable absorber material is borosilicate glass and is designed so that the absorber material is below its softening temperature 1510°F ± 18°F for 12.5 weight-percent boron rod. The softening temperature for borosilicate glass is defined in ASTM C 338.

The wet annular burnable absorber (WABA) material is B_4C contained in an alumina matrix. Thermal-physical and gas release properties of Al_20_3-B_4C are described in references 4 and 22. Wet annular burnable absorber rods are designed so that the absorber temperature does not exceed 1200°F during normal operation or an overpower transient. The 1200°F maximum temperature He gas release in a WABA rod will not exceed 30 percent (ref. 22).

C. Neutron Source Rods

The neutron source rods are designed to withstand the following:

1. The external pressure equal to RCS operating pressure with appropriate allowance for overpressure transients.

2. An internal pressure equal to the pressure generated by released gases over the source rod life.

D. Thimble Plug Assembly

The thimble plug assembly may be used to restrict bypass flow through those thimbles not occupied by absorber, source, or BA rods.

When used, the thimble plug assemblies satisfy the following:

1. Accommodate the differential thermal expansion between the fuel assembly and the core internals.

2. Maintain positive contact with the fuel assembly and the core internals.

3. Limit the flow through each occupied thimble to acceptable design value.

E. Stainless Steel Rod Insert Assembly

The SSRIA may be used to provide power suppression and power shaping capability in a fuel assembly to restore design margin to meet the fuel rod internal pressure criterion. The SSRIA core component is comprised of stainless steel

rods mounted to a conventional fuel assembly insert holddown device. The SSRIA satisfies all applicable core component design criteria.

4.2.1.7 Surveillance Program

Paragraph 4.2.4.5 and sections 8 and 23 of references 3 and 10 discuss the testing and fuel surveillance operation experience program that has been and is being conducted to verify the adequacy of the fuel performance and design bases. Fuel surveillance and testing results, as they become available, are used to improve fuel rod design and manufacturing processes and to ensure that the design bases and safety criteria are satisfied. The improved corrosion resistance of ZIRLO fuel rod cladding has been demonstrated to high burnups in the BR-3 and North Anna demonstration programs. Cladding corrosion measurements showed that the reduced corrosion exhibited by the ZIRLO clad fuel rods was better than anticipated.

Reference 28 discusses the differences between ZIRLO and Optimized ZIRLO cladding material as well as provides information on the additional fuel surveillance programs demonstrating the similarities with ZIRLO cladding material.

4.2.2 DESCRIPTION AND DESIGN DRAWINGS

The fuel assembly, fuel rod, and incore control component design data are given in table 4.3-1.

The VANTAGE 5 assembly has the same cross-sectional envelope as the LOPAR assembly. The VANTAGE 5 assembly is, however, 0.210-in. longer than the initial core/Cycle 1 LOPAR assembly for both units. The grid centerline elevations of the VANTAGE 5 are identical to those of the Region 5/Cycle 3 LOPAR assembly for Unit 1 and Region 4/Cycle 2 LOPAR assembly for Unit 2. The VANTAGE 5 bottom grid is 0.355-in. lower than the LOPAR design of Cycle 1, and the top grid is 0.360-in. lower than the same LOPAR design. However, any integral contact between the two fuel assemblies will be grid-to-grid. By matching grid elevations, any crossflow maldistribution between the LOPAR and VANTAGE 5 fuel assemblies is minimized. To accommodate the VANTAGE 5 fuel assembly with ZIRLO clad fuel rods and the protective bottom grid with the elongated bottom end plug, Inconel grid, No. 1, was raised by 0.7 in., and the first Zircaloy-4/ZIRLO grid, No. 2, was lowered 0.3 in. to reduce the lower most span length in the ZIRLO fuel assembly. This resulted in span No. 1 being shortened by 1.0 in. and span No. 2 being lengthened by 0.3 in. as shown in figure 4.2-2.

Commencing with Region 10 in Unit 1 Cycle 8 and Region 9 in Unit 2 Cycle 7, the fuel assembly skeleton includes ZIRLO fabricated guide thimble tubes and instrumentation tubes. The ZIRLO guide thimble tube and instrumentation tube lengths have been reduced, resulting in a slightly shorter overall fuel assembly height to allow for additional growth at high burnup. The top nozzle holddown spring design for the shorter ZIRLO fuel assembly has a slightly increased height compared to the standard top nozzle holddown spring design to maintain comparable holddown forces. The top Inconel grid was lowered by 0.2 inch because of the shorter overall height of the ZIRLO skeleton.

Commencing with Region 12 in Unit 1 Cycle 10 and Region 11 in Unit 2 Cycle 9, the ZIRLO guide thimble tube and instrumentation tube lengths have been restored to the same length as the VANTAGE 5 design with the Zircaloy-4 skeleton. The top Inconel grid for the longer ZIRLO skeleton design has been returned to the same elevation as in the VANTAGE 5 design with the Zircaloy-4 skeleton. The standard top nozzle holddown spring is used on the longer ZIRLO fuel assembly to maintain comparable holddown forces.

Commencing with Region 27 (Cycle 25) reload for Unit 1 and Region 25 (Cycle 23) reload for Unit 2, the Vogtle units implement the Westinghouse 17x17 PRIME™ fuel assembly design which is an improved version of the 17x17 VANTAGE+ fuel design. The PRIME™ fuel assembly design incorporates advanced features to improve fuel reliability, dimensional stability and corrosion resistance of the 17x17 VANTAGE+ with Debris Mitigation Features fuel design will be implemented. The PRIME™ fuel features include Low Tin ZIRLO grid strap material to improve corrosion resistances, the PRIME™ Bottom Nozzle incorporates a low pressure drop design along with lower side skirts to help improve debris resistance and the external dashpot tube which stiffens the dashpot region of the fuel assembly to minimize the potential for incomplete rod insertion. The PRIME™ advanced fuel design has been extensively evaluated, tested and analyzed and it was demonstrated that it meets all of the applicable mechanical design and safety criteria.

Optimized ZIRLO cladding material has been approved for use in Vogtle 1 and 2 by the NRC, reference 29.

Each fuel assembly consists of 264 fuel rods, 24 guide thimble tubes, and 1 instrumentation thimble tube arranged within a supporting structure. A fuel assembly may have limited substitution of zirconium alloy or stainless steel filler rods in place of fuel rods, in accordance with NRC approved applications of fuel rod configuration. The instrumentation thimble is located in the center position and provides a channel for insertion of an incore neutron detector, if the fuel assembly is located in an instrumented core position. The guide thimbles provide channels for insertion of either an RCCA, a neutron source assembly, a BA assembly, or a thimble plug assembly, depending on the position of the particular fuel assembly in the core. Figure 4.2-1 shows a cross-section of the fuel assembly array, and figure 4.2-2 shows a fuel assembly full-length view. The fuel rods are loaded into the fuel assembly structure so that there is clearance between the fuel rod ends and the top and bottom nozzles.

Fuel assemblies are installed vertically in the reactor vessel and stand upright on the lower core plate, which is fitted with alignment pins to locate and orient each assembly. After all fuel assemblies are set in place, the upper support structure is installed. Alignment pins, built into the upper core plate, engage and locate the upper ends of the fuel assemblies. The upper core plate then bears down against the holddown springs on the top nozzle of each fuel assembly to hold the fuel assemblies in place.

Improper orientation of fuel assemblies within the core is prevented by the use of an indexing hole in one corner of the top nozzle top plate. The assembly is oriented with respect to the handling tool and the core by means of a pin inserted into this indexing hole. Visual confirmation of proper orientation is also provided by an engraved identification number on the opposite corner clamp.

4.2.2.1 Fuel Rods

The fuel rods consist of uranium dioxide ceramic pellets contained in slightly cold-worked Zircaloy-4 tubing plugged and seal-welded at the ends to encapsulate the fuel. A schematic of the fuel rod is shown in figure 4.2-3. The fuel pellets are right circular cylinders consisting of slightly enriched uranium dioxide powder which has been compacted by cold pressing and then sintered to the required density. The ends of each pellet are dished slightly to allow greater axial expansion at the center of the pellets. For reloads, the ends of each pellet also have a small chamfer at the outer cylindrical surface which improves manufacturability.

The VANTAGE 5 fuel rod has the same clad wall thickness as the LOPAR fuel rod, but the VANTAGE 5 fuel rod diameter is reduced to optimize the water-to-uranium ratio. The VANTAGE 5 fuel rod length is greater than the LOPAR fuel rod length to provide a longer plenum and bottom end plug. The bottom end plug has an internal-grip feature to facilitate rod loading on both designs and is longer to provide a longer lead-in for the removable top nozzle reconstitution feature.

Commencing with the Region 8 fuel rods in Unit 2 Cycle 6 and the Region 10 fuel rods in Unit 1 Cycle 8, the fuel rod bottom end plug was elongated for use with the protective bottom grid. In conjunction with the elongated bottom end plug, the fuel rod top end plug was elongated and fitted with an external gripper.

Commencing with the Region 12 fuel rods in Unit 1 Cycle 10 and Region 11 fuel rods in Unit 2 Cycle 9, the ZIRLO fuel rod length has been increased based on the growth model for ZIRLO (reference 25). In addition, the fuel rod top end plug is reduced in length by eliminating the external gripper feature. The reduced top end plug length allows a further increase in the fuel rod tube length, and, consequently, an increase in the fuel rod plenum.

Optimized ZIRLO cladding material has been approved for use in Vogtle 1 and 2 by the NRC, reference 29.

The axial blanket region is the nominal 6 inches of fuel pellets located at each end of the fuel rod pellet stack. The fuel in the axial blanket region may be natural, mid-enriched, or fully enriched, solid or annular pellets. The natural or mid-enriched axial blankets reduce neutron leakage and improve fuel utilization. The annular blanket pellets are used to increase the void volume for gas accommodation within the fuel rod. The axial blankets utilize chamfered pellets which are physically different (length) than the enriched pellets to help prevent accidental mixing during manufacturing.

The integral fuel burnable absorber (IFBA) coated fuel pellets are identical to the enriched uranium dioxide pellets except for the addition of a thin zirconium diboride (ZrB_2) coating on the pellet cylindrical surface. Coated pellets occupy the central portion of the fuel stack. The number and pattern of IFBA rods within an assembly may vary depending on specific application. The ends of the enriched coated pellets are dished to allow for greater axial expansion at the pellet centerline and to increase the void volume for fission gas release. This coating may be applied with a linear B-10 loading (mg/in.) that is greater than the original IFBA design for added flexibility in the core design.

Void volume and clearances are provided within the rods to accommodate fission gases released from the fuel, differential thermal expansion between the clad and the fuel, and fuel density changes during irradiation. Shifting of the fuel within the clad during handling or shipping prior to core loading is prevented by a stainless steel helical spring which bears on top of the fuel. At assembly, the pellets are stacked in the clad to the required fuel height. The spring is then inserted into the top end of the fuel tube and the end plugs pressed into the ends of the tube and welded. All fuel rods are internally pressurized with helium during the welding process to minimize compressive clad stresses and prevent clad flattening under coolant operating pressures.

The fuel rods are prepressurized and designed so that:

- The internal gas pressure mechanical design limit referred to in paragraph 4.2.1.3 is not exceeded.

- The cladding stress-strain limits (paragraph 4.2.1.1) are not exceeded for Condition 1 and 2 events.

- Clad flattening will not occur during the fuel core life.

4.2.2.2 Fuel Assembly Structure

The fuel assembly structure consists of a bottom nozzle, top nozzle, guide thimbles, and grids, as shown in figure 4.2-2.

4.2.2.2.1 Bottom Nozzle

The bottom nozzle serves as a bottom structural element of the fuel assembly and directs the coolant flow distribution to the assembly. The nozzle is fabricated from type 304 stainless steel and is shown in figure 4.2-2. The legs form a plenum for the inlet coolant flow to the fuel assembly. The plate prevents accidental downward ejection of the fuel rods from the fuel assembly. The bottom nozzle is fastened to the fuel assembly guide tubes by locked thimble screws which penetrate through the nozzle and mate with a threaded plug in each guide tube.

Coolant flows from the plenum in the bottom nozzle upward through the penetrations in the plate to the channels between the fuel rods. The penetrations in the plate are positioned between the rows of the fuel rods.

Axial loads (holddown) imposed on the fuel assembly and the weight of the fuel assembly are transmitted through the bottom nozzle to the lower core plate. Indexing and positioning of the fuel assembly is controlled by alignment holes in two diagonally opposite bearing plates which mate with locating pins in the lower core plate. Lateral loads on the fuel assembly are transmitted to the lower core plate through the locating pins.

A debris filter bottom nozzle (DFBN) was introduced as a replacement to the standard nozzle design described above to inhibit debris from entering the active fuel region of the core. This nozzle utilized the same material, geometry, functional, and welding requirements as the standard bottom nozzle as described above. The revised end plate flow hole patterns are shown on figure 4.2-2 to illustrate the increased number of smaller flow holes that reduce the passage of debris into the active region of the fuel assembly. Additional debris protection was provided by the protective bottom grid assembly and the elongated fuel rod bottom end plug described in paragraph 4.2.2.2.4.

A modification introducing a skirt on the DFBN was made to improve the structural integrity of the nozzle on the VANTAGE 5 design. In addition, five holes were placed on each face of this skirt to allow lateral flow communication. This change in bottom nozzle design was referred to as the modified DFBN and is illustrated on figure 4.2-2 (VANTAGE 5).

Commencing with the fresh fuel installed in Unit 1 Cycle 18, Unit 2 Cycle 17, and subsequent Vogtle reloads, the standardized debris filter bottom nozzle (SDFBN), which was developed for 17X17 fuel and is designed to have a loss coefficient that is the same, independent of supplier, will be implemented. The SDFBN has eliminated the side skirt communication flow holes as a means of improving the debris mitigation performance of the bottom nozzle, as shown in figure 4.2-2. This nozzle has been extensively evaluated and analyzed and it was demonstrated that it meets all of the applicable mechanical design criteria. In addition, specific testing was performed to demonstrate that there is no adverse effect on the thermal hydraulic performance of the SDFBN either with respect to the pressure drop or with respect to DNB.

Beginning with the Region 27 (Cycle 25) reload for Unit 1 and Region 25 (Cycle 23) reload for Unit 2, the Vogtle units implement the Westinghouse PRIME^{TM} fuel assembly design. The PRIME^{TM} fuel assembly bottom nozzle design has a two chamfer inlet flow hole design to

improve the pressure drop (lower the loss coefficient). In addition, the PRIME™ bottom nozzle design lowers the side skirts to help improve the debris filtering capability of the bottom nozzle by eliminating the large lateral flow path between the bottom nozzle legs in the SDFBN design by lowering the side skirts of the PRIME™ bottom nozzle. In addition, small flow holes are added to the side skirts to ensure that there is adequate lateral flow to the baffle barrel region of the core to ensure that the reactor vessel former plants are cooled. These features are shown in Figure 4.2-2 (Sheet 7 of 7). This advanced bottom nozzle design has been extensively evaluated, tested and analyzed and it was demonstrated that it meets all of the applicable mechanical design and safety criteria.

4.2.2.2.2 Top Nozzle

Standard Top Nozzle

The standard top nozzle functions as the upper structural element of the fuel assembly in addition to providing a partial protective housing for the RCCA or other components. The top nozzle consists of an adapter plate, enclosure, top plate, and pads. Holddown springs are mounted on the assembly, as shown in figure 4.2-2. The springs and bolts are made of Inconel-718, and -600, respectively; other components are made of type 304 stainless steel.

The adapter plate is provided with round penetrations and semicircular-ended slots to permit the flow of coolant upward through the top nozzle. Other round holes are provided to accept sleeves which are welded to the adapter plate and mechanically attached to the thimble tubes. The ligaments in the plate cover the tops of the fuel rods and prevent their upward ejection from the fuel assembly. The enclosure is a box-like structure which sets the distance between the adapter plate and the top plate. The top plate has a large hole in the center to permit access for the control rods and the control rod spiders. Holddown springs are mounted on the top plate and are fastened in place by bolts and clamps located at two diagonally opposite corners. Integral pads which contain alignment holes for locating the upper end of the fuel assembly are positioned on the other two corners.

Reconstitutable Top Nozzle

The RTN design differs from the above standard nozzle design in the following ways. A groove is provided in each thimble thru-hole in the nozzle plate to facilitate attachment and removal. Round holes in the adapter plate are provided to accept nozzle inserts which are locked into the grooves in the adapter plate using lock tubes and mechanically attached to the thimble tubes at the lower ends of the inserts (figure 4.2-5). The nozzle plate thickness is reduced to provide additional axial space for fuel rod growth. Holddown springs are mounted on the top plate and are fastened in place by spring screws.

Commencing with the fresh fuel installed in Unit 1 Cycle 11 and in Unit 2 Cycle 9, Alloy 718 is used instead of Alloy 600 for the fuel assembly holddown spring screws on the RTN to improve resistance to primary water stress corrosion cracking.

To remove the RTN, a tool is first inserted through a lock tube (figure 4.2-5) and expanded radially to engage the bottom edge of the tube. An axial force is then exerted on the tool which overrides local lock tube deformations and withdraws the lock tube from the nozzle insert. After the lock tubes have been withdrawn, the RTN is removed by raising it off the upper slotted ends of the nozzle inserts, which deflect inwardly under the axial lift load.

With the RTN removed, direct access is provided for fuel rod examination or replacement. Reconstitution is completed by the remounting of the RTN and the insertion of lock tubes.

Additional details of this design feature, the design bases, and evaluation of the RTN are given in subsection 2.3.2 in reference 21.

A composite (cast) top nozzle was introduced in Unit 1 Cycle 8 and in Unit 2 Cycle 7, and replaced the integral welded assembly. This design change, for manufacturing process improvement, reduces the total number of components required to fabricate and assemble the top nozzle. The cast and welded top nozzles are interchangeable regarding form, fit, and function. Therefore, either of these RTN designs may be used.

Westinghouse Integral Nozzle

Commencing with Vogtle Unit 1, Cycle 20, the Westinghouse Integral Nozzle (WIN) will replace the RTN. The WIN top nozzle functions as the upper structural element of the fuel assembly in addition to providing a partial protective housing for the RCCA or other components. The top nozzle consists of an adapter plate, enclosure, top plate, and pads. Holddown springs are mounted on the assembly, as shown in figure 4.2-17. For the WIN, the springs are made of Alloy 781 and the main nozzle body and the pins are made of Type 304 stainless steel.

The WIN design, while similar to the RTN, incorporates design and manufacturing improvements to eliminate the Alloy 718 spring screw for attachment of the holddown springs. In the WIN nozzle, the springs are assembled into the nozzle pad and pinned in place. The WIN design provides a wedged rather than a clamped (bolted) joint for transfer of the fuel assembly holddown forces into the top nozzle structure. Integral pads which contain alignment holes for locating the upper end of the fuel assembly are positioned on the other two corners for the WIN. The flow plate, thermal characteristics, and method of attachment of the nozzle are all unchanged from the RTN top nozzle design.

Replacement Reconstitutable Top Nozzle (RRTN)

A replacement reconstitutable top nozzle (RRTN) design may be used in a reload cycle to replace the original reconstitutable top nozzle (RTN) or Westinghouse Integral Top Nozzle (WIN) on an irradiated fuel assembly. The mechanical features of the RRTN are the same as those for the RTN (see figure 4.2-5) or WIN with some minor dimensional differences in the top nozzle adapter plate thimble hole to facilitate attachment to an irradiated fuel assembly. The RRTN may be manufactured by either the composite (cast) process or the integral welded process. The cast and integral welded top nozzles are interchangeable regarding form, fit and function. Therefore, either of these RRTN designs may be used to replace an RTN or WIN regardless of whether the original RTN or WIN on the assembly was the composite (cast) design or the integral welded design. Either Alloy 718 or Alloy 600 may be used for the fuel assembly holddown spring screws on the RRTN.

4.2.2.2.3 Guide Thimbles and Instrument Tube

The guide thimbles are structural members which also provide channels for the neutron absorber rods, BA rods, neutron source, or thimble plug assemblies. With the exception of a reduction in the guide thimble diameter and length above the dashpot, the VANTAGE 5 guide thimbles are identical to those in the LOPAR design. A reduction to the guide thimble outside diameter and inside diameter is required due to the thicker Zircaloy grid straps and reduced cell size. The VANTAGE 5 thimble tube is shorter than the LOPAR thimble tube due to the RTN or WIN and nozzle insert features. Each thimble is fabricated from Zircaloy-4/ ZIRLO tubing having two different diameters. The tube diameter at the top section provides the annular area necessary to permit rapid control rod insertion during a reactor trip. Holes are provided on the thimble tube above the dashpot to reduce the rod drop time. The lower portion of the guide thimble is swaged to a smaller diameter to reduce diametral clearances and produce a dashpot

action near the end of the control rod travel during normal trip operation. The dashpot is closed at the bottom by means of an end plug, which is provided with a small flow port to avoid fluid stagnation in the dashpot volume during normal operation. The top end of the guide thimble is fastened to a tubular sleeve by three expansion swages on the standard top nozzle. The sleeve fits into and is welded to the standard top nozzle adapter plate. The top end of the guide thimble is fastened to a nozzle insert by three expansion swages. The nozzle insert fits into and is locked into the RTN or WIN adapter plate using a lock tube. The lower end of the guide thimble is fitted with an end plug, which is captured by the bottom grid insert and then fastened to the bottom nozzle by a crimp locked thimble screw.

Fuel rod support grids are fastened to the guide thimble assemblies to create an integrated structure. Since welding of the grids to the thimbles is not possible, the fastening technique depicted in figures 4.2-4 and 4.2-5 is used for all but the bottom grid in a fuel assembly.

An expanding tool is inserted into the inner diameter of the Zircaloy/ZIRLO thimble tube at the elevation of the grid sleeves that have been previously attached to the grid assembly. The four-lobed tool forces the thimble and sleeve outward to a predetermined diameter, thus joining the two components.

The top grid-to-thimble attachment is shown in figure 4.2-5 for the standard top nozzle design. The stainless steel sleeves are brazed into the Inconel grid assembly. The Zircaloy/ZIRLO guide thimbles are fastened to the long sleeves by expanding the two members as shown in figures 4.2-4 and 4.2-6. Finally, the top ends of the sleeves are welded to the top nozzle adapter plate as shown in figure 4.2-5.

In assemblies with reconstitutable top nozzles or Westinghouse Integral Nozzles, the guide thimbles are fastened inside the top grid sleeves and nozzle inserts as shown in figure 4.2-5. A bulge in the nozzle insert is then captured in a corresponding groove in the hole in the top nozzle plate. The insert is fixed in place by the insertion of a lock tube into the insert, thus providing a mechanical connection between the guide thimble and the top nozzle.

The top Inconel grid sleeve, top nozzle insert, and thimble of the VANTAGE 5 design are joined together using bulge joint mechanical attachments as shown in figure 4.2-5. This bulge joint connection was mechanically tested and found to meet all applicable design criteria.

The intermediate mixing vane and intermediate flow mixer Zircaloy/ZIRLO/Low Tin ZIRLO grids employ a single bulge connection to the sleeve and thimble as compared to a two bulge connection used in the top Inconel grid (figure 4.2-6). Mechanical testing of this bulge joint connection was also found to be acceptable.

The bottom grid assembly is joined to the assembly as shown in figure 4.2-7. The stainless steel insert is spotwelded to the bottom grid and later captured between the guide thimble end plug and the bottom nozzle by means of a stainless steel thimble screw.

The described methods of grid fastening are standard and have been used successfully since the introduction of Zircaloy guide thimbles in 1969.

The central instrumentation tube of each fuel assembly is constrained by seating in a counterbore in the bottom nozzle at its lower end and is attached to the top and midgrid in the same manner as above for the guide thimbles. This tube has a constant diameter and guides the incore neutron detectors. The VANTAGE 5 instrumentation tube also has a reduction in diameter when compared to the LOPAR assembly instrumentation tube. This decrease still allows sufficient diametral clearance for the flux thimble to traverse the tube without binding.

Beginning with the Region 27 (Cycle 25) reload for Unit 1 and the Region 25 (Cycle 23) reload for Unit 2, the Vogtle units implement the Westinghouse PRIME^{TM} fuel assembly design which incorporates an external dashpot tube to stiffen the dashpot region of the fuel assembly to

minimize the potential for incomplete rod insertion. This advanced dashpot design has been extensively evaluated, tested and analyzed and it was demonstrated that it meets all of the applicable mechanical design and safety criteria.

4.2.2.2.4 Grid Assemblies

The fuel rods, as shown in figure 4.2-2, are supported at intervals along their length by grid assemblies which maintain the lateral spacing between the rods. Each fuel rod is supported within each grid by the combination of support dimples and springs. The grid assembly consists of individual slotted straps assembled and interlocked into an egg crate arrangement with the straps permanently joined at their points of intersection.

Two types of grid assemblies are used in each fuel assembly. One type, with mixing vanes projecting from the edges of the straps into the coolant stream, is used in the high heat flux region of the fuel assemblies to promote mixing of the coolant. The other type, located at the ends of the assembly, does not contain mixing vanes on the internal straps. The outside straps on all grids contain mixing vanes which, in addition to their mixing function, aid in guiding the grids and fuel assemblies past projecting surfaces during handling or during loading and unloading of the core.

The top and bottom Inconel-718 (nonmixing vane) grids of the VANTAGE 5 fuel assemblies are similar in design to the Inconel grids of the Cycle 1, LOPAR fuel assemblies for VEGP Units 1 and 2. The six intermediate (mixing vane) grids on the VANTAGE 5 design are made of Zircaloy/ZIRLO/Low Tin ZIRLO material rather than the intermediate Inconel (mixing vane) grids which are currently used in the LOPAR design. Beginning with Unit 1 Cycle 8 and Unit 2 Cycle 7, the intermediate grids and intermediate flow mixer (IFM) grids are made of ZIRLO material.

The Zircaloy/ZIRLO/Low Tin ZIRLO grids have thicker straps than the Inconel. Also, the Zircaloy/ZIRLO/Low Tin ZIRLO grid height is higher compared to the Inconel midgrid. These dimensional changes were made to compensate for differences in material strength properties. The Zircaloy/ZIRLO/Low Tin ZIRLO grid incorporates the same grid cell support configuration as the Inconel grid. The Zircaloy/ZIRLO/Low Tin ZIRLO interlocking strap joints and grid/sleeve joints are fabricated by laser welding, whereas the Inconel grid joints are brazed.

The VANTAGE 5 IFM grids shown on figure 4.2-2 are located in the three uppermost spans between the Zircaloy/ZIRLO/Low Tin ZIRLO mixing vane structural grids and incorporate a similar mixing vane array. Their prime function is midspan flow mixing in the hottest fuel assembly spans. Each IFM grid cell contains four dimples which are designed to prevent midspan channel closure in the spans containing IFMs and fuel rod contact with the mixing vanes. This simplified cell arrangement allows short grid cells so that the IFM grid can accomplish its flow mixing objective with minimal pressure drop.

The IFM grids, like the VANTAGE 5 mixing vane grids, are fabricated from Zircaloy/ZIRLO/Low Tin ZIRLO. This material was selected to take advantage of the material's inherent low neutron capture cross-section. The Zircaloy/ZIRLO/Low Tin ZIRLO grid straps are manufactured using the same basic techniques as the Zircaloy/ZIRLO/Low Tin ZIRLO grid assemblies used for the Westinghouse optimized fuel assembly (OFA) design and are joined to the guide thimbles via sleeves which are welded at the bottom of appropriate grid cells.

The IFM grids are not intended to be structural members. The outer strap configuration was to be similar to current fuel designs to preclude grid hang-up and damage during fuel handling. Additionally, the grid envelope is smaller which further minimizes the potential for damage and reduces calculated forces during seismic/LOCA events. A coolable geometry is assured at the IFM grid elevation, as well as at the structural grid elevation.

Commencing with the fresh feed fuel assemblies for Unit 2 Cycle 6 and Unit 1 Cycle 8, the fuel incorporated a bottom protective grid and a modification to the bottom fuel rod end plug. The protective grid illustrated in figure 4.2-2 is a partial height grid, similar in configuration to the intermediate flow mixing grid, fabricated of Inconel without mixing vanes, and positioned on the top plate of the bottom nozzle. In conjunction with the protective grid, the bottom fuel rod end plug is elongated. The protective grid and elongated bottom end plug together provide a zone below the active fuel in which debris can be entrapped.

Commencing with the fresh fuel installed in Unit 1 Cycle 18, Unit 2 Cycle 17, and subsequent Vogtle reload, the robust protective grid (RPG) which was developed as a result of observed failures in the field as noted in post irradiation exams (PIE) performed at several different plants, will be implemented. It was determined that observed failures were the result of two primary issues: 1) fatigue failure within the protective grid itself at the top of the end strap and 2) stress corrosion cracking (SCC) primarily within the rod support dimples. The RPG implements design changes such as increasing the maximum nominal height of the grid, increasing the ligament length and the radii of the ligament cutouts, and the use of four additional spacers for a total of eight spacers to help strengthen the grid. The nominal height of the grid was increased to allow "V-notch" window cutouts to be added to help minimize flow-induced vibration caused by vortex shedding at the trailing edge of the inner grid straps. These design changes incorporated into the RPG design help address the issues of fatigue failures and failures due to SCC. It was demonstrated that the above changes do not impact the thermal hydraulic performance of the RPG as there is no change to the pressure loss coefficient. In addition, the RPG retains the original protective grid function as a debris mitigation feature.

Beginning with the Region 27 (Cycle 25) reload for Unit 1 and the Region 25 (Cycle 23) reload Unit 2, the Vogtle units implement the Westinghouse PRIME^{TM} fuel assembly design which incorporates Low Tin ZIRLO grid strap material to improve corrosion resistance as compared to grids manufactured with ZIRLO grid strap material. This Low Tin ZIRLO grid strap material has been extensively evaluated, tested and analyzed and it was demonstrated that all of the applicable mechanical design and safety criteria remain satisfied.

4.2.2.3 Incore Control Components

Reactivity control is provided by neutron absorbing rods and a soluble chemical neutron absorber (boric acid). The boric acid concentration is varied to control long-term reactivity changes such as:

A. Fuel depletion and fission product buildup.

B. Cold to hot, zero power reactivity changes.

C. Reactivity change produced by intermediate-term fission products such as xenon and samarium.

D. Burnable poison depletion.

The chemical and volume control system (CVCS) is discussed in chapter 9.

The RCCAs provide reactivity control for:

A. Shutdown.

B. Reactivity changes due to coolant temperature changes in the power range.

C. Reactivity changes associated with the power coefficient of reactivity.

D. Reactivity changes due to void formation.

It is necessary to maintain a negative power coefficient at hot full power conditions throughout the entire cycle to reduce possible deleterious effects caused by a positive coefficient during loss-of-coolant or loss-of-flow accidents. The first fuel cycle contains more excess reactivity than subsequent cycles due to the loading of all fresh (unburned) fuel. Since soluble boron alone is insufficient to ensure a negative moderator coefficient, BA assemblies are also used.

The RCCAs and their control rod drive mechanisms (CRDMs) are the only moving parts in the reactor. Figure 4.2-8 illustrates the rod cluster control (RCC) and CRDM assembly, in addition to the arrangement of these components in the reactor, relative to the interfacing fuel assembly and guide tubes. In the following paragraphs, each reactivity control component is described in detail. The CRDM assembly is described in subsection 3.9.4.

The neutron source assemblies provide a means of monitoring the core during periods of low neutron activity. The thimble plug assemblies may be used to limit bypass flow through those fuel assembly thimbles which do not contain control rods, BA rods, or neutron source rods.

4.2.2.3.1 Rod Cluster Control Assemblies

The RCCAs are divided into two categories: control and shutdown. The control groups compensate for reactivity changes due to variations in operating conditions of the reactor (i.e., power and temperature variations). Two nuclear design criteria have been employed for selection of the control group. First, the total reactivity worth must be adequate to meet the nuclear requirements of the reactor. Second, in view of the fact that these rods may be partially inserted at power operation, the total power peaking factor should be low enough to ensure that the power capability is met. The control and shutdown groups provide adequate shutdown margin.

An RCCA is comprised of a group of individual neutron absorber rods fastened at the top end to a common spider assembly, as illustrated in figure 4.2-9.

The absorber materials used in the VEGP control rods are either solid Ag-In-Cd bar or hafnium (Hf) bar which are essentially "black" to thermal neutrons and have sufficient additional resonance absorption to significantly increase their worth. The absorber material is sealed in cold worked, high purity stainless steel tubes. (See figure 4.2-10.) A thin chrome electroplate is applied to the tubing outer surface of the Ag-In-Cd RCCA over a specified length which is in contact with the reactor internal guides for the Westinghouse RCCAs; for the Framatome RCCAs, the exterior of the rods are ion-nitrided to harden the surface. The cladding provides increased resistance to tube wear. Sufficient diametral and end clearances are provided to accommodate relative thermal expansion. In addition, the absorber diameter is slightly reduced at the lower extremity of the rodlets in order to accommodate absorber swelling and minimize cladding interaction.

The bottom plugs are made bullet-nosed to reduce the hydraulic drag during reactor trip and to guide smoothly into the dashpot section of the fuel assembly guide thimbles.

The material used in the absorber rod end plugs is type 308 stainless steel for the Westinghouse RCCAs; for the Framatome RCCAs, the absorber rod end plugs are 308L stainless steel. The design stresses used for the type 308P and 308L material are the same as those defined in the ASME Code, Section III, for type 304 stainless steel. At room temperature the yield and ultimate stresses per American Society of Testing Materials (ASTM) 580 are exactly the same for the two alloys. In view of the similarity of composition of the alloys, the temperature dependence of strength for the two materials is also assumed to be the same.

The allowable stresses used as a function of temperature are listed in table 1-1.2 of Section III of the ASME Code. The fatigue strength for the type 308 material is based on the S-N curve for austenitic stainless steels in figure 1-9.2 of Section III.

The spider assembly is in the form of a central hub with radial vanes containing cylindrical fingers from which the absorber rods are suspended. Handling detents and detents for connection to the drive rod assembly are machined into the upper end of the hub. Coil springs inside the spider body absorb the impact energy at the end of a trip insertion. The Westinghouse RCCAs have two coil springs and the Framatome RCCAs have a single coil spring. The radial vanes are joined to the hub by tack-welding and brazing, and the fingers are joined to the vanes by brazing for the Westinghouse RCCAs; for the Framatome RCCAs, the spider is a one-piece casting. A bolt which holds the springs and retainer is threaded into the hub within the skirt and welded to prevent loosening in service. All components of the Westinghouse RCCA spider assembly are made from types 304 and 308 stainless steel except for the retainer, which is of 17-4 PH material, and the springs, which are Inconel-718 alloy. For the Framatone RCCA spider assembly, the spider is made from CF3M (316L) stainless steel, the retainer is 17-4 PH stainless steel, and the spring is Inconel-718 alloy.

The absorber rods are fastened securely to the spider. The rods are first threaded into the spider fingers for the Westinghouse RCCAs; for the Framatome RCCAs, the rods pass through the spider boss and have nuts that thread onto the top of the rods. The Westinghouse and Framatome RCCAs are both pinned to maintain joint tightness, after which the pins are welded in place. The end plug below the pin position is designed with a reduced section to permit flexing of the rods to correct for small operating or assembly misalignments.

The overall length is such that when the assembly is withdrawn through its full travel, the tips of the absorber rods remain engaged in the guide thimbles so that alignment between rods and thimbles is always maintained. Since the rods are long and slender, they are relatively free to conform to any small misalignments with the guide thimble.

4.2.2.3.2 BA Assembly

Each BA assembly consists of BA rods attached to a holddown assembly. The BA assemblies are shown in figure 4.2-11. When needed for nuclear considerations, BA assemblies are inserted into selected thimbles within fuel assemblies.

The standard BA rods consist of borosilicate glass tubes contained within type 304 stainless steel tubular cladding plugged and seal-welded at the ends to encapsulate the glass. The glass is also supported along the length of its inside diameter by a thin-wall, tubular inner liner. The top end of the liner is open to permit the diffused helium to pass into the void volume, and the liner overhangs the glass. The liner has an outward flange at the bottom end to maintain the position of the liner with the glass. The cladding in the standard BA rods is slightly cold worked type 304 stainless steel. All other structural materials are type 304 or 308 stainless steel except for the springs, which are Inconel-718. The borosilicate glass tube provides sufficient boron content to meet the criteria discussed in subsection 4.3.1. A typical standard BA rod is shown in longitudinal and transverse cross-sections in figure 4.2-12.

Wet annual burnable absorber rods consist of annular pellets of alumina-boron carbide (AL_20_3-B_4C) burnable absorber material contained within two concentric Zircaloy tubes. These Zircaloy tubes which form the inner and the outer clad for the WABA rod are plugged, pressurized with helium, and seal-welded at each end to encapsulate the annular stack of absorber material. The absorber stack length (figure 4.2-12) is positioned axially within the WABA rods by the use of Zircaloy bottom-end spacers.

An annular plenum is provided within the rod to accommodate the helium gas released from the absorber material as it depletes during irradiation. The reactor coolant flows inside the inner tube and outside the outer tube of the annular rod. A typical WABA rod is shown in longitude and cross-section in figure 4.2-12. Additional design details are given in Section 3.0 of reference 22.

The BA rods in each fuel assembly are grouped and attached together at the top end of the rods to a holddown assembly by a flat, perforated retaining plate, which fits within the fuel assembly top nozzle and rests on the adapter plate.

The retaining plate and the BA rods are held down and restrained against vertical motion through a spring pack which is attached to the plate and is compressed by the upper core plate when the reactor upper internals assembly is lowered into the reactor. This arrangement ensures that the BA rods cannot be ejected from the core by flow forces. Each WABA rod is permanently attached to the base plate by a crimped attaching nut.

4.2.2.3.3 Neutron Source Assembly

The purpose of the neutron source assembly is to provide a base neutron level to ensure that the detectors are operational and responding to core multiplication neutrons. A neutron source is placed in the reactor to provide a positive neutron count of at least one-half count per second on the source range detectors attributable to core neutrons. The detectors, called source range detectors, are used primarily when the core is subcritical and during special subcritical modes of operations.

The source assembly also permits detection of changes in the core multiplication factor during core loading, refueling, control rod testing, and approach to criticality. This can be done since the multiplication factor is related to an inverse function of the detector count rate. Changes in the multiplication factor can be detected during addition of fuel assemblies while loading the core, changes in control rod positions, and changes in boron concentration.

Both primary and secondary neutron source rods are used. The primary source rod, containing a radioactive material, spontaneously emits neutrons during initial core loading, reactor startup, and initial operation of the first core. After the primary source rod decays beyond the desired neutron flux level, neutrons are then supplied by the secondary source rod. The secondary source rod contains a stable material, which must be activated during reactor operation. The activation results in the subsequent release of neutrons.

Four source assemblies are installed in the reactor core: two primary source assemblies and two secondary source assemblies. Each primary source assembly contains one primary source rod and a number of BA rods. Each secondary source assembly contains a symmetrical grouping of four secondary source rods. Locations not filled with a source or BA rod contain a thimble plug. The source assemblies are shown in figures 4.2-13 and 4.2-14.

Neutron source assemblies are employed at opposite sides of the core. The assemblies are inserted into the RCC guide thimbles in fuel assemblies at selected unrodded locations.

As shown in figures 4.2-13 and 4.2-14, the source assemblies contain a holddown assembly identical to that of the BA assembly.

The primary and secondary source rods both utilize the same cladding material as the absorber rods. The secondary source rods contain Sb-Be pellets stacked to a height of approximately 88 in. The primary source rods contain capsules of californium (Pu-Be possible alternate) source material and alumina spacer to position the source material within the cladding. The rods in each assembly are permanently fastened at the top end to a holddown assembly.

The other structural members, except for the springs, are constructed of type 304 stainless steel. The springs exposed to the reactor coolant are Inconel-718.

A double-encapsulated, secondary source rod assembly was introduced as a replacement to the single-encapsulated, secondary source rod assembly in Unit 1 Cycle 8 and Unit 2 Cycle 7. The double-encapsulated, secondary source design provides additional margin against source material leakage. This assembly has the same exterior dimensions as the single-encapsulated, secondary source assembly. The antimony-beryllium pellets (stack height 88 in.) are encapsulated in a pressurized, 304 stainless-steel tube and then inserted in an outer-pressurized, stainless-steel tube as indicated on figure 4.2-14. This assembly makes up the new double-encapsulated, secondary source rod assembly design.

4.2.2.3.4 Thimble Plug Assembly

Thimble plug assemblies may be used to limit bypass flow through the RCC guide thimbles in fuel assemblies which do not contain either control rods, source rods, or BA rods.

The thimble plug assemblies consist of a flat baseplate with short rods suspended from the bottom surface and a spring pack assembly, as shown in figure 4.2-15. The 24 short rods, called thimble plugs, project into the upper ends of the guide thimbles to reduce the bypass flow. Each thimble plug is permanently attached to the baseplate by a nut which is lock-welded or crimped to the threaded end of the plug. Similar short rods are also used on the source assemblies and BA assemblies to plug the ends of all vacant fuel assembly guide thimbles. When in the core, the thimble plug assemblies interface with both the upper core plate and with the fuel assembly top nozzles by resting on the adapter plate. The spring pack is compressed by the upper core plate when the upper internals assembly is lowered into place.

All components in the thimble plug assembly, except for the springs, are constructed from type 304 stainless steel. The springs are Inconel-718.

4.2.2.3.5 Stainless-Steel Rod Insert Assembly

The SSRIA is to provide power suppression and power shaping ability to restore design margin to meet the fuel rod internal pressure criterion.

The stainless-steel rods are mounted to a conventional insert holddown assembly, 24 rods per assembly. The rods are either solid design or solid for the top 3-foot section and stainless-steel tube for the lower 9-foot section. The rods are the same length and diameter as RCCA rodlets. Only one type of stainless-steel rod is used on an individual insert assembly. The SSRIA is shown in figure 4.2-16.

All components in the SSRIA, except for the springs, are constructed from type 304 and/or 308 stainless steel. The springs are Inconel-718.

4.2.3 DESIGN EVALUATION

The fuel assemblies, fuel rods, and incore control components are designed to satisfy the performance and safety criteria of section 4.2, the mechanical design bases of subsection 4.2.1, and other interfacing nuclear and thermal and hydraulic design bases specified in sections 4.3 and 4.4.

Effects of Conditions 2, 3, 4, or anticipated transients without trip on fuel integrity are presented in chapter 15 or supporting topical reports.

The initial step in fuel rod design evaluation for a region of fuel is to determine the limiting rod(s). Limiting rods are defined as those rods whose predicted performance provides the minimum margin to each of the design criteria. For a number of design criteria, the limiting rod is the lead burnup rod of a fuel region. In other instances, it may be the maximum power or the minimum burnup rod. For the most part, no single rod is limiting with respect to all design criteria.

After identifying the limiting rod(s), a worst-case performance analysis is performed, which considers the effects of rod operating history, model uncertainties, and dimensional variation. To verify adherence to the design criteria, the evaluation considers the effects of postulated transient power changes during operation consistent with Conditions 1 and 2. These transient power increases can affect both rod average and local power levels. Parameters considered include rod internal pressure, fuel temperature, clad stress, and clad strain. In fuel rod design analyses, these performance parameters provide the basis for comparison between expected fuel rod behavior and the corresponding design criteria limits.

Fuel rod and assembly models used for the performance evaluations are documented and maintained under an appropriate control system. Materials properties used in the design evaluations are given in reference 4.

4.2.3.1 Cladding

A. Vibration and Wear

Fuel rod vibrations are flow induced. The effect of vibration on the fuel assembly and individual fuel rods is minimal. The cyclic stress range associated with deflections of such small magnitude is insignificant and has no effect on the structural integrity of the fuel rod.

The reaction force on the grid supports due to rod vibration motions is also small and is much less than the spring preload. Firm fuel clad spring contact is maintained. No significant wear of the clad or grip supports is expected during the life of the fuel assembly, based on out-of-pile flow tests, performance of similarly designed fuel in operating reactors, and design analyses.

Clad fretting and fuel vibration has been experimentally investigated, as shown in reference 11.

B. Fuel Rod Internal Pressure and Cladding Stresses

A burnup-dependent fission gas release model[23, 27] is used in determining the internal gas pressures as a function of irradiation time. The plenum height of the fuel rod has been designed to ensure that the maximum internal pressure of the fuel rod will not exceed the value which would cause:

- The fuel/clad diametral gap to increase during steady-state operation.
- Extensive DNB propagation to occur.

The clad stresses at a constant local fuel rod power are low. Compressive stresses are created by the pressure differential between the coolant pressure and the rod internal gas pressure. Stresses due to the temperature gradient are not included in the volume average effective stress because thermal stresses

are, in general, negative at the clad inside diameter and positive at the clad outside diameter, and their contribution to the clad volume average stress is small. Furthermore, the thermal stress decreases with time during steady-state operation due to stress relaxation. The stress due to pressure differential is highest in the minimum power rod at beginning of life (BOL) due to low internal gas pressure, and the thermal stress is highest in the maximum power rod due to steep temperature gradient.

The volume average effective stress at BOL is substantially below the unirradiated clad strength (approximately 55,500 psi) at a typical clad mean operating temperature of 700°F.

Tensile stresses could be created once the clad has come in contact with the pellet. These stresses would be induced by the fuel pellet swelling during irradiation.

Swelling of the fuel pellet can result in small clad stains (less than 1 percent) for expected discharge burnups, but the associated clad stresses are very low because of clad creep (thermal- and irradiation-induced creep). The 1-percent strain criterion is extremely conservative for fuel-swelling driven clad strain because the strain rate associated with solid fission products swelling is very slow. A detailed discussion of fuel rod performance is given in paragraph 4.2.3.3.

C. Materials and Chemical Evaluation

Zircaloy-4/ZIRLO/Optimized ZIRLO clad have a high corrosion resistance to the coolant, fuel, and fission products. As shown in reference 3, there is considerable PWR operating experience on the capability of Zircaloy as a clad material. ZIRLO clad fuel rods were introduced in a Westinghouse core in 1991. Optimized ZIRLO cladding material has been approved for use in Vogtle 1 and 2 by the NRC, reference 29. Controls on fuel fabrication specify maximum moisture levels to preclude clad hydriding.

Metallographic examination of irradiated commercial fuel rods has shown occurrences of fuel/clad chemical interaction. Reaction layers of less than 1 mil in thickness have been observed between fuel and clad at limited points around the circumference. Metallographic data indicates that this interface layer remains very thin even at high burnup. Thus, there is no indication of propagation of the layer and eventual clad penetration.

Stress corrosion cracking is another postulated phenomenon related to fuel/clad chemical interaction. Out-of-pile tests have shown that in the presence of high clad tensile stresses, large concentrations of iodine can chemically attack the Zircaloy/ZIRLO/Optimized ZIRLO tubing and lead to eventual clad cracking. Extensive post-irradiation examination has produced no conclusive inpile evidence that this mechanism is operative in commercial fuel.

D. Rod Bowing

Reference 12 presents the model used for evaluation of fuel rod bowing. To the present time, this model has been used for bow assessment in 14 x 14, 15 x 15, and 17 x 17 type cores.

E. Consequences of Power Coolant Mismatch

This subject is discussed in chapter 15.

F. Creep Collapse and Creep-Down

This subject and the associated irradiation stability of cladding have been evaluated using the models described in references 7 and 26. It has been established that the design basis of no clad collapse during planned core life can be satisfied by limiting fuel densification and by having a sufficiently high initial internal rod pressure.

G. Fuel Assembly Design Evaluation with ZIRLO Clad Fuel Rods

Evaluations were performed using NRC approved fuel rod performance codes to ensure that the fuel rod design bases and design criteria stated in section 4.2 were met for the fresh fuel assemblies containing ZIRLO clad fuel rods commencing in Unit 2, Cycle 6. The fuel rod design bases, criteria, and models which are particularly affected by the ZIRLO clad are described in reference 25.

The design and predicted nuclear characteristics for each fuel rod clad with ZIRLO are similar to those described in section 4.3. The evaluations have shown that the nuclear design bases for fuel rods clad with ZIRLO are satisfied. The change to ZIRLO will not affect the use of the standard nuclear design analytical models and methods noted in table 4.1-2 and described in section 4.3 to accurately evaluate the neutronic behavior of fuel rods clad with ZIRLO.

The thermal and hydraulic design bases for the fuel rods clad with ZIRLO are identical to those discussed in section 4.4. Since the use of ZIRLO clad fuel does not represent changes of any magnitude affecting the parameters which are major contributors in this area (i.e., DNB, core flow, and rod bow), the design bases described in section 4.4 remain valid.

The two non-LOCA accidents potentially affected by the use of ZIRLO clad material are the locked rotor/shaft break and RCCA ejection accidents. For the locked rotor/shaft break accident, it was determined that the ZIRLO cladding resulted in a very small increase in peak clad temperature, and the effect on the metal-to-water reaction rate was negligible when compared to Zircaloy-4. However, sufficient margin exists in the VEGP plant safety analysis to accommodate the small PCT increase. For the RCCA ejection accident, the ZIRLO cladding results in a negligible effect in both the fraction of fuel melting at the hot spot and the fuel peak stored energy when compared to the results of Zircaloy-4. The conclusions in subsections 15.3.3, 15.3.4, and 15.4.8 for these two affected non-LOCA accidents remain valid.

The loss of coolant accident analyses for the VANTAGE 5 fuel in VEGP units were performed using the 1981 evaluation model with BASH (large break LOCA) and the NOTRUMP evaluation model (small break LOCA) described in paragraphs 15.6.5.3.1.1 and 15.6.5.3.1.2. Revisions to these evaluation models for use in the analyses of fuel with ZIRLO cladding have been identified and reported in reference 25. The revisions include the cladding specific heat, high-temperature creep (swelling), burst temperature, burst strain, and fuel assembly blockage. Calculations performed with the above revised evaluation models have shown that the effects of ZIRLO cladding on the large break and small break LOCA analysis results given in paragraphs 15.6.5.2 and 15.6.5.3 are minor.

H. Fuel Assembly Design Evaluation with Optimized ZIRLO Clad Fuel Rods

Consistent with the preceding item G for ZIRLO clad fuel rods, NRC approved fuel rod performance codes and methods are utilized to ensure the design criteria presented in section 4.2 are met during normal operation, including anticipated operational occurrences on a reload basis, reference 28.

4.2.3.2 Fuel Materials Considerations

Sintered, high-density uranium dioxide fuel reacts only slightly with the clad at core operating temperatures and pressures. In the event of clad defects, the high resistance of uranium dioxide to attack by water protects against fuel deterioration, although limited fuel erosion can occur. As has been shown by operating experience and extensive experimental work, the thermal design parameters conservatively account for changes in the thermal performance of the fuel elements due to pellet fracture which may occur during power operation. The consequences of defects in the clad are greatly reduced by the ability of uranium dioxide to retain fission products, including those which are gaseous or highly volatile. Observations from several operating Westinghouse PWRs[10] have shown that fuel pellets can densify under irradiation to a density higher than the manufactured values. Fuel densification and subsequent settling of the fuel pellets can result in local and distributed gaps in the fuel rods. Fuel densification has been minimized by improvements in the fuel manufacturing process and by specifying a nominal 95-percent initial fuel density.

The evaluation of fuel densification effects and the treatment of fuel swelling and fission gas release are described in references 23 and 27.

The effects of waterlogging on fuel behavior are discussed in paragraph 4.2.3.3.

4.2.3.3 Fuel Rod Performance

In the calculation of the steady-state performance of a nuclear fuel rod, the following interacting factors must be considered:

A. Clad creep and elastic deflection.

B. Pellet density changes, thermal expansion, gas release, and thermal properties as a function of temperature and fuel burnup.

C. Internal pressure as a function of fission gas release, rod geometry, and temperature distribution.

These effects are evaluated using fuel rod design models (ref. 23 and 27) which include appropriate models for time dependent fuel densification. With these interacting factors considered, the model determines the fuel rod performance characteristics for a given rod geometry, power history, and axial power shape.

In particular, internal gas pressure, fuel and clad temperatures, and clad deflections are calculated. The fuel rod is divided into several axial sections and radially into a number of annular zones. Fuel density changes are calculated separately for each segment. The effects are integrated to obtain the internal rod pressure.

The initial rod internal pressure is selected to delay fuel/clad mechanical interaction and to avoid the potential for flattened rod formation. It is limited, however, by the design criteria for the rod internal pressure (paragraph 4.2.1.3).

The gap conductance between the pellet surface and the clad inner diameter is calculated as a function of the composition, temperature and pressure of the gas mixture, and the gap size of contact pressure between clad and pellet. After computing the fuel temperature for each pellet annular zone, the fractional fission gas release is assessed using an empirical model derived from experimental data. (Ref. 23 and 27) The total amount of gas released is based on the average fractional release within each axial and radial zone and the gas generation rate, which in turn is a function of burnup. Finally, the gas released is summed over all zones, and the pressure is calculated.

The model shows close agreement in fit for a variety of published and proprietary data on fission gas release, fuel temperatures, and clad deflections (ref. 23, 25, and 27). These data include variations in power, time, fuel density, and geometry.

4.2.3.3.1 Fuel/Cladding Mechanical Interaction

One factor in fuel element duty is potential mechanical interaction of fuel and clad. This fuel/clad interaction produces cyclic stresses and strains in the clad, and these in turn reduce clad life. The reduction of fuel/clad interaction is therefore a goal of design. The technology for using prepressurized fuel rods in Westinghouse PWRs has been developed to further this objective.

The gap between the fuel and clad is initially sufficient to prevent hard contact between the two. However, during power operation a gradual compressive creep of the clad onto the fuel pellet occurs due to the external pressure exerted on the rod by the coolant. Clad compressive creep eventually results in the fuel/clad contact. Once fuel/clad contact occurs, changes in power level result in changes in clad stresses and strains. By using prepressurized fuel rods to partially offset the effect of the coolant external pressure, the rate of clad creep toward the surface of the fuel is reduced. Fuel rod prepressurization delays the time at which fuel/clad contact occurs and hence significantly reduces the extent of cyclic stresses and strains experienced by the clad both before and after fuel/clad contact. These factors result in an increase in the fatigue life margin of the clad and lead to greater clad reliability. If gaps should form in the fuel stacks, clad flattening will be prevented by the rod prepressurization so that the flattening time will be greater than the fuel core life.

A two-dimensional (r,Θ) finite element model has been established to investigate the effects of radial pellet cracks on stress concentrations in the clad. "Stress concentration" herein is defined as the difference between the maximum clad stress in the Θ direction and the mean clad stress. The first case has the fuel and clad in mechanical equilibrium; and, as a result, the stress in the clad is close to zero. In subsequent cases the pellet power is increased in steps and the resultant fuel thermal expansion imposes tensile stress in the clad. In addition to uniform clad stresses, stress concentrations develop in the clad adjacent to radial cracks in the pellet. These radial cracks have a tendency to open during a power increase, but the frictional forces between fuel and clad oppose the opening of these cracks and result in localized increases in clad stress. As the power is further increased, large tensile stresses exceed the ultimate tensile strength of UO_2, and additional cracks in the fuel are created, limiting the magnitude of the stress concentration in the clad.

As part of the standard fuel rod design analysis, the maximum stress concentration evaluated from finite element calculations is added to the volume-averaged effective stress in the clad as determined from the stress/strain calculations. The resultant clad stress is then compared to the temperature-dependent cladding yield stress in order to ensure that the stress/strain criteria are satisfied.

The transient evaluation method is described in the following paragraphs.

Pellet thermal expansion due to power increases is considered the only mechanism by which significant stresses and strains can be imposed on the clad.

Power increases in commercial reactors can result from fuel shuffling (e.g., region 3 positioned near the center core for cycle 2 operation after operating near the periphery during cycle 1), reactor power escalation following extended reduced power operation, and full-length control rod movement. In the mechanical design model, lead rods are depleted using best- estimate power histories as determined by core physics calculations. During burnup, the amount of diametral gap closure is evaluated based upon the pellet expansion cracking model, clad creep model, and fuel swelling model. At various times during the depletion, the power is increased locally on the rod to the burnup-dependent attainable power density as determined by core physics calculations. The radial, tangential, and axial clad stresses resulting from the power increase are combined into a volume average effective clad stress.

The Von Mises criterion is used to determine whether the clad yield stress has been exceeded. This criterion states that an isotropic material in multiaxial stress will begin to yield plastically when the effective stress exceeds the yield stress as determined by an axial tensile test. The yield stress correlation is that for irradiated cladding, since fuel/clad interaction occurs at high burnup. In applying this criterion, the effective stress is increased by an allowance which accounts for stress concentrations in the clad adjacent to radial cracks in the pellet, prior to the comparison with the yield stress. This allowance was evaluated using a two-dimensional (r,Θ) finite element model.

Slow transient power increases can result in large clad strains without exceeding the clad yield stress because of clad creep and stress relaxation. Therefore, in addition to the yield stress criterion, a criterion on allowable clad strain is necessary. Based upon high strain rate burst and tensile test data on irradiated tubing, 1-percent strain was determined to be conservative lower limit on irradiated clad ductility and thus was adopted as a design criterion.

A comprehensive review of the available strain fatigue models was conducted by Westinghouse as early as 1968. This included the Langer-O'Donnell model,[13] the Yao-Munse model, and the Manson-Halford model. Upon completion of this review, using the results of the Westinghouse experimental programs discussed below, it was concluded that the approach defined by Langer-O'Donnell would be retained and the empirical factors of their correlation modified in order to conservatively bound the results of the Westinghouse testing program.

The Langer-O'Donnell empirical correlation has the following form:

$$S_a = \frac{E}{4\sqrt{N_f}} \ln \frac{\left(\quad 100 \quad \right)}{100 - RA} + S_e$$

where:

S_a	=	$1/2\ E\ \Delta\ \varepsilon_t$ = pseudostress amplitude which causes failure in N cycles ($lb/in.^2$).
$\Delta\ \varepsilon_t$	=	total strain range (in./in.).
E	=	Young's Modulus ($lb/in.^2$).
N_f	=	number of cycles to failure.
RA	=	reduction in area at fracture in a uniaxial tensile.
S_e	=	endurance limit ($lb/in.^2$).

Both RA and S_e are empirical constants which depend on the type of material, the temperature, and irradiation.

The Westinghouse testing program was subdivided into the following subprograms:

A. A rotating bend fatigue experiment on unirradiated Zircaloy-4 specimens at room temperature and at 725°F. Both hydrided and nonhydrided Zircaloy-4 cladding was tested.

B. A biaxial fatigue experiment in gas autoclave on unirradiated Zircaloy-4 cladding, both hydrided and nonhydrided.

C. A fatigue test program on irradiated cladding from the Carolina-Virginia Tube Reactor and Yankee Core V conducted at Battelle Memorial Institute.

The results of these test programs provided information on different cladding conditions, including the effect of irradiation, hydrogen level, and temperature.

The design equations followed the concept for the fatigue design criterion according to the ASME Code, Section III:

A. The calculated pseudostress amplitude (S_a) has to be multiplied by a factor of 2 in order to obtain the allowable number of cycles (N_f).

B. The allowable cycles for a given S_a is 5 percent of N_f, or a safety factor of 20 on cycles.

The lesser of the two allowable numbers of cycles is selected. The cumulative fatigue life fraction is then computed as:

$$\sum_{1}^{k} \frac{n_k}{N_{fk}} \leq 1$$

where:

n_k = number of diurnal cycles of mode k.

N_{fk} = number of allowable cycles.

It is recognized that a possible limitation to the satisfactory behavior of the fuel rods in a reactor which is subjected to daily load follow is the failure of the clad by low-cycle strain fatigue. During their normal residence time in the reactor, the fuel rods may be subjected to approximately 1000 cycles with typical changes in power level from 50 to 100 percent of their steady-state values.

The assessment of the fatigue life of the fuel rod clad is subject to a considerable uncertainty due to the difficulty of evaluating the strain range with results from the cyclic interaction of the fuel pellets and clad. This difficulty arises, for example, from such highly unpredictable phenomena as pellet cracking, fragmentation, and relocation. Nevertheless, since early 1968, this particular phenomenon has been investigated analytically and experimentally. (Ref. 13) Strain fatigue tests on irradiated and nonirradiated hydrided Zircaloy-4 claddings were performed, which permitted a definition of a conservative fatigue life limit and recommendation on a methodology to treat the strain fatigue evaluation of the Westinghouse reference fuel rod designs.

It is believed that the final proof of the adequacy of a given fuel rod design to meet the load follow requirements can only come from incore experiments performed on actual reactors.

Experience in load follow operation dates back to early 1970 with the load follow operation of the Saxton reactor. Successful load follow operation has been performed on reactor A

(approximately 400 load follow cycles) and reactor B (approximately 500 load follow cycles). In both cases, there was no significant coolant activity increase that could be associated with the load follow mode of operation.

4.2.3.3.2 Irradiation Experience

Westinghouse fuel operational experience is presented in reference 3. Additional test assembly and test rod experience is given in sections 8 and 23 of reference 10. Optimized ZIRLO operating experience is documented in reference 28.

4.2.3.3.3 Fuel and Cladding Temperature

The methods used for evaluation of fuel rod temperatures are presented in paragraph 4.4.2.11.

4.2.3.3.4 Waterlogging

Local cladding deformations typical for waterlogging [c] bursts have never been observed in commercial Westinghouse fuel. Experience has shown that the small number of rods which have acquired clad defects, regardless of primary mechanism, remain intact and do not progressively distort or restrict coolant flow. In fact, such small defects are normally observed through reductions in coolant activity to be progressively closed upon further operation due to the buildup of zirconium oxide and other substances. Secondary failures which have been observed in defected rods are attributed to hydrogen embrittlement of the cladding. Post-irradiation examinations point to the hydriding failure mechanism rather than a waterlogging mechanism; the secondary failures occur as axial cracks in the cladding and are similar regardless of the primary failure mechanism. Such cracks do not result in flow blockage or increase the effects of any postulated transients.

More information is provided in references 14 and 15.

4.2.3.3.5 Potentially Damaging Temperature Effects During Transients

The fuel rod experiences many operational transients (intentional maneuvers) during its residence in the core. A number of thermal effects must be considered when analyzing the fuel rod performance.

The clad can be in contact with the fuel pellet at some time in the fuel lifetime. Clad/pellet interaction occurs if the fuel pellet temperature is increased after the clad is in contact with the pellet. Clad/pellet interaction is discussed in paragraph 4.2.3.3.1.

The potential effects of operation with waterlogged fuel are discussed in paragraph 4.2.3.3.4, which concluded that waterlogging is not a concern during operational transients.

Clad flattening, as shown in reference 7, has been observed in some operating power reactors. Thermal expansion (axial) of the fuel rod stack against a flattened section of clad could cause

[c] Waterlogging damage of a previously defected fuel rod has occasionally been postulated as a mechanism for subsequent rupture of the cladding. Such damage has been postulated as a consequence of a power increase on a rod after water has entered such a rod through a clad defect of appropriate size. Rupture is postulated upon power increase if the rod internal pressure increase is excessive due to insufficient venting of water to the reactor coolant.

failure of the clad. This is no longer a concern because clad flattening is precluded during the fuel residence in the core (paragraph 4.2.3.1).

Potential differential thermal expansion between the fuel rods and the guide thimbles during a transient is considered in the design. Excessive bowing of the fuel rods is precluded because the grid assemblies allow axial movement of the fuel rods relative to the grids. Specifically, thermal expansion of the fuel rods is considered in the grid design so that axial loads imposed on the fuel rods during a thermal transient will not result in excessively bowed fuel rods.

4.2.3.3.6 Fuel Element Burnout and Potential Energy Release

As discussed in paragraph 4.4.2.2, the core is protected from DNB over the full range of possible operating conditions. In the extremely unlikely event that DNB should occur, the clad temperature will rise due to the steam blanketing at the rod surface and the consequent degradation in heat transfer. During this time there is a potential for chemical reaction between the cladding and the coolant. However, because of the relatively good film boiling heat transfer following DNB, the energy release resulting from this reaction is insignificant compared to the power produced by the fuel.

4.2.3.3.7 Coolant Flow Blockage Effects on Fuel Rods

This evaluation is presented in paragraph 4.4.4.7.

4.2.3.4 Spacer Grids

The coolant flow channels are established and maintained by the structure composed of grids and guide thimbles. The lateral spacing between fuel rods is provided and controlled by the support dimples of adjacent grid cells. Contact of the fuel rods on the dimples is maintained through the clamping force of the grid springs. Lateral motion of the fuel rods is opposed by the spring force and the internal moments generated between the spring and the support dimples. Grid testing is discussed in reference 16.

4.2.3.5 Fuel Assembly

4.2.3.5.1 Stresses and Deflections

The fuel assembly component stress levels are limited by the design. For example, stresses in the fuel rod due to thermal expansion and Zircaloy/ZIRLO/Optimized ZIRLO irradiation growth are limited by the relative motion of the rod as it slips over the grid spring and dimple surfaces. Clearances between the fuel rod ends and nozzles are provided so that Zircaloy/ZIRLO/Optimized ZIRLO irradiation growth does not result in rod end interferences. Stresses in the fuel assembly caused by tripping of the RCCA have little influence on fatigue because of the small number of events during the life of an assembly. Assembly components and prototype fuel assemblies made from production parts have been subjected to structural tests to verify that the design bases requirements are met.

The fuel assembly design loads for shipping have been established at 4 g axial and 6 g lateral. Accelerometers are permanently placed in the shipping cask to monitor and detect fuel

assembly accelerations that would exceed the criteria. Past history and experience have indicated that loads which exceed the allowable limits rarely occur. Exceeding the limits requires reinspection of the fuel assembly for damage. Tests on various fuel assembly components, such as the grid assembly, sleeves, inserts, and structure joints, have been performed to ensure that the shipping design limits do not result in impairment of fuel assembly function. Seismic analysis of the fuel assembly is presented in reference 16.

To demonstrate that the fuel assemblies will maintain a geometry that is capable of being cooled under the worst-case accident Condition 4 event, Westinghouse has performed the following analyses.

The fuel assembly response resulting from safe shutdown earthquake (SSE) condition was analyzed using the history numerical techniques. The vessel motion for this type of accident primarily causes lateral loads on the reactor core. Consequently, the finite element seismic model as described in references 16 and 17 was used to assess the fuel assembly deflections and impact forces. However, the input parameters were modified to appropriately represent the Westinghouse 17 x 17 8-ft Inconel grid fuel assembly to be used in the VEGP units.

The motions of the upper and lower core plates and the barrel at the upper core plate elevation, which are simultaneously applied to the simulated reactor core model as input motion, were obtained from the time-history analysis of the reactor vessel and internals. The fuel assembly response, namely the displacements and impact forces, was obtained with the reactor core model by using the motions resulting from a reactor pressure vessel inlet nozzle break which produced the limiting structural loads for the fuel assembly.

4.2.3.5.1.1 Grid Analyses. The maximum grid impact force obtained from seismic analyses is less than the allowable grid strength. With respect to the guidelines of Appendix A of SRP Section 4.2, Westinghouse has demonstrated that a simultaneous SSE and LOCA event is highly unlikely. The fatigue cycles, crack initiation, and crack growth due to normal operating and seismic events will not realistically lead to a pipe rupture. (Ref. 18)

Based on the deterministic fracture mechanics evaluation of small flaws in piping components, Westinghouse has demonstrated that the dynamic effects of a large pipe rupture in the primary coolant piping system for the VEGP units is reduced. An exemption from a portion of the requirements of General Design Criterion 4 of Appendix A to 10 CFR Part 50 has been granted to the VEGP units. (Ref. 19)

The result of a pipe leakage accident would be to impose insignificant asymmetric loadings on the reactor core system. The fuel assembly grid load due to pipe ruptures was not applied to the analysis results.

4.2.3.5.1.2 Nongrid Analyses. The stresses induced in the various fuel assembly nongrid components were assessed based on the most limiting seismic condition. The fuel assembly axial forces resulting from the normal spring hold-down load together with its own weight distribution are the primary source of the stresses in the thimble guide tube and fuel assembly nozzles. The fuel-rod-accident-induced stresses, which are generally very small, are caused by bending due to the fuel assembly deflections during the seismic accident. A summary of the seismic-induced stresses, which are expressed in terms of a percentage of allowable stress limits for the fuel assembly major components, is given in table 4.2-1. The component stresses, which include normal operating stresses, are substantially below the established allowable limits. Consequently, the structural designs of the fuel assembly components are acceptable under the postulated accident design conditions for the VEGP.

4.2.3.5.2 Dimensional Stability

A prototype fuel assembly has been subjected to column loads in excess of those expected in normal service and faulted conditions. (Ref. 16)

No interference with control rod insertion into thimble tubes will occur during a postulated seismic transient due to fuel rod swelling, thermal expansion, or bowing. In the early phase of the transient following the coolant break, the high axial loads, which could be generated by the difference in thermal expansion between fuel clad and thimbles, are relieved by slippage of the fuel rods through the grids. The relatively low drag force restraint on the fuel rods will induce only minor thermal bowing, which is insufficient to close the fuel rod-to-thimble tube gap.

4.2.3.6 Reactivity Control Assembly and Burnable Absorber Rods

4.2.3.6.1 Internal Pressure and Cladding Stresses During Normal, Transient, and Accident Conditions

The designs of the BA and source rods provide a sufficient cold void volume to accommodate the internal pressure increase during operation. This is not a concern for the RCCA absorber rod because no gas is released by the absorber material (whether it be Ag-In-Cd or hafnium).

For the standard BA rod, the use of glass in tubular form provides a central void volume along the length of the rods (figure 4.2-12). For the WABA rod, there is also sufficient cold void volume to limit the internal pressure to a value, which satisfies the design criteria. For the source rods, a void volume is provided within the rod in order to limit the internal pressure increase until end of life (EOL) (figures 4.2-13 and 4.2-14).

The stress analysis of these rods assumes 100-percent gas release to the rod void volume in addition to the initial pressure within the rod.

During normal transient and accident conditions, the void volume limits the internal pressures to values which satisfy the criteria in paragraph 4.2.1.6. These limits are established not only to ensure that peak stresses do not reach unacceptable values, but also to limit the amplitude of the oscillatory stress component in consideration of the fatigue characteristics of the materials.

Rod, guide thimble, and dashpot flow analyses indicate that the flow is sufficient to prevent coolant boiling within the guide thimble. Therefore, clad temperatures at which the clad material has adequate strength to resist coolant operating pressures and rod internal pressures are maintained.

4.2.3.6.2 Thermal Stability of the Absorber Material, Including Changes and Thermal Expansion

The radial and axial temperature profiles within the source and absorber rods have been determined by considering gap conductance, thermal expansion, neutron or gamma heating of the contained material as well as gamma heating of the clad.

The maximum temperatures of the Ag-In-Cd or Hf rod absorber material were calculated and found to be significantly less than the respective material melting point and to occur axially at only the highest flux region. The thermal expansion properties of the absorber materials and the phase changes are discussed in reference 4 for Ag-In-Cd and reference 9 for Hf.

The maximum temperature of the borosilicate glass in the standard burnable absorber was calculated to be about 1300°F, which occurs following the initial rise to power. As the operating cycle proceeds, the glass and pellet temperature decreases for the following reasons:

A. Reduction in power generation due to boron-10 depletion.

B. Better gap conductance as the helium produced diffuses to the gap.

C. External gap reduction due to borosilicate glass creep.

The maximum temperature of the Al_20_3-B_4C burnable absorber pellet is calculated to be less than 1200°F which takes place following the initial rise to power. As the operating cycle proceeds the burnable absorber pellet temperature decreases for the following reasons: (1) a reduction in heat generation due to boron depletion, and (2) better gap conduction as the helium produced diffuses into the gap.

Sufficient diametral and end clearances have been provided in the control rods, burnable absorber, and source rods to accommodate the relative thermal expansions between the enclosed material and the surrounding clad and end plug.

4.2.3.6.3 Irradiation Stability of the Absorber Material, Taking into Consideration Gas Release and Swelling

The irradiation stability of the Ag-In-Cd and Hf absorber material is discussed in references 4 and 9, respectively. Irradiation produces no deleterious effects in the Ag-In-Cd absorber material.

As mentioned in paragraph 4.2.3.6.1, gas release is not a concern for the control rod material because no gas is released by the absorber material. Sufficient diametral and end clearances are provided to accommodate swelling of the absorber material.

Based on experience with borosilicate glass and on nuclear and thermal calculations, gross swelling or cracking of the glass in the standard burnable absorber tubing is not expected during operation. Some minor creep of the glass at the hot spot could occur but would only continue until boron-10 depletion and helium gap closure by creep had lowered the glass temperature to values which cause negligible creep. The wall thickness of the inner liner is sized to provide adequate support in the event of slumping and to collapse locally before rupture of the exterior cladding if unexpected large volume changes due to swelling or cracking should occur. The ends of the inner liner are open to allow helium, which diffuses out of the glass, to occupy the central void.

The Al_20_3-B_4C WABA pellets are designed such that gross swelling or crumbling of the pellets is not expected to occur during reactor operation. Some minor cracking of the pellets may occur, but this cracking should not affect the overall absorber and stack integrity.

4.2.3.6.4 Potential for Chemical Interaction, Including Possible Waterlogging Rupture

The structural materials selected have good resistance to irradiation damage and are compatible with the reactor environment.

Corrosion of the materials exposed to the coolant is quite low, and proper control of chloride and oxygen in the coolant will prevent the occurrence of stress corrosion. The potential for the interference with RCC movement due to possible corrosion phenomena is very low.

Waterlogging rupture is not a failure mechanism associated with VEGP control rods. However, a breach of the cladding for any postulated reason does not result in serious consequences.

Both the Ag-In-Cd and Hf absorber materials are relatively inert and would still remain remote from high coolant velocity regions. Rapid loss of material resulting in significant loss of reactivity control material would not occur. Bettis test results (ref. 4) concluded that additions of indium and cadmium to silver, in the amounts to form the Westinghouse absorber material composition, result in small corrosion rates.

The consequences of a clad breach in the standard BA cladding would be small. It is anticipated that upon clad breach, the borosilicate glass would be leached by the coolant water and that localized power peaking of a few percent would occur; no design criteria would be expected to be violated.

For the WABA, in the unlikely event that the Zircaloy clad is breached, the B_4C in the affected rod(s) could be leached-out by the coolant water. If this occurred early, incore instruments could detect large peaking factor changes, and corrective action would be taken, if warranted. A postulated clad breach after substantial irradiation would have no significant effect on peaking factors since the boron will have been burned-out. Breaching of the Zircaloy clad by internal hydriding is not expected due to moisture controls employed during fabrication. Rods of this design have also performed very well with no failures observed.

4.2.4 TESTING AND INSPECTION PLAN

4.2.4.1 Quality Assurance Program

The quality assurance program plan of the Westinghouse Nuclear Fuel Division for the VEGP is summarized in reference 20.

The program provides for control over all activities affecting product quality, commencing with design and development and continuing through procurement, materials handling, fabrication, testing and inspection, storage, and transportation. The program also provides for the indoctrination and training of personnel and for the auditing of activities affecting product quality through a formal auditing program.

Westinghouse drawings and product, process, and material specifications identify the inspections to be performed.

4.2.4.2 Quality Control

Quality control philosophy is generally based on the following inspections being performed to a 95-percent confidence that at least 95 percent of the product meets specification, unless otherwise noted.

A. Fuel System Components and Parts

The characteristics inspected depend upon the component parts; the quality control program includes dimensional and visual examinations, check audits of test reports, material certification, and nondestructive examination, such as X-ray and ultrasonic.

All material used in this core is accepted and released by quality control.

B. Pellets

Inspection is performed for dimensional characteristics such as diameter, density, length, and squareness of ends. Additional visual inspections are performed for cracks, chips, and surface conditions according to approved standards.

Density is determined in terms of weight per unit length and is plotted on zone charts used in controlling the process. Chemical analyses are taken on a specified sample basis throughout pellet production.

C. Rod Inspection

Fuel rod, control rodlet, BA rod, and source rod inspection consists of the following nondestructive examination techniques and methods, as applicable:

1. Each rod is leak tested using a calibrated mass spectrometer, with helium being the detectable gas.
2. Rod welds are inspected by ultrasonic test or X-ray in accordance with a qualified technique and Westinghouse specifications meeting the requirements of ASTM-E-142.
3. All rods are dimensionally inspected prior to final release. The requirements include such items as length, camber, and visual appearance.
4. All fuel rods are inspected by gamma scanning or other approved methods, as discussed in paragraph 4.2.4.5, to ensure proper plenum dimensions.
5. All fuel rods are inspected by gamma scanning, or other approved methods, as discussed in paragraph 4.2.4.5, to ensure that no significant gaps exist between pellets.
6. All fuel rods are active gamma scanned to verify enrichment control prior to acceptance for assembly loading.
7. Traceability of rods and associated rod components is established by quality control.

D. Assemblies

Each fuel rod, control rod, BA rod, and source rod assembly is inspected for compliance with drawing and/or specification requirements. Other incore control component inspection and specification requirements are given in paragraph 4.2.4.4.

E. Other Inspections

The following inspections are performed as part of the routine inspection operation:

1. Tool and gauge inspection and control, including standardization to primary and/or secondary working standards. Tool inspection is performed at prescribed intervals on all serialized tools. Complete records are kept of calibration and conditions of tools.

2. Audits are performed of inspection activities and records to ensure that prescribed methods are followed and that records are correct and properly maintained.

3. Surveillance inspection, where appropriate, and audits of outside contractors are performed to ensure conformance with specified requirements.

F. Process Control

To prevent the possibility of mixing enrichments during fuel manufacture and assembly, strict enrichment segregation and other process controls are exercised.

The UO_2 powder is kept in sealed containers. The contents are fully identified. A Westinghouse identification tag completely describing the contents is affixed to the containers before transfer to powder storage. Isotopic content is confirmed by analysis.

Powder withdrawal from storage can be made by only one authorized group, which directs the powder to the correct pellet production line. All pellet production lines are physically separated from each other, and pellets of only a single nominal enrichment are present in any one section of a given production line at any given time. Enrichment barriers prevent mixing of product on a production line.

Finished pellets are placed on trays and transferred to segregated storage racks within the confines of the pelleting area. Samples from each pellet lot are tested for isotopic content and impurity levels prior to acceptance by quality control. Physical barriers prevent mixing of pellets of different nominal densities and enrichments in this storage area. Unused powder and substandard pellets are returned to storage in the appropriate item control area.

Pellets are loaded into fuel cladding tubes on isolated production lines. Each production line contains only rods of one fuel type at any one time. The cladding tubes are identified by serialized traceability codes. The code uniquely identifies each rod and is maintained with the rod throughout production.

After inspection, the rods are loaded into a magazine for subsequent loading into a fuel assembly. At the time the magazines are loaded, the fuel rod identification numbers are entered into a computer system which then identifies the location of each rod within a given fuel assembly. After the loading of the fuel assembly, the top nozzle, which is inscribed with a permanent identification number, is attached to the assembly.

Similar traceability is provided for BA, source rods, and control rodlets, as required.

4.2.4.3 Online Fuel Failure Monitoring

The function of the CVCS letdown monitor is to monitor the CVCS letdown liquid process and to provide indication of abnormal activity levels in the RCS. This monitor can act as a means of failed fuel warning because failed fuel would be a cause of an increase in activity. However, confirmation of the cause of any abnormal activity levels will be made by laboratory analysis of primary coolant. For a discussion of the CVCS letdown monitor, refer to information provided

on liquid process and effluent monitors presented in section 11.5, paragraph 11.5.2.3, and table 11.5.2-1.

4.2.4.4 Incore Control Component Testing and Inspection

Tests and inspections are performed on each reactivity control component to verify the mechanical characteristics. In the case of the full-length RCCA, prototype testing has been conducted; and both manufacturing test/inspections and functional testing at the plant site are performed.

During the component manufacturing phase, the following requirements apply to the reactivity control components to ensure the proper functioning during reactor operation:

A. All materials are procured to specifications to attain the desired standard of quality.

B. All Westinghouse spider assemblies (a spider from each braze lot for Hf RCCAs) are proof tested by applying a 5000-lb load to the spider body, so that approximately 310 lb are applied to each vane. This proof load provides a bending moment at the spider body approximately equivalent to 1.4 times the load caused by the acceleration imposed by the CRDM.[(a)]

C. All rods are checked for integrity by the methods described in paragraph 4.2.4.2C.

D. To ensure proper fit with the fuel assembly, the rod cluster control, BA, and source assemblies are installed in the fuel assembly and checked for binding in the dry condition.

The RCCAs are functionally tested, following core loading but prior to criticality, to demonstrate reliable operation of the assemblies. Each assembly is operated (and tripped) one time at full-flow/hot conditions.

In order to demonstrate continuous free movement of the RCCAs and to ensure acceptable core power distributions during operations, partial movement checks are performed on every RCCA, as required by the Technical Specifications. In addition, periodic drop tests of the full-length RCCAs are performed at each refueling shutdown to demonstrate continued ability to meet trip time requirements.

If an RCCA cannot be moved by its mechanism, adjustments in the boron concentration of the coolant ensure that adequate shutdown margin would be achieved following a trip. Thus, inability to move one RCCA can be tolerated. More than one inoperable RCCA could be tolerated but would impose additional demands on the plant operator. Therefore, the number of inoperable RCCAs has been limited to one.

4.2.4.5 Tests and Inspections by Others

If any tests and inspections are to be performed on behalf of Westinghouse, Westinghouse will review and approve the quality control procedures, inspection plans, etc., to be utilized to ensure that they are equivalent to the description provided in paragraphs 4.2.4.1 through 4.2.4.4 and are performed properly to meet all Westinghouse requirements.

---

a. Requirement B is not applicable to the Framatome RCCA spider assemblies.

4.2.4.6 Inservice Surveillance

As detailed in reference 3, significant 17 x 17, 12-ft Inconel grid fuel assembly operating experience has been obtained. VEGP will establish a surveillance program for inspection of post-irradiated fuel assemblies. This surveillance program will establish the schedule, guidelines, and inspection criteria for conducting visual inspection of post-irradiated fuel assemblies and/or insert components. As a minimum, the surveillance program will include a quantitative visual examination of some discharged fuel assemblies from each refueling. This program includes criteria for additional inspection requirements for post-irradiated fuel assemblies if unusual characteristics are noticed in the visual inspection or plant instrumentation and subsequent laboratory analysis indicates gross failed fuel. The VEGP post irradiated fuel surveillance program will address disposition of fuel assemblies and/or insert components receiving an unsatisfactory visual inspection. Those post-irradiated fuel assemblies receiving an unsatisfactory visual inspection shall not be reinserted into the core until a more detailed inspection and/or evaluation can be performed. Normally the fuel assemblies will be taken to the spent fuel inspection station.

The engineering group is responsible for initiating the necessary corrective actions.

4.2.4.7 Onsite Inspection

Written procedures are used by the station staff for the post- shipment inspection of all new fuel and associated components, such as control rods, plugs, and inserts. Fuel handling procedures specify the sequence in which handling and inspection take place.

Loaded fuel containers, when received onsite, are externally inspected to ensure that labels and markings are intact and seals are unbroken. After the containers are opened, the shock indicators attached to the suspended internals are inspected to determine whether movement during transit exceeded design limitations.

Following removal of the fuel assembly from the container in accordance with detailed procedures, the fuel assembly plastic wrapper is examined for evidence of damage. The polyethylene wrapper is then removed, and a visual inspection of the entire bundle is performed.

Control rod, source, and BA assemblies usually are shipped in fuel assemblies and are inspected prior to removal of the fuel assembly from the container. The control rod assembly is withdrawn a few inches from the fuel assembly to ensure free and unrestricted movement, and the exposed section is visually inspected for mechanical integrity, replaced in the fuel assembly, and stored with the fuel assembly. Control rod, source, or BA assemblies may be stored separately or within fuel assemblies in the new fuel storage area.

Westinghouse designed an experimental program to obtain in-reactor creep and growth behavior data for various cladding and structural zirconium-based alloys to fluence levels that support long-term target values for fuel burnup. The program involves the irradiation of non-fueled test samples in symmetric core locations in VEGP Unit 2 commencing with Cycle 10.

For the duration of the program, the test samples will be inserted into as many as four selected host fuel assemblies in the reload core. The test samples that will be irradiated for more than one cycle will be moved to the new once-burned fuel assemblies after each cycle of operation. Neutronically equivalent dummy samples will be used as needed to preserve core symmetry. The reload evaluation for each cycle will address the cycle-specific test samples.

The discharged test samples will be removed from the fuel assemblies and prepared for shipment. The test samples will be sheared and loaded into casks for shipment to a hot cell test facility. The remaining test parts and the dummy samples can be stored in the spent fuel pool.

4.2.4.8 References

1. Letter, T. M. Anderson (Westinghouse) to J. R. Miller (NRC), dated August 15, 1980.
2. Letter, T. M. Anderson (Westinghouse) to J. R. Miller (NRC), dated April 21, 1981.
3. Slagle, W. H., "Operational Experience with Westinghouse Cores," WCAP-8183 (revised annually).
4. Beaumont, M. D., et al., "Properties of Fuel and Core Component Materials," WCAP-9179, Revision 1 (Proprietary), and WCAP-9224 (Nonproprietary), July 1978.
5. Slagle, W. H., et al., “17x17 Next Generation Fuel (17x17 NGF) Reference Core Report,” May 2011.
6. Deleted.
7. George, R. A., Lee, Y. C., and Eng, G. H., "Revised Clad Flattening Model," WCAP-8377 (Proprietary) and WCAP-8381 (Nonproprietary), July 1974.
8. Risher, D., et al., "Safety Analysis for the Revised Fuel Rod Internal Pressure Design Basis," WCAP-8963 (Proprietary), November 1976, and WCAP-8964 (Nonproprietary), August 1977.
9. "Hafnium," Appendix A to Reference 2, October 1980.
10. Eggleston, F. T., "Safety-Related Research and Development for Westinghouse Pressurized Water Reactors, Program Summaries - Winter 1976 - Summer 1978," WCAP-8768, Revision 2, October 1977.
11. Demario, E. E., "Hydraulic Flow Test of the 17 x 17 Fuel Assembly," WCAP-8278 (Proprietary) and WCAP-8279 (Nonproprietary), February 1974.
12. Skaritka, J., ed, "Fuel Rod Bow Evaluation," WCAP-8691, Rev 1, July 1979.
13. O'Donnell, W. J. and Langer, B. F., "Fatigue Design Basis for Zircaloy Components," Nuclear Science and Engineering 20, pp 1-12, 1964.
14. Stephan, L. A., "The Effects of Cladding Material and Heat Treatment on the Response of Waterlogged UO_2 Fuel Rods to Power Bursts," IN-ITR-111, January 1970.
15. Western New York Nuclear Research Center Correspondence With the U.S. Atomic Energy Commission on February 11 and August 27, 1971, Docket No. 50-57.
16. Gesinski, L. and Chiang, D., "Safety Analysis of the 17 x 17 Fuel Assembly for Combined Seismic and Loss-of-Coolant Accident," WCAP-8236 (Proprietary) and WCAP-8288 (Nonproprietary), December 1973.
17. Beaumont, M. D., et al., "Verification, Testing, and Analysis of the 17 x 17 Optimized Fuel Assembly," WCAP-9401-P-A (Proprietary) and WCAP-9402-A (Nonproprietary), August 1981.
18. Witt, F. J., Bamford, W. H., and Esselman, T. C., "Integrity of the Primary Piping Systems of Westinghouse Nuclear Power Plants During Postulated Seismic Events," WCAP-9283, March 1978.

19. "Georgia Power Company, et al., (Vogtle Electric Generating Plant, Units 1 and 2), Exemption," Federal Register, Volume 50, No. 27, February 8, 1985.

20. "Nuclear Fuel Division Quality Assurance Program Plan," WCAP-7800, Revision 4-A, March 1975.

21. Davidson, S. L. ed et al., "Reference Core Report VANTAGE 5 Fuel Assembly," WCAP-10444-P-A, September 1985.

22. Skaritka, J., et al., "Westinghouse Wet Annular Burnable Absorber Evaluation Report," WCAP-10021-P-A, Revision 1 (Proprietary), October 1983.

23. Weiner, R. P., et al., "Improved Fuel Performance Models for Westinghouse Fuel Rod Design and Safety Evaluations," WCAP-10851-P-A (Proprietary) and WCAP-11873-A (Nonproprietary), August 1988.

24. Davidson, S. L. ed et al., "Extended Burnup Evaluation of Westinghouse Fuel, "WCAP-10125-P-A and WCAP-10126-N1-P (Nonproprietary), December 1985.

25. Davidson, S. L., et al., "VANTAGE + Fuel Assembly Reference Core Report," WCAP-12610-P-A, April 1995.

26. Kersting, P. J., et al., "Assessment of Clad Flattening and Densification Power Spike Factor Elimination in Westinghouse Nuclear Fuel," WCAP-13589-A, March 1995.

27. Foster, J. P., et al., "Westinghouse Improved Performance Analysis and Design Model (PAD 4.0)," WCAP-15063-P-A, Revision 1, with Errata, July 2000.

28. Shah, H., “Optimized ZIRLO™,” WCAP-12610-P-A & CENPD-404-P-A Addendum 1-A, July 2006.

29. U.S. NRC, R. E. Martin letter to SNC, C. R. Pierce, “Joseph M. Farley Nuclear Plant, Units 1 and 2, and Vogtle Electric Generating Plant, Units 1 and 2, Issuance of Amendments Regarding Use of Optimized ZIRLO (CAC Nos. MF7480, MF7481, MF7482, AND MF7483),” August 04, 2016 (Agencywide Documents Access and Management System (ADAMS) Accession No. ML16179A386).

TABLE 4.2-1

FUEL ASSEMBLY COMPONENT STRESSES
(PERCENT OF ALLOWABLE)

Component	Uniform Stresses (Membrane/Direct)	Combined Stresses (Membrane and Bending)
Thimble	54.9	37.8
Fuel rod[a]	23.7	15.8
Top nozzle plate	(b)	6.6
Bottom nozzle plate	(b)	12.7
Bottom nozzle leg	2.0	9.1

a. Includes primary operating stresses.

b. Indicates a negligible value.

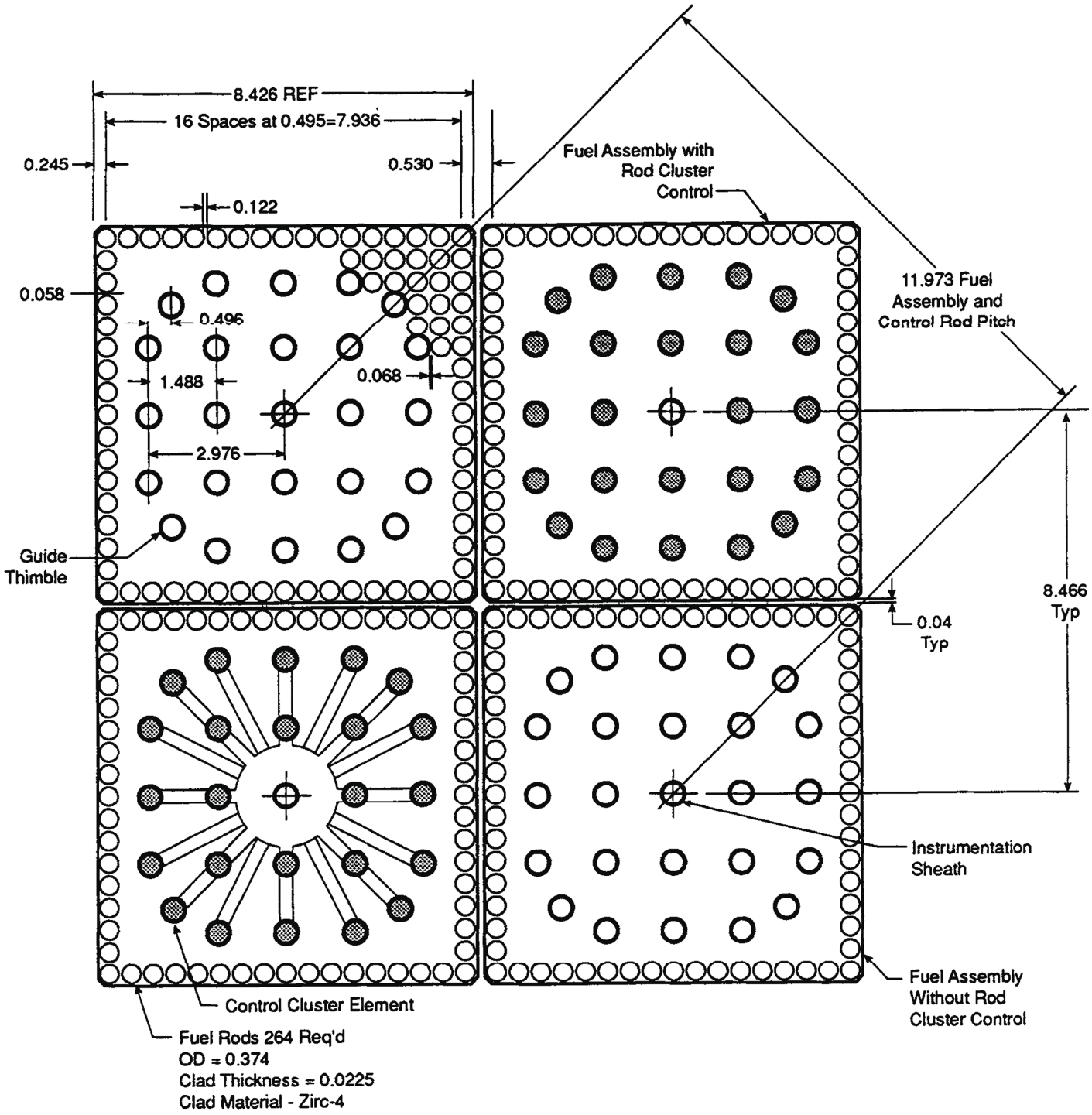

REV 14 10/07

SOUTHERN COMPANY
Energy to Serve Your World®

VOGTLE
ELECTRIC GENERATING PLANT
UNIT 1 AND UNIT 2

FUEL ASSEMBLY CROSS–SECTION
17 X 17 LOPAR

FIGURE 4.2–1 (SHEET 1 OF 2)

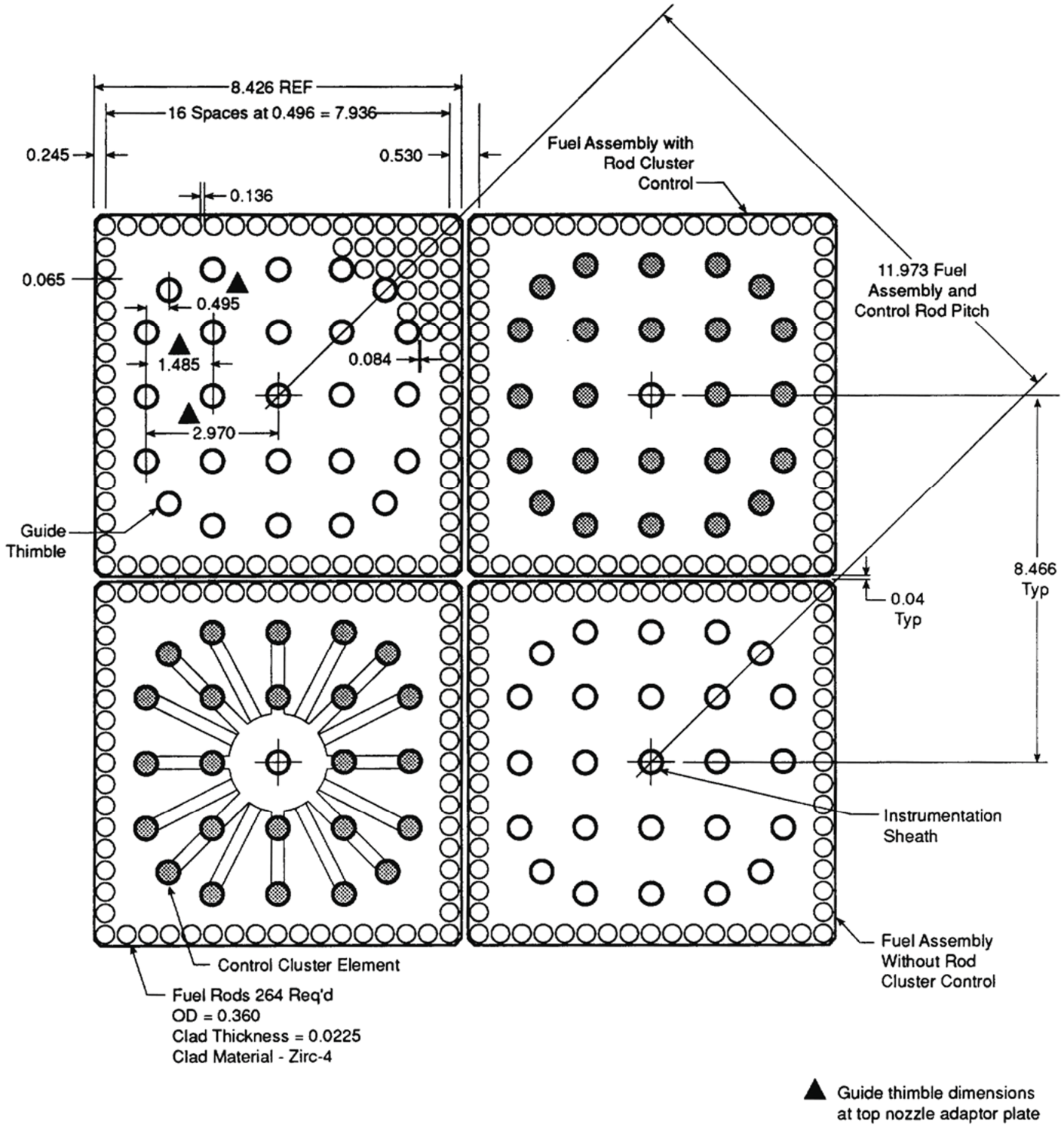

REV 14 10/07

SOUTHERN COMPANY
Energy to Serve Your World®

VOGTLE
ELECTRIC GENERATING PLANT
UNIT 1 AND UNIT 2

FUEL ASSEMBLY CROSS–SECTION
17 X 17 VANTAGE 5

FIGURE 4.2–1 (SHEET 2 OF 2)

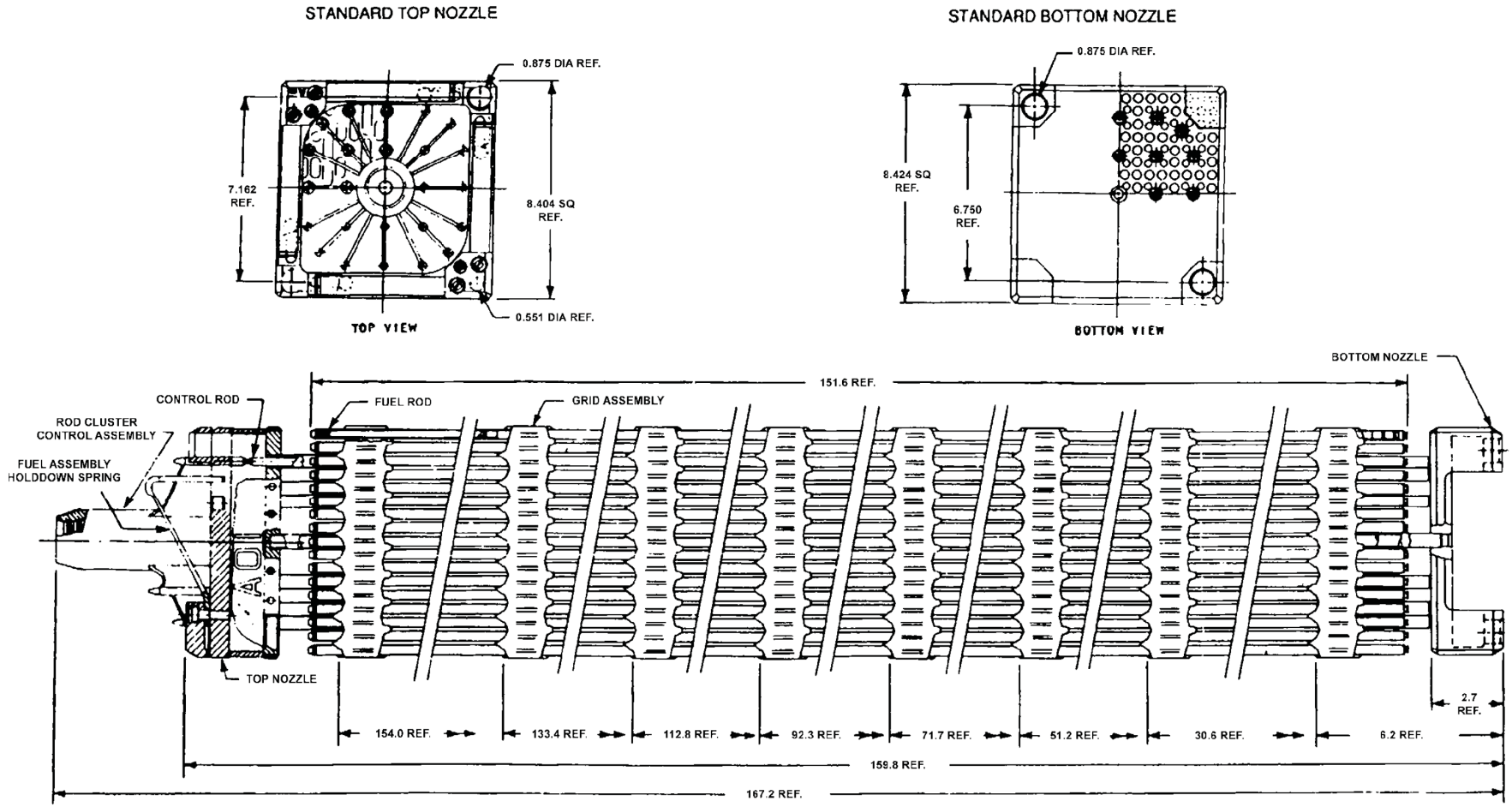

REV 24 10/22

SOUTHERN COMPANY
Energy to Serve Your World®

VOGTLE
ELECTRIC GENERATING PLANT
UNIT 1 AND UNIT 2

FUEL ASSEMBLY OUTLINE, 17 X 17
LOPAR, REGIONS 5A, 5B, 5C
5D, 5L, 5M, 5N

FIGURE 4.2–2 (SHEET 1 OF 7)

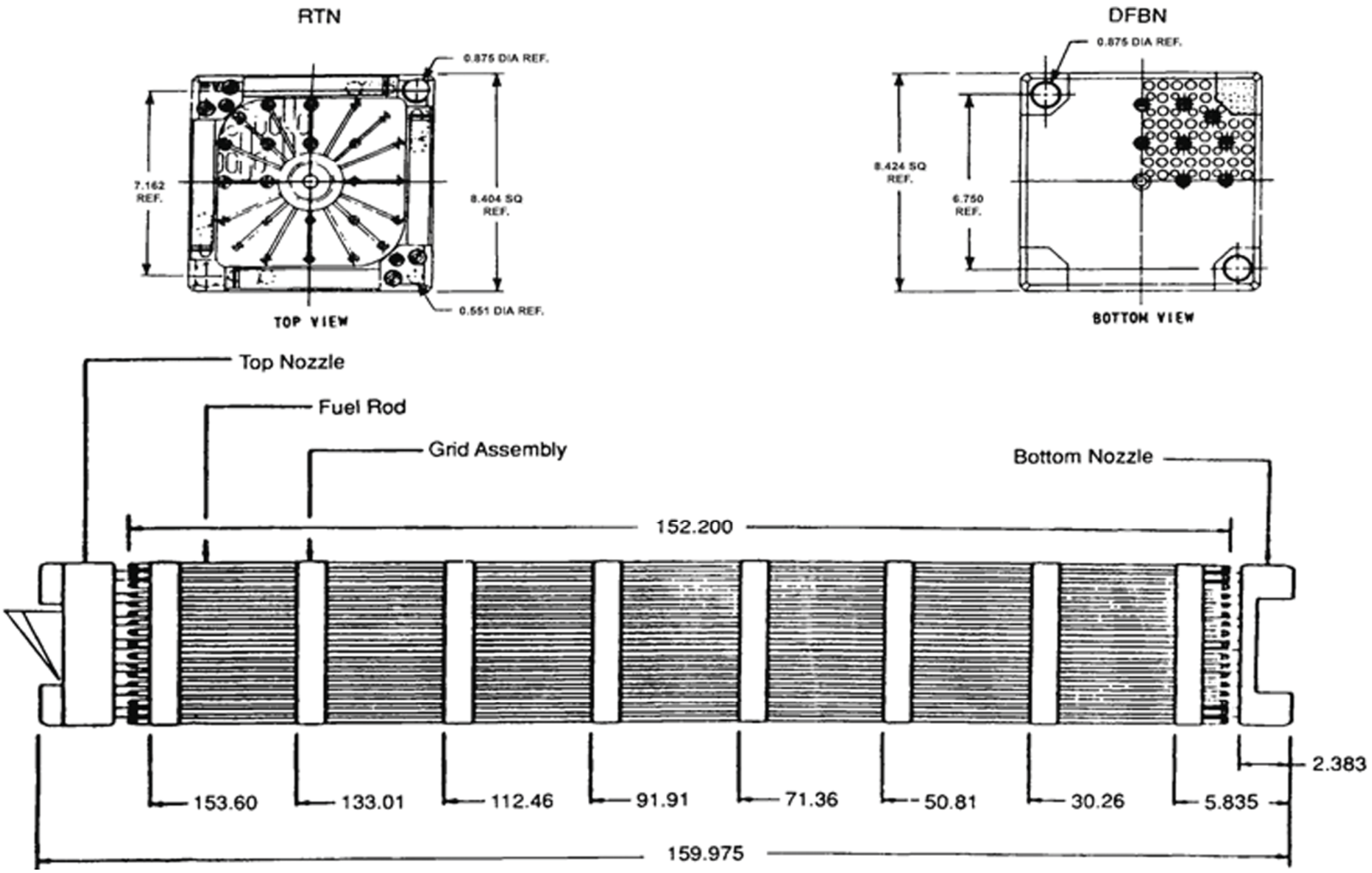

REV 24 10/22

SOUTHERN COMPANY
Energy to Serve Your World®

VOGTLE
ELECTRIC GENERATING PLANT
UNIT 1 AND UNIT 2

FUEL ASSEMBLY OUTLINE, 17 X 17
LOPAR, REGIONS 5E, 5P

FIGURE 4.2–2 (SHEET 2 OF 7)

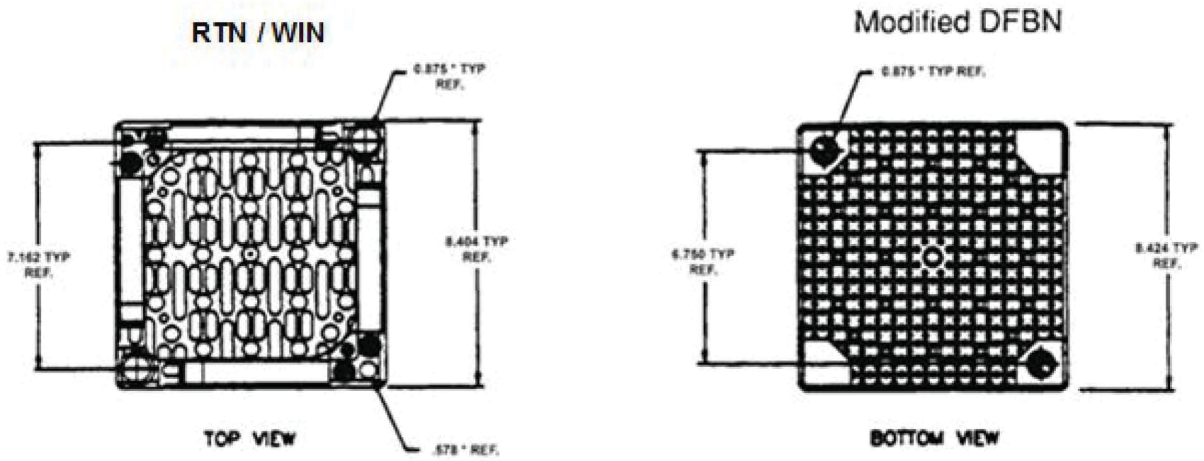

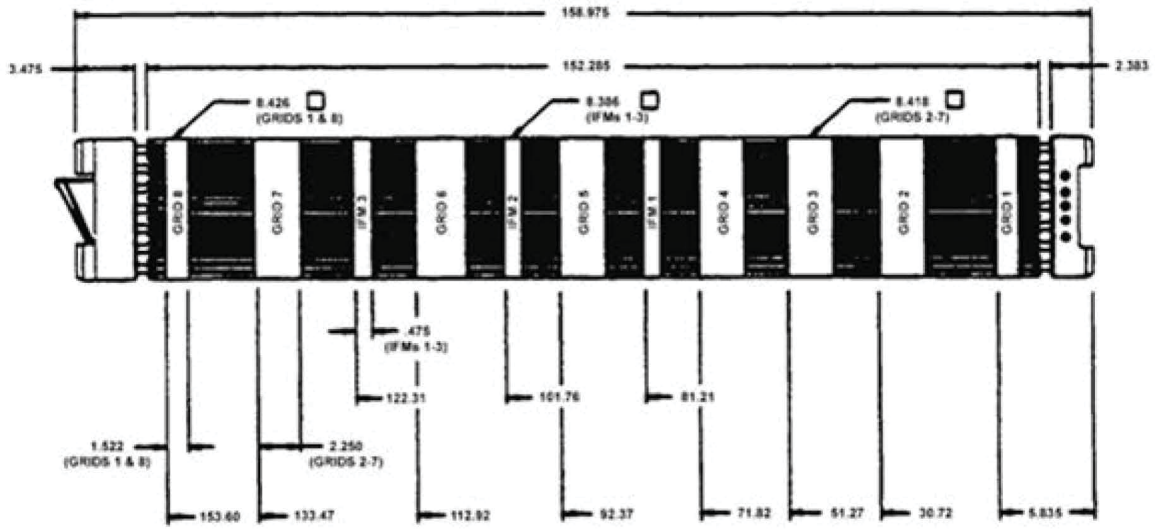

17 X 17 VANTAGE 5 FUEL ASSEMBLY

REV 24 10/22

SOUTHERN COMPANY
Energy to Serve Your World®

VOGTLE
ELECTRIC GENERATING PLANT
UNIT 1 AND UNIT 2

FUEL ASSEMBLY OUTLINE
17 X 17 VANTAGE 5

FIGURE 4.2–2 (SHEET 3 OF 7)

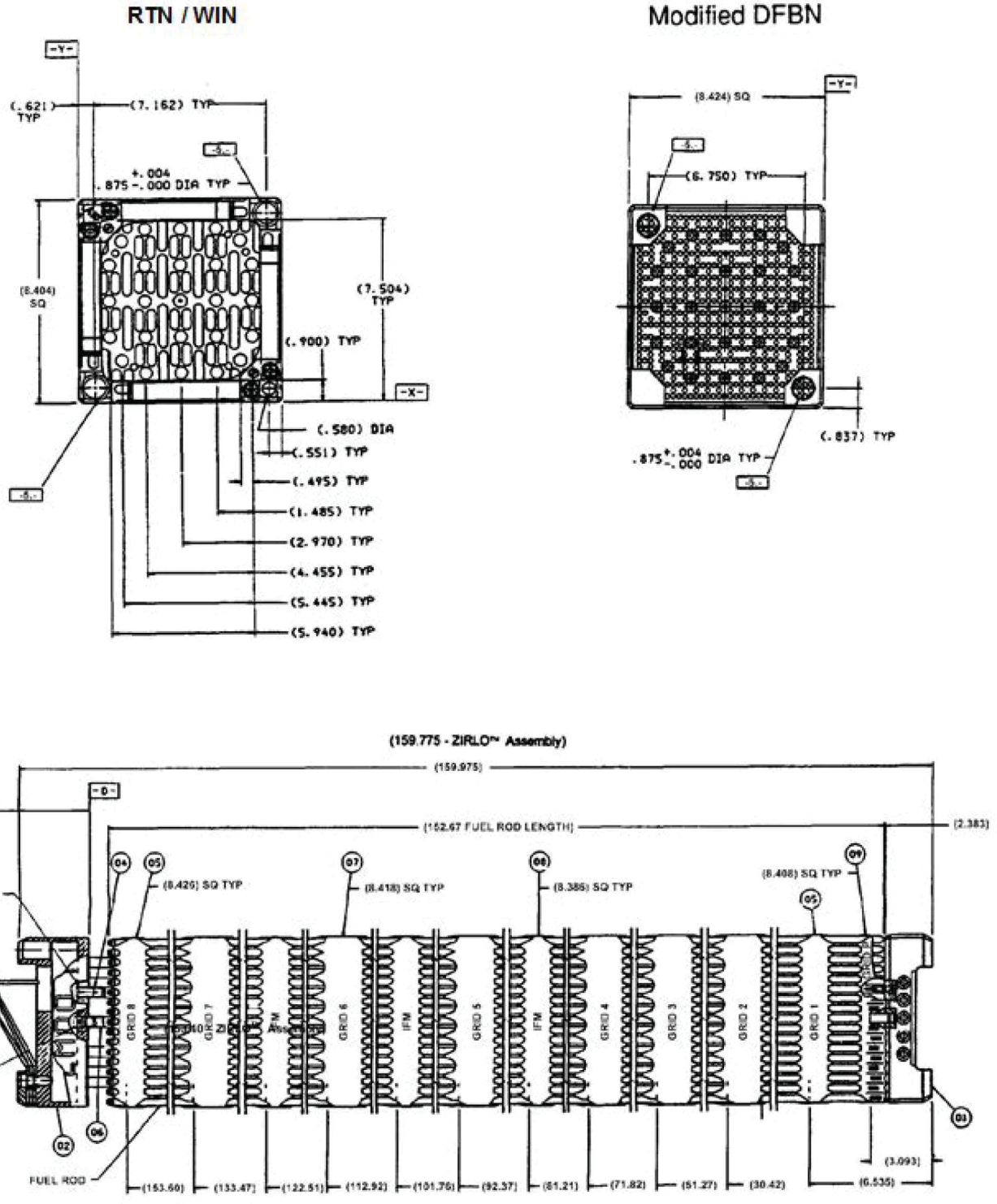

REV 21 4/18

SOUTHERN COMPANY
Energy to Serve Your World®

VOGTLE
ELECTRIC GENERATING PLANT
UNIT 1 AND UNIT 2

FUEL ASSEMBLY OUTLINE
17 X 17 OFA P+ ZIRC–4/ZIRLO®/
ZIRLO/OPTIMIZED ZIRLO™ FUEL RODS

FIGURE 4.2–2 (SHEET 4 OF 7)

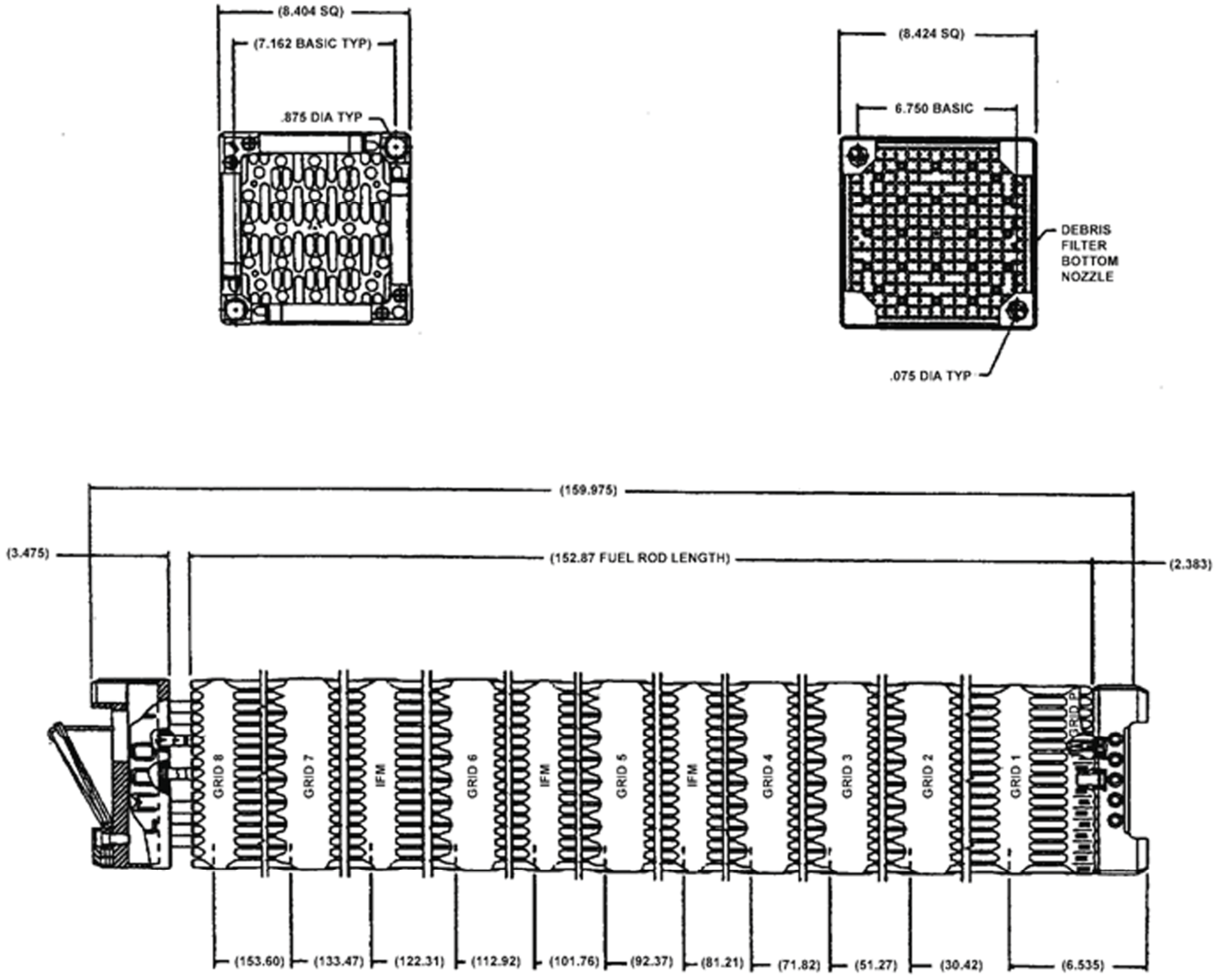

REV 24 10/22

SOUTHERN COMPANY
Energy to Serve Your World®

VOGTLE
ELECTRIC GENERATING PLANT
UNIT 1 AND UNIT 2

FUEL ASSEMBLY OUTLINE
17 X 17 VANTAGE+ WITH LOW ROD
INTERNAL PRESSURE FUEL RODS

FIGURE 4.2–2 (SHEET 5 OF 7)

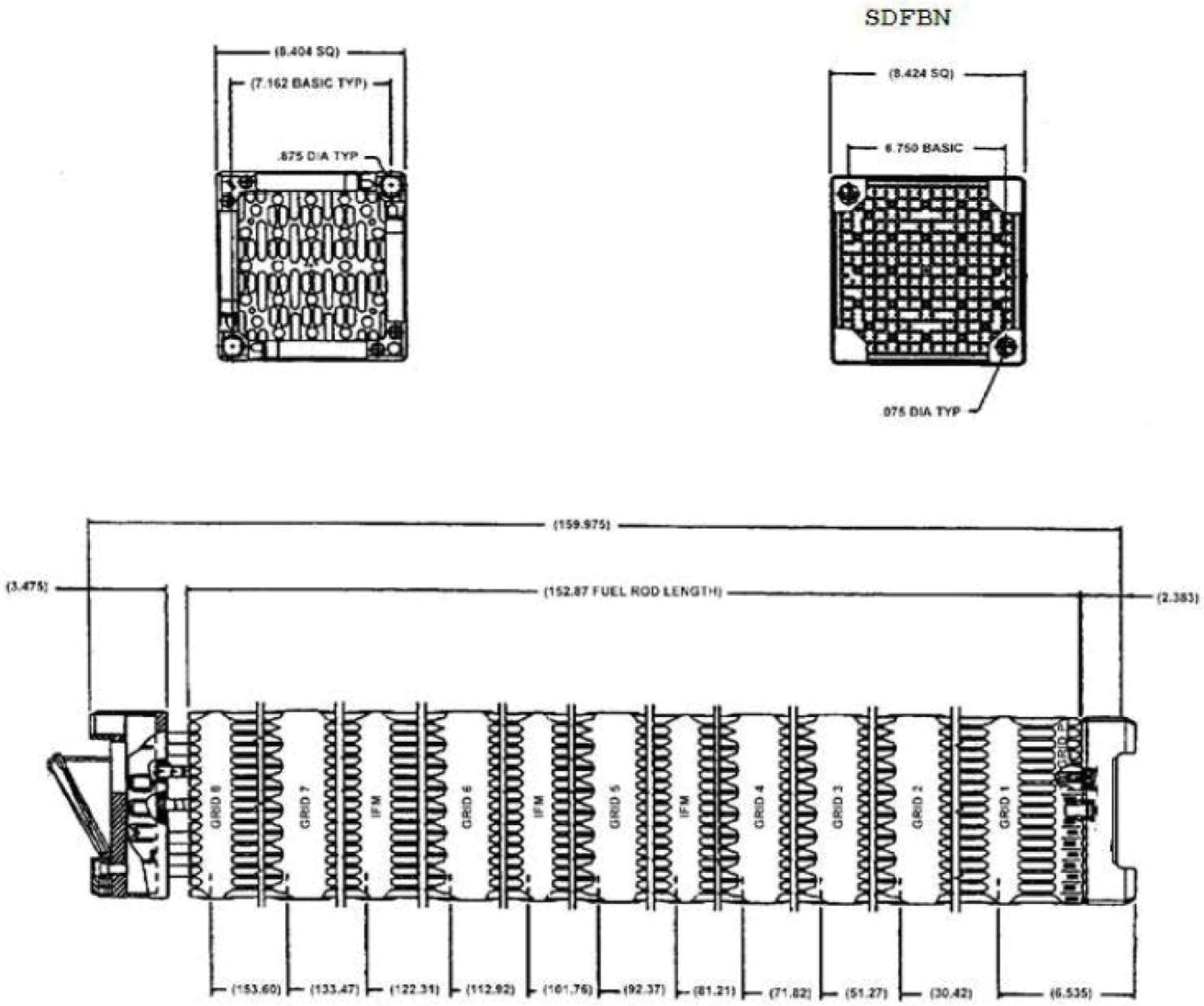

REV 24 10/22

SOUTHERN COMPANY *Energy to Serve Your World®* **VOGTLE** **ELECTRIC GENERATING PLANT** **UNIT 1 AND UNIT 2**	FUEL ASSEMBLY OUTLINE 17 X 17 VANTAGE+ WITH LOW ROD INTERNAL PRESSURE FUEL RODS AND SDFBN FIGURE 4.2-2 (SHEET 6 OF 7)

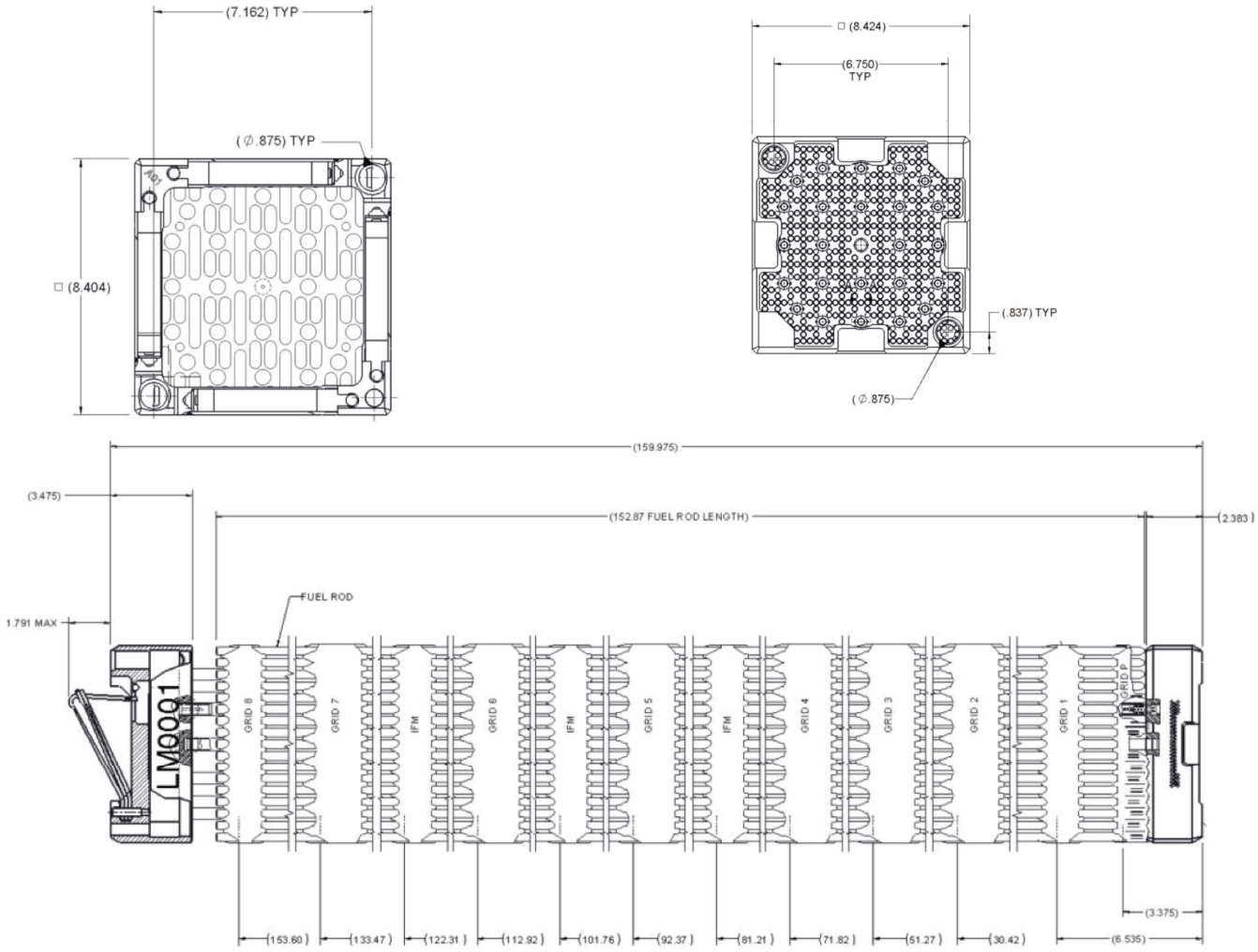

REV 24 10/22

SOUTHERN COMPANY *Energy to Serve Your World®* **VOGTLE ELECTRIC GENERATING PLANT UNIT 1 AND UNIT 2**	FUEL ASSEMBLY OUTLINE, 17 X 17 PRIME FUEL ASSEMBLY
	FIGURE 4.2-2 (SHEET 7 OF 7)

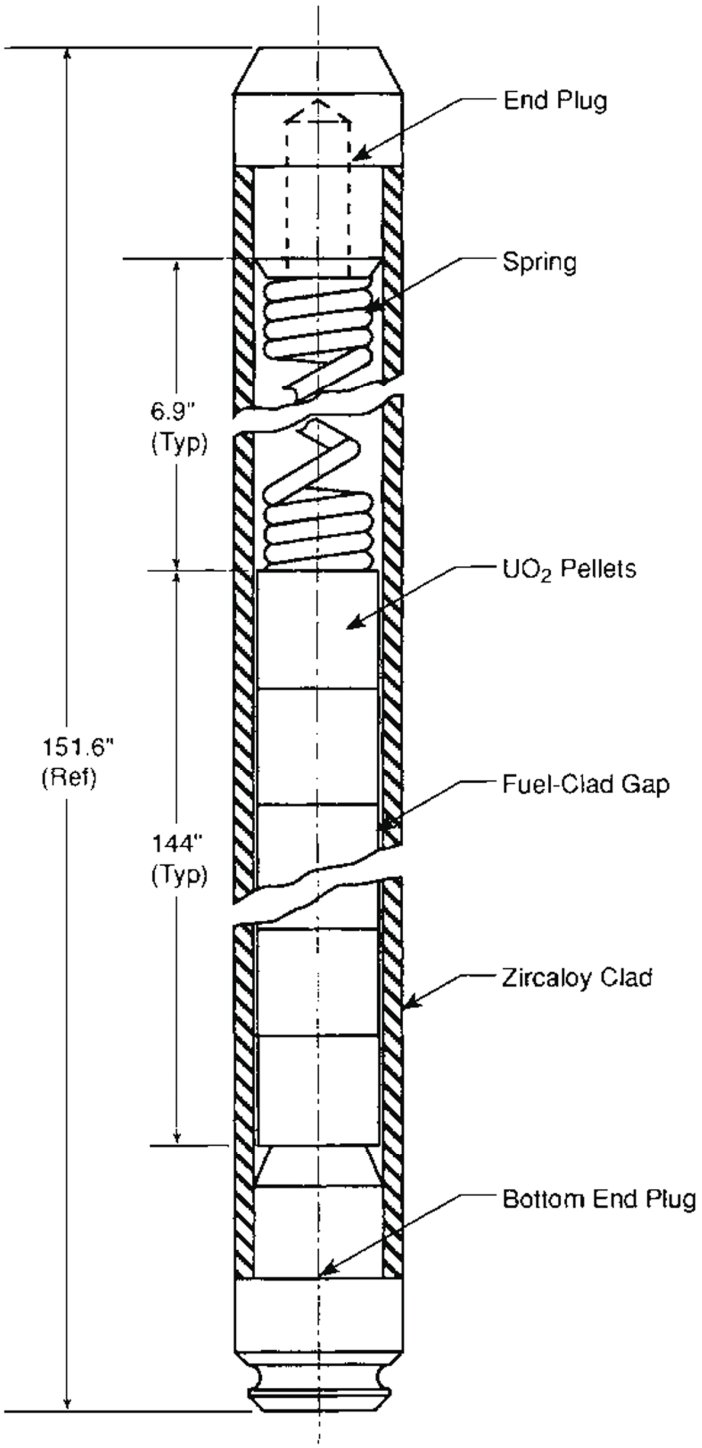

Specific dimensions depend on design variables such as prepressurization, power history, and discharge burnup.

REV 14 10/07

SOUTHERN COMPANY
Energy to Serve Your World®

VOGTLE
ELECTRIC GENERATING PLANT
UNIT 1 AND UNIT 2

FUEL ROD SCHEMATIC
LOPAR, REGIONS 5A, 5B, 5C, 5D, 5L
5M, 5N,

FIGURE 4.2–3 (SHEET 1 OF 4)

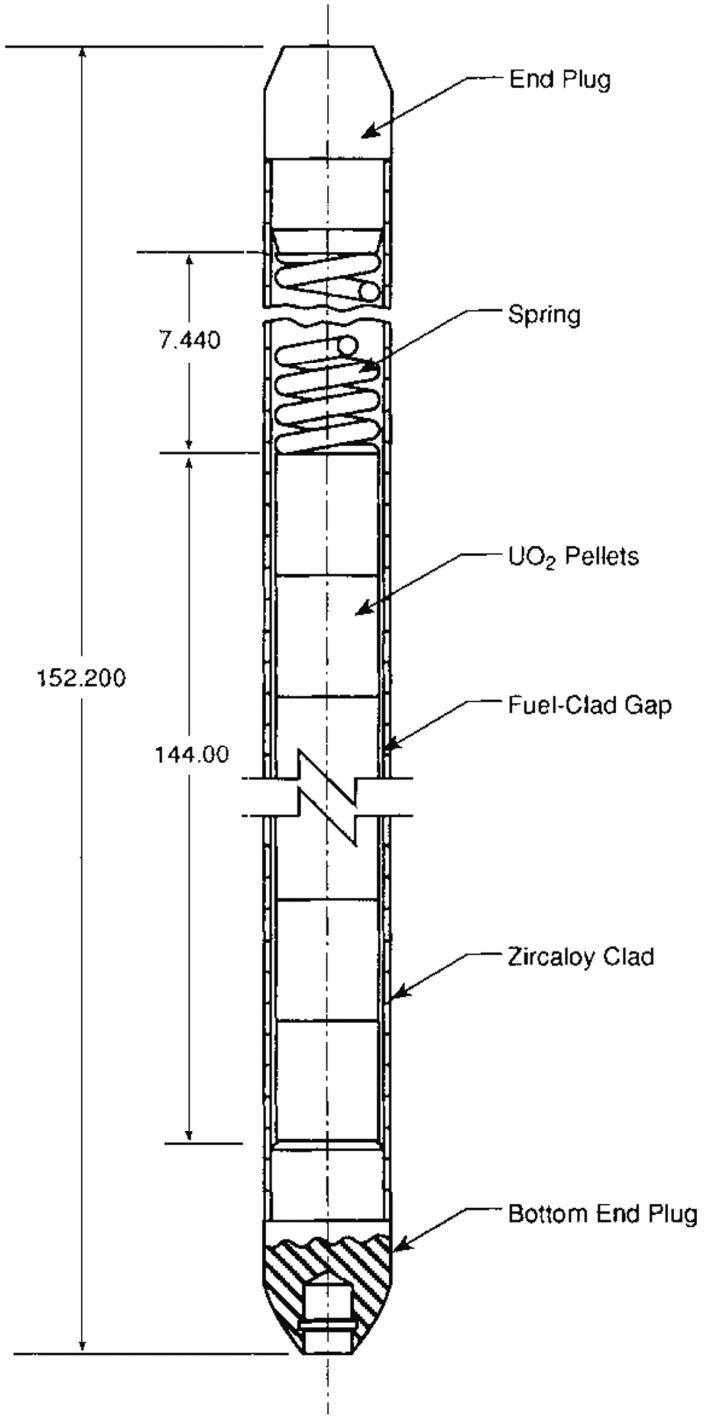

Specific dimensions depend on design variables such as prepressurization, power history, and discharge burnup.

REV 14 10/07

SOUTHERN COMPANY
Energy to Serve Your World®

VOGTLE
ELECTRIC GENERATING PLANT
UNIT 1 AND UNIT 2

FUEL ROD SCHEMATIC
LOPAR, REGIONS 5E, 5P

FIGURE 4.2–3 (SHEET 2 OF 4)

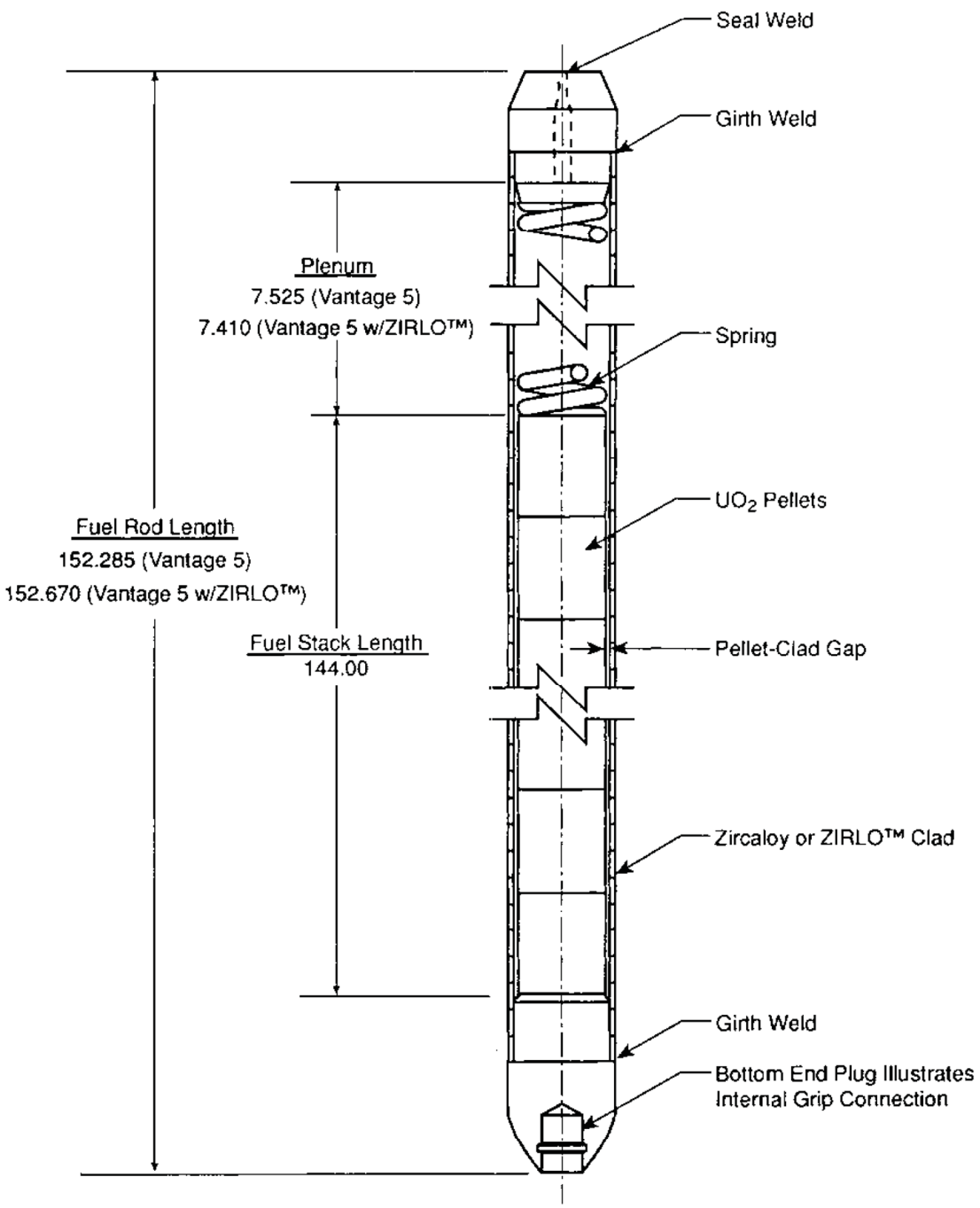

17x17 Fuel Rod Assembly

Specific dimensions depend on design variables such as prepressurization, power history, and discharge burnup.

Dimensions are in inches (nominal)

REV 14 10/07

SOUTHERN COMPANY *Energy to Serve Your World®*	**VOGTLE ELECTRIC GENERATING PLANT UNIT 1 AND UNIT 2**	FUEL ROD SCHEMATIC VANTAGE 5
		FIGURE 4.2–3 (SHEET 3 OF 4)

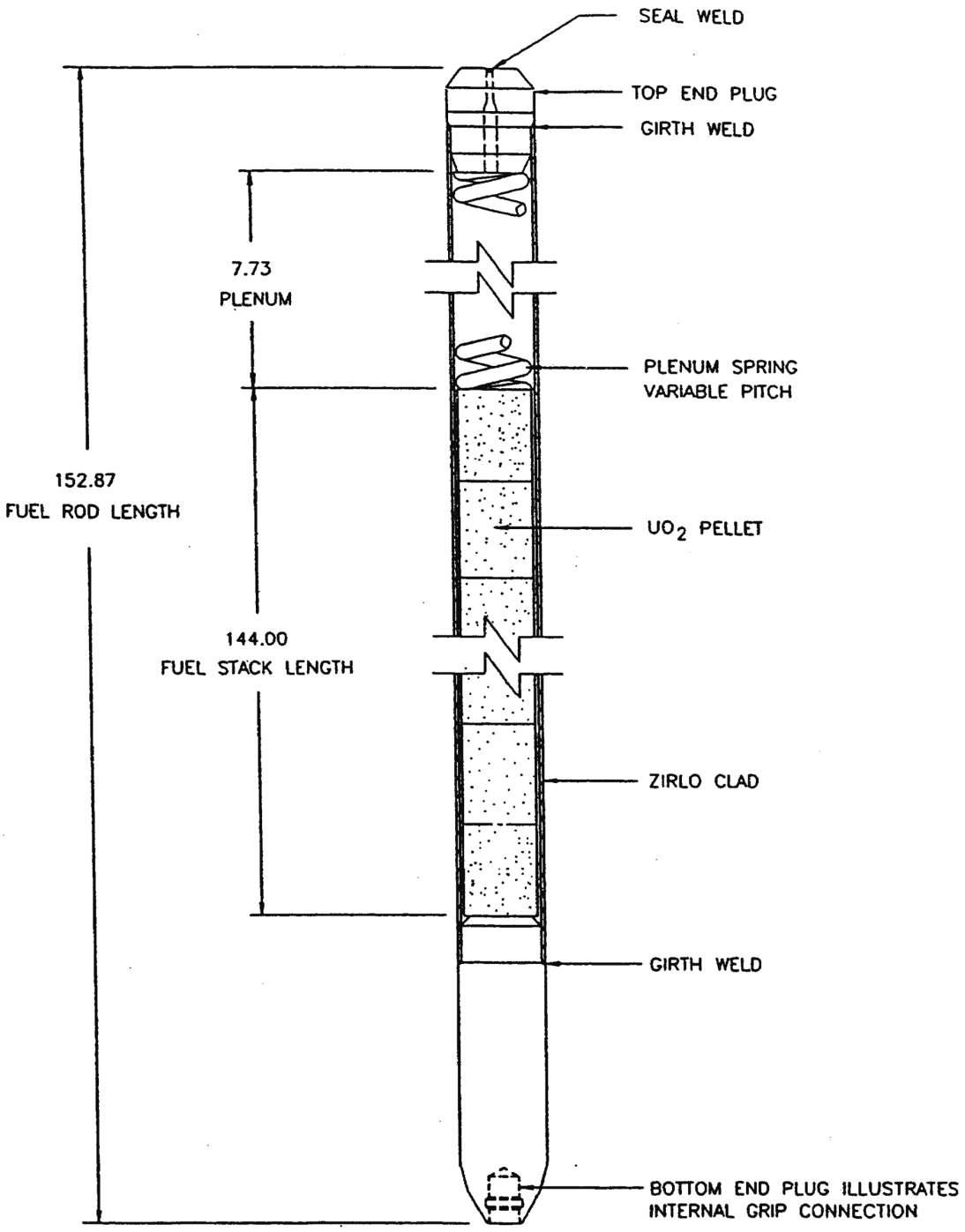

SPECIFIC DIMENSIONS DEPEND ON DESIGN VARIABLES SUCH AS PRE-PRESSURIZATION, POWER HISTORY, AND DISCHARGE BURNUP

REV 14 10/07

SOUTHERN COMPANY
Energy to Serve Your World®

VOGTLE
ELECTRIC GENERATING PLANT
UNIT 1 AND UNIT 2

FUEL ROD SCHEMATIC
LOW ROD INTERNAL PRESSURE DESIGN

FIGURE 4.2–3 (SHEET 4 OF 4)

Midgrid Expansion Joint Design

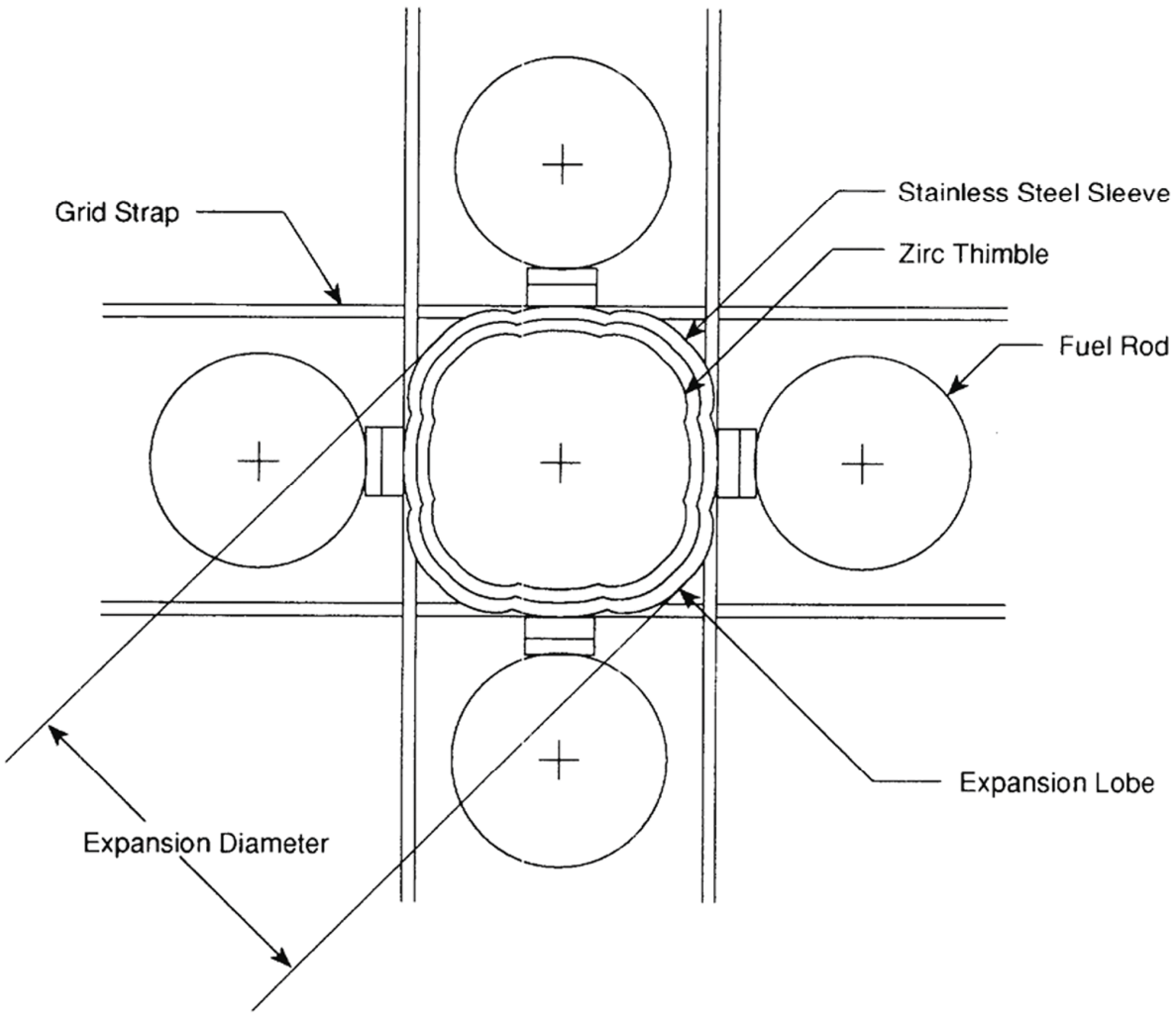

REV 14 10/07

SOUTHERN COMPANY
Energy to Serve Your World®

VOGTLE
ELECTRIC GENERATING PLANT
UNIT 1 AND UNIT 2

PLAN VIEW
LOPAR

FIGURE 4.2–4 (SHEET 1 OF 2)

IFM and Midgrid Expansion Joint Design

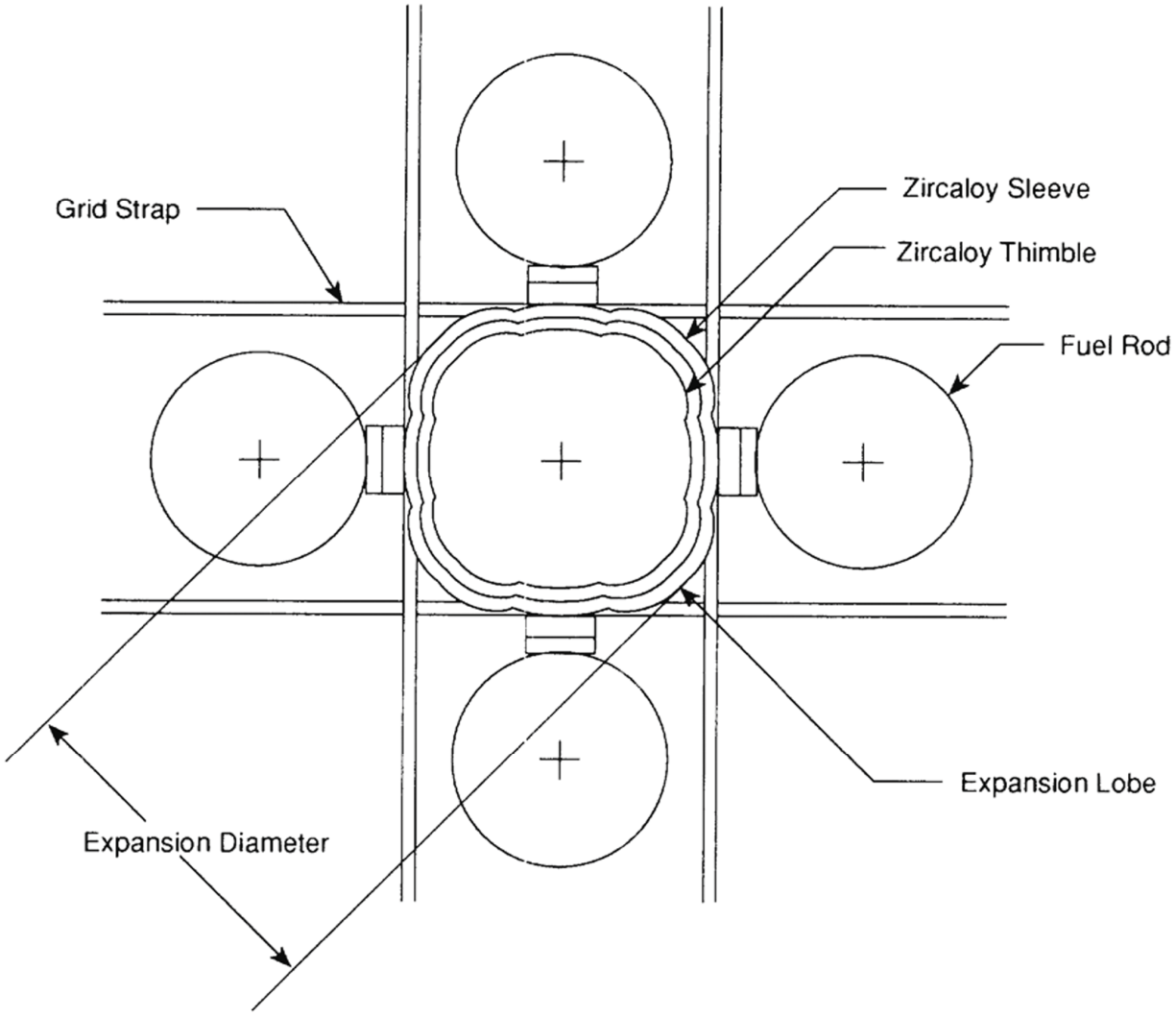

REV 14 10/07

SOUTHERN COMPANY
Energy to Serve Your World®

VOGTLE
ELECTRIC GENERATING PLANT
UNIT 1 AND UNIT 2

PLAN VIEW
VANTAGE 5

FIGURE 4.2–4 (SHEET 2 OF 2)

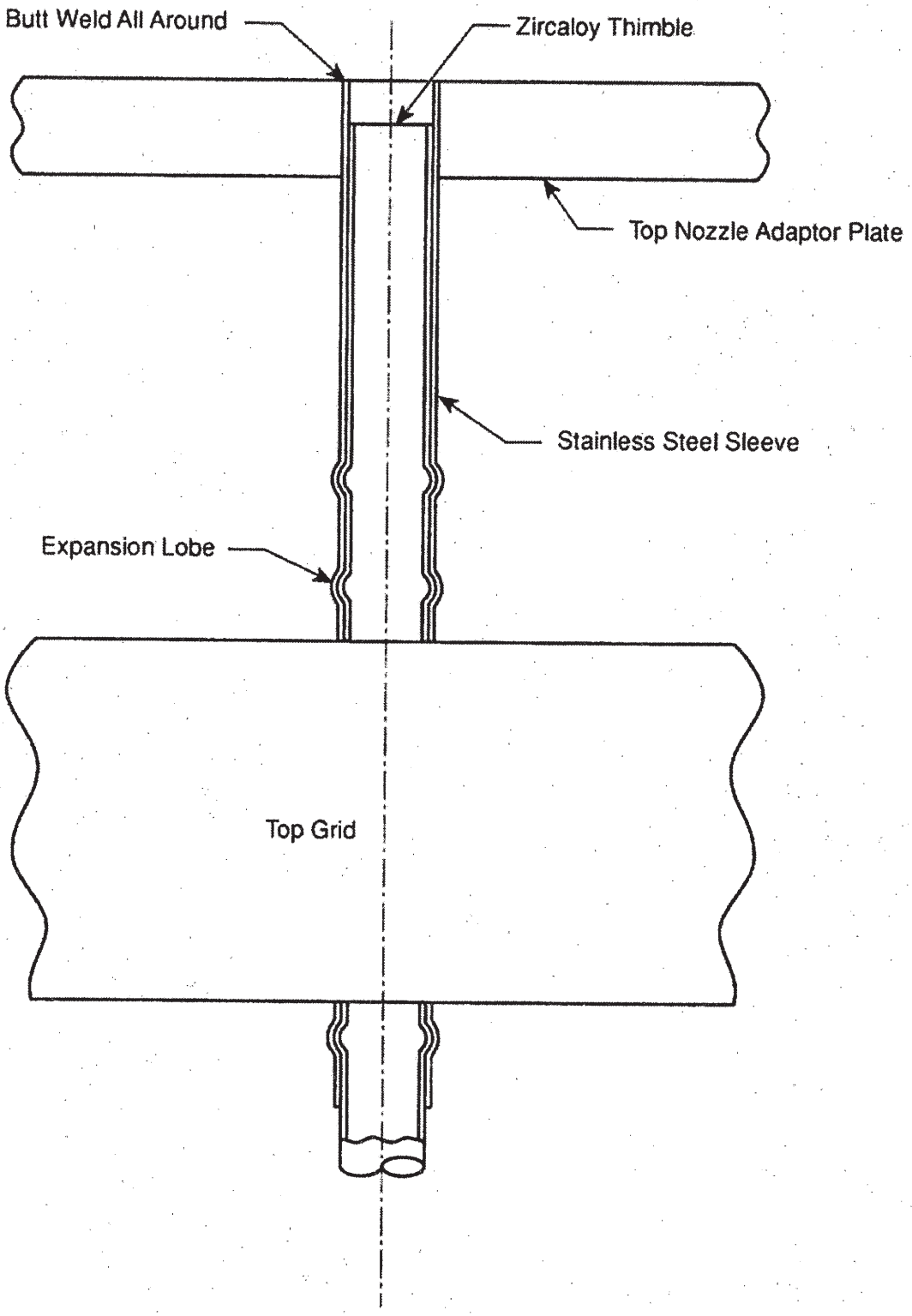

REV 21 4/18

SOUTHERN COMPANY
Energy to Serve Your World®

VOGTLE
ELECTRIC GENERATING PLANT
UNIT 1 AND UNIT 2

INITIAL CORE TOP GRID TO STANDARD NOZZLE ATTACHMENT LOPAR

FIGURE 4.2–5 (SHEET 1 OF 4)

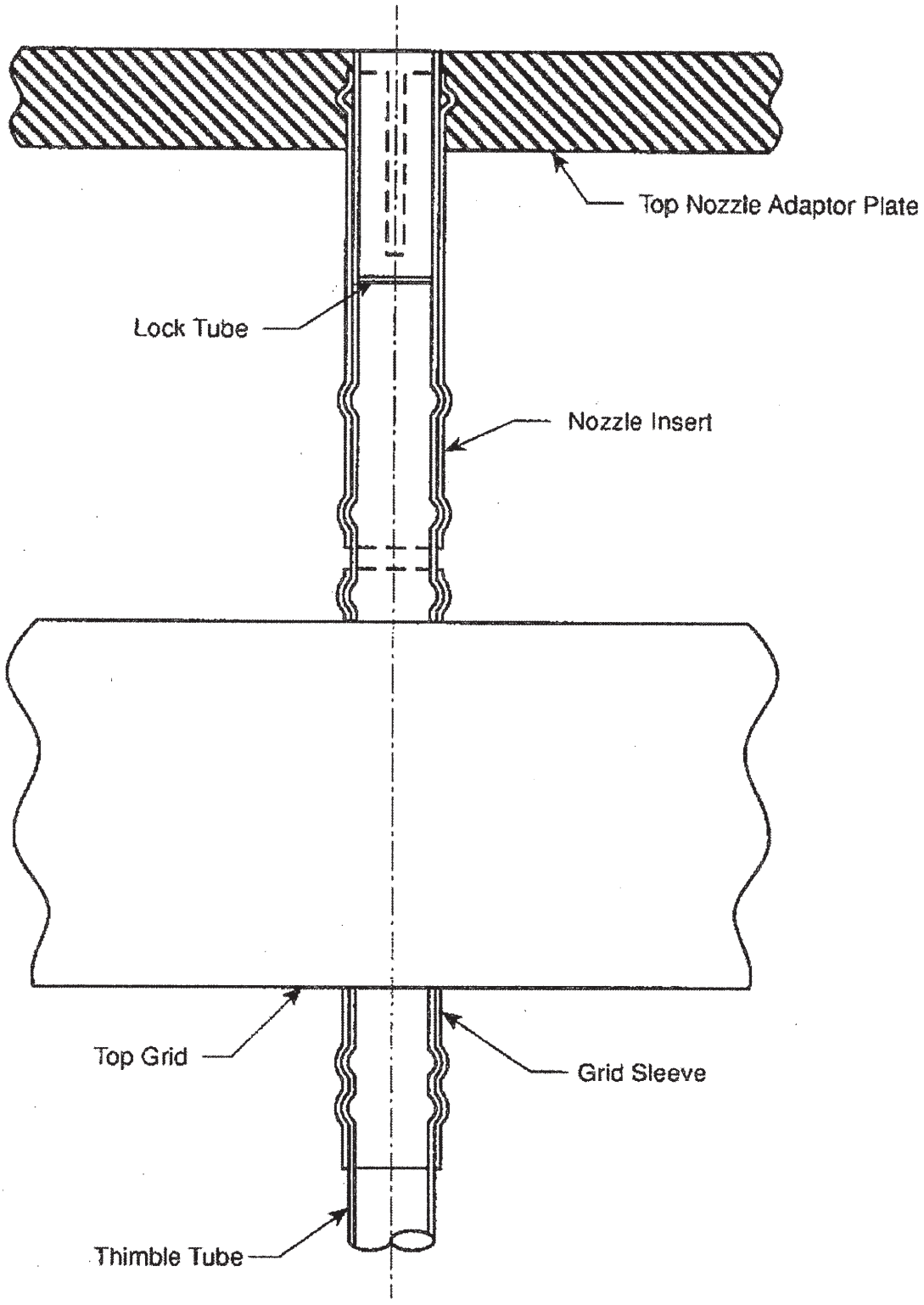

REV 21 4/18

SOUTHERN COMPANY
Energy to Serve Your World®

VOGTLE
ELECTRIC GENERATING PLANT
UNIT 1 AND UNIT 2

RELOAD CYCLE RECONSTITUTABLE TOP GRID TO NOZZLE ATTACHMENT LOPAR

FIGURE 4.2–5 (SHEET 2 OF 4)

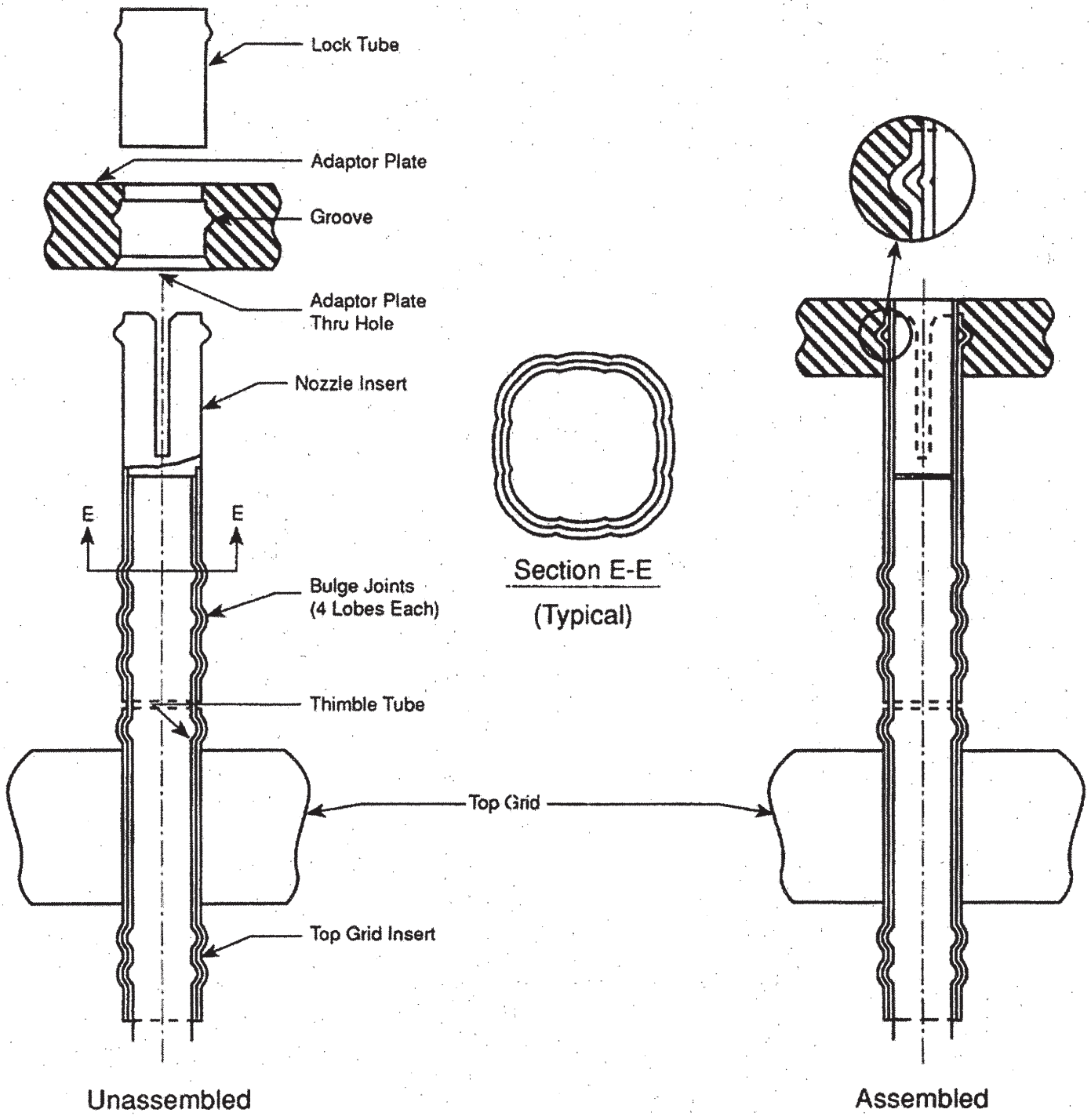

REV 21 4/18

SOUTHERN COMPANY
Energy to Serve Your World®

VOGTLE
ELECTRIC GENERATING PLANT
UNIT 1 AND UNIT 2

THIMBLE/INSERT/TOP GRID SLEEVE
BULGE JOINT GEOMETRY VANTAGE
5/VANTAGE+ VOGTLE 1 CYCLES 3-21, VOGTLE
2 CYCLES 2-19

FIGURE 4.2–5 (SHEET 3 OF 4)

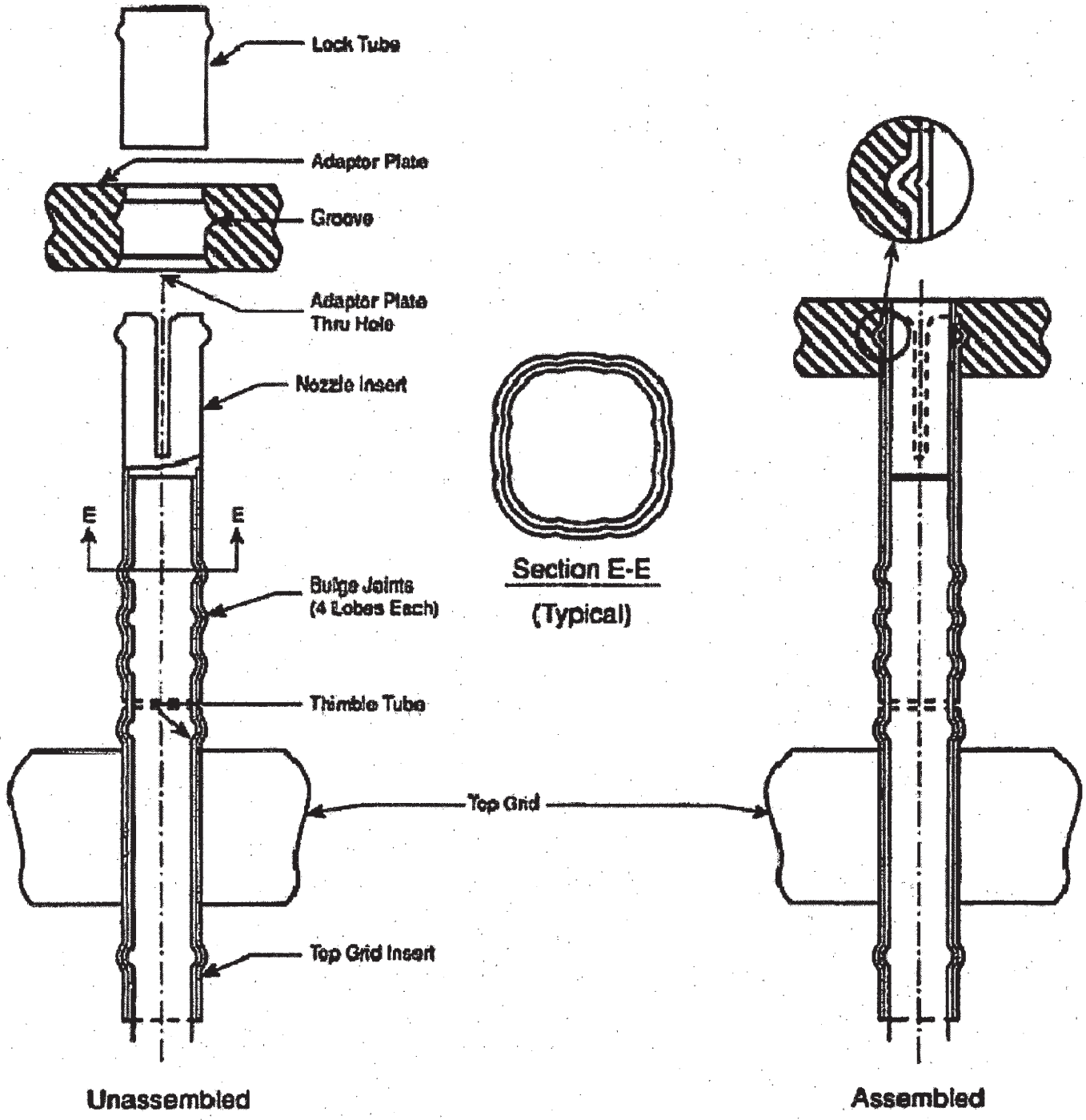

REV 21 4/18

SOUTHERN COMPANY Energy to Serve Your World® VOGTLE ELECTRIC GENERATING PLANT UNIT 1 AND UNIT 2	THIMBLE/INSERT/TOP GRID SLEEVE BULGE JOINT GEOMETRY VANTAGE 5/VANTAGE+ VOGTLE 1 CYCLE 22, VOGTLE 2 CYCLE 20 AND LATER
	FIGURE 4.2-5 (SHEET 4 OF 4)

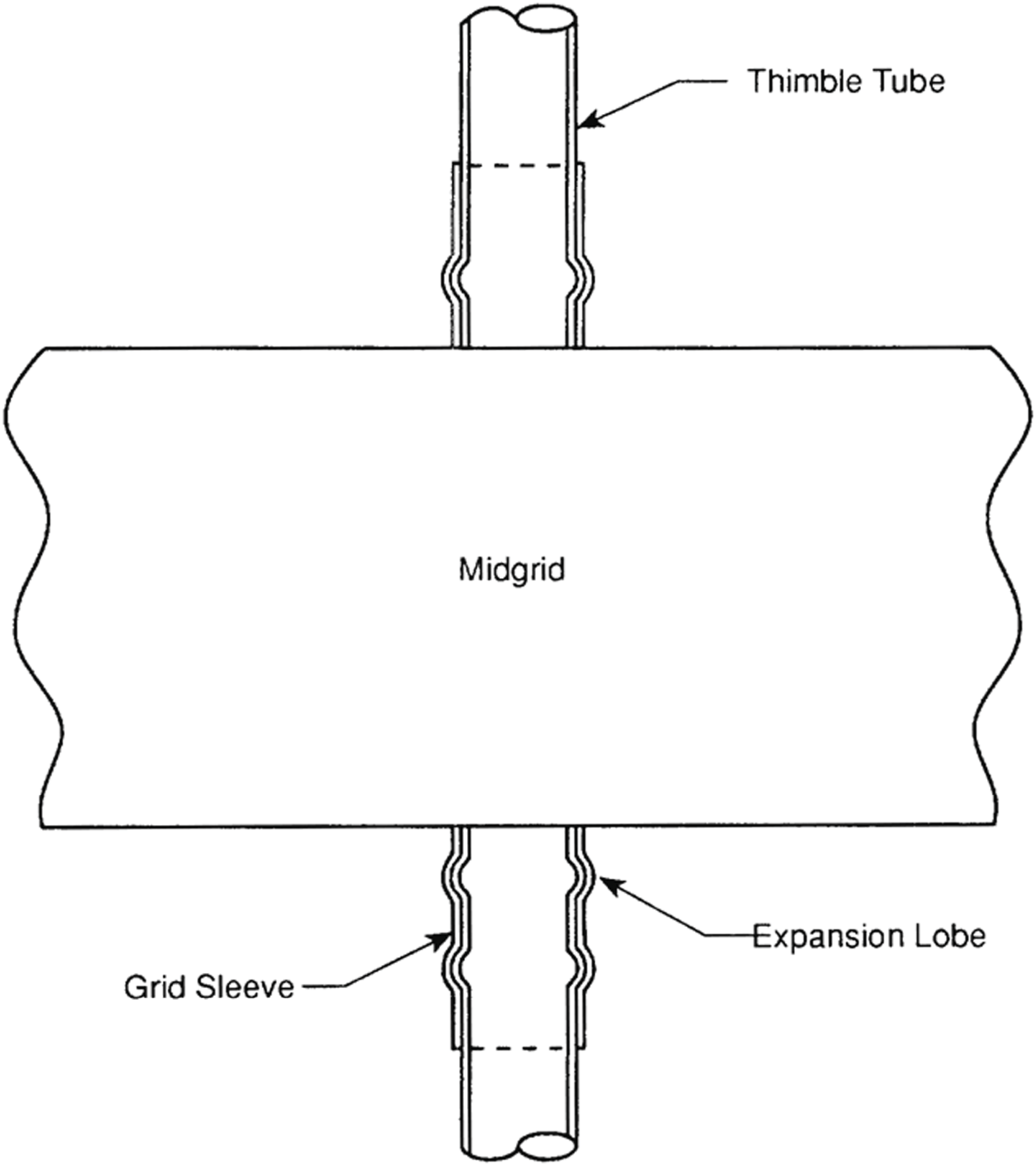

REV 14 10/07

SOUTHERN COMPANY
Energy to Serve Your World®

VOGTLE
ELECTRIC GENERATING PLANT
UNIT 1 AND UNIT 2

ELEVATION VIEW, GRID TO THIMBLE ATTACHMENT LOPAR

FIGURE 4.2–6 (SHEET 1 OF 2)

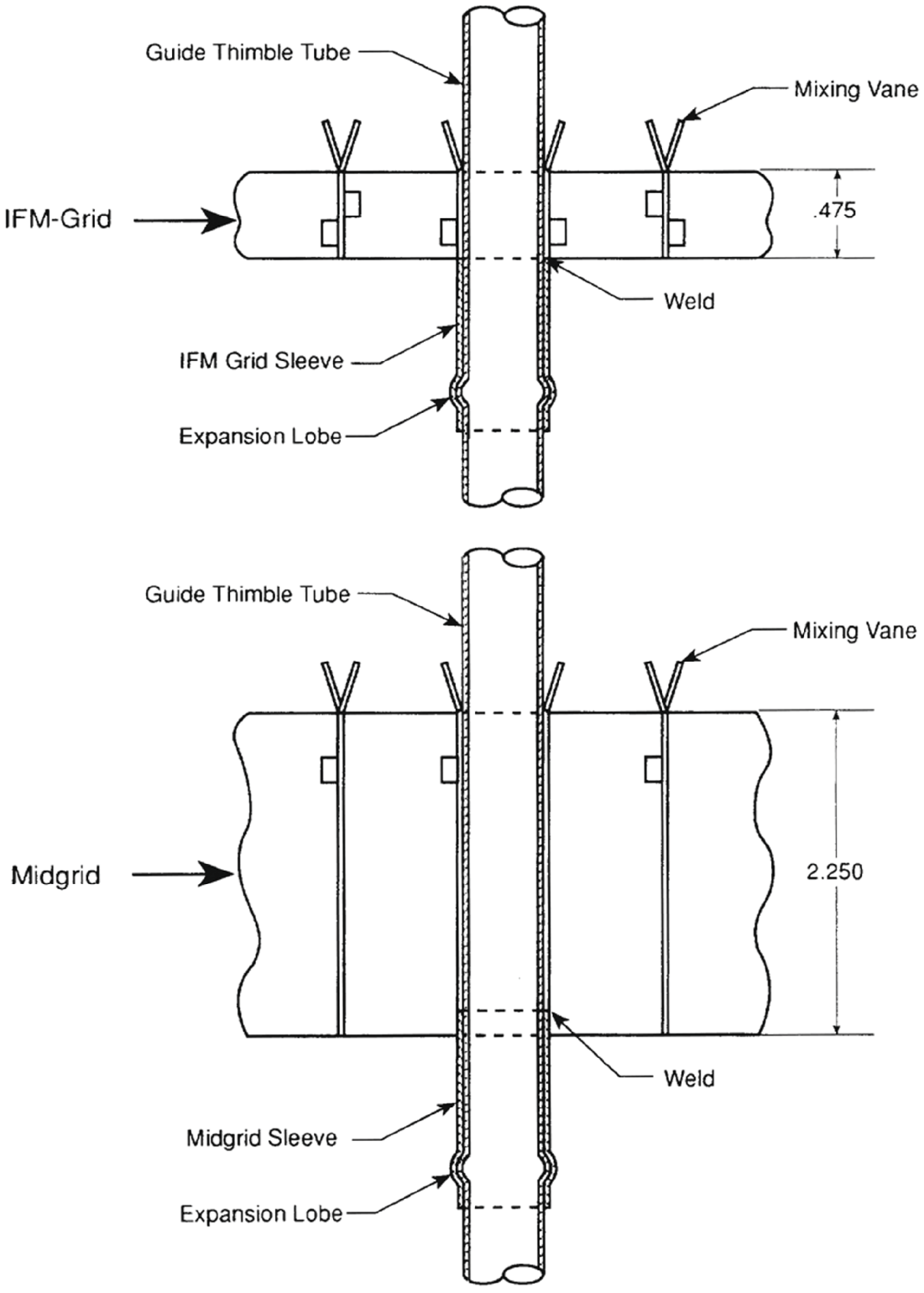

Dimensions are in inches (nominal)

REV 14 10/07

SOUTHERN COMPANY
Energy to Serve Your World®

VOGTLE
ELECTRIC GENERATING PLANT
UNIT 1 AND UNIT 2

GRID TO THIMBLE ATTACHMENT JOINTS
VANTAGE 5

FIGURE 4.2–6 (SHEET 2 OF 2)

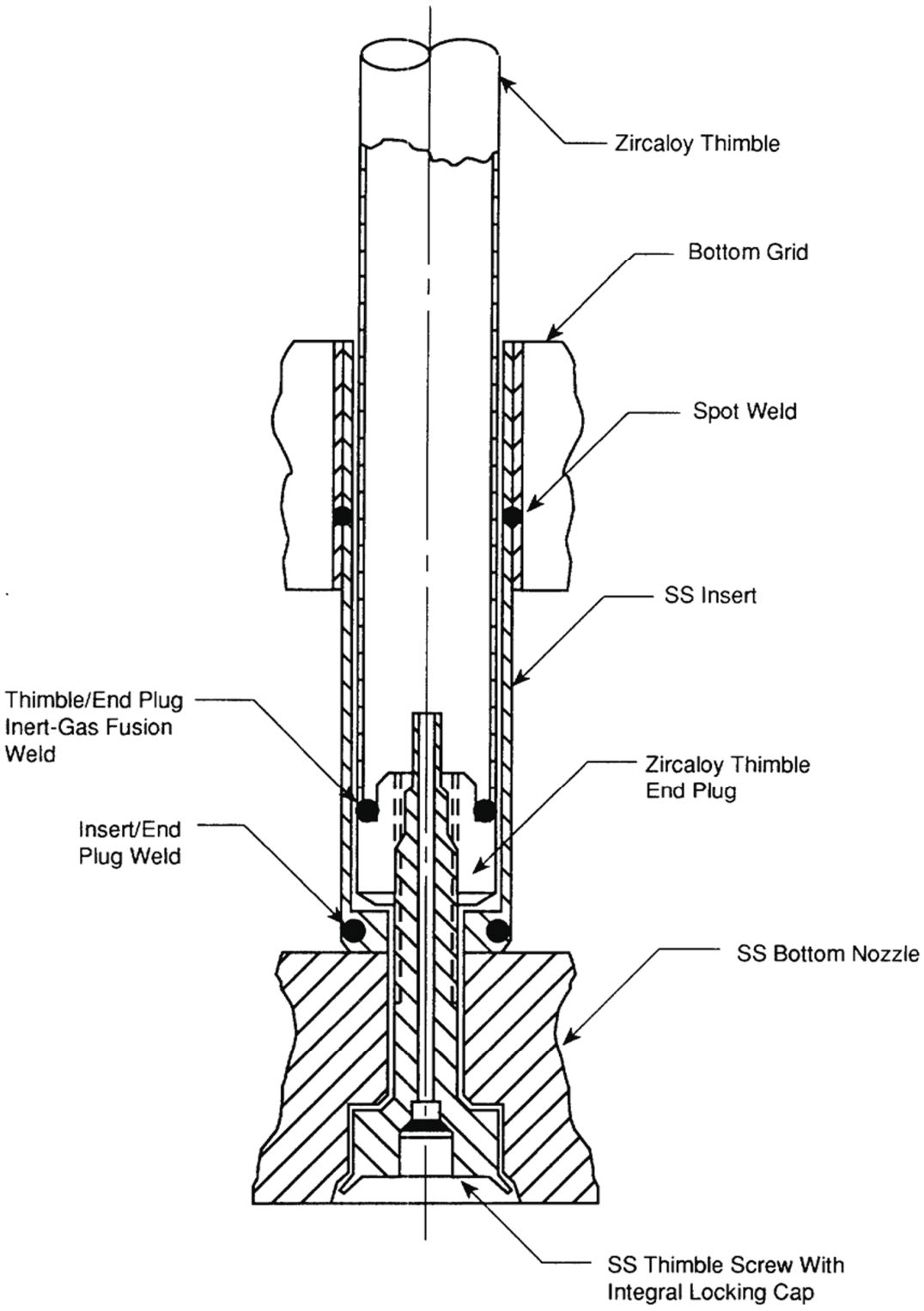

REV 14 10/07

SOUTHERN COMPANY
Energy to Serve Your World®

VOGTLE
ELECTRIC GENERATING PLANT
UNIT 1 AND UNIT 2

GUIDE THIMBLE TO BOTTOM NOZZEL JOINT
LOPAR

FIGURE 4.2–7 (SHEET 1 OF 2)

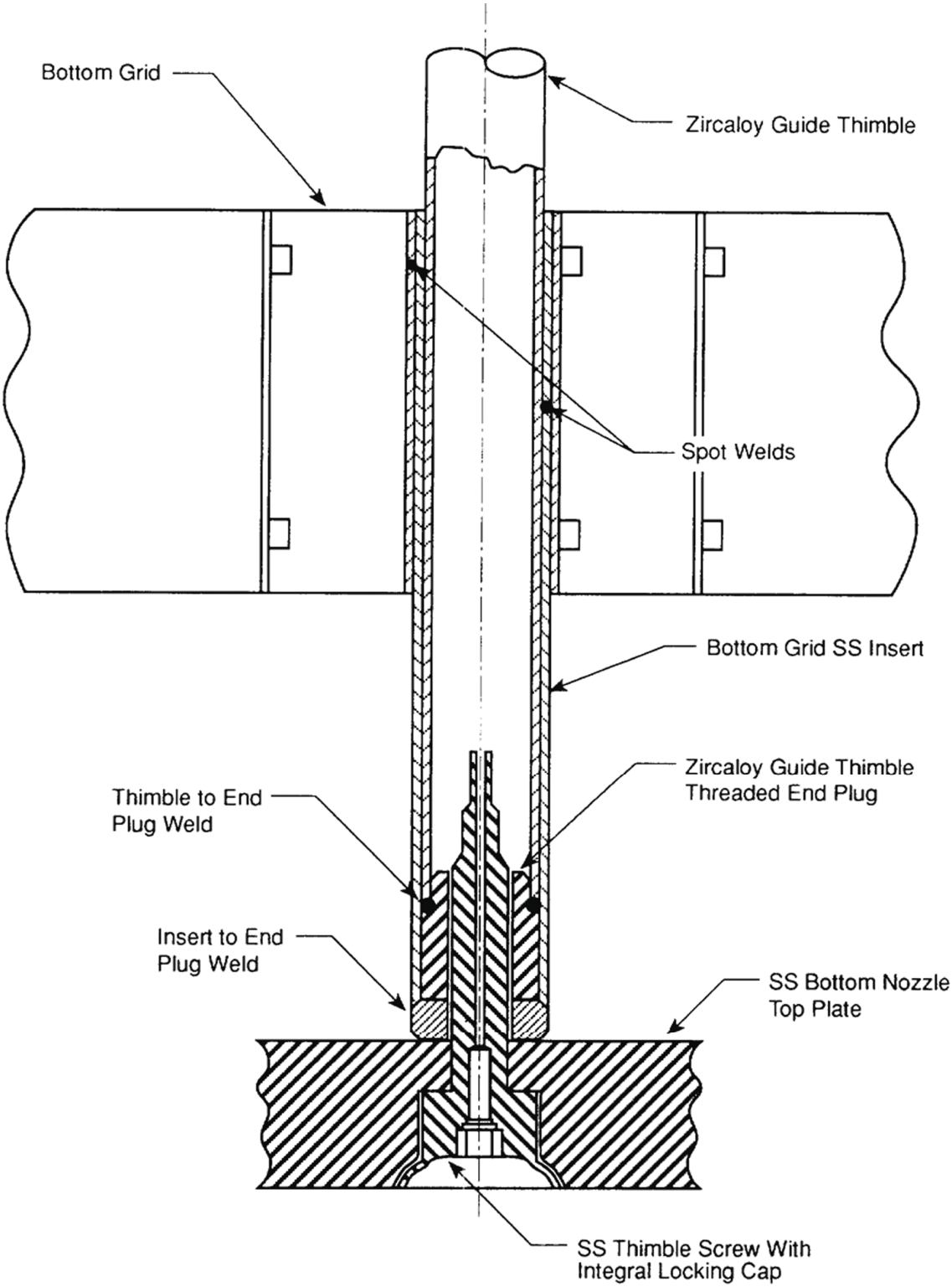

REV 14 10/07

SOUTHERN COMPANY
Energy to Serve Your World®

VOGTLE
ELECTRIC GENERATING PLANT
UNIT 1 AND UNIT 2

GUIDE THIMBLE TO BOTTOM NOZZEL JOINT
VANTAGE 5

FIGURE 4.2–7 (SHEET 2 OF 2)

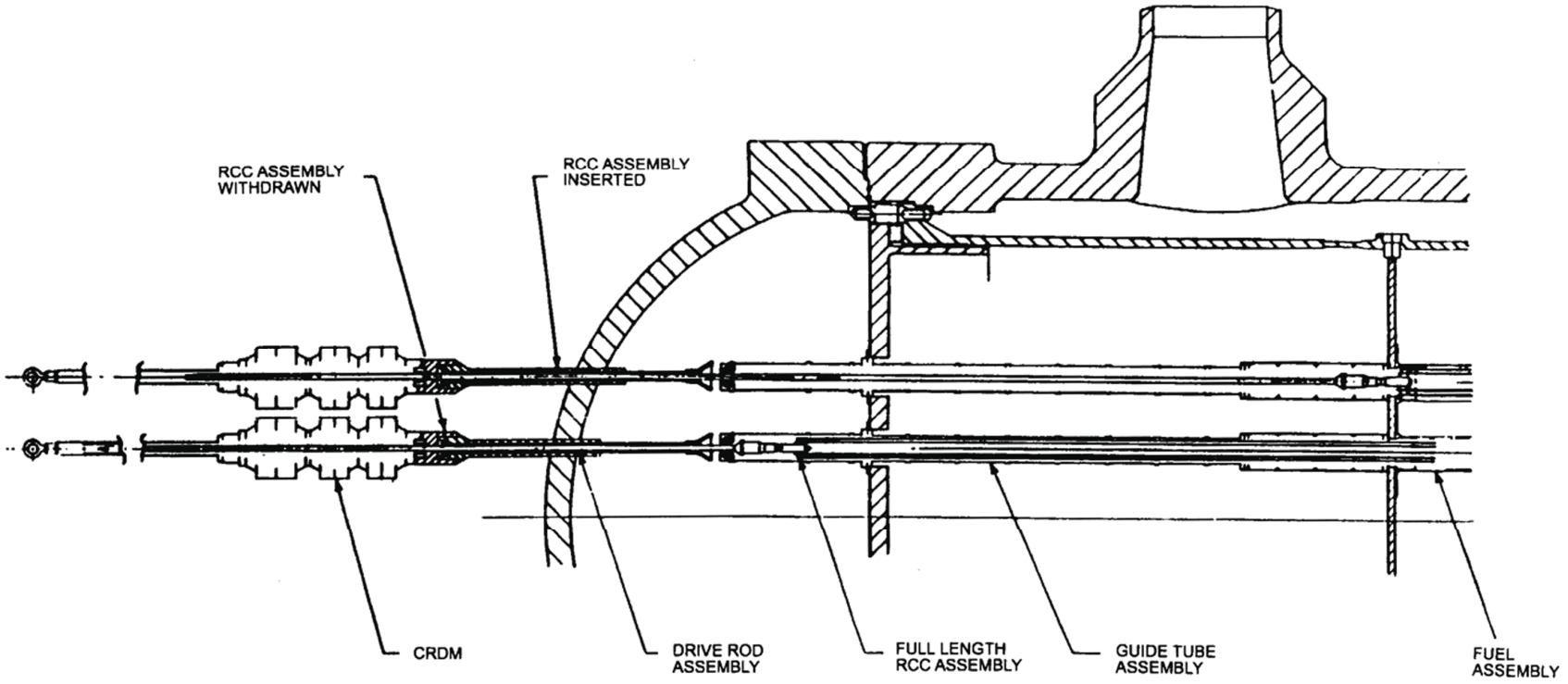

REV 14 10/07

SOUTHERN COMPANY
Energy to Serve Your World®

VOGTLE
ELECTRIC GENERATING PLANT
UNIT 1 AND UNIT 2

RCC AND DRIVE ROD ASSEMBLY
WITH INTERFACE COMPONENTS

FIGURE 4.2–8

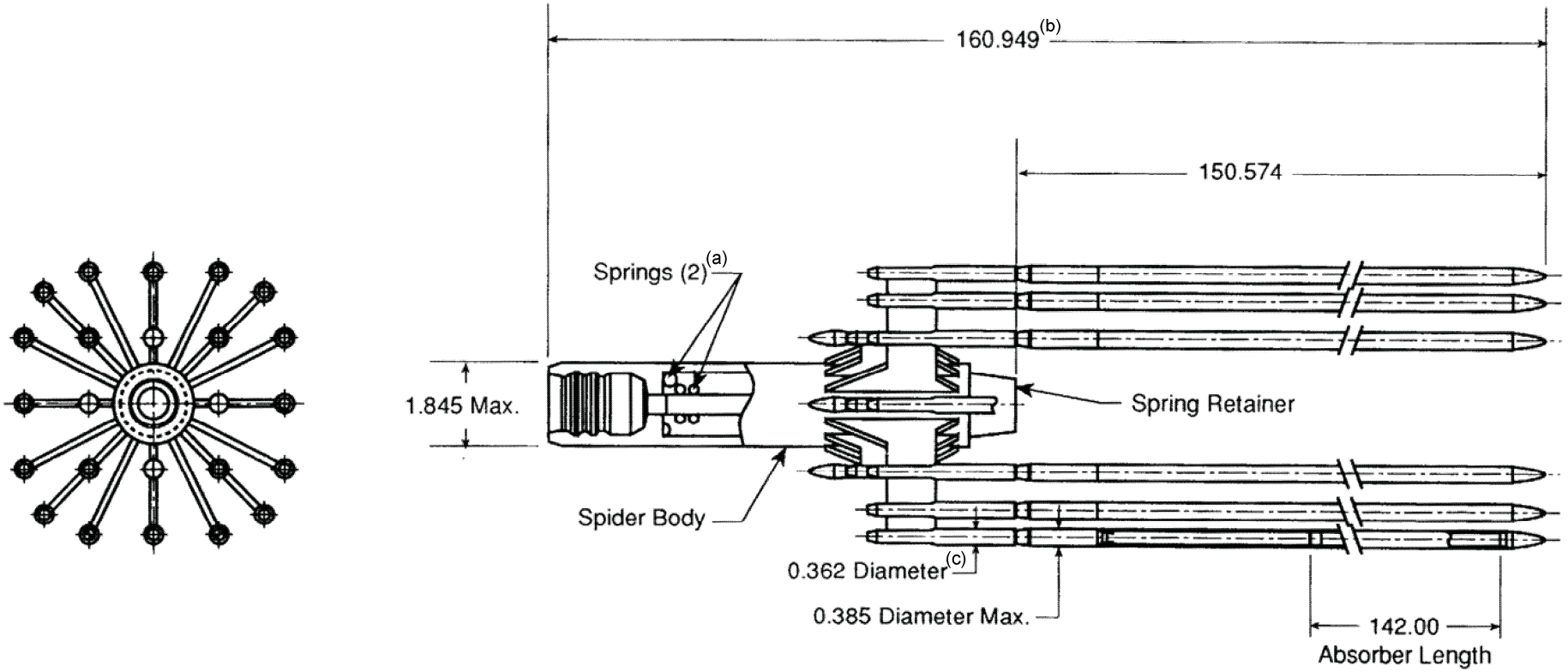

a A single coil spring applicable to Framatome RCCAs only
b Overall assembly length of 161.0 inches applicable to Framatome RCCAs only
c Spider boss diameter of 0.355 applicable to Framatome RCCAs only

REV 23 3/21

SOUTHERN COMPANY
Energy to Serve Your World®

VOGTLE
ELECTRIC GENERATING PLANT
UNIT 1 AND UNIT 2

FULL–LENGTH RCCA OUTLINE

FIGURE 4.2–9

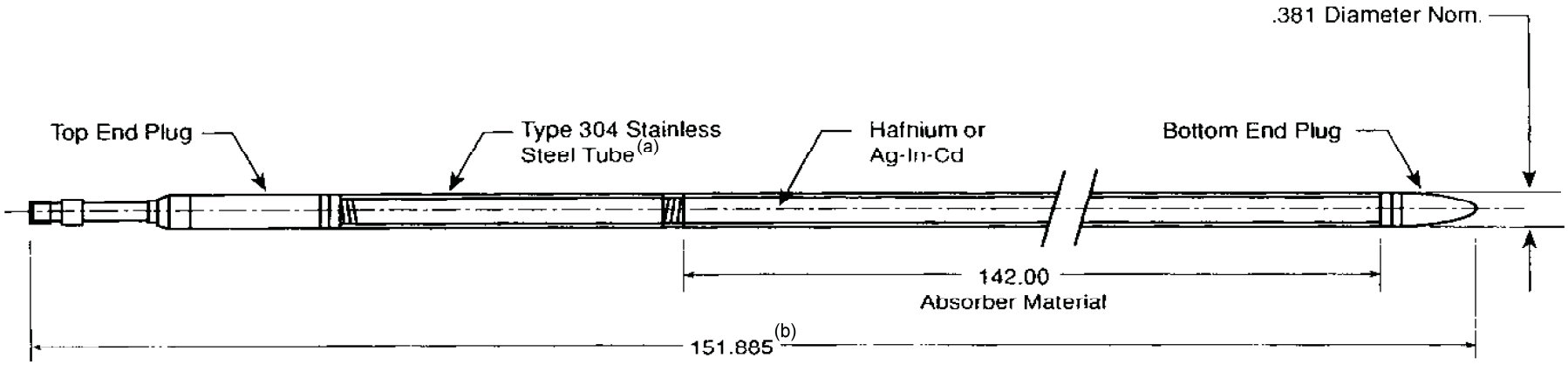

a 316 stainless steel low contaminant cladding material applicable to Framatome RCCA only
b Overall absorber rod length of 153.831 applicable to Framatome RCCAs only

REV 23 3/21

SOUTHERN COMPANY
Energy to Serve Your World®

VOGTLE
ELECTRIC GENERATING PLANT
UNIT 1 AND UNIT 2

ABSORBER ROD

FIGURE 4.2–10

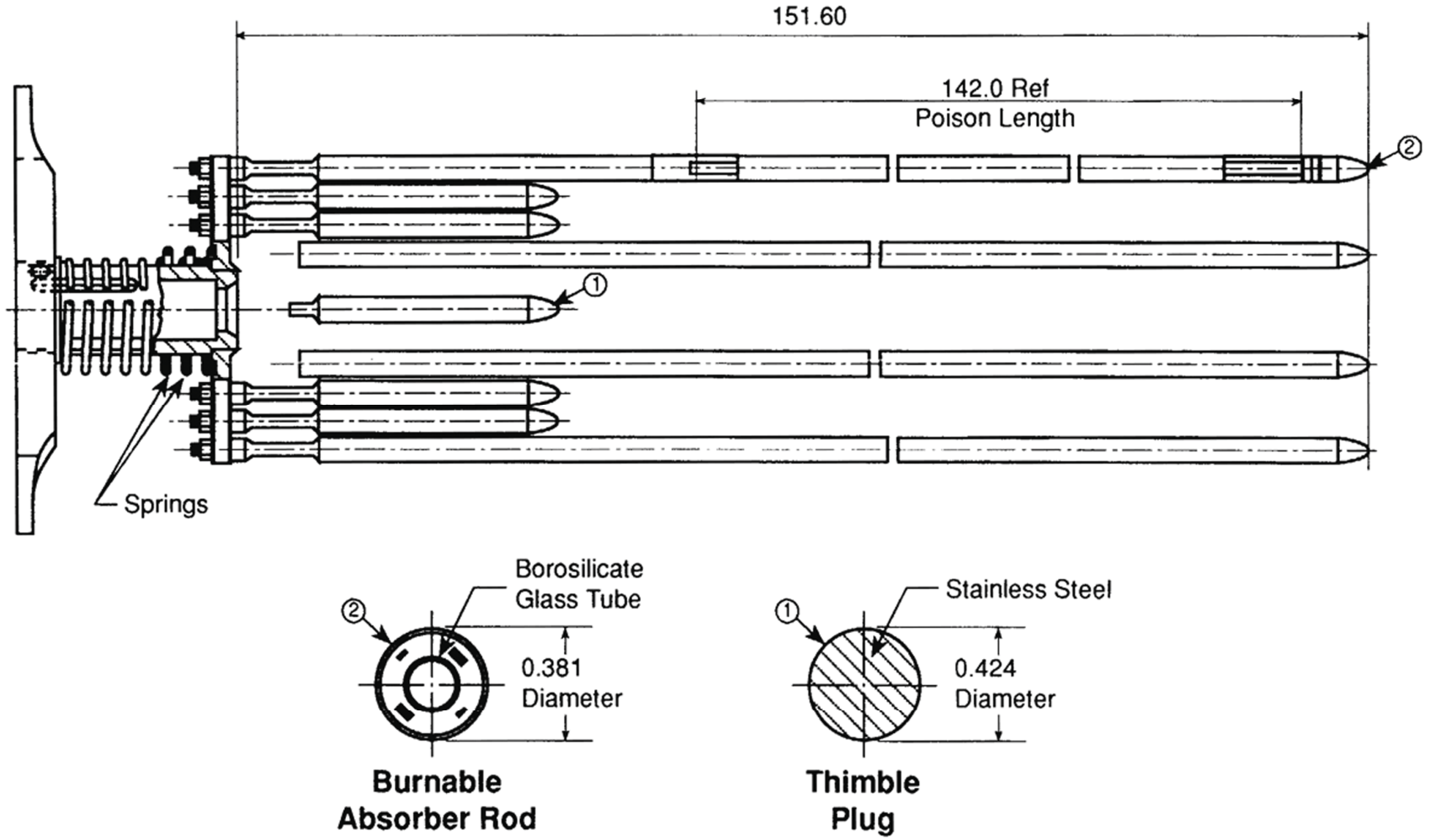

REV 14 10/07

SOUTHERN COMPANY
Energy to Serve Your World®

VOGTLE
ELECTRIC GENERATING PLANT
UNIT 1 AND UNIT 2

BURNABLE ABSORBER ASSEMBLY
(STANDARD BOROSILICATE GLASS)

FIGURE 4.2–11 (SHEET 1 OF 2)

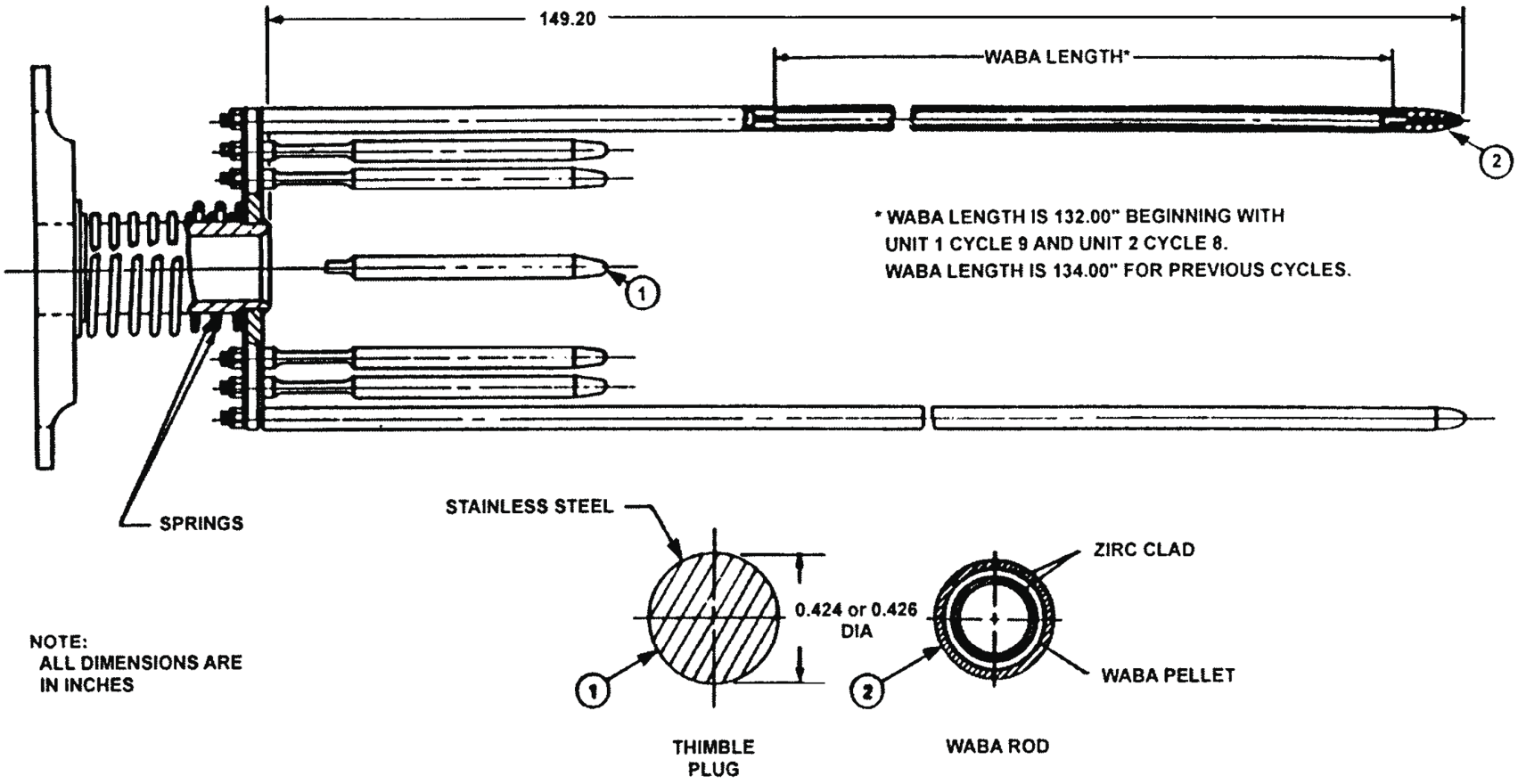

REV 14 10/07

SOUTHERN COMPANY
Energy to Serve Your World®

VOGTLE
ELECTRIC GENERATING PLANT
UNIT 1 AND UNIT 2

WET ANNULAR BURNABLE ABSORBER
(WABA) ASSEMBLY

FIGURE 4.2-11 (SHEET 2 OF 2)

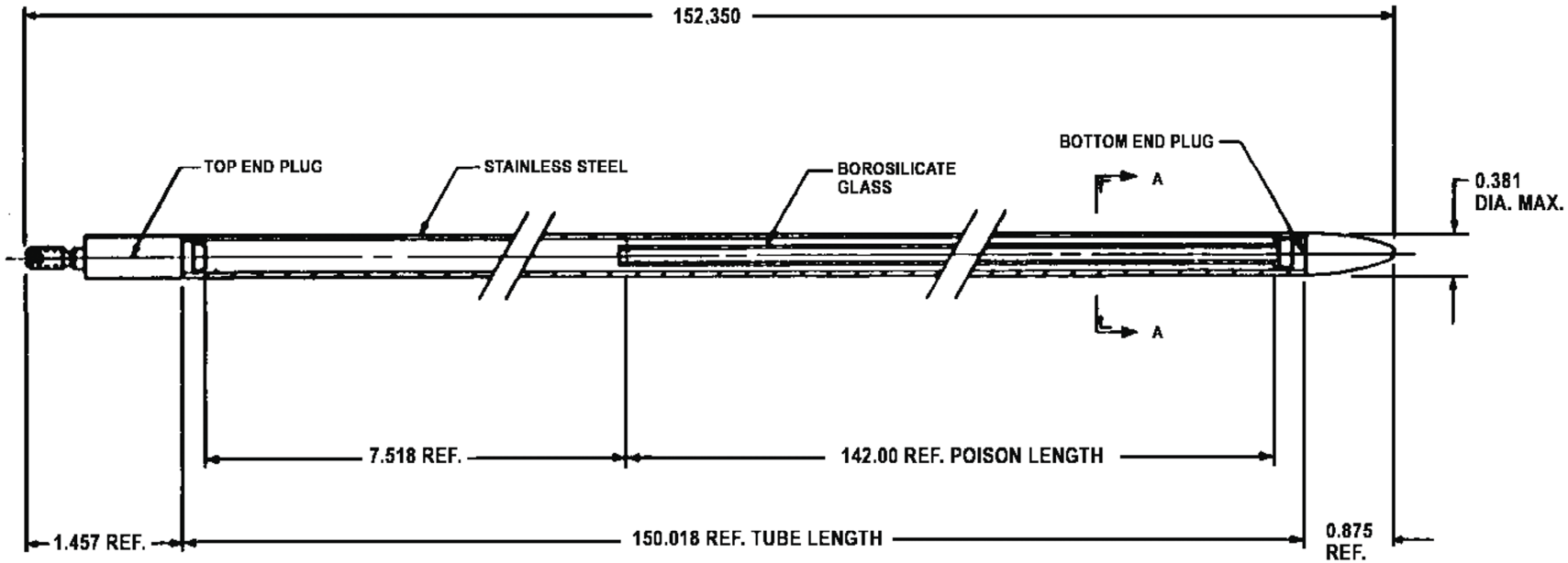

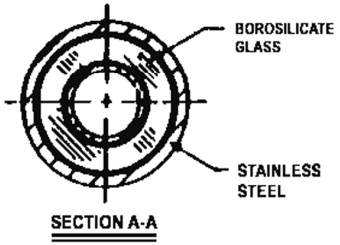

REV 14 10/07

SOUTHERN COMPANY
Energy to Serve Your World®

VOGTLE
ELECTRIC GENERATING PLANT
UNIT 1 AND UNIT 2

BA ROD CROSS SECTION
(STANDARD BOROSILICATE GLASS)

FIGURE 4.2-12 (SHEET 1 OF 2)

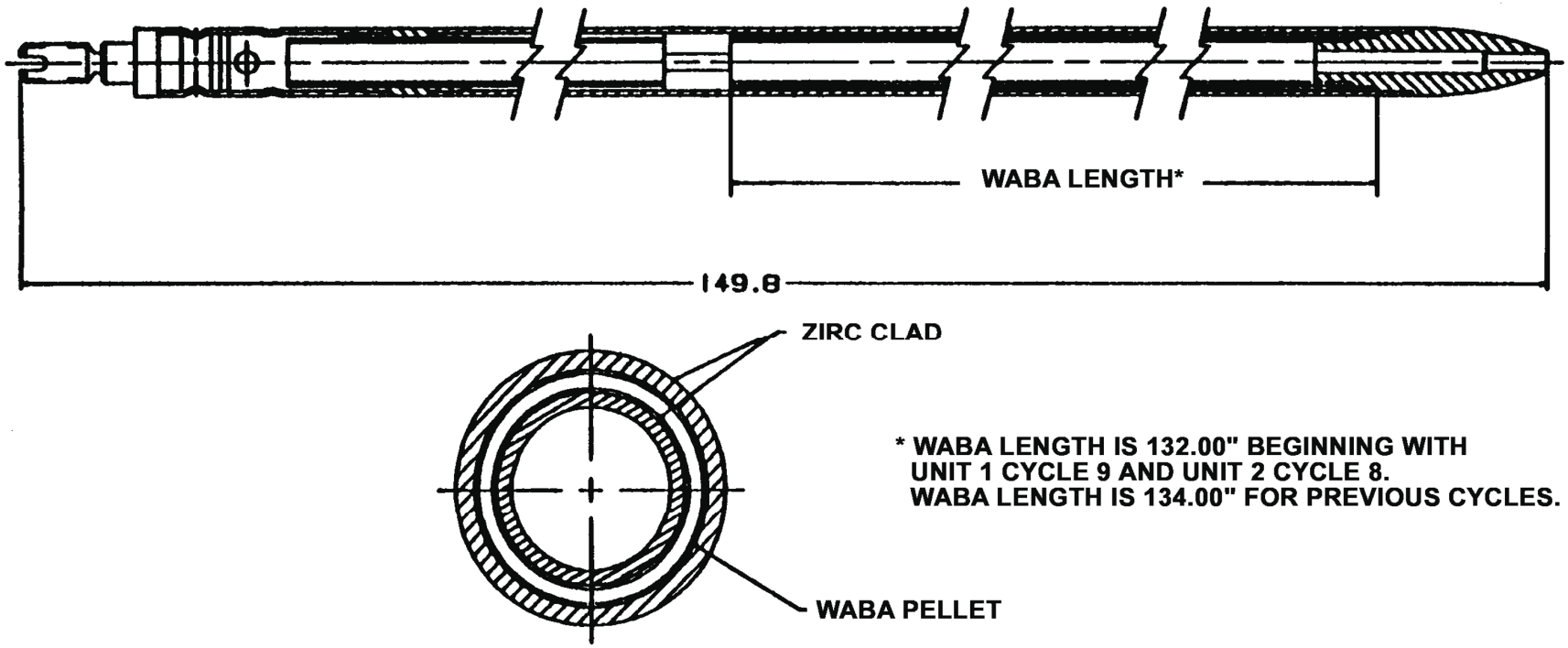

* WABA LENGTH IS 132.00" BEGINNING WITH
UNIT 1 CYCLE 9 AND UNIT 2 CYCLE 8.
WABA LENGTH IS 134.00" FOR PREVIOUS CYCLES.

REV 14 10/07

SOUTHERN COMPANY
Energy to Serve Your World®

VOGTLE
ELECTRIC GENERATING PLANT
UNIT 1 AND UNIT 2

BA ROD CROSS SECTION
(WET ANNULAR BURNABLE ABSORBER)

FIGURE 4.2-12 (SHEET 2 OF 2)

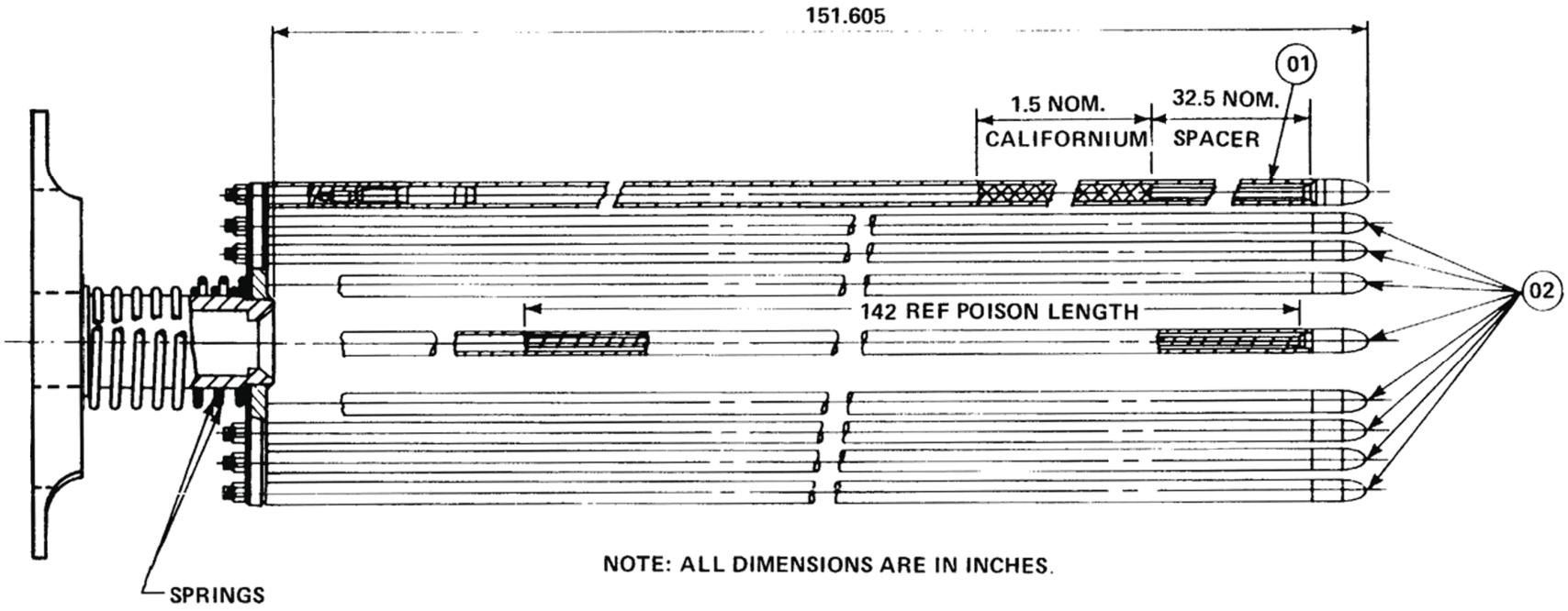

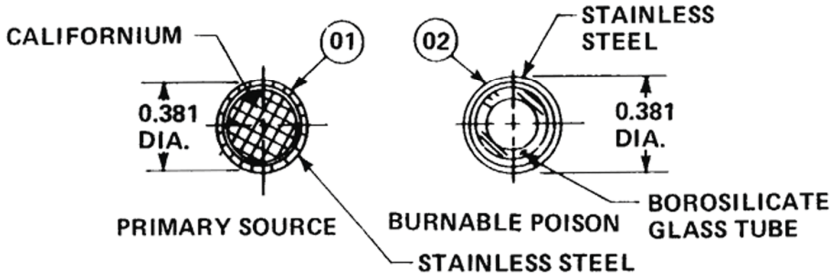

REV 14 10/07

SOUTHERN COMPANY
Energy to Serve Your World®

VOGTLE
ELECTRIC GENERATING PLANT
UNIT 1 AND UNIT 2

PRIMARY SOURCE ASSEMBLY

FIGURE 4.2–13

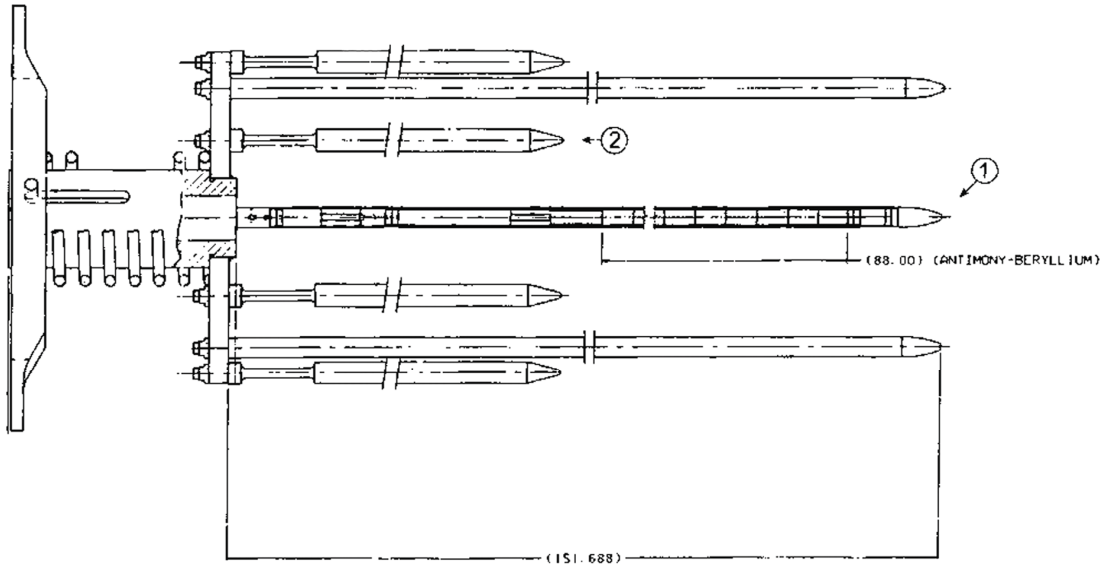

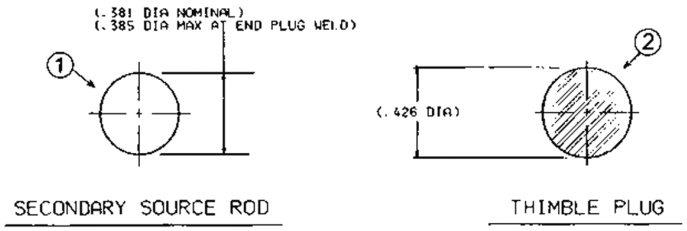

SECONDARY SOURCE ROD

THIMBLE PLUG

NOTE: All dimensions are in inches.

REV 14 10/07

SOUTHERN COMPANY
Energy to Serve Your World®

VOGTLE
ELECTRIC GENERATING PLANT
UNIT 1 AND UNIT 2

DOUBLE–ENCAPSULATED SECONDARY SOURCE ASSEMBLY (SIX ROD PATTERN)

FIGURE 4.2–14 (SHEET 1 OF 2)

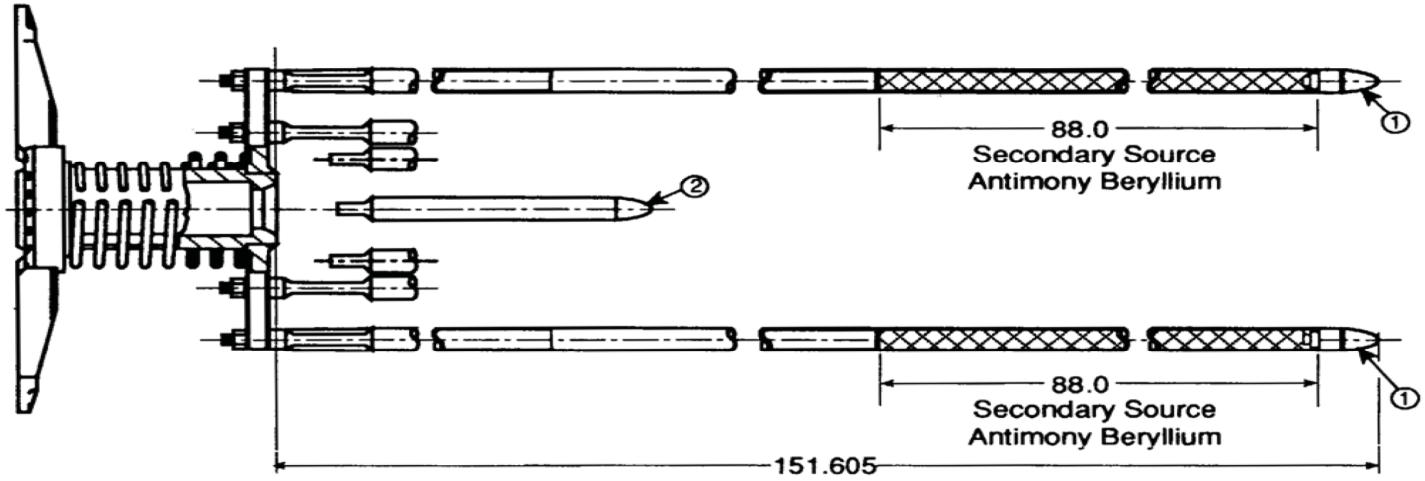

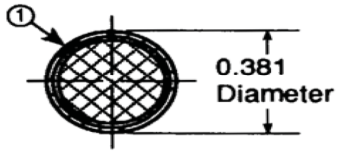

Secondary Source

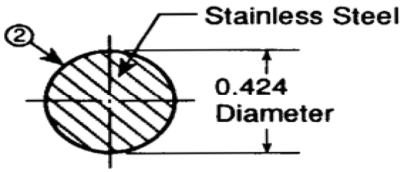

Thimble Plug

REV 14 10/07

SOUTHERN COMPANY
Energy to Serve Your World®

VOGTLE
ELECTRIC GENERATING PLANT
UNIT 1 AND UNIT 2

SINGLE–ENCAPSULATED SECONDARY SOURCE ASSEMBLY
(FOUR ROD PATTERN)

FIGURE 4.2–14 (SHEET 2 OF 2)

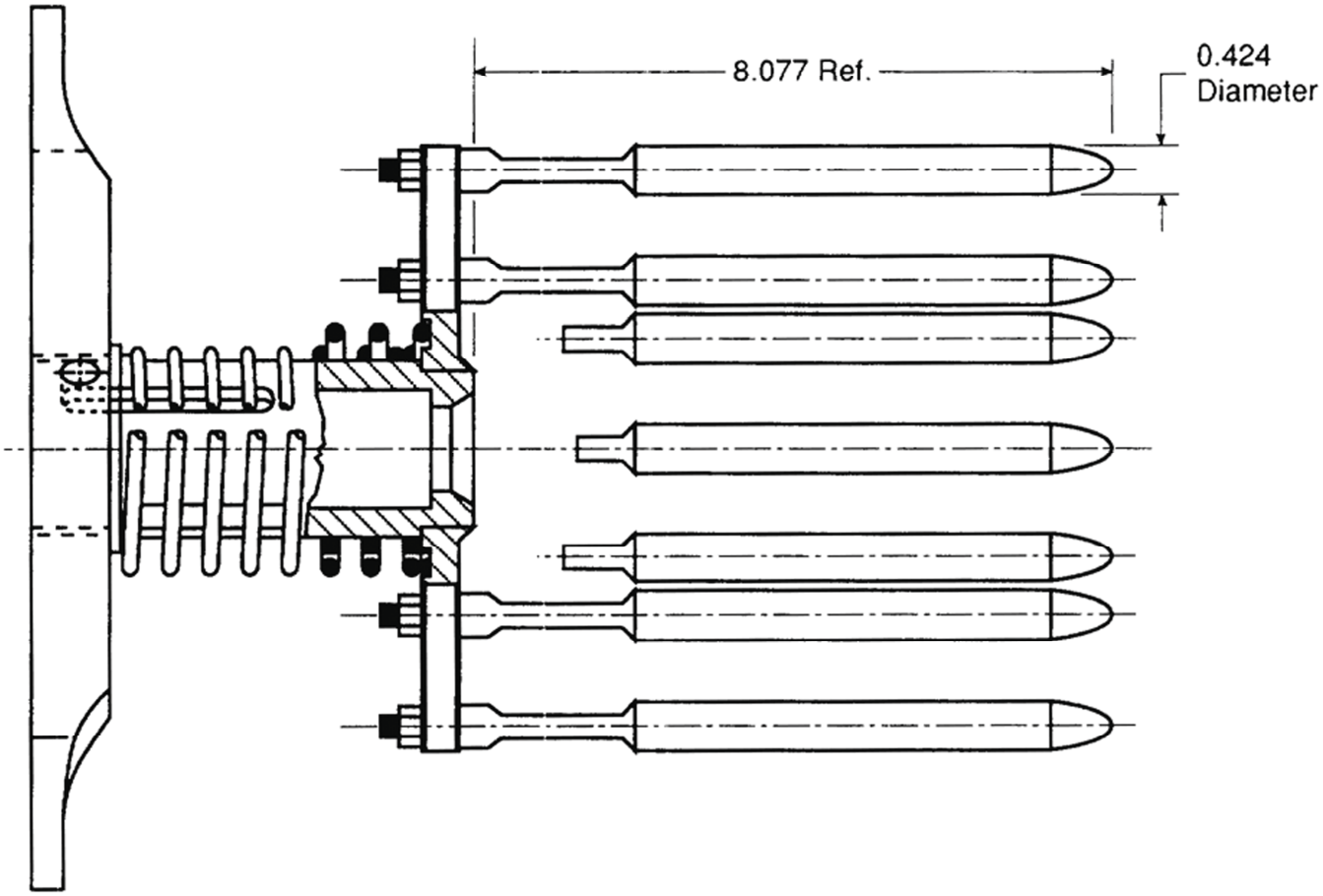

REV 14 10/07

SOUTHERN COMPANY
Energy to Serve Your World®

VOGTLE
ELECTRIC GENERATING PLANT
UNIT 1 AND UNIT 2

THIMBLE PLUG ASSEMBLY

FIGURE 4.2–15 (SHEET 1 OF 2)

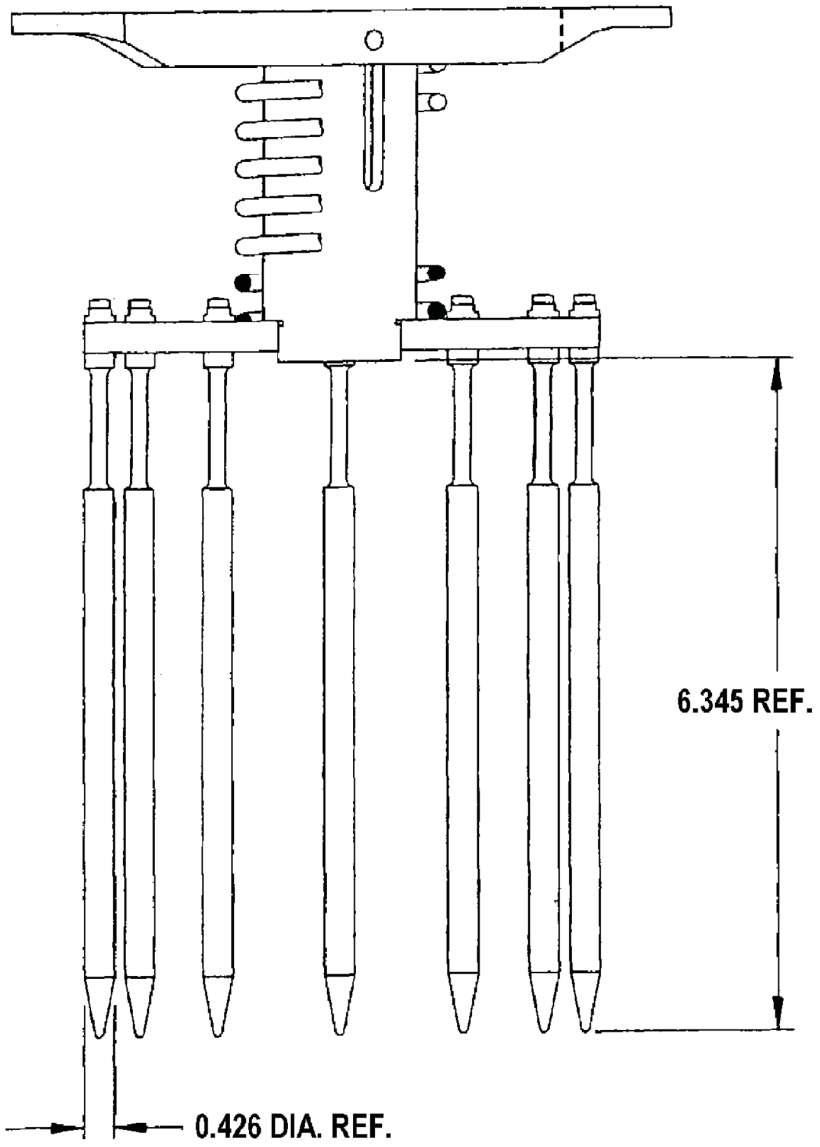

VOGTLE UNIT 1 CYCLE 12 AND AFTER

Section 1.01 VOGTLE UNIT 2 CYCLE 11 AND AFTER

REV 14 10/07

SOUTHERN COMPANY *Energy to Serve Your World®* **VOGTLE** **ELECTRIC GENERATING PLANT** **UNIT 1 AND UNIT 2**	STANDARDIZED THIMBLE PLUG ASSEMBLY
	FIGURE 4.2–15 (SHEET 2 OF 2)

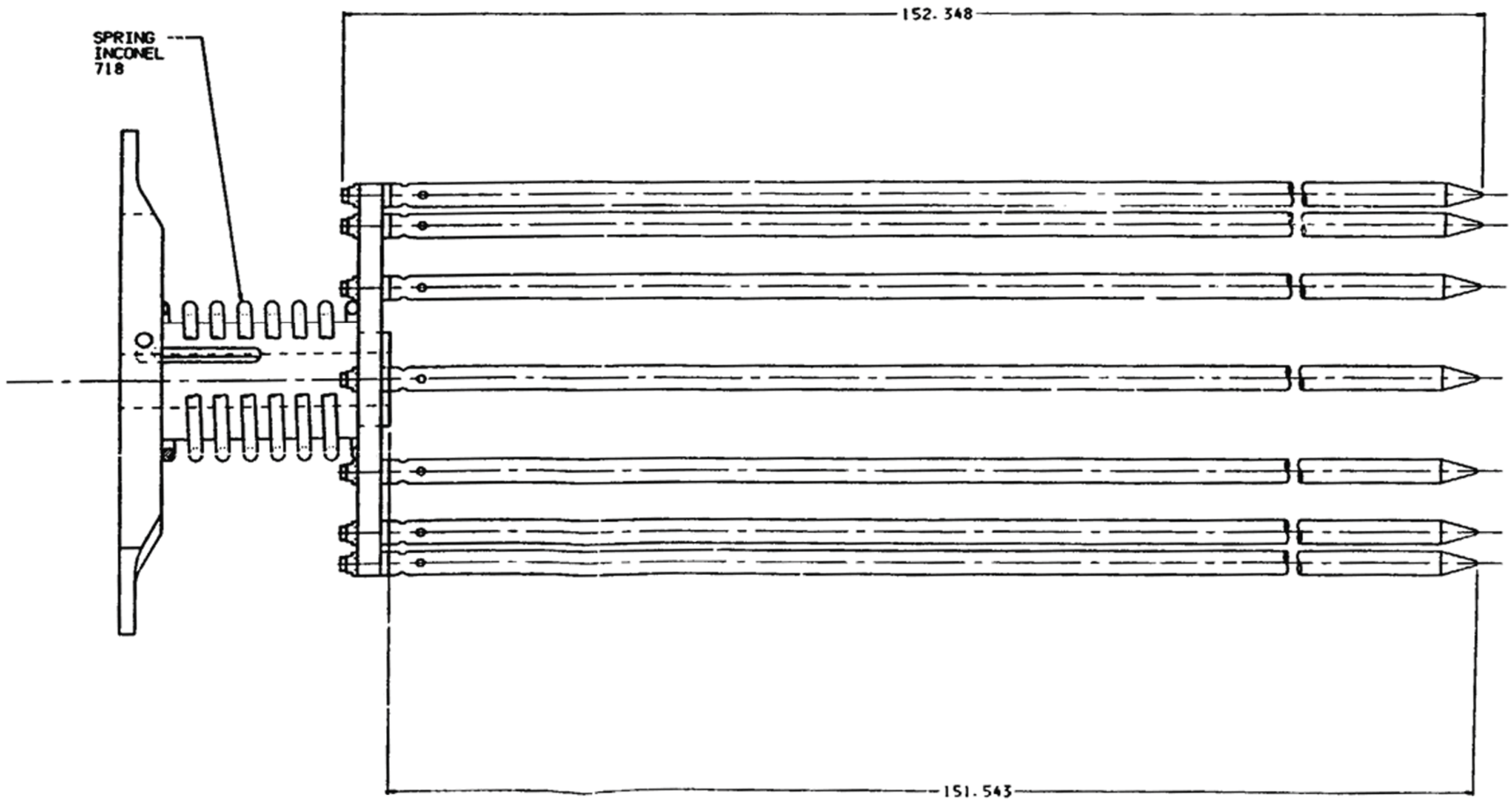

REV 14 10/07

SOUTHERN COMPANY
Energy to Serve Your World®

VOGTLE
ELECTRIC GENERATING PLANT
UNIT 1 AND UNIT 2

STAIN STEEL ROD
INSERT ASSEMBLY

FIGURE 4.2–16

4.3 NUCLEAR DESIGN

4.3.1 DESIGN BASES

This section describes the design bases and functional requirements used in the nuclear design of the fuel and reactivity control system and relates these design bases to the general design criteria (GDC) presented in 10 CFR 50, Appendix A. Where applicable, supplemental criteria, such as Final Acceptance Criteria for Emergency Core Cooling Systems, are addressed. However, before discussing the nuclear design bases, it is appropriate to briefly review the four major categories as ascribed to conditions of plant operation.

The full spectrum of plant conditions is divided into four categories, in accordance with the anticipated frequency of occurrence and risk to the public:

- Condition 1 - Normal operation.
- Condition 2 - Incidents of moderate frequency.
- Condition 3 - Infrequent faults.
- Condition 4 - Limiting faults.

In general, Condition 1 occurrences are accommodated with margin between any plant parameter and the value of that parameter which would require either automatic or manual protective action. Condition 2 incidents are accommodated with, at most, a shutdown of the reactor with the plant capable of returning to operation after corrective action. Fuel damage (fuel damage as used here is defined as penetration of the fission product barrier; i.e., the fuel rod clad) is not expected during Condition 1 and Condition 2 events. It is not possible, however, to preclude a very small number of rod failures. These are within the capability of the chemical and volume control system (CVCS) and are consistent with the plant design basis.

Condition 3 incidents do not cause more than a small fraction of the fuel elements in the reactor to be damaged, although sufficient fuel element damage might occur to preclude immediate resumption of operation. The release of radioactive material due to Condition 3 incidents is not sufficient to interrupt or restrict public use of those areas beyond the exclusion area boundary. Furthermore, a Condition 3 incident does not by itself generate a Condition 4 fault or result in a consequential loss of function of the reactor coolant or reactor containment barriers.

Condition 4 occurrences are faults that are not expected to occur but are defined as limiting faults which must be designed against. Condition 4 faults do not cause a release of radioactive material that results in exceeding the limits of 10 CFR 100.

The core design power distribution limits related to fuel integrity are met for Condition 1 occurrences through conservative design and maintained by the action of the control system. The requirements for Condition 2 occurrences are met by providing an adequate protection system which monitors reactor parameters. The control and protection systems are described in chapter 7, and the consequences of condition 2, 3, and 4 occurrences are given in chapter 15.

4.3.1.1 Fuel Burnup

4.3.1.1.1 Basis

A limitation on initial installed excess reactivity or average discharge burnup is not required other than as is quantified in terms of other design bases, such as core negative reactivity feedback and shutdown margin discussed below.

4.3.1.1.2 Discussion

Fuel burnup is a measure of fuel depletion which represents the integrated energy output of the fuel in MWd/tonne of uranium and is a convenient means for quantifying fuel exposure criteria.

The core design lifetime or design discharge burnup is achieved by installing sufficient initial excess reactivity in each fuel region and by following a fuel replacement program (such as that described in subsection 4.3.2) that meets all safety-related criteria in each cycle of operation.

Initial excess reactivity installed in the fuel, although not a design basis, must be sufficient to maintain core criticality at full-power operating conditions throughout cycle life with equilibrium xenon, samarium, and other fission products present. The end of design cycle life is defined to occur when the chemical shim concentration is essentially zero with control rods present to the degree necessary for operational requirements (e.g., the controlling bank at the "bite" position). In terms of chemical shim boron concentration, this represents approximately 10 ppm with no control rod insertion.

After the end of design cycle life is reached and reactivity is no longer sufficient to maintain criticality at full-power operating conditions, core criticality is maintained at reduced-power conditions.

4.3.1.2 Negative Reactivity Feedbacks (Reactivity Coefficient)

4.3.1.2.1 Basis

The fuel temperature coefficient will be negative, and the moderator temperature coefficient of reactivity will be nonpositive for full power operating conditions, thereby providing negative reactivity feedback characteristics at full power. Below 70-percent power, a moderator temperature coefficient of up to +7.0 pcm/°F is allowed. From 70-percent to 100-percent power, the moderator temperature coefficient limit decreases linearly from +7.0 to 0.0 pcm/°F. The design basis meets GDC 11.

4.3.1.2.2 Discussion

When compensation for a rapid increase in reactivity is considered, there are two major effects. These are the resonance absorption (Doppler) effects associated with changing fuel temperature and the neutron spectrum and reactor composition change effects resulting from changing moderator density. These basic physics characteristics are often identified by reactivity coefficients. The use of slightly enriched uranium ensures that the Doppler coefficient of reactivity is negative. This coefficient provides the most rapid reactivity compensation.

The core is also designed to have an overall moderator temperature coefficient of reactivity which is nonpositive at 100-percent power and less than or equal to +7.0 pcm/°F below 70-percent power. From 70-percent power to 100-percent power, the maximum allowed moderator temperature coefficient decreases linearly from +7.0 pcm/°F to 0.0 pcm/°F. At full power, void content provides another, slower compensatory effect. The moderator temperature coefficient is maintained at or below the above stated limit through the use of fixed burnable absorber (BA) rods, and/or integral fuel burnable absorbers (IFBA) in the form of a zirconium diboride (ZrB_2) coating on the enriched fuel pellets, and/or control rods by limiting the reactivity held down by soluble boron.

Burnable absorber content (quantity and distribution) is not stated as a design basis. However, for some reloads, the use of burnable absorbers may be necessary for peaking factor limit control and for the accomplishment of meeting the moderator temperature coefficient limits discussed above.

4.3.1.3 Control of Power Distribution

4.3.1.3.1 Basis

The nuclear design basis is that, with at least a 95-percent confidence level:

A. The fuel will not be operated at greater than 14.5 kW/ft under normal operating conditions, including an allowance of 2 percent for calorimetric error.

B. Under abnormal conditions, including the maximum overpower condition, the fuel peak power will not cause melting, as defined in paragraph 4.4.1.2.

C. The fuel will not operate with a power distribution that violates the departure from nucleate boiling (DNB) design basis (i.e., the departure from nucleate boiling ratio (DNBR) shall not be less than the design limit DNBR discussed in subsection 4.4.1) under Condition 1 and 2 events, including the maximum overpower condition.

D. Fuel management will be such as to produce values of fuel rod power and burnup consistent with the assumptions in the fuel rod mechanical integrity analysis of section 4.2.

The above basis meets GDC 10.

4.3.1.3.2 Discussion

Calculation of extreme power shapes which affect fuel design limits is performed with proven methods and verified frequently with measurements from operating reactors. The conditions under which limiting power shapes are assumed to occur are chosen conservatively with regard to any permissible operating state.

Even though there is close agreement between calculated peak power and measurements, a nuclear uncertainty (paragraph 4.3.2.2.1) is applied to calculated peak local power. Such a margin is provided both for the analysis for normal operating states and for anticipated transients.

4.3.1.4 Maximum Controlled Reactivity Insertion Rate

4.3.1.4.1 Basis

The maximum reactivity insertion rate due to withdrawal of rod cluster control assemblies (RCCAs) at power or by boron dilution is limited. During normal at power operation, the maximum controlled reactivity insertion rate is limited. A maximum reactivity change rate for accidental withdrawal of two control banks is set so that peak heat generation rate and DNBR do not exceed the maximum allowable at overpower conditions. This satisfies GDC 25.

The maximum reactivity worth of control rods and the maximum rates of reactivity insertion employing control rods are limited to preclude rupture of the coolant pressure boundary or disruption of the core internals to a degree which would impair core cooling capacity due to a rod withdrawal or an ejection accident. (See chapter 15.)

Following any Condition 4 event (rod ejection, steam line break, etc.) the reactor can be brought to the shutdown condition, and the core will maintain acceptable heat transfer geometry. This satisfies GDC 28.

4.3.1.4.2 Discussion

Reactivity addition associated with an accidental withdrawal of a control bank (or banks) is limited by the maximum rod speed (or travel rate) and by the worth of the bank(s). For this reactor, the maximum control rod speed is 45 in./min.

The reactivity change rates are conservatively calculated, assuming unfavorable axial power and xenon distributions. The peak xenon burnout rate is significantly lower than the maximum reactivity addition rate for normal operation and for accidental withdrawal of two banks.

4.3.1.5 Shutdown Margins

4.3.1.5.1 Basis

Minimum shutdown margin as specified in the Technical Specifications or Technical Requirements Manual is required in all operating modes, in the hot standby shutdown condition, and in the cold shutdown condition.

In all analyses involving reactor trip, the single, highest worth rod cluster control assembly is postulated to remain untripped in its full-out position (stuck rod criterion). This satisfies GDC 26.

4.3.1.5.2 Discussion

Two independent reactivity control systems are provided: control rods and soluble boron in the coolant. The control rod system can compensate for the reactivity effects of the fuel and water temperature changes accompanying power level changes over the range from full load to no load. In addition, the control rod system provides the minimum shutdown margin under Condition 1 events and is capable of making the core subcritical rapidly enough to prevent

exceeding acceptable fuel damage limits (very small number of rod failures), assuming that the highest worth control rod is stuck out upon trip.

The boron system can compensate for all xenon burnout reactivity changes and will maintain the reactor in the cold shutdown condition. Thus, backup and emergency shutdown provisions are provided by mechanical and chemical shim control systems which satisfy GDC 26.

4.3.1.5.3 Basis

When fuel assemblies are in the pressure vessel and the vessel head is not in place, k_{eff} will be maintained at or below 0.95 with control rods and soluble boron. Further, the fuel will be maintained sufficiently subcritical that removal of all rod cluster control assemblies will not result in criticality.

4.3.1.5.4 Discussion

American National Standards Institute (ANSI) N18.2 specifies a k_{eff} not to exceed 0.95 in spent fuel storage racks and transfer equipment flooded with pure water and a k_{eff} not to exceed 0.98 in normally dry new fuel storage racks, assuming optimum moderation. No criterion is given for the refueling operation. However, a 5-percent margin, which is consistent with spent fuel storage and transfer and the new fuel storage, is adequate for the controlled and continuously monitored operations involved.

The boron concentration required to meet the refueling shutdown criteria is specified in the Core Operating Limits Report, which is referenced in the Technical Specifications. Verification that these shutdown criteria are met, including uncertainties, is achieved using standard design methods. The subcriticality of the core is continuously monitored as described in the Technical Specifications.

4.3.1.6 Stability

4.3.1.6.1 Basis

The core will be inherently stable to power oscillations at the fundamental mode. This satisfies GDC 12.

Spatial power oscillations within the core with a constant core power output, should they occur, can be reliably and readily detected and suppressed.

4.3.1.6.2 Discussion

Oscillations of the total power output of the core, from whatever cause, are readily detected by the loop temperature sensors and by the nuclear instrumentation. The core is protected by these systems; a reactor trip would occur if power increased unacceptably, preserving the design margins to fuel design limits. The stability of the turbine/steam generator/core systems and the reactor control system is such that total core power oscillations are not normally possible. The redundancy of the protection circuits ensures an extremely low probability of exceeding design power levels.

The core is designed so that diametral and azimuthal oscillations due to spatial xenon effects are self-damping, and no operator action or control action is required to suppress them. The stability to diametral oscillations is so great that this excitation is highly improbable. Convergent azimuthal oscillations can be excited by prohibited motion of individual control rods. Such oscillations are readily observable and alarmed, using the excore long ion chambers. Indications are also continuously available from incore thermocouples and loop temperature measurements. Movable incore detectors can be activated to provide more detailed information. In all proposed cores, these horizontal plane oscillations are self-damping by virtue of reactivity feedback effects designed into the core.

However, axial xenon spatial power oscillations may occur in the middle to end of core life. The control bank and excore detectors are provided for control and monitoring of axial power distributions.

Assurance that fuel design limits are not exceeded is provided by reactor overpower ΔT and overtemperature ΔT trip functions, which use the measured axial power imbalance as an input. Detection and suppression of xenon oscillations are discussed in paragraph 4.3.2.7.

4.3.1.7 Anticipated Transients Without SCRAM

The effects of anticipated transients with failure to trip are not considered in the design bases of the plant. Analysis has shown that the likelihood of such a hypothetical event is negligibly small. Furthermore, analysis of the consequences of hypothetical failure to trip following anticipated transients has shown that no significant core damage would result, system peak pressures would be limited to acceptable values, and no failure of the reactor coolant system would result.(1)

4.3.2 DESCRIPTION

4.3.2.1 Nuclear Design Description

The reactor core consists of a specified number of fuel rods held in bundles by spacer grids and top and bottom fittings. The fuel rods are constructed of Zircaloy/ZIRLO/Optimized ZIRLO cylindrical tubes containing UO_2 fuel pellets. The bundles, known as fuel assemblies, are arranged in a pattern which approximates a right circular cylinder.

Each fuel assembly contains a 17 x 17 rod array composed of 264 fuel rods, 24 guide thimbles, and an incore instrumentation tube. Figure 4.2-1 shows a cross-sectional view of the 17 x 17 fuel assemblies. Further details of the fuel assembly are given in section 4.2.

For initial core loading, the fuel rods within a given assembly have the same uranium enrichment in both the radial and axial planes. Fuel assemblies of three different enrichments are used in the initial core loading to establish a favorable radial power distribution. Figure 4.3-1 shows the fuel loading pattern to be used in the first core. Two regions consisting of the two lower enrichments are interspersed to form a checkerboard pattern in the central portion of the core. The third region is arranged around the periphery of the core and contains the highest enrichment. The enrichments for the VEGP initial cycle are shown in table 4.3-1.

For reload cores, VANTAGE 5 fuel assemblies may be used. Detailed descriptions of the VANTAGE 5 fuel features are given in section 4.2. Integral fuel burnable absorbers (IFBA) in the central portion of the fuel stack may be used in reload cores to control excess reactivity.

Axial blankets consisting of unenriched, mid-enriched, or fully enriched solid or annular fuel pellets may be placed at the ends of the enriched pellet stack. The unenriched or mid-enriched axial blanket pellets are used in reload cores to reduce neutron leakage and to improve fuel utilization. The annular blanket pellets are used to increase the void volume for gas accommodation within the fuel rod.

A typical reloading pattern is also shown in figure 4.3-1 with new fuel interspersed checkerboard-style in the center and depleted fuel on the periphery. The core will normally operate approximately 18 months between refueling, accumulating approximately 20,000 MWd/tonne of uranium per year. The exact reloading pattern, the initial and final positions of assemblies, and the number of fresh assemblies and their placement are dependent on the energy requirement for the next cycle and burnup and power histories of the previous cycles.

The core average enrichment is determined by the amount of fissionable material required to provide the desired core lifetime and energy requirements. The physics of the burnout process is such that operation of the reactor depletes the amount of fuel available due to the absorption of neutrons by the U-235 atoms and their subsequent fission. In addition, the fission process results in the formation of fission products, some of which readily absorb neutrons. These effects, depletion and the buildup of fission products, are partially offset by the buildup of plutonium shown in figure 4.3-2 for a typical 17 x 17 fuel assembly, which occurs due to the nonfission absorption of neutrons in U-238. Therefore, at the beginning of any cycle a reactivity reserve equal to the depletion of the fissionable fuel and the buildup of fission product poisons over the specified cycle life must be built into the reactor. This excess reactivity is controlled by removable neutron-absorbing material in the form of boron dissolved in the primary coolant and BA rods and/or ZrB_2-coated fuel pellets. The stack length of the coated fuel pellets may vary for different reload designs, with the optimum length determined on a design-specific basis.

The concentration of the soluble boron is varied to compensate for reactivity changes due to fuel burnup, fission product poisoning including xenon and samarium, BA depletion, and the cold-to-operating moderator temperature change. Using its normal or emergency boration path, the CVCS is capable of inserting negative reactivity at a rate of approximately 30 pcm/min when the reactor coolant boron concentration is 1000 ppm and approximately 35 pcm/min when the reactor coolant boron concentration is 100 ppm. The peak burnout rate for xenon is 25 pcm/min. (Subsection 9.3.4 discusses the capability of the CVCS to counteract xenon decay.) Rapid transient reactivity requirements and safety shutdown requirements are met with control rods.

As the boron concentration is increased, the moderator temperature coefficient becomes less negative. High boron concentrations will cause the moderator temperature coefficient to be positive at beginning of life (BOL). Therefore, burnable absorber rods and/or IFBAs are used to reduce the soluble boron concentration sufficiently to ensure that the moderator coefficient is nonpositive at full power, is less than or equal to +7.0 pcm/°F below 70-percent power, and below a linearly decreasing limit of +7.0 pcm/°F to 0.0 pcm/°F between 70-percent power and 100-percent power, respectively.

During operation, the poison content in these rods is depleted, thus adding positive reactivity to offset some of the negative reactivity from fuel depletion and fission product buildup. The depletion rate of the BA rods and/or IFBA coated rods is not critical, since chemical shim is always available and flexible enough to cover any possible deviations in the expected BA depletion rate. Figure 4.3-3 is a plot of core depletion with and without BA rods, (as is typical of the first cycle and a typical reload containing IFBAs). Note that even at end of life (EOL) conditions some residual poison remains in the BA rods, resulting in a net decrease in the cycle lifetime. The IFBA coating at EOL conditions leaves no residual poison.

In addition to reactivity control, the BA rods and/or fuel rods containing ZrB_2-coated fuel pellets are strategically located to provide a favorable radial power distribution. Figure 4.3-4 shows the BA distributions within a fuel assembly for the several BA patterns used in a 17 x 17 array and also shows the standard within-assembly configurations of the fuel rods containing ZrB_2-coated fuel pellets for several IFBA patterns. Typical reload core BA loading patterns for discrete BAs (WABA or borosilicate glass) and IFBAs are shown in figure 4.3-5. These burnable absorber (IFBA) loading patterns were reassessed to achieve the most efficient absorber orientation. The revised patterns provide improved peaking factor and reactivity holddown benefits. Use of the revised patterns commenced with Vogtle Unit 1 Region 9 and Vogtle Unit 2 Region 7.

Tables 4.3-1 through 4.3-3 contain summaries of reactor core design parameters including reactivity coefficients, delayed neutron fraction, and neutron lifetimes. Sufficient information is included to permit an independent calculation of the nuclear performance characteristics of the core.

4.3.2.2 Power Distribution

The accuracy of power distribution calculations has been confirmed through approximately 1000 flux maps during some 20 years of operation under conditions very similar to those expected. Details of this confirmation are given in reference 2 and in paragraph 4.3.2.2.7.

4.3.2.2.1 Definitions

Power distributions are quantified in terms of hot channel factors. These factors are a measure of the peak pellet power within the reactor core and the total energy produced in a coolant channel, relative to the total reactor power output, and are expressed in terms of quantities related to the nuclear or thermal design; namely, power density is the thermal power produced per unit volume of the core (kW/l).

Linear power density is the thermal power produced per unit length of active fuel (kW/ft). Since fuel assembly geometry is standardized, this is the unit of power density most commonly used. For all practical purposes, it differs from kilowatts per liter by a constant factor, which includes geometry effects and the fraction of the total thermal power generated in the fuel rod.

Average linear power density is the total thermal power produced in the fuel rods divided by the total active fuel length of all rods in the core.

Local heat flux is the heat flux at the surface of the cladding ($Btu/ft^2/h$). For nominal rod parameters, this differs from linear power density by a constant factor.

Rod power or rod integral power is the length integrated linear power density in one rod (kW).

Average rod power is the total thermal power produced in the fuel rods divided by the number of fuel rods (assuming all rods have equal length).

The hot channel factors used in the discussion of power distributions in this section are defined as follows:

F_Q heat flux hot channel factor, is defined as the maximum local heat flux on the surface of a fuel rod divided by the average fuel rod heat flux, allowing for manufacturing tolerances on fuel pellets and rods.

F_Q^N, nuclear heat flux hot channel factor, is defined as the maximum local fuel rod linear power density divided by the average fuel rod linear power density, assuming nominal fuel pellet and rod parameters.

F_Q^E, engineering heat flux hot channel factor, is the allowance on heat flux required for manufacturing tolerances. The engineering factor allows for local variation in enrichment, pellet density and diameter, surface area of the fuel rod, and eccentricity of the gap between pellet and clad. Combined statistically, the net effect is a factor of 1.03 to be applied to fuel rod surface heat flux.

$F_{\Delta H}^N$, nuclear enthalpy rise hot channel factor, is defined as the ratio of the integral of linear power along the rod with the highest integrated power to the average rod power.

Manufacturing tolerances, hot channel power distribution, and surrounding channel power distributions are treated explicitly in the calculation of the DNBR described in section 4.4.

It is convenient for the purposes of discussion to define subfactors of F_Q. However, design limits are set in terms of the total peaking factor.

F_Q = total peaking factor or heat flux hot channel factor.

$$= \frac{\text{maximum } kW/ft}{\text{average } kW/ft}$$

Without densification effects:

$$F_Q = F_Q^N \times F_Q^E$$
$$= F_{XY}^N \times F_Z^N \times F_U^N \times F_Q^E$$

where F_Q^N and F_Q^E are defined above and :

F_U^N = factor for measurement conservatism, assumed to be 1.05, when using $\geq$ 44 detector thimbles, and is 1.05 + [2.0 {3-T / (14.5)}] / 100, where T equals the number of thimbles, when using $\geq$ 29 and < 44 detector thimbles.

F_{XY}^N = ratio of peak power density to average power density in the horizontal plane of peak local power.

F_Z^N = ratio of the power per unit core height in the horizontal plane of peak local power to the average value of power per unit core height. If the plane of peak local power coincides with the plane of maximum power per unit core height, the F_Z^N is the core average axial peaking factor.

To include the allowances made for densification effects, which are height dependent, the following quantities are defined:

S(Z) = the allowances made for densification effects at height Z in the core (paragraph 4.3.2.2.5.).

$P(Z)$ = ratio of the power per unit core height in the horizontal plane at height Z to the average value of power per unit core height.

$F^N_{XY}(Z)$ = ratio of peak power density to average power density in the horizontal plane of height Z.

then:

F_Q = total peaking factor.

$$= \frac{\text{maximum } kW/ft}{\text{average } kW/ft}$$

Including densification allowance:

$$F_Q = \max (F^N_{XY}(Z) \times P(Z) \times S(Z)) \times F^N_U \times F^E_Q$$

4.3.2.2.2 Radial Power Distributions

The power shape in horizontal sections of the core at full power is a function of the fuel assembly and BA loading patterns, the control rod pattern, and the fuel burnup distribution. Thus, at any time in the cycle, a horizontal section of the core can be characterized as unrodded or with group D control rods. These two situations combined with burnup effects determine the radial power shapes which can exist in the core at full power. Typical first cycle values of F^N_{XY} are the radial factors (BOL to EOL) given in table 4.3-2. The effect on radial power shapes of power level, xenon, samarium, and moderator density effects are also considered, but these are quite small. The effect of nonuniform flow distribution is negligible. While radial power distributions in various planes of the core are often illustrated, since the moderator density is directly proportional to enthalpy, the core radial enthalpy rise distribution, as determined by the integral of power up each channel, is of greater interest. Figures 4.3-6 through 4.3-11 show typical reload radial power distributions for one-fourth of the core for representative operating conditions. These conditions are as follows:

A. Hot full power (HFP) at BOL, unrodded, no xenon.

B. HFP at BOL, unrodded, equilibrium xenon.

C. HFP near BOL, bank D in, equilibrium xenon.

D. HFP near middle of life (MOL), unrodded equilibrium xenon.

E. HFP near EOL, unrodded, equilibrium xenon.

F. HFP at EOL, bank D in, equilibrium xenon.

Since the position of the hot channel varies from time to time, a single-reference radial design power distribution is selected for DNB calculations. This reference power distribution is chosen conservatively to concentrate power in one area of the core, minimizing the benefits of flow redistribution. Assembly powers are normalized to core average power. The radial power distribution within a fuel rod and its variation with burnup as utilized in thermal calculations and fuel rod design are discussed in section 4.4.

4.3.2.2.3 Assembly Power Distributions

For the purpose of illustration, typical rodwise power distributions from the BOL and EOL conditions corresponding to figures 4.3-7 and 4.3-10, respectively, are given for the same assembly in figures 4.3-12 and 4.3-13, respectively.

Since the detailed power distribution surrounding the hot channel varies from time to time, a conservatively flat radial assembly power distribution is assumed in the DNB analysis, described in section 4.4, with the rod of maximum integrated power artificially raised to the design value of $F^N_{\Delta H}$. Care is taken in the nuclear design of all fuel cycles and all operating conditions to ensure that a flatter assembly power distribution does not occur with limiting values of $F^N_{\Delta H}$.

4.3.2.2.4 Axial Power Distributions

The shape of the power profile in the axial or vertical direction is largely under the control of the operator through either the manual operation of the control rods or automatic motion of rods responding to manual operation of the CVCS. Nuclear effects which cause variations in the axial power shape include moderator density, Doppler effect on resonance absorption, spatial distribution of xenon, burnup, and axial distribution of fuel enrichment and burnable absorbers. Automatically controlled variations in total power output and full-length rod motion are also important in determining the axial power shape at any time. Signals are available to the operator from the excore ion chambers, which are long ion chambers outside the reactor vessel running parallel to the axis of the core. Separate signals are taken from the top and bottom halves of the chambers. The difference between top and bottom signals from each of four pairs of detectors is displayed on the control panel and called the flux difference, ΔI. Calculations of core average peaking factor for many plants and measurements from operating plants under many operating situations are associated with either ΔI or axial offset in such a way that an upper bound can be placed on the peaking factor. For these correlations, axial offset is defined as:

$$\text{axial offset} = \frac{\phi_t - \phi_b}{\phi_t + \phi_b}$$

and ϕ_t and ϕ_b are the top and bottom detector readings.

Representative reload axial power shapes for BOL, MOL, and EOL conditions are shown in figures 4.3-14 through 4.3-16. These figures cover a wide range of axial offset, including values achieved by skewing xenon distributions.

4.3.2.2.5 Local Power Peaking

Past creep collapse methods have assumed that pellet hangup occurs and an axial gap exists in all fuel rods within a reactor core. The size of the axial gap is estimated from conservative early-in-life fuel densification as determined from out-of-reactor sintering tests described in Regulatory Guide 1.126. The size of the axial gap determines the magnitude of the power spike factor applied to fuel designs. Axial gaps greater than 0.5 in. can lead to clad collapse and significant flux and power spiking. Axial gaps less than 0.5 in. have been shown, reference 26, to result in no clad collapse and are associated with a relatively small power spike of 1 percent or less. Reference 26, presents data that demonstrates that no large axial gaps, i.e., > 0.3 in., exist in current fuel designs during in-reactor performance. Therefore, the power spike factor is no longer considered in the nuclear design.

4.3.2.2.6 Limiting Power Distributions

According to the ANSI classification of plant conditions (chapter 15), Condition 1 occurrences are those expected frequently or regularly in the course of power operation, maintenance, or maneuvering of the plant. As such, Condition 1 occurrences are accommodated with margin between any plant parameter and the value of that parameter which would require either automatic or manual protective action. Inasmuch as Condition 1 events occur frequently or regularly, they must be considered from the point of view of affecting the consequences of fault conditions (Conditions 2, 3, and 4). In this regard, analysis of each fault condition described is generally based on a conservative set of initial conditions corresponding to the most adverse set of conditions which can occur during Condition 1 operation.

The list of steady-state and shutdown conditions, permissible deviations, and operational transients is given in chapter 15. Implicit in the definition of normal operation is proper and timely action by the reactor operator; that is, the operator follows recommended operating procedures for maintaining appropriate power distributions and takes any necessary remedial actions when alerted to do so by the plant instrumentation. Thus, as stated above, the worst or limiting power distribution which can occur during normal operation is to be considered as the starting point for analysis of Conditions 2, 3, and 4 events.

Improper procedural actions or errors by the operator are assumed in the design as occurrences of moderate frequency (Condition 2). Some of the consequences which might result are discussed in chapter 15. Therefore, the limiting power shapes which result from such Condition 2 events are those power shapes which deviate from the normal operating condition at the recommended axial offset band; e.g., due to lack of proper action by the operator during a xenon transient following a change in power level brought about by control rod motion. Power shapes which fall in this category are used for determination of the reactor protection system setpoints to maintain margin to overpower or DNB limits.

The means for maintaining power distributions within the required hot channel factor limits are described in the Core Operating Limits Report and the Technical Specifications. A complete discussion of power distribution control in Westinghouse pressurized water reactors (PWRs) is included in reference 6. Detailed background information on the design constraints on local power density in a Westinghouse PWR, on the defined operating procedures, and on the measures taken to preclude exceeding design limits is presented in the Westinghouse topical report on power distribution control and load following procedures.[7] The following paragraphs summarize these reports and describe the calculations used to establish the upper bound on peaking factors.

The calculations used to establish the upper bound on peaking factors, F_Q and $F_{\Delta H}^N$, include all of the nuclear effects which influence the radial and/or axial power distributions throughout core life for various modes of operation, including load follow, reduced power operation, and axial xenon transients.

Radial power distributions are calculated for the full-power condition. Fuel and moderator temperature feedback effects are included for the average enthalpy plane of the reactor. The steady-state nuclear design calculations are done for normal flow with the same mass flow in each channel and flow redistribution effects neglected. The effect of flow redistribution is calculated explicitly where it is important in the DNB analysis of accidents. The effect of xenon on radial power distribution is small (compare figures 4.3-6 and 4.3-7) but is included as part of the normal design process.

The core average axial profile can experience significant changes, which can occur rapidly as a result of rod motion and load changes and more slowly due to xenon distribution. For the study

of points of closest approach to axial power distribution limits, several thousand cases are examined. Since the properties of the nuclear design dictate what axial shapes can occur, boundaries on the limits of interest can be set in terms of the parameters which are readily observed on the plant. Specifically, the nuclear design parameters significant to the axial power distribution analysis are as follows:

- Core power level.
- Core height.
- Coolant temperature and flow.
- Coolant temperature program as a function of reactor power.
- Fuel cycle lifetimes.
- Rod bank worths.
- Rod bank overlaps.

Normal operation of the plant assumes compliance with the following conditions:

A. Control rods in a single bank move together with no individual rod insertion differing by more than 12 steps (indicated) from the bank demand position.

B. Control banks are sequenced with overlapping banks.

C. The control full-length bank insertion limits are not violated.

D. Axial power distribution control procedures, which are given in terms of flux difference control and control bank position, are observed.

The axial power distribution procedures referred to above are part of the required operating procedures followed in normal operation.

Limits placed on the axial flux difference are designed to assure that the heat flux hot channel factor F_Q is maintained within acceptable limits. The constant axial offset control (CAOC) operating procedures described in reference 7 require control of the axial flux difference at all power levels within a permissible operating band about a target value corresponding to the equilibrium full power value. The relaxed axial offset control (RAOC) procedures to be implemented in Unit 1 Cycle 4 and Unit 2 Cycle 3 and beyond, described in reference 39, were developed to provide wider control band widths and, consequently, more operating flexibility. These wider operating limits, particularly at lower power levels, can increase plant availability by allowing quicker plant startups and increased maneuvering flexibility without trip or reportable occurrences.

Further operating flexibility is achieved by combining RAOC operation with an F_Q surveillance technical specification. F_{xy} (z) surveillance requires periodic plant surveillance on the height-dependent radial peaking factor, F_{xy} (z), for partial verification that operation will not cause the F_Q (z) limit to be exceeded. In the F_Q surveillance technical specification to be implemented in Unit 1 Cycle 4 and Unit 2 Cycle 3, F_{xy} (z) surveillance will be replaced by F_Q (z) surveillance. Monitoring F_Q (z) and increasing the measured value for expected plant maneuvers provides a more convenient form of assuring plant operation below the F_Q (z) limit while retaining the intent of using a measured parameter to verify Technical Specification compliance.

In standard CAOC analysis described in reference 7, the generation of the normal operation power distributions is constrained by the rod insertion limits (RIL) and the ΔI band limits. The purpose of RAOC is to find the widest permissible ΔI-Power operating space by analyzing a

wide range of ΔI. Therefore, the generation of normal operation power distributions is constrained only by the RIL for RAOC.

For a CAOC analysis, load-follow simulations are performed covering the allowed CAOC operating space to generate a typical range of allowed axial xenon distributions, which in turn are used to calculate axial power distributions in both normal operation and Condition II accident conditions. For a RAOC analysis, however, a reconstruction model described in reference 39 is used as a more practical method to create axial xenon distributions covering the wider ΔI-Power operating space allowed with RAOC operation. Each resulting power shape is analyzed to determine if LOCA constraints are met or exceeded. The total peaking factor, F_Q^T, is determined using standard synthesis methods as described in reference 7.

The $F_Q(z)$'s are synthesized from axial calculations combined with radial factors appropriate for rodded and unrodded planes in the first cycle. In these calculations, the effects on the unrodded radial peak of xenon redistribution that occurs following the withdrawal of a control bank (or banks) from a rodded region is obtained from two-dimensional X-Y calculations. A 1.03 factor to be applied on the unrodded radial peak was obtained from calculations in which xenon distribution was preconditioned by the presence of control rods and then allowed to redistribute for several hours. A detailed discussion of this effect may be found in reference 7. The calculated values have been increased by a factor of 1.05, when using $\geq$ 44 detector thimbles, and is 1.05 + [2.0 {3-T / (14.5)}] / 100, where T equals the number of thimbles, when using $\geq$ 29 and < 44 detector thimbles for conservatism and a factor of 1.03 for the engineering factor F_Q^E.

The envelope drawn over the calculated maximum ($F_Q(Z)$ × power) points in figure 4.3-21 represents an upper bound envelope on local power density versus elevation in the core. It should be emphasized that this envelope is a conservative representation of the bounding values of local power density.

Finally, as previously discussed, this upper bound envelope is based on procedures of load follow which require operation within specified axial flux difference limits. Operation within this upperbound envelope is ensured by limits contained in the Technical Specifications which rely only upon excore surveillance supplemented by the normal monthly full core map requirement and by computer-based alarms on deviation from the allowed flux difference band.

Allowing for fuel densification effects, the average linear power at 3626 MW is 5.79 kW/ft. From figure 4.3-21, the conservative upper bound value of normalized local power density, including power uncertainty allowance, is 2.50, corresponding to a peak linear power of 14.5 kW/ft.

To determine reactor protection system setpoints with respect to power distributions, three categories of events are considered: rod control equipment malfunctions, operator errors of commission, and operator errors of omission. In evaluating these three categories of events, the core is assumed to be operating within the four constraints described above.

The first category comprises uncontrolled rod withdrawal (with rods moving in the normal bank sequence) for full-length banks. Also included are motions of the full-length banks below their insertion limits, which could be caused, for example, by uncontrolled dilution or primary coolant cooldown. Power distributions were calculated throughout these occurrences, assuming short-term corrective action; that is, no transient xenon effects were considered to result from the malfunction. The event was assumed to occur from typical normal operating situations, which include normal xenon transients. It was further assumed in determining the power distributions that total core power level would be limited by reactor trip to below 120 percent. Since the study is to determine protection limits with respect to power and axial offset, no credit was taken for trip setpoint reduction due to flux difference. Representative results are given in figure 4.3-22 in units of kW/ft. The peak power density which can occur in such events, assuming reactor trip at

or below 120 percent, is less than that required for centerline melt, including uncertainties and densification effects.

The second category, also appearing in figure 4.3-22, assumes that the operator mispositions the full-length rod bank in violation of the insertion limits and creates short-term conditions not included in normal operating conditions.

The third category assumes that the operator fails to take action to correct a flux difference violation (such as boration/dilution transient). Representative results for peak linear power density include an allowance for calorimetric error. The peak linear power does not exceed 22.4 kW/ft, including the above factors. This value applies to Zircaloy, ZIRLO, and/or Optimized ZIRLO clad fuel.

The appropriate hot channel factors F_Q and $F^N_{\Delta H}$ for peak local power density and for DNB analysis at full power based on analyses of possible operating power shapes are addressed in the Core Operating Limits Report and the Technical Specifications.

The maximum allowable F_Q can be increased with decreasing power, as shown in the Core Operating Limits Report and the Technical Specifications. Increasing $F^N_{\Delta H}$ with decreasing power is permitted by the DNB protection setpoints and allows radial power shape changes with rod insertion to the insertion limits, as described in paragraph 4.4.4.3. The allowance for increased $F^N_{\Delta H}$ permitted is addressed in the Technical Specifications.

This becomes a design basis criterion which is used for establishing acceptable control rod patterns and control bank sequencing. Likewise, fuel loading patterns for each cycle are selected with consideration of this design criterion. The worst values of $F^N_{\Delta H}$ for possible rod configurations occurring in normal operation are used in verifying that this criterion is met. Typical radial power distributions are shown in figures 4.3-6 through 4.3-11. The worst values generally occur when the rods are assumed to be at their insertion limits. Operation with rod positions above the allowed rod insertion limits provides increasing margin to the $F^N_{\Delta H}$ criterion. As discussed in section 3.2 of reference 8, it has been determined that the Technical Specifications limits are met, provided the above conditions A and B are observed. These limits are taken as input to the thermal-hydraulic design basis, as described in paragraph 4.4.4.3.1.

When a situation is possible in normal operation which could result in local power densities in excess of those assumed as the precondition for a subsequent hypothetical accident, but which would not itself cause fuel failure, administrative controls and alarms are provided for returning the core to a safe condition. These alarms are described in detail in chapter 7.

The independence of the various individual uncertainties constituting the uncertainty factor on F_Q enables the uncertainty (F^U_Q) to be calculated by statistically combining the individual uncertainties on the limiting rod. The standard deviation of the resultant distribution of F^U_Q is determined by taking the square root of the sum of the variances of each of the contributing distributions.(2) The measurement uncertainty is 1.05 (reference 2) and is applicable when using $\geq$ 44 detector thimbles. Reference 45 evaluated using $\geq$ 29 and < 44 detector thimbles, and the measurement uncertainty is 1.05 + [2.0 {3-T / {14.5)}] / 100, where T equals the number of thimbles used. The value for F^E_Q is 1.03. The value for the rod bow factor, F^B_Q, is 1.013, which accounts for the initial as-built rod bow.

4.3.2.2.7 Experimental Verification of Power Distribution Analysis

This subject is discussed in depth in reference 2. A summary of this report is given below. It should be noted that power-distribution-related measurements are incorporated into the evaluation of calculated power distribution information, using an incore instrumentation processing code described in reference 9 or reference 41. The measured-versus-calculational comparison is normally performed periodically throughout the cycle lifetime of the reactor, as required by Technical Specifications.

In a measurement of the heat flux hot channel factor, F_Q, with the movable detector system described in subsections 7.7.1 and 4.4.6, the following uncertainties must be considered:

A. Reproducibility of the measured signal.

B. Errors in the calculated relationship between detector current and local flux.

C. Errors in the calculated relationship between detector flux and peak rod power some distance from the measurement thimble.

The appropriate allowance for category A above has been quantified by repetitive measurements made with several intercalibrated detectors by using the common thimble features of the incore detector system. This system allows more than one detector to access any thimble. Errors in category B above are quantified to the extent possible, by using the detector current measured at one thimble location to predict fluxes at another location, which is also measured. Local power distribution predictions are verified in critical experiments on arrays of rods with simulated guide thimbles, control rods, BAs, etc. These critical experiments provide quantification of errors of categories A and C above.

Reference 2 describes critical experiments performed at the Westinghouse Reactor Evaluation Center and measurements taken on two Westinghouse plants with incore systems of the same type used in the VEGP. The report concludes that the uncertainty associated with F_Q (heat flux) is 4.58 percent at the 95-percent confidence level with only 5 percent of the measurements greater than the inferred value. This is the equivalent of a 1.645σ limit on a normal distribution and is the uncertainty to be associated with a full core flux map with movable detectors reduced with a reasonable set of input data incorporating the influence of burnup on the radial power distribution. The uncertainty is usually rounded up to 5 percent.

In comparing measured power distributions (or detector currents) with calculations for the same operating conditions, it is not possible to isolate the detector reproducibility. Thus, a comparison between measured and predicted power distributions has to include some measurement error. Such a comparison is given in figure 4.3-24 for one of the maps used in reference 2. Since the first publication of reference 2, hundreds of maps have been taken on these and other reactors. The results confirm the adequacy of the 5-percent uncertainty allowance on the calculated F_Q, when using ≥ 44 detector thimbles. When using ≥ 29 and < 44 detector thimbles, the measurement uncertainty is $1.05 + [2.0 \{3\text{-}T / \{14.5)\}] / 100$, where T equals the number of thimbles (reference 45). .

A similar analysis for the uncertainty in $F^N_{\Delta H}$ (rod integral power) measurements results in an allowance of 3.60 percent at the equivalent of a 1.645σ confidence level. For historical reasons, an 8-percent uncertainty factor is allowed in the nuclear design calculational basis; that is, the predicted rod integrals at full power must not exceed the design $F^N_{\Delta H}$ less 8 percent.

A measurement in the second cycle of a 121-assembly, 12-ft core is compared with a simplified one-dimensional core average axial calculation in figure 4.3-25. This calculation does not give explicit representation to the fuel grids.

The accumulated data on power distributions in actual operation are basically of three types:

A. Much of the data is obtained in steady-state operation at constant power in the normal operating configuration.

B. Data with unusual values of axial offset are obtained as part of the excore detector calibration exercise performed monthly.

C. Special tests have been performed in load follow and other transient xenon conditions which have yielded useful information on power distributions.

These data are presented in detail in reference 8. Figure 4.3-26 contains a summary of measured values of F_Q as a function of axial offset for five plants from that report.

4.3.2.2.8 Testing

An extensive series of physics tests has been performed on the first core. These tests and the criteria for satisfactory results are described in chapter 14. Since not all limiting situations can be created at BOL, the main purpose of the tests is to provide a check on the calculational methods used in the predictions for the conditions of the test. Tests performed at the beginning of each reload cycle are limited to verification of the selected safety-related parameters of the reload design.

4.3.2.2.9 Monitoring Instrumentation

The adequacy of instrument numbers, spatial deployment, required correlations between readings and peaking factors, calibration, and errors are described in references 2, 6, and 8. The relevant conclusions are summarized in paragraph 4.3.2.2.7 and subsection 4.4.6.

Provided the limitations given in paragraph 4.3.2.2.6 on rod insertion and flux difference are observed, the excore detector system provides adequate online monitoring of power distributions. Further details of specific limits on the observed rod positions and flux difference are given in the Core Operating Limits Report and the Technical Specifications, together with a discussion of the Bases.

Limits for alarms, reactor trip, etc., are given in the Technical Specifications. Descriptions of the systems provided are given in section 7.7.

4.3.2.3 Reactivity Coefficients

The kinetic characteristics of the reactor core determine the response of the core to changing plant conditions or to operator adjustments made during normal operation, as well as the core response during abnormal or accidental transients. These kinetic characteristics are quantified in reactivity coefficients. The reactivity coefficients reflect the changes in the neutron multiplication due to varying plant conditions, such as power, moderator or fuel temperatures, or pressure or void conditions, although the latter are relatively unimportant in the VEGP reactors. Since reactivity coefficients change during the life of the core, ranges of coefficients are employed in transient analysis to determine the response of the plant throughout life. The results of such simulations and the reactivity coefficients used are presented in chapter 15. The reactivity coefficients are calculated on a corewide basis by diffusion theory methods. The effect of radial and axial power distribution on core average reactivity coefficients is implicit in those calculations and is not significant under normal operating conditions. For example, a

skewed xenon distribution which results in changing axial offset by 5 percent changes the moderator and Doppler temperature coefficients by less than 0.01 pcm/°F, and 0.03 pcm/°F, respectively. An artificially skewed xenon distribution which results in changing the radial $F^N_{\Delta H}$ by 3 percent changes the moderator and Doppler temperature coefficients by less than 0.03 pcm/°F and 0.001 pcm/°F, respectively. The spatial effects are accentuated in some transient conditions, for example, in postulated rupture of the main steam line break and rupture of an RCCA mechanism housing described in subsections 15.1.5 and 15.4.8, and are included in these analyses.

The analytical methods and calculational models used in calculating the reactivity coefficients are given in subsection 4.3.3. These models have been confirmed through extensive testing of more than 30 cores similar to the plant described herein; results of these tests are discussed in subsection 4.3.3.

Quantitative information for calculated reactivity coefficients including fuel-Doppler coefficient, moderator coefficients (density, temperature, pressure, and void), and power coefficient, is given in the following sections.

4.3.2.3.1 Fuel Temperature (Doppler) Coefficient

The fuel temperature (Doppler) coefficient is defined as the change in reactivity per degree change in effective fuel temperature and is primarily a measure of the Doppler broadening of U-238 and Pu-240 resonance absorption peaks. Doppler broadening of other isotopes is also considered, but their contribution to the Doppler effect is small. An increase in fuel temperature increases the effective resonance absorption cross-sections of the fuel and produces a corresponding reduction in reactivity.

The fuel temperature coefficient is calculated by performing two-group two-dimensional or three-dimensional calculations. Moderator temperature is held constant, and the power level is varied. Spatial variation of fuel temperature is taken into account by calculating the effective fuel temperature as a function of power density, as discussed in paragraph 4.3.3.1.

A typical Doppler temperature coefficient is shown in figure 4.3-27 as a function of the effective fuel temperature (at BOL and EOL conditions). The effective fuel temperature is lower than the volume-averaged fuel temperature, since the neutron flux distribution is nonuniform through the pellet and gives preferential weight to the surface temperature. A typical Doppler-only contribution to the power coefficient, defined later, is shown in figure 4.3-28 as a function of relative core power. The integral of the differential curve in figure 4.3-28 is the Doppler contribution to the power defect and is shown in figure 4.3-29 as a function of relative power. The Doppler coefficient becomes more negative as a function of life as the Pu-240 content increases, thus increasing the Pu-240 resonance absorption, but the overall value becomes less negative, since the fuel temperature changes with burnup, as described in paragraph 4.3.3.1. The upper and lower limits of Doppler coefficient used in accident analyses are given in chapter 15.

4.3.2.3.2 Moderator Coefficients

The moderator coefficient is a measure of the change in reactivity due to a change in specific coolant parameters, such as density, temperature, pressure, or void. The coefficients so obtained are moderator density, temperature, pressure, and void coefficients.

4.3.2.3.2.1 Moderator Density and Temperature Coefficients. The moderator temperature (density) coefficient is defined as the change in reactivity per degree change in the moderator temperature. Generally, the effects of the changes in moderator density and the temperature are considered together.

The soluble boron used in the reactor as a means of reactivity control also has an effect on the moderator density coefficient, since the soluble boron density and the water density are decreased when the coolant temperature rises. A decrease in the soluble boron density introduces a positive component in the moderator coefficient. If the concentration of soluble boron is large enough, the net value of the coefficient may be positive. However, with the BA rods and or IFBAs present, the beginning of life core hot boron concentration is sufficiently low that the moderator temperature coefficient is nonpositive at 100-percent power, less than or equal to +7.0 pcm/°F below 70-percent power, and less than a linearly decreasing limit of +7.0 pcm/°F to 0.0 pcm/°F between 70-percent and 100-percent power, respectively. The effect of control rods is to make the moderator coefficient more negative, since the thermal neutron mean free path, and hence the volume affected by the control rods, increase with an increase in temperature.

With burnup, the moderator coefficient becomes more negative, primarily as a result of boric acid dilution, but also to a significant extent from the effects of the depletion of uranium and buildup of fission products.

The moderator coefficient is calculated for a range of plant conditions by performing two-group two- or three-dimensional calculations, in which the moderator temperature is varied by about ±5°F about each of the mean temperatures and the density is changed consistent with the temperature. The moderator coefficient is shown as a function of core temperature and boron concentration for unrodded configurations of typical reload cores in figures 4.3-30 through 4.3-32. The temperature range covered is from cold (68°F) to about 600°F. The contribution due to Doppler coefficient (because of change in moderator temperature) has been subtracted from these results. Figure 4.3-33 shows the hot, full-power moderator temperature coefficient plotted as a function of lifetime for the critical boron concentration condition based on a typical reload boron letdown.

The moderator coefficients presented here are calculated on a corewide basis, since they are used to describe the core behavior in normal and accident situations when the moderator temperature changes can be considered to affect the entire core.

4.3.2.3.2.2 Moderator Pressure Coefficient. The moderator pressure coefficient relates the change in moderator density, resulting from a reactor coolant pressure change, to the corresponding effect on neutron production. This coefficient is of much less significance than the moderator temperature coefficient. A change of 50 psi in pressure has approximately the same effect on reactivity as a 1/2-degree change in moderator temperature. This coefficient can be determined from the moderator temperature coefficient by relating change in pressure to the corresponding change in density. The moderator pressure coefficient is negative over a portion of the moderator temperature range at BOL ≤(-0.004 pcm/psi, BOL) but is always positive at operating conditions and becomes more positive during life (+0.3 pcm/psi, EOL).

4.3.2.3.2.3 Moderator Void Coefficient. The moderator void coefficient relates the change in neutron multiplication to the presence of voids in the moderator. In a PWR, this coefficient is not very significant because of the low void content in the coolant. The core void content is less than one-half of 1 percent and is due to local or statistical boiling. The void coefficient varies

from 50 pcm/percent void at BOL and at low temperatures to -250 pcm/percent void at EOL and at operating temperatures. The void coefficient at operating temperature becomes more negative with fuel burnup.

4.3.2.3.3 Power Coefficient

The combined effect of moderator temperature and fuel temperature change as the core power level changes is called the total power coefficient and is expressed in terms of reactivity change per percent power change. A typical power coefficient at BOL and EOL conditions is given in figure 4.3-34.

The total power coefficient becomes more negative with burnup, reflecting the combined effect of moderator and fuel temperature coefficients with burnup. The power defect (integral reactivity effect) at BOL and EOL is given in figure 4.3-35.

4.3.2.3.4 Comparison of Calculated and Experimental Reactivity Coefficients

Subsection 4.3.3 describes the comparison of calculated and experimental reactivity coefficients in detail. Based on the data presented there, the accuracy of the current analytical model is:

- $\pm$0.2 percent $\Delta\rho$ for Doppler and power defect.
- $\pm$2.0 pcm/°F for the moderator coefficient.

Experimental evaluation of the reactivity coefficients is performed during the reload physics startup tests.

4.3.2.3.5 Reactivity Coefficients Used in Transient Analysis

Table 4.3-2 gives the limiting values as well as the best-estimate values for the reactivity coefficients for the initial cycle. The limiting values were used as design limits in the transient analysis. The exact values of the coefficient used in the analysis depend on whether the transient of interest is examined at the BOL or EOL, whether the most negative or the most positive (least negative) coefficients are appropriate, and whether spatial nonuniformity must be considered in the analysis. Conservative values of coefficients, considering various aspects of analysis, are used in the transient analysis. This is described in chapter 15.

The reactivity coefficients shown in figures 4.3-27 through 4.3-35 are typical best-estimate values calculated for a typical reload cycle. Limiting values are chosen to encompass the best-estimate reactivity coefficients, including the uncertainties given in paragraph 4.3.3.3 over appropriate operating conditions. The most positive, as well as the most negative, values are selected to form the design basis range used in the transient analysis. A direct comparison of the best-estimate and design limit values for the initial cycle shown in table 4.3-2 can be misleading, since in many instances the most conservative combination of reactivity coefficients was used in the transient analysis even though the extreme coefficients assumed may not simultaneously occur at the conditions assumed in the analysis. The need for a reevaluation of any accident in a subsequent cycle is contingent upon whether the coefficients for that cycle fall within the identified range used in the analysis presented in chapter 15 with due allowance for the calculational uncertainties given in paragraph 4.3.3.3. Control rod requirements are given in table 4.3-3 for the initial cycle and for a hypothetical equilibrium cycle, since these are markedly different.

4.3.2.4 Control Requirements

To ensure the shutdown margin required by the Technical Specifications or Technical Requirements Manual, as applicable, under conditions where a cooldown to ambient temperature is required, concentrated soluble boron is added to the coolant. Boron concentrations for several core conditions are listed in table 4.3-2 for the initial cycle. For all core conditions including refueling, the boron concentration is well below the solubility limit. The RCCAs are employed to bring the reactor to the shutdown condition. The minimum required shutdown margin is given in the Core Operating Limits Report.

The ability to accomplish the shutdown for hot conditions is demonstrated in table 4.3-3 by comparing the difference between the RCCA reactivity available with an allowance for the worst stuck rod with that required for control and protection purposes. The shutdown margin includes an allowance of 10 percent for analytic uncertainties (paragraph 4.3.2.4.9). The 10-percent uncertainty can be reduced to 7 percent with the use of Ag-In-Cd RCCAs. Use of a 7-percent uncertainty allowance on RCCA worth is discussed and shown to be acceptable in references 40 and 44. The largest reactivity control requirement appears at the EOL when the moderator temperature coefficient reaches its peak negative value as reflected in the larger power defect.

The control rods are required to provide sufficient reactivity to account for the power defect from full power to zero power and to provide the required shutdown margin. The reactivity addition resulting from power reduction consists of contributions from Doppler effect, moderator temperature, flux redistribution, and reduction in void content as discussed below.

4.3.2.4.1 Doppler Effect

The Doppler effect arises from the broadening of U-238 and Pu-240 resonance cross-sections with an increase in effective pellet temperature. This effect is most noticeable over the range of zero power to full power due to the large pellet temperature increase with power generation.

4.3.2.4.2 Variable Average Moderator Temperature

When the core is shut down to the hot zero-power condition, the average moderator temperature changes from the equilibrium full-load value determined by the steam generator and turbine characteristics (steam pressure, heat transfer, tube fouling, etc.) to the equilibrium no-load value, which is based on the steam generator shell side design pressure. The design change in temperature is conservatively increased by 6°F to account for the control dead band and measurement errors.

When the moderator coefficient is negative (except early in core life, when higher boron concentrations may result in a moderator temperature coefficient as high as +7.0 pcm/°F for powers below 70 percent and decreasing linearly to a value of 0.0 pcm/°F at 100-percent power), there is a reactivity addition with power reduction. The moderator coefficient becomes more negative as the fuel depletes because the boron concentration is reduced. This effect is the major contributor to the increased requirement at EOL.

4.3.2.4.3 Redistribution

During full-power operation, the coolant density decreases with core height, and this, together with partial insertion of control rods, results in less fuel depletion near the top of the core. Under

steady-state conditions, the relative power distribution will be slightly asymmetric toward the bottom of the core. On the other hand, at hot zero-power conditions, the coolant density is uniform up the core, and there is no flattening due to Doppler effect. The result will be a flux distribution which at zero power can be skewed toward the top of the core. The reactivity insertion due to the skewed distribution is calculated with an allowance for effects of xenon distribution.

4.3.2.4.4 Void Content

A small void content in the core is due to nucleate boiling at full power. The void collapse coincident with power reduction makes a small positive reactivity contribution.

4.3.2.4.5 Rod Insertion Allowance

At full power, the control bank is operated within a prescribed band of travel to compensate for small changes in boron concentration, changes in temperature, and very small changes in the xenon concentration not compensated for by a change in boron concentration. When the control bank reaches either limit of this bank, a change in boron concentration is required to compensate for additional reactivity changes. Since the insertion limit is set by a rod travel limit, a conservatively high calculation of the inserted worth is made, which exceeds the normally inserted reactivity.

4.3.2.4.6 Installed Excess Reactivity for Depletion

Excess reactivity of approximately 10 percent $\Delta\rho$ (hot) is installed at the beginning of each cycle to provide sufficient reactivity to compensate for fuel depletion and fission product buildup throughout the cycle. This reactivity is controlled by the addition of soluble boron to the coolant and by BA. The soluble boron concentration for several core configurations, the unit boron worth, and the BA worth are given in tables 4.3-1 and 4.3-2 for the initial cycle. Since the excess reactivity for burnup is controlled by soluble boron and/or BA, it is not included in control rod requirements.

4.3.2.4.7 Xenon and Samarium Poisoning

Changes in xenon and samarium concentrations in the core occur at a sufficiently slow rate, even following rapid power level changes, that the resulting reactivity change can be controlled by changing the soluble boron concentration. (Also see paragraph 4.3.2.4.16.)

4.3.2.4.8 pH Effects

Changes in reactivity due to a change in coolant pH, if any, are sufficiently small in magnitude and occur slowly enough to be controlled by the boron system.[11]

4.3.2.4.9 Experimental Confirmation

Following a normal shutdown, the total core reactivity change during cooldown with a stuck rod has been measured on a 121-assembly, 10-ft-high core and a 121-assembly, 12-ft-high core. In each case, the core was allowed to cool down until it reached criticality simulating the steam line break accident. For the 10-ft core, the total reactivity change associated with the cooldown is overpredicted by about 0.3-percent $\Delta\rho$ with respect to the measured result. This represents an error of about 5 percent in the total reactivity change and is about half the uncertainty allowance for this quantity. For the 12-ft core, the difference between the measured and predicted reactivity change is an even smaller 0.2-percent $\Delta\rho$. These measurements and others demonstrate the capability of the methods described in subsection 4.3.3.

4.3.2.4.10 Control

Core reactivity is controlled by means of a chemical poison dissolved in the coolant, RCCAs, and burnable absorbers as described below.

4.3.2.4.11 Chemical Shim

Boron in solution as boric acid is used to control relatively slow reactivity changes associated with:

A. The moderator temperature defect in going from cold shutdown at ambient temperature to the hot operating temperature at zero power.

B. The transient xenon and samarium poisoning, such as that following power changes or changes in rod cluster control position.

C. The reactivity effects of fissile inventory depletion and buildup of long-life fission products.

D. The depletion of the burnable absorbers.

The boron concentrations for various core conditions are presented in table 4.3-2 for the initial cycle.

4.3.2.4.12 Rod Cluster Control Assemblies

The number of RCCAs is shown in table 4.3-1. The RCCAs are used for shutdown and control purposes to offset fast reactivity changes associated with:

A. The required shutdown margin in the hot zero power, stuck rods condition.

B. The reactivity compensation as a result of an increase in power above hot zero power (power defect, including Doppler and moderator reactivity changes).

C. Unprogrammed fluctuations in boron concentration, coolant temperature, or xenon concentration (with rods not exceeding the allowable rod insertion limits).

D. Reactivity ramp rates resulting from load changes.

The allowed control bank reactivity insertion is limited at full power to maintain shutdown capability. As the power level is reduced, control rod reactivity requirements are also reduced, and more rod insertion is allowed. The control bank position is monitored, and the operator is

notified by an alarm if the limit is approached. The determination of the insertion limit uses conservative xenon distributions and axial power shapes. In addition, the RCCA withdrawal pattern determined from the analyses is used in determining power distribution factors and in determining the maximum worth of an inserted RCCA ejection accident. For further discussion, refer to the Technical Specifications on rod insertion limits.

Power distribution, rod ejection, and rod misalignment analyses are based on the arrangement of the shutdown and control groups of the RCCAs shown in figure 4.3-36. All shutdown RCCAs are withdrawn before withdrawal of the control banks is initiated.

In going from 0- to 100-percent power, control banks A, B, C, and D are withdrawn sequentially. The limits of rod insertion and further discussion on the basis for rod insertion limits are provided in the Technical Specifications.

4.3.2.4.13 Reactor Coolant Temperature

Reactor coolant (or moderator) temperature control has added flexibility in reactivity control of the Westinghouse pressurized water reactor. This feature takes advantage of the negative moderator temperature coefficient inherent in a PWR to:

- Maximize return to power capabilities.
- Provide ±5-percent power load regulation capabilities.
- Extend the time in cycle life to which daily load follow operations can be accomplished.

Reactor coolant temperature control supplements the dilution capability of the plant by lowering the reactor coolant temperature to supply positive reactivity through the negative moderator coefficient of the reactor. After the transient is over, the system returns the reactor coolant temperature to the programmed value.

Moderator temperature control of reactivity, like soluble boron control, has the advantage of not significantly affecting the core power distribution. However, unlike boron control, temperature control can be rapid enough to achieve reactor power change rates of 5 percent/min.

4.3.2.4.14 Burnable Absorbers

The discrete BA rods or integral fuel burnable absorbers may be used to provide partial control of the excess reactivity available during any fuel cycle. In doing so, these rods control peaking factors and prevent the moderator temperature coefficient from being positive at full power conditions, from exceeding +7.0 pcm/°F at power levels below 70-percent power, and from exceeding a limit which decreases linearly from 7.0 pcm/°F to 0.0 pcm/°F between 70-percent power and 100-percent power, respectively. They perform this function by reducing the requirement for soluble boron in the moderator at the beginning of the cycle, as described previously. For purposes of illustration, typical reload cycle burnable absorber patterns are shown in figure 4.3-5, and the arrangements within an assembly are displayed in figure 4.3-4. The boron in the rods is depleted with burnup but at a sufficiently slow rate so that the peaking factor limits are not exceeded and the resulting critical concentration of soluble boron is such that the moderator temperature coefficient remains within the limits stated above at all times for power operating conditions.

4.3.2.4.15 Peak Xenon Startup

Compensation for the peak xenon buildup may be accomplished using the boron control system. Startup from the peak xenon condition is accomplished with a combination of rod motion and boron dilution. The boron dilution may be made at any time, including during the shutdown period, provided the shutdown margin is maintained.

4.3.2.4.16 Load Follow Control and Xenon Control

During load follow maneuvers, power changes are accomplished using control rod motion and dilution or boration by the boron system as required. Control rod motion is limited by the control rod insertion limits on full-length rods, as provided in the Technical Specifications and Core Operating Limits Report and discussed in paragraph 4.3.2.4.12. The power distribution is maintained within acceptable limits through location of the full-length rod bank. Reactivity changes due to the changing xenon concentration can be controlled by rod motion and/or changes in the soluble boron concentration.

Late in cycle life, extended load follow capability is obtained by augmenting the limited boron dilution capability at low soluble boron concentrations by temporary moderator temperature reductions.

Rapid power increases (5 percent/min) from part power during load follow operation are accomplished with a combination of rod motion, moderator temperature reduction, and boron dilution. Compensation for the rapid power increase is accomplished initially by a combination of rod withdrawal and moderator temperature reduction. As the slower boron dilution takes effect after the initial rapid power increase, the moderator temperature is returned to the programmed value.

4.3.2.4.17 Burnup

Control of the excess reactivity for burnup is accomplished using soluble boron and/or burnable absorbers. The boron concentration must be limited during operating conditions to ensure that the moderator temperature coefficient is nonpositive at full power, less than or equal to +7.0 pcm/°F below 70-percent power, and less than or equal to a limit which varies linearly from +7.0 pcm/°F to 0.0 pcm/°F between 70-percent power and 100-percent power, respectively. Sufficient burnable absorbers are installed at the beginning of a cycle to give the desired cycle lifetime, and limit the boron concentration to assure achieving the moderator temperature coefficient limits discussed above. The practical minimum boron concentration is in the range of 0 to 10 ppm.

4.3.2.5 Control Rod Patterns and Reactivity Worths

The RCCAs are designated by function as the control groups and the shutdown groups. The terms "group" and "bank" are used synonymously throughout this report to describe a particular grouping of control assemblies. The RCCA pattern, which is not expected to change during the life of the plant, is displayed in figure 4.3-36. The control banks are labeled A, B, C, and D; and the shutdown banks are labeled SA, SB, SC, SD, and SE. Each bank, although operated and controlled as a unit, is composed of two subgroups. The axial position of the RCCAs may be controlled manually or automatically. The RCCAs are all dropped into the core following actuation of reactor trip signals.

Two criteria have been employed for selection of the control groups. First, the total reactivity worth must be adequate to meet the requirements specified in table 4.3-3. Second, in view of the fact that these rods may be partially inserted at power operation, the total power peaking factor should be low enough to ensure that the power capability requirements are met.

Analyses indicate that the first requirement can be met either by a single group or by two or more banks whose total worth equals at least the required amount. The axial power shape would be more peaked following movement of a single group of rods worth 3- to 4-percent $\Delta\rho$ Therefore, four banks (designated A, B, C, and D in figure 4.3-36), each worth approximately 1 percent $\Delta\rho$, have been selected. Typical control bank worths for the initial cycle are shown in table 4.3-2.

The position of control banks for criticality under any reactor condition is determined by the concentration of boron in the coolant. On an approach to criticality, boron is adjusted to ensure that criticality will be achieved with control rods above the insertion limits and other considerations. (See the Technical Specifications and the Core Operating Limits Report.) Early in the cycle, there may also be a withdrawal limit at low power to maintain the moderator temperature coefficient that is less than or equal to the limit value for that power level.

Ejected rod worths for several different conditions are given in subsection 15.4.8.

Allowable deviations due to misaligned control rods are discussed in the Technical Specifications.

A representative differential rod worth calculation for two banks of control rods withdrawn simultaneously (rod withdrawal accident) is given in figure 4.3-37.

Calculation of control rod reactivity worth versus time following reactor trip involves both control rod velocity and differential reactivity worth. The rod position versus time of travel after rod release assumed is given in figure 4.3-38. For nuclear design purposes, the reactivity worth versus rod position is calculated by a series of steady-state calculations at various control positions, assuming all rods out of the core as the initial position in order to minimize the initial reactivity insertion rate. Also, to be conservative, the rod of highest worth is assumed stuck out of the core, and the flux distribution (and thus reactivity importance) is assumed to be skewed to the bottom of the core. The result of these calculations is shown in figure 4.3-39.

The shutdown groups provide additional negative reactivity to ensure an adequate shutdown margin. Shutdown margin is defined as the amount by which the core would be subcritical at hot shutdown if all RCCAs were tripped, but assuming that the highest worth assembly remained fully withdrawn and no changes in xenon or boron took place. The loss of control rod worth due to the depletion of the absorber material is negligible, since only bank D may be in the core under normal operating conditions (near full power).

The values given in table 4.3-3 show that the available reactivity in withdrawn RCCAs provides the design bases minimum shutdown margin, allowing for the highest worth cluster to be at its fully withdrawn position. An allowance for the uncertainty in the calculated worth of N-1 rods is made before determination of the shutdown margin.

4.3.2.6 Criticality of the Reactor During Refueling

The basis for maintaining the reactor subcritical during refueling is presented in paragraph 4.3.1.5, and a discussion of how control requirements are met is given in paragraphs 4.3.2.4 and 4.3.2.5.

4.3.2.6.1 Fuel Storage Criticality

The following information describes the design criteria and analysis techniques for storage of fuel in the spent fuel racks. The Unit 1 and Unit 2 spent fuel racks were analyzed in accordance with the methodology contained in reference 42 which credits the soluble boron contained in the spent fuel pool water. The analyses have been reviewed by the NRC and documented in their safety evaluation for Technical Specification Amendments 139 and 118 for Unit 1 and Unit 2, respectively (reference 43).

4.3.2.6.1.1 Storage of Fuel Assemblies. - The fuel storage pools contain high-density fuel storage racks which are designed to store Westinghouse 17x17 fuel assemblies with a maximum enrichment of up to 5.0 wt% U-235.

One factor which prevents criticality of fuel assemblies in a fuel storage rack is the design of the rack which limits fuel assembly interaction by fixing the minimum separation between fuel assemblies. Other factors include limits on the enrichment, burnup, fixed absorbers, burnable absorbers, decay time, soluble boron, and placement of assemblies within the fuel storage racks.

The design basis for preventing criticality outside the reactor is that, including uncertainties, there is a 95-percent probability at a 95-percent confidence level (95/95) that the effective neutron multiplication factor, K_{eff}, of the fuel rack array will be less than or equal to 0.95.

The spent fuel racks have been analyzed such that K_{eff} remains less than 1.0 including uncertainties and tolerances on a 95/95 basis without the presence of any soluble boron in the storage pool (No Soluble Boron 95/95 Conditions) as defined in reference 42. Soluble boron credit is used to provide safety margin by maintaining $K_{eff} \leq 0.95$ including uncertainties, tolerances, and accident conditions in the presence of spent fuel pool soluble boron. The amount of soluble boron required for the allowable storage conditions excluding accidents is 511 ppm (Unit 1), 394 ppm (Unit 2). The presence of Boral panels in the Unit 1 spent fuel racks is credited in the Unit 1 criticality analyses. The presence of any Boraflex panels in the Unit 2 spent fuel racks is ignored. The criticality analyses include a calculational bias, mechanical uncertainties, and consideration of 0.05 wt% enrichment variability.

The analysis methodology employs: (1) SCALE-PC, a personal computer version of the SCALE-4.3 code system, with the updated SCALE-4.3 version of the 44 group ENDF/B-V neutron cross section library, and (2) the two-dimensional integral transport code DIT with an ENDF/B-VI neutron cross section library.

SCALE-PC was used for calculations involving infinite arrays for the “2-out-of-4”, “3-out-of-4”, “All-Cell,” and “3x3” fuel assembly storage configurations. In addition, it was employed in a full pool representation of the storage racks to evaluate soluble boron worth and postulated accidents.

SCALE-PC, used in both the benchmarking and the fuel assembly storage configurations, includes the control module CSAS25 and the following functional modules: BONAMI, NITAWL-II, and KENO V.a.

The DIT code is used for simulation of in-reactor fuel assembly depletion. KENO V.a was used in the calculation of biases and uncertainties.

Models were made for each storage configuration as well as for the entire pools. Each configuration was modeled as an infinitely repeating pattern in the X-Y plane. A water reflector

was modeled above and below the spent fuel storage cells to account for axial reactivity effects. The KENO model for the entire pool modeled each individual storage rack module.

KENO was used to calculate K_{eff} for the various storage configurations considered as well as for the entire pool. For demonstrating that K_{eff} remains below unity for zero soluble boron, SNC chose to apply an acceptance criterion of 0.995. For the storage configurations considered, the target value of K_{eff} for these calculations was selected to be less than 0.995 by an amount sufficient to cover the magnitude of the analytical biases and uncertainties. KENO was also used to determine burnup and IFBA versus enrichment requirements to meet the target K_{eff} for configurations that credit burnup or IFBA.

Calculations were performed for the entire pool with various fuel storage configurations to demonstrate that the K_{eff} for the entire pool remains below 0.995 with zero soluble boron. KENO was used to determine the soluble boron requirements for nonaccident and accident conditions to ensure that K_{eff} remains less than or equal to 0.95.

The details of the modeling and analyses are described in reference 42.

For the analyses described in reference 43, three Westinghouse fuel assembly designs were considered: 17x17 STANDARD (STD), 17x17 Optimized Fuel Assembly (OFA), and the 17x17 Robust Fuel Assembly (RFA). The most reactive design for each storage configuration was used to bound the other fuel designs for both fresh and depleted fuel.

The spent fuel racks have been analyzed to allow storage of Westinghouse 17x17 fuel assemblies with nominal initial enrichments up to 5.00 wt% U-235 in storage cell locations using credit for checkerboard configurations, burnup credit, and integral fuel burnable absorber (IFBA) credit. Although the analysis covers nominal initial enrichments up to 5.0 wt% U-235, the Technical Specifications allows only 5.0 wt% U-235 maximum. The presence of Boral panels in the Unit 1 spent fuel racks is credited in the Unit 1 criticality analyses. This analysis does not take any credit for the presence of the spent fuel rack Boraflex poison panels in the Unit 2 spent fuel racks. The following storage configurations and enrichment limits resulted from this analysis:

Unit 1

New or partially spent fuel assemblies with a combination of burnup and initial nominal enrichment in the “acceptable burnup domain” of figures 4.3-46 or satisfying a minimum IFBA requirement as shown in figure 4.3-54 may be allowed unrestricted storage in the Unit 1 fuel storage pool.

New or partially spent fuel assemblies with a maximum initial enrichment of 5.0 weight percent U-235 may be stored in the Unit 1 fuel storage pool in a 3-out-of-4 checkerboard storage configuration as shown in figure 4.3-48.

Interfaces between storage configurations in the Unit 1 fuel storage pool shall be in compliance with figure 4.3-50. “A” assemblies are new or partially spent fuel assemblies with a combination of burnup and initial nominal enrichment in the “acceptable burnup domain” of figure 4.3-46, or which satisfy a minimum IFBA requirement as shown in figure 4.3-54. “B” assemblies are assemblies with initial enrichments up to a maximum of 5.0 weight percent U-235.

Unit 2

New or partially spent fuel assemblies with a combination of burnup and initial nominal enrichment in the “acceptable burnup domain” of figure 4.3-47 may be allowed unrestricted storage in the Unit 2 fuel storage pool.

New or partially spent fuel assemblies with a combination of burnup and initial nominal enrichment in the “acceptable burnup domain” of figure 4.3-55 may be stored in the Unit 2 fuel storage pool in a 3-out-of-4 checkerboard storage configuration as shown in figure 4.3-48.

New or partially spent fuel assemblies with a maximum initial enrichment of 5.0 weight percent U-235 may be stored in the Unit 2 fuel storage pool in a 2-out-of-4 checkerboard storage configuration as shown in figure 4.3-48.

New or partially spent fuel assemblies with a combination of burnup, decay time, and initial nominal enrichment in the “acceptable burnup domain” of figure 4.3-57 may be stored in the Unit 2 fuel storage pool as “low enrichment” fuel assemblies in the 3x3 checkerboard storage configuration as shown in figure 4.3-49. New or partially spent fuel assemblies with initial nominal enrichments less than or equal to 3.20 weight percent U-235 or which satisfy a minimum IFBA requirement as shown in figure 4.3-56 for higher initial enrichments may be stored in the Unit 2 fuel storage pool as “high enrichment” fuel assemblies in the 3x3 checkerboard storage configuration as shown in figure 4.3-49.

Interfaces between storage configurations in the Unit 2 fuel storage pool shall be in compliance with figures 4.3-50, 4.3-51, 4.3-52, and 4.3-53. “A” assemblies are new or partially spent fuel assemblies with a combination of burnup and initial nominal enrichment in the “acceptable burnup domain” of figure 4.3-47. “B” assemblies are new or partially spent fuel assemblies with a combination of burnup and initial nominal enrichment in the “acceptable burnup domain” of figure 4.3-55. “C” assemblies are assemblies with initial enrichments up to a maximum of 5.0 weight percent U-235. “L” assemblies are new or partially spent fuel assemblies with a combination of burnup, decay time, and initial nominal enrichment in the “acceptable burnup domain” of figure 4.3-57. “H” assemblies are new or partially spent fuel assemblies with initial nominal enrichments less than or equal to 3.20 weight percent U-235 or which satisfy a minimum IFBA requirement as shown in figure 4.3-56 for higher initial enrichments.

The analytical methods conform with ANSI N18.2-1973, "Nuclear Safety Criteria for the Design of Stationary Pressurized Water Reactor Plants," Section 5.7, Fuel Handling System; ANSI 57.2-1983, "Design Objectives for Light Water Reactor Spent Fuel Storage Facilities at Nuclear Power Stations," Section 6.4.2; ANSI N16.9-1975, "Validation of Calculational Methods for Nuclear Criticality Safety"; and the NRC Standard Review Plan, Section 9.1.2, "Spent Fuel Storage."

4.3.2.6.1.2 Credit for Soluble Boron - Reference 42 describes how credit for fuel storage pool soluble boron is used under normal storage configuration conditions. The storage configuration is defined using K_{eff} calculations to ensure that the K_{eff} will be less than 1.0 with no soluble boron under normal storage conditions including tolerances and uncertainties. Soluble boron credit is then used to maintain K_{eff} less than or equal to 0.95. The analyses assumed 19.9% of the boron atoms have atomic weight 10 (B-10). However, to account for the effects of variations in the natural abundance of B-10, the calculated boron concentrations, as well as the concentrations for accidents, were adjusted to correspond to a B-10 fraction of 19.7%. The Unit 1 pool requires 511 ppm and the Unit 2 pool requires 394 ppm to maintain K_{eff} less than or equal to 0.95 for all allowed combinations of storage configurations, enrichments, and burnups.

The soluble boron concentration required to maintain K_{eff} less than or equal to 0.95 under accident conditions is determined by first surveying all possible events which increase the K_{eff} value of the spent fuel pool. The accident event which produced the largest increase in spent fuel pool K_{eff} value is employed to determine the required soluble boron concentration necessary to mitigate this and all less severe accident events. The list of accident cases considered includes:

- Dropped fresh fuel assembly on top of the storage racks,
- Misloaded fresh fuel assembly into an incorrect storage rack location,
- Misloaded fresh fuel assembly outside of the storage racks,
- Reduction in rack module-to-module water gap due to seismic event,
- Spent fuel pool temperature outside the normal range of 50 °F to 185 °F.

From a criticality standpoint, a dropped assembly accident occurs when a fuel assembly in its most reactive condition is dropped onto the storage racks. The rack structure from a criticality standpoint is not excessively deformed. Previous accident analysis with unborated water showed that the dropped assembly which comes to rest horizontally on top of the rack has sufficient water separating it from the active fuel height of stored assemblies to preclude neutronic interaction. For the borated water condition, the interaction is even less since the water contains boron, an additional thermal neutron absorber.

Several fuel mishandling events were simulated with KENO V.a to assess the possible increase in the K_{eff} value of the spent fuel pools. The fuel mishandling events all assumed that a fresh Westinghouse OFA fuel assembly enriched to 5.0 weight percent U-235 (and no burnable poisons) was misloaded into the described area of the spent fuel pool. These cases were simulated with the KENO V.a model for the entire spent fuel pool.

For Unit 1, the fuel mishandling event which produced the largest increase in spent fuel pool K_{eff} value is the misloading of a fresh fuel assembly between a 3-out-of-4 fuel assembly storage configuration and the pool wall. The additional soluble boron concentration necessary to mitigate this and all less severe accident events is 340 ppm.

For Unit 2, the fuel mishandling event which produced the largest increase in spent fuel pool K_{eff} value is the misloading of a fresh fuel assembly in an incorrect storage rack location for the 2-out-of-4 configuration. The additional soluble boron concentration necessary to mitigate this and all less severe accident events is 704 ppm.

For the accident due to a seismic event, the gap between rack modules was reduced to zero. For both Units 1 and 2, the reactivity increase is an order of magnitude less than that for the fuel mishandling events.

An increase in the temperature of the water passing through the stored fuel assemblies causes a decrease in water density which results in an addition of negative reactivity for flux trap design racks such as the Unit 1 racks. However, since Boraflex is not considered to be present for the Unit 2 racks and the fuel storage pool water has a high concentration of boron, a density decrease causes a positive reactivity addition. The reactivity effects of a temperature range from 32° F to 240° F were evaluated. This bounds the temperature range assumed in the criticality analyses (50° F to 185° F). The increase in reactivity due to the decrease in temperature below 50° F is bounded by the misplacement of a fuel assembly between the rack and pool walls for the Unit 1 racks. The increase in reactivity due to the increase in temperature is bounded by the misload accident for the Unit 2 racks.

Including the effects of accidents, the maximum required boron concentration to maintain $K_{eff} \leq 0.95$ is 851 ppm for Unit 1 and 1098 ppm for Unit 2, which is well below the minimum Technical Specification limit of 2000 ppm.

The results of all analyses including accidents verify that there is a 95-percent probability at a 95-percent confidence level (including uncertainties) that K_{eff} of the spent fuel storage racks will be less than 0.95 when flooded with water borated to a concentration of 851 ppm for Unit 1 and

1098 ppm for Unit 2. Normal nominal boron concentration in the fuel storage pool is about 2400 ppm which is greater than that used in the evaluation of pool dilution.

A spent fuel pool boron dilution evaluation was performed to determine the volume necessary to dilute the spent fuel pool from 2000 ppm to 600 ppm (the boron concentration required to maintain $K_{eff} \leq 0.95$ in the absence of an unrelated accident). The boron dilution evaluation determined that approximately 465,000 gal of water would be required to dilute the spent fuel pool from 2000 ppm to 600 ppm. A dilution event that would result in this large volume of water would require the transfer of a large quantity of water from the dilution source and significant increase in the spent fuel pool level, which would ultimately overflow the pool. This large volume of water would be readily detected and terminated by plant personnel. A spent fuel pool dilution event of this magnitude is not a credible event.

4.3.2.6.2 Rod Storage Canister

The fuel rod storage canister (FRSC) must be treated as if it were an assembly with enrichment and burnup of the rod in the canister with the most limiting combination of enrichment and burnup. Storage of the FRSC is based upon meeting the requirements for each of the allowable storage configurations.

4.3.2.7 Stability

4.3.2.7.1 Introduction

The stability of the PWR cores against xenon-induced spatial oscillations and the control of such transients are discussed extensively in references 6, 18, 19, and 20. A summary of these reports is given in the following discussion, and the design bases are given in paragraph 4.3.1.6.

In a large reactor core, xenon-induced oscillations can take place with no corresponding change in the total power of the core. The oscillation may be caused by a power shift in the core which occurs rapidly by comparison with the xenon-iodine time constants. Such a power shift occurs in the axial direction when a plant load change is made by control rod motion and results in a change in the moderator density and fuel temperature distributions. Such a power shift could occur in the diametral plane of the core as a result of abnormal control action.

Due to the negative power coefficient of reactivity, PWR cores are inherently stable to oscillations in total power. Protection against total power instabilities is provided by the control and protection system, as described in section 7.7. Hence, the discussion on the core stability will be limited here to xenon-induced spatial oscillations.

4.3.2.7.2 Stability Index

Power distributions, either in the axial direction or in the X-Y plane, can undergo oscillations due to perturbations introduced in the equilibrium distributions without changing the total core power. The overtones in the current PWRs and the stability of the core against xenon-induced oscillations can be determined in terms of the eigenvalues of the first flux overtones. Writing the eigenvalue ξ of the first flux harmonic as:

$$\xi = b = ic \quad (1)$$

Then b is defined as the stability index and T = $2\pi/c$ as the oscillation period of the first harmonic. The time dependence of the first harmonic $\delta\phi$ in the power distribution can now be represented as:

$$\delta\phi(t) = A\, e^{\xi t} = ae^{bt}\cos ct \quad (2)$$

where A and a are constants. The stability index can also be obtained approximately by:

$$b = \frac{1}{T} \ln \frac{A_{n+1}}{A_n}$$

where A_n and A_{n+1} are the successive peak amplitudes of the oscillation and T is the time period between the successive peaks.

4.3.2.7.3 Prediction of the Core Stability

The stability of the core described herein (i.e., with 17 x 17 fuel assemblies) against xenon-induced spatial oscillations is expected to be equal to or better than that of earlier designs for cores of similar size. The prediction is based on a comparison of the parameters which are significant in determining the stability of the core against the xenon-induced oscillations, namely:

A. The overall core size is unchanged and spatial power distributions will be similar.

B. The moderator temperature coefficient is expected to be similar or slightly more negative.

C. The Doppler coefficient of reactivity is expected to be equal or slightly more negative at full power.

Analysis of both the axial and X-Y xenon transient tests, discussed in paragraph 4.3.2.7.5, shows that the calculational model is adequate for the prediction of core stability.

4.3.2.7.4 Stability Measurements

4.3.2.7.4.1 Axial Measurements. Two axial xenon transient tests conducted in a PWR with a core height of 12 ft and 121 fuel assemblies are reported in reference 21 and will be briefly discussed here. The tests were performed at approximately 10 percent and 50 percent of cycle life.

Both a free-running oscillation test and a controlled test were performed during the first test. The second test at midcycle consisted of a free-running oscillation test only. In each of the free-running oscillation tests, a perturbation was introduced to the equilibrium power distribution through an impulse motion of the control bank D and the subsequent oscillation period was monitored. In the controlled test conducted early in the cycle, the part-length rods were used to follow the oscillations to maintain an axial offset within the prescribed limits. The axial offset of power was obtained from the excore ion chamber readings (which had been calibrated against the incore flux maps) as a function of time for both free-running tests, as shown in figure 4.3-40.

The total core power was maintained constant during these spatial xenon tests, and the stability index and the oscillation period were obtained from a least-square fit of the axial offset data in

the form of equation 2. The axial offset of power is the quantity that properly represents the axial stability in the sense that it essentially eliminates any contribution from even-order harmonics, including the fundamental mode. The conclusions of the tests are:

A. The core was stable against induced axial xenon transients, at the core average burnups of both 1550 MWd/tonne uranium and 7700 MWd/tonne uranium. The measured stability indices are -0.041 h^{-1} for the first test (curve 1 of figure 4.3-40) and -0.014 h^{-1} for the second test (curve 2 of figure 4.3-40). The corresponding oscillation periods are 32.4 and 27.2 h, respectively.

B. The reactor core becomes less stable as fuel burnup progresses, and the axial stability index is essentially zero at 12,000 MWd/tonne uranium. However, the movable control rod systems can control axial oscillations, as described in paragraph 4.3.2.7.6.1.

4.3.2.7.4.2 Measurements in the X-Y Plane. Two X-Y xenon oscillation tests were performed at a PWR plant with a core height of 12 ft and 157 fuel assemblies. The first test was conducted at a core average burnup of 1540 MWd/tonne uranium and the second at a core average burnup of 12,900 MWd/tonne uranium. Both of the X-Y xenon tests show that the core was stable in the X-Y plane at both burnups. The second test shows that the core became more stable as the fuel burnup increased, and all Westinghouse PWRs with 121 and 157 assemblies are expected to be stable throughout their burnup cycles. The results of these tests are applicable to the 193-assembly VEGP core as discussed in paragraph 4.3.2.7.3.

In each of the two X-Y tests, a perturbation was introduced to the equilibrium power distribution through an impulse motion of one rod cluster control unit located along the diagonal axis. Following the perturbation, the uncontrolled oscillation was monitored, using the movable detector and thermocouple system and the excore power range detectors. The quadrant tilt difference (QTD) is the quantity that properly represents the diametral oscillation in the X-Y plane of the reactor core in that the differences of the quadrant average powers over two symmetrically opposite quadrants essentially eliminates the contribution to the oscillation from the azimuthal mode. The QTD data were fitted in the form of equation 2 through a least-square method. A stability index of -0.076 h^{-1} with a period of 29.6 h was obtained from the thermocouple data shown in figure 4.3-41.

It was observed in the second X-Y xenon test that the PWR core with 157 fuel assemblies had become more stable due to an increased fuel depletion, and the stability index was not determined.

4.3.2.7.5 Comparison of Calculations with Measurements

The analysis of the axial xenon transient tests was performed in an axial slab geometry, using a flux synthesis technique. The direct simulation of the axial offset data was carried out using the PANDA code.[22] The analysis of the X-Y xenon transient tests was performed in an X-Y geometry, using a modified TURTLE code.[10] Both the PANDA and TURTLE codes solve the two-group, time-dependent neutron diffusion equation with time-dependent xenon and iodine concentrations. The fuel temperature and moderator density feedback is limited to a steady-state model. All the X-Y calculations were performed in an average enthalpy plane.

The basic nuclear cross-sections used in this study were generated from a unit cell depletion program which has evolved from the codes LEOPARD[23] and CINDER.[24] The detailed experimental data during the tests, including the reactor power level, the enthalpy rise, and the

impulse motion of the control rod assembly, as well as the plant follow burnup data, were closely simulated in the study.

The results of the stability calculation for the axial tests are compared with the experimental data in table 4.3-5. The calculations show conservative results for both of the axial tests with a margin of approximately -0.01 h^{-1} in the stability index.

An analytical simulation of the first X-Y xenon oscillation test shows a calculated stability index of -0.081 h^{-1}, in close agreement with the measured value of -0.076 h^{-1}. As indicated earlier, the second X-Y xenon test showed that the core had become more stable compared to the first test, and no evaluation of the stability index was attempted. This increase in the core stability in the X-Y plane due to increased fuel burnup is due mainly to the increased magnitude of the negative moderator temperature coefficient.

Previous studies of the physics of xenon oscillations, including three-dimensional analysis, are reported in a series of topical reports.[18][19][20] A more detailed description of the experimental results and analysis of the axial and X-Y xenon transient tests is presented in reference 21 and section 1 of reference 25.

4.3.2.7.6 Stability Control and Protection

The excore detector system is utilized to provide indications of xenon-induced spatial oscillations. The readings from the excore detectors are available to the operator and also form part of the protection system.

4.3.2.7.6.1 Axial Power Distribution. For maintenance of proper axial power distributions, the operator is instructed to maintain an axial offset within a prescribed operating band, based on the excore detector readings. Should the axial offset be permitted to move far enough outside this band, the protection limit will be reached, and the power will be manually reduced.

As fuel burnup progresses, 12-ft PWR cores become less stable to axial xenon oscillations. However, free xenon oscillations are not allowed to occur, except for special tests. The full-length control rod banks are sufficient to dampen and control any axial xenon oscillations present. Should the axial offset be inadvertently permitted to move far enough outside the allowed band due to an axial xenon oscillation or for any other reason, the protection limit on axial offset will be reached and the power will be manually reduced.

4.3.2.7.6.2 Radial Power Distribution. The core described herein is calculated to be stable against X-Y xenon-induced oscillations at all times in life.

The X-Y stability of large PWRs has been further verified as part of the startup physics test program for PWR cores with 193 fuel assemblies. The measured X-Y stability of the cores with 157 and 193 assemblies was in close agreement with the calculated stability, as discussed in paragraphs 4.3.2.7.4 and 4.3.2.7.5. In the unlikely event that X-Y oscillations occur, backup actions are possible and would be implemented, if necessary, to increase the natural stability of the core. This is based on the fact that several actions could be taken to reduce the moderator temperature coefficient, which would increase the stability of the core in the X-Y plane.

Provisions for protection against nonsymmetric perturbations in the X-Y power distribution that could result from equipment malfunctions are made in the protection system design. This includes control rod drop, rod misalignment, and asymmetric loss of coolant flow.

A more detailed discussion of the power distribution control in PWR cores is presented in references 6 and 7.

4.3.2.8 Vessel Irradiation

A brief review of the methods and analyses used in the determination of neutron and gamma ray flux attenuation between the core and the pressure vessel is given below. A more complete discussion on the pressure vessel irradiation and surveillance program is given in section 5.3.

The materials that serve to attenuate neutrons originating in the core and gamma rays from both the core and structural components consist of the core baffle, core barrel, neutron panels, and associated water annuli, all of which are within the region between the core and the pressure vessel.

In general, few group neutron diffusion theory codes are used to determine fission power density distributions within the active core, and the accuracy of these analyses is verified by incore measurements on operating reactors. Region and rodwise power-sharing information from the core calculations is then used as source information in two-dimensional S_N transport calculations which compute the flux distributions throughout the reactor.

The neutron flux distribution and spectrum in the various structural components vary significantly from the core to the pressure vessel. Representative values of the neutron flux distribution and spectrum are presented in table 4.3-6. The values listed are based on time-averaged equilibrium cycle reactor core parameters and power distributions and thus are suitable for long-term neutron velocity time projections and for correlation with radiation damage estimates.

As discussed in section 5.3, the irradiation surveillance program utilizes actual test samples to verify the accuracy of the calculated fluxes at the vessel.

4.3.3 ANALYTICAL METHODS

Calculations required in nuclear design consist of three distinct types, which are performed in sequence:

- Determination of effective fuel temperatures.
- Generation of microscopic few-group parameters.
- Space-dependent, few-group diffusion calculations.

These calculations are carried out by computer codes which can be executed individually. However, at Westinghouse most of the codes required have been linked to form an automated design sequence which minimizes design time, avoids errors in transcription of data, and standardizes the design methods.

4.3.3.1 Fuel Temperature (Doppler) Calculations

Temperatures vary radially within the fuel rod, depending on the heat generation rate in the pellet; the conductivity of the materials in the pellet, gap, and clad; and the temperature of the coolant.

The fuel temperatures for use in most nuclear design Doppler calculations are obtained from a simplified version of the Westinghouse fuel rod design model described in paragraph 4.2.1.3,

which considers the effect of radial variation of pellet conductivity, expansion coefficient and heat generation rate, elastic deflection of the clad, and a gap conductance which depends on the initial fill gas, the hot open gap dimension, and the fraction of the pellet over which the gap is closed. The fraction of the gap assumed closed represents an empirical adjustment used to produce close agreement with observed reactivity data at BOL. Further gap closure occurs with burnup and accounts for the decrease in Doppler defect with burnup which has been observed in operating plants.

Radial power distributions in the pellet as a function of burnup are obtained from LASER[26] calculations.

The effective U-238 temperature for resonance absorption is obtained from the radial temperature distribution by applying a radially dependent weighting function. The weighting function was determined from REPAD[27] Monte Carlo calculations of resonance escape probabilities in several steady-state and transient temperature distributions. In each case, a flat pellet temperature was determined which produced the same resonance escape probability as the actual distribution. The weighting function was empirically determined from these results.

The effective Pu-240 temperature for resonance absorption is determined by a convolution of the radial distribution of Pu-240 densities from LASER burnup calculations and the radial weighting function. The resulting temperature is burnup dependent, but the difference between U-238 and Pu-240 temperatures, in terms of reactivity effects, is small.

The effective pellet temperature for pellet dimensional change is that value which produces the same outer pellet radius in a virgin pellet as that obtained from the temperature model. The effective clad temperature for dimensional change is its average value.

The temperature calculational model has been validated by plant Doppler defect data, as shown in table 4.3-7, and Doppler coefficient data, as shown in figure 4.3-42. Stability index measurements also provide a sensitive measure of the Doppler coefficient near full power (paragraph 4.3.2.7). It can be seen that Doppler defect data is typically within 0.2 percent $\Delta\rho$ of prediction.

4.3.3.2 Macroscopic Group Constants

There are two lattice codes which have been used for the generation of macroscopic group constants needed in the spatial, few-group diffusion codes. One is PHOENIX-P which has historically been the sources of the macroscopic group constants. The other is PARAGON, which will be used in forthcoming reload designs. Following is a detailed description of each.

PHOENIX-P has been approved by the NRC as a lattice code for the generation of macroscopic and microscopic few-group cross-sections for PWR analysis (reference 37). PHOENIX-P is a two-dimensional, multigroup, transport-based lattice code capable of providing all necessary data for PWR analysis. Since it is a dimensional lattice code, PHOENIX-P does not rely on predetermined spatial/spectral interaction assumptions for the heterogeneous fuel lattice and can provide a more accurate multigroup flux solution.

The solution for the detailed spatial flux and energy distribution is divided into two major steps in PHOENIX-P (reference 37). First, a two-dimensional fine energy group nodal solution is obtained, coupling individual sub-cell regions (pellet, clad, and moderator) as well as surrounding pins, using a method based on Carivik's collision probability approach and heterogeneous response fluxes which preserve the heterogeneity of the pin cells and their surroundings. The nodal solution provides an accurate and detailed local flux distribution, which is then used to homogenize the pin cells spatially to fewer groups. Then, a standard S4

discrete ordinates calculation solves for the angular distribution, based on the group-collapsed and homogenized cross-sections from the first step. These S4 fluxes normalize the detailed spatial and energy nodal fluxes, which are then used to compute reaction rates and power distributions and to deplete the fuel and burnable absorbers. A standard B1 calculation evaluates the fundamental mode critical spectrum, providing an improved fast diffusion coefficient for the core spatial codes.

PHOENIX-P employs a 70 energy group library derived from the ENDF/B-6 basic data. This library was designed to capture the integral properties of the multigroup data properly during group collapse and to model important resonance parameters properly. It contains all neutronics data necessary for modeling fuel, fission products, cladding and structural materials, coolant, and control and burnable absorber materials present in PWRs. Group constants for burnable absorber cells, control rod cells, guide thimbles and instrumentation thimbles, or other nonfuel cells, can be obtained directly from PHOENIX-P without adjustments such as those required in the cell or 1D lattice codes.

Paragon has been approved by the NRC as the new generation of Westinghouse lattice code (reference 47). PARAGON is a replacement for PHOENIX-P and its primary use will be to provide the same types of input data that PHOENIX-P generates for use in three-dimensional core simulator codes. This includes macroscopic cross-sections, microscopic cross-sections, pin factors for pin-power reconstruction calculations, discontinuity factors for a nodal method solution, and other data needed for safety analysis or other downstream applications.

PARAGON is based on collision probability-interface current cell coupling methods. PARAGON provides flexibility in modeling that was not available in PHOENIX-P including exact cell geometry representation instead of cylinderization, multiple rings and regions within the fuel pin and the moderator cell geometry, and variable cell pitch. The solution method permits flexibility in choosing the quality of the calculation through both increasing the number of regions modeled within the cell and the number of angular current directions tracked at the cell interfaces.

The calculation scheme in PARAGON is based on the conventional lattice modules: resonance calculation, flux solution, leakage correction, and depletion. The detailed theory of these modules is described in reference 47. The cross-section resonance calculation module is based on the space-dependent Dancoff method (reference 47); it is a generalization of the PHOENIX-P methodology that permits to subdivide the fuel pin into many rings and, therefore, generates space-dependent self-shielded isotopic cross-sections. The flux solution module uses the interface current collision probability method and permits a detailed representation of the fuel cells (reference 47). The other two modules (leakage and depletion) are similar to the ones used in PHOENIX-P.

The current PARAGON cross-section library is a 70-group library, based on the ENDF/B basic nuclear data, with the same group structure as the library currently used with PHOENIX-P. The PARAGON qualification library has been improved through the addition of more explicit fission products and fission product chains (reference 47). PARAGON is, however, designed to employ any number of energy groups.

The new NEXUS cross-section generation system uses PARAGON as the lattice code (reference 48).

4.3.3.3 Spatial Few-Group Diffusion Calculations

Spatial few-group diffusion calculations are performed using 3D ANC (reference 36). A two-group, two- and three-dimensional nodal code will be used for dimensional modeling of the

core. The three-dimensional nature of this code provides both radial and axial power distributions. For some applications, the updated version of the PANDA will continue to be used for axial calculations, and a two-dimensional collapse of 3D ANC that properly accounts for the three-dimensional features of the fuel will be used for X-Y calculations.

Nodal calculations (four radial mesh per assembly) are carried out to determine the critical boron concentrations and power distributions. The moderator coefficient is evaluated by varying the inlet temperature in the same kind of calculations as those used for power distribution and reactivity predictions.

Validation of the reactivity calculations is associated with the validation of the group constants themselves, as discussed in paragraph 4.3.3.2. Validation of the Doppler calculations is associated with the fuel temperature validation discussed in paragraph 4.3.3.1. Validation of the moderator coefficient calculations is obtained by comparison with plant measurements at HZP conditions, as shown in table 4.3-11.

Axial calculations are used to determine differential control rod worth curves (reactivity versus rod insertion) and axial power shapes during steady-state and transient xenon conditions (flyspeck curve). Group constants are obtained from the three-dimensional nodal model by flux-volume weighting on an axial slicewise basis. Radial bucklings are determined by varying parameters in the buckling model while forcing the one-dimensional model to reproduce the axial characteristics (axial offset, midplane power) of the three-dimensional model.

Validation of the spatial codes for calculating power distributions involves the use of incore and excore detectors and is discussed in paragraph 4.3.2.2.7.

Based on comparison with measured data, it is estimated that the accuracy of current analytical methods is:

- $\pm$0.2 percent $\Delta\rho$ for Doppler defect.
- $\pm 2 \times 10^{-5}/^{\circ}F$ for moderator coefficient.
- $\pm$50 ppm for critical boron concentration with depletion.
- $\pm$3 percent for power distributions.
- $\pm$0.2 percent $\Delta\rho$ for rod bank worth.
- $\pm$4 pcm/step for differential rod worth.
- $\pm$0.5 pcm/ppm for boron worth.
- $\pm$0.1 percent $\Delta\rho$ for moderator defect.

4.3.4 REFERENCES

1. "Westinghouse Anticipated Transients Without Reactor Trip Analysis," WCAP-8330, August 1974.
2. Spier, E. M., "Evaluation of Nuclear Hot Channel Factor Uncertainties," WCAP-7308-L-P-A (Proprietary) and WCAP-7308-L-A, (Nonproprietary), June 1988.
3. Hellman, J. M., ed, "Fuel Densification Experimental Results and Model for Reactor Application," WCAP-8218-P-A (Proprietary) and WCAP-8219-A (Nonproprietary), March 1975.
4. Meyer, R. O., "The Analysis of Fuel Densification," Division of Systems Safety, U.S. Nuclear Regulatory Commission, NUREG-0085, July 1976.

5. Hellman, J. M., Olson, C. A., and Yang, J. W., "Effects of Fuel Densification Power Spikes on Clad Thermal Transients," WCAP-8359, July 1974.

6. "Power Distribution Control of Westinghouse Pressurized Water Reactors," WCAP-7811, December 1971.

7. Morita, T., et al., "Power Distribution Control and Load Following Procedures," WCAP-8385 (Proprietary) and WCAP-8403 (Nonproprietary), September 1974.

8. McFarlane, A. F., "Power Peaking Factors," WCAP-7912-P-A (Proprietary) and WCAP-7912-A (Nonproprietary), January 1975.

9. Meyer, C. E., and Stover, R. L., "Incore Power Distribution Determination in Westinghouse Pressurized Water Reactors," WCAP-8498, July 1975.

10. Barry, R. F., and Altomare, S., "The TURTLE 24.0 Diffusion Depletion Code," WCAP-7213-A (Proprietary) and WCAP-7758-A (Nonproprietary), February 1975.

11. Cermak, J. O., et al., "Pressurized Water Reactor pH -Reactivity Effect Final Report," WCAP-3696-8 (EURAEC-2074), October 1968.

12. Ford, W. E., III, "CSRL-V: Processed ENDF1B-V 227-Neutron-Group and Pointwise Cross-Section Libraries for Criticality Safety, Reactor and Shielding Studies," ORNL/CSD/TM-160, June 1982.

13. Deleted.

14. Petrie, L. M., and Cross, N. F., "KENO IV--An Improved Monte Carlo Criticality Program," ORNL-4938, November 1975.

15. Deleted.

16. Deleted.

17. Deleted.

18. Poncelet, C. G., and Christie, A. M., "Xenon-Induced Spatial Instabilities in Large Pressurized Water Reactors," WCAP-3680-20 (EURAEC-1974), March 1968.

19. Skogen, F. B., and McFarlane, A. F., "Control Procedures for Xenon-Induced X-Y Instabilities in Large Pressurized Water Reactors," WCAP-3680-21 (EURAEC-2111), February 1969.

20. Skogen, F. B., and McFarlane, A. F., "Xenon-Induced Spatial Instabilities in Three Dimensions," WCAP-3680-22 (EURAEC-2116), September 1969.

21. Lee, J. C., et al., "Axial Xenon Transient Tests at the Rochester Gas and Electric Reactor," WCAP-7964, June 1971.

22. Barry, R. F., and Minton, G., "The PANDA Code," WCAP-7084-P-A (Nonproprietary), February 1975.

23. Barry, R. F., "LEOPARD - A Spectrum Dependent Non-Spatial Depletion Code for the IBM-7094," WCAP-3269-26, September 1963.

24. England, T. R., "CINDER - A One-Point Depletion and Fission Product Program," WAPD-TM-334, August 1962.

25. Eggleston, F. R., "Safety-Related Research and Development for Westinghouse Pressurized Water Reactors, Program Summaries - Winter 1977 - Summer 1978," WCAP-8768, Revision 2, October 1978.

26. Poncelet, C. G., "LASER - A Depletion Program for Lattice Calculations Based on MUFT and THERMOS," WCAP-6073, April 1966.

27. Olhoeft, J. E., "The Doppler Effect for a Non-Uniform Temperature Distribution in Reactor Fuel Elements," WCAP-2048, July 1962.

28. Nodvik, R. J., "Supplementary Report on Evaluation of Mass Spectrometric and Radiochemical Analyses of Yankee Core I Spent Fuel, Incuding Isotopes of Elements Thorium Through Curium," WCAP-6086, August 1969.

29. Drake, M. K., ed, "Data Formats and Procedure for the ENDF/B Neutron Cross Section Library," BNL-50274, ENDF-102, Vol. 1, 1970.

30. Suich, J. E., and Honeck, H. C., "The HAMMER System, Heterogeneous Analysis by Multigroup Methods of Exponentials and Reactors," DP-1064, January 1967.

31. Flatt, H. P., and Buller, D. C., "AIM-5, A Multigroup, One Dimensional Diffusion Equation Code," NAA-SR-4694, March 1960.

32. "Nuclear Design of Westinghouse Pressurized Water Reactors with Burnable Poison Rods," WCAP-7806, December 1971.

33. Strawbridge, L. E., and Barry, R. F., "Criticality Calculation for Uniform Water-Moderated Lattices," Nuclear Science and Engineering 23, p 58, 1965.

34. Nodvik, R. J., "Saxton Core II Fuel Performance Evaluation," WCAP-3385-56, Part II, "Evaluation of Mass Spectrometric and Radiochemical Materials Analyses of Irradiated Saxton Plutonium Fuel," July 1970.

35. Leamer, R. D., et al., "PuO_2 -UO_2 Fueled Critical Experiments," WCAP-3726-1, July 1967.

36. Davidson, S. L., ed, et al., "ANC: Westinghouse Advanced Nodal Computer Code," WCAP-10965-P-A, September 1986.

37. Nguyen, T. Q., et al., "Qualification of the PHOENIX-P/ANC Nuclear Design System for Pressurized Water Reactor Cores," WCAP-11596-P-A, June 1988.

38. Mildrum, C. M., Mayhue, L. T., Baker, M. M., and Isaac, P. G., "Qualification of the PHOENIX/POLCA Nuclear Design and Analysis Program for Boiling Water Reactors," WCAP-10841 (Proprietary), and WCAP-10842 (Nonproprietary), June 1985.

39. WCAP-10216-P-A, Revision 1A, "Relaxation of Constant Axial Offset Control, FQ Surveillance Technical Specification," February 1994.

40. Chao, y. a., et al., "Westinghouse Dynamic Rod Worth Measurement Technique," WCAP-13360-P-A, January 1996.

41. Beard, C.L. and T. Morita, "Beacon Core Monitoring and Operations Support System," WCAP-12472-P-A Addendum 1-A, January 2000.

42. Vogtle Electric Generating Plant, Request to Revise Technical Specifications to Reflect Updated Spent Fuel Rack Criticality Analyses for Units 1 and 2, SNC Letter NL-04-0973, J. T. Gasser to NRC, August 13, 2004.

43. Issuance of Amendments that Revise the Spent Fuel Pool Rack Criticality Analyses, NRC to D. E. Grissette, September 22, 2005 (Amendments 139/118).

44. WCAP-16260-P-A, Revision 0, "The Spatially Corrected Inverse Count Rate (SCICR) Method for Subcritical Reactivity Measurement," September 2005.

45. GP-18735, "Evaluation of a Reduction in the Required Number of Movable Incore Detector Thimbles," January 31, 2011.

46. GP-18767," Southern Nuclear Operating Company, Vogtle Electric Generating Plant Units 1 and 2, Cycle 17 Movable Incore Detector Thimble Evaluation," April 4, 2011.

47. Ouisloumen, M., et al., “Qualification of the Two-dimensional Transport Code PARAGON,” WCAP-16045-P-A, Westinghouse, 2004.

48. Zhang, B., et al., “Qualification of the NEXUS Nuclear Data Methodology,” WCAP-16045-P-A, Addendum 1, Westinghouse, 2005.

4.3.5 BIBLIOGRAPHY

Dominick, I. E., and Orr, W. L., "Experimental Verification of Wet Fuel Storage Criticality Analyses," WCAP-8682 (Proprietary) and WCAP-8683 (Nonproprietary), December 1975.